Nanoscale Science Research Centers

2009 Contractors' Meeting

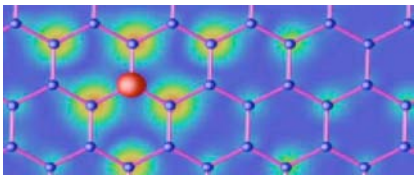

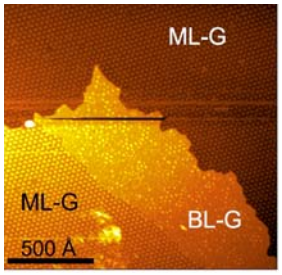

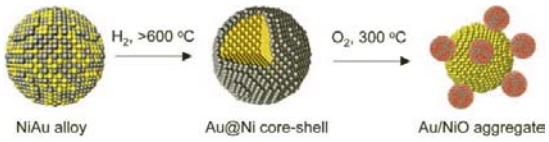

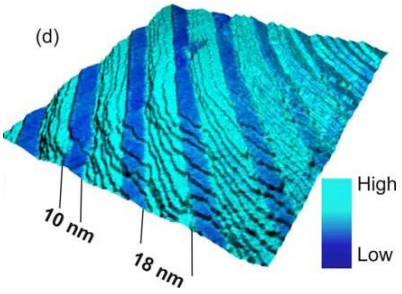

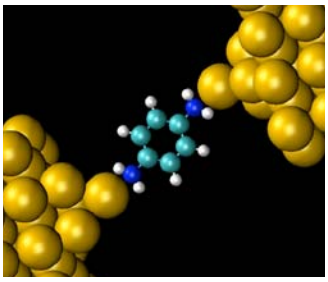

The Westin Annapolis
Annapolis, Maryland

June 3-5, 2009

U.S. DEPARTMENT OF ENERGY
Office of Basic Energy Sciences

NOTE: The printed version of this abstract book is provided in black-and-white; the accompanying CD contains full color versions of all the abstracts.

This document was produced under contract number DE-AC05-06OR23100 between the U.S. Department of Energy and Oak Ridge Associated Universities.

Nanoscale Science Research Centers (NSRCs) Contractors' Meeting

The Westin Annapolis
100 Westgate Circle
Annapolis, Maryland 21401
Phone: (410) 972-4300; Fax: (410) 295-7420
Meeting in Capitol D Room
Poster Boards in A-B-C Rooms
Dinner in Senate Room

AGENDA

Wednesday, June 3, 2009

6:00 p.m. Welcome and introductory remarks
P. Montano and A. H. Carim, DOE-Basic Energy Sciences

6:15 p.m. Buffet dinner available

6:45 p.m. Update on overall NSRC status, progress, and user programs
A. H. Carim, DOE-BES

7:15 p.m. **Invited plenary presentation**
J. Heath, CalTech

8:00 p.m. The Interplay of Theory and Experiment in Nanoscience
P. T. Cummings, Vanderbilt U. and CNMS

8:30 p.m. Enabling nanocrystal science and applications with WANDA, a custom robotic laboratory
D. J. Milliron, Foundry

9:00 p.m. Adjourn for evening

Thursday, June 4, 2009

7:30 a.m. Continental breakfast available

8:30 a.m. Improved Hybrid Organic-Inorganic Photovoltaics via In Situ UV-Polymerization in Nanotube Arrays
S. J. Sibener, U. Chicago

9:00 a.m. Visualizing 3-D Directed Assembly of Block-Copolymer Thin Films on Nanoparticle Substrates using Neutron Scattering
A. Karim, U. Akron

9:30 a.m. Solvent Vapor-Assisted Self-Assembly of Patternable Block Copolymers
J. K. Bosworth, Hitachi Global Storage Technologies

10:00 a.m. Break

10:30 a.m. Core-Shell particle restructuring during CO oxidation cycles: A DRIFTS investigation
B. Eichhorn, U. Maryland

11:00 a.m. Catalysis and Corrosion on Transition Metal Nanoclusters
J. P. Greeley, CNM

11:30 a.m. Tracking single quantum dots in three dimensions: Following receptor traffic and membrane topology
J. H. Werner, CINT

12:00 noon Lunch buffet

1:15 p.m. Combinatorial Discovery of Biomimetic Atomically-Defined Soft Nanomaterials
R. N. Zuckermann, Foundry

1:45 p.m. Multicomponent Nanoscale Systems Fabricated with a Macromolecular Toolbox
O. Gang, CFN

2:15 p.m. Break

2:45 p.m. Methods for the Synthesis of Defined Protein Nanotubes
J. D. Mougous, U. Washington

3:15 p.m. Bioinspired Templates for the Growth of Semiconductor Nanowires
C. A. Batt, Cornell U.

3:45 p.m. Poster session

5:00 p.m. Adjourn for day

Friday, June 5, 2009

7:30 a.m. Continental breakfast available

8:30 a.m. Nanostructure characterization of resistive oxides
O. Heinonen, Seagate

9:00 a.m. Linear and Nonlinear Properties of Large-Area Metamaterials
S. R. J. Brueck, U. New Mexico

9:30 a.m. Hybrid Plasmonics: New Routes to Imaging, Spectroscopy, and Efficient Energy Flow at the Nanoscale
G. P. Wiederrecht, CNM

10:00 a.m. Break

10:30 a.m. Transition Metal Catalyzed Graphene
P. Sutter, CFN

11:00 a.m. Single Molecules Junctions: Conductance, Formation and Evolution Statistics
L. Venkataraman, Columbia U.

11:30 a.m. Deciphering the Mechanisms of Bias-Induced Phase Transitions on a Single Defect Level
S. V. Kalinin, CNMS

12:00 noon Lunch buffet

1:15 p.m. **Invited plenary presentation**
Small Is Different: The Non-Scalable Nano Range
U. Landman, Georgia Tech

2:00 p.m. Experimental and theoretical studies of molecular-scale quantum dots at carbon nanotube heterojunctions
J. Hone, Columbia U.

2:30 p.m. Discovery Platforms™ for Nanoscience
J. P. Sullivan, CINT

3:00 p.m. Closing remarks
P. Montano and A. H. Carim, DOE-Basic Energy Sciences

3:15 p.m. Adjourn meeting

Table of Contents

Speaker Extended Abstracts

Poster Extended Abstracts

Biomaterials

Catalysis

Electronic and Photonic Materials

Scanning Probes

Theory and Simulation

X-Ray Probes

Other Topics

Speaker Extended Abstracts

The Interplay of Theory and Experiment in Nanoscience

Peter T. Cummings
Department of Chemical and Biomolecular Engineering
Vanderbilt University
Nashville, TN 37235-1604
and
Center for Nanophase Materials Sciences
Oak Ridge National Laboratory
Oak Ridge, TN 37831-6496

Theory and simulation have played, and continue to play, a central role in nanoscience. In fact, it can be argued that theory and simulation play a greater role in nanoscience than in macroscopic materials and chemical sciences for at least three reasons: first, many experiments performed at the nanoscale can only be interpreted through theory; second, theory and simulation can provide a convenient framework to isolate effects and phenomena in a way that may be difficult or impossible to achieve in an experiment (i.e., in theory and/or simulation, the boundary and initial conditions are under complete control, which may be impossible to achieve in an experiment), thus making theory and simulation a crucial tool in understanding emergent phenomena in nanoscale systems; and, finally, theory and simulation can be used to design new nanostructured materials, as well as systems based on nanoscale phenomena.

In this presentation, these roles of theory and simulation will be illustrated through examples from the published literature, from the speaker's own research program, from user research projects at the Center for Nanophase Materials Sciences (CNMS), and from the CNMS internal scientific research program. The latter has three major themes: imaging nanoscale functionality, synthesis and dynamics of nanostructured polymeric and hybrid materials, and emergent behavior in nanoscale systems. Theory and simulation play prominent roles in all three themes, in addition to leading the emergent behavior theme.

In conclusion, the prospects for the future role of theory and simulation in nanoscience will be assessed, in light of continuing advances in theory, computational methods and computing hardware.

Enabling nanocrystal science and applications with WANDA, a custom robotic laboratory

Emory Chan[1], Gang Han[1], Shiwei Wu[1], Bruce E. Cohen[1], P. James Schuck[1], Jonathan S. Owen[2], A. Paul Alivisatos[2], Delia J. Milliron[1]

[1]The Molecular Foundry, Lawrence Berkeley National Laboratory, 1 Cyclotron Road, Berkeley, CA 94720; [2]Department of Chemistry, University of California, Berkeley, CA 94720. Correspondence to DJM: dmilliron@lbl.gov.

Scientific Thrust Area

This project is lead by the Molecular Foundry's Inorganic Nanostructures Facility, in collaboration with the Biological Nanostructures and the Imaging & Manipulation Facilities.

Research Achievement

From 2007 to 2008, the Molecular Foundry took on the challenge of enabling automated synthesis of colloidal nanocrystals. Symyx Technologies built and tested the product of a collaborative design process over the course of 7 months and installed the Workstation for Automated Nanomaterials Discovery and Analysis (WANDA) at the Molecular Foundry in October 2008. Although WANDA has been operational for only six months, it is already facilitating nanoscience in unprecedented ways. The custom low-thermal-mass reactor bay at the heart of WANDA's core module has performed impeccably, synthesizing colloidal nanocrystals ranging from semiconductors to metals, and characterizing their growth processes using high-throughput optical spectroscopy.

Colloidal nanocrystals are a centerpiece of modern nanoscience, investigated worldwide for their size-dependent properties and their potential applications in catalysis, photovoltaics, light-emitting diodes, and bio-imaging, among others. Nanocrystal synthesis is conventionally carried out in a round bottom flask which is stirred magnetically, heated by an electric mantle, and connected to a Schlenk line to prevent inadvertent oxidation. Using this approach, a tremendous diversity of size-controlled nanocrystals have been synthesized including metals, and oxide, chalcogenide, and pnictide semiconductors with rounded, faceted, anisotropic, or even branched shapes. Nonetheless, the conventional flask makes synthetic development slow and reproducibility challenging, especially as the product can be highly sensitive to synthetic variables such as heating and cooling rates, or the rate of reactant addition. Problems with batch-to-batch reproducibility limit the systematic investigation of size-dependent properties, typically making it necessary to perform all measurements on a single batch of nanocrystals. By developing an automated synthesis platform, we seek to a) accelerate the rate of synthetic development and the investigation of synthetic pathways and b) produce completely reproducible nanocrystals to facilitate property assessments and applications of all kinds.

The result of our development effort, WANDA, contains eight custom reactors, which can be operated in parallel and which are capability of executing the extreme thermal profiles required for nanocrystal synthesis, including reaction temperatures up to 350 ℃ and rapid, active cooling at the reaction end point. Aliquots collected by a sampling needle are characterized in a 96-well plate reader by photoluminescence and absorption spectroscopy. In addition, a quartz plate can be automatically spotted for x-ray diffraction analysis by the Facility's existing diffractometer.

Nanocrystals of the semiconductor CdSe have been extensively investigated and are still the subject of active research for optoelectronics applications and as bio-imaging probes. The synthesis of monodisperse CdSe nanocrystals with exceptionally reproducible growth kinetics has been demonstrated using WANDA. We have taken advantage of this reproducibility, and the high-throughput capabilities of WANDA to optimize the CdSe synthesis with respect to size distribution. Then, varying reactant concentrations, temperature, and time over 160 samples, we were able to determine kinetic rate orders, activation energies, and pre-exponential factors for nanocrystal growth. These results demonstrates the power of automation to enable rapid refinement and detailed investigation of synthetic methods.

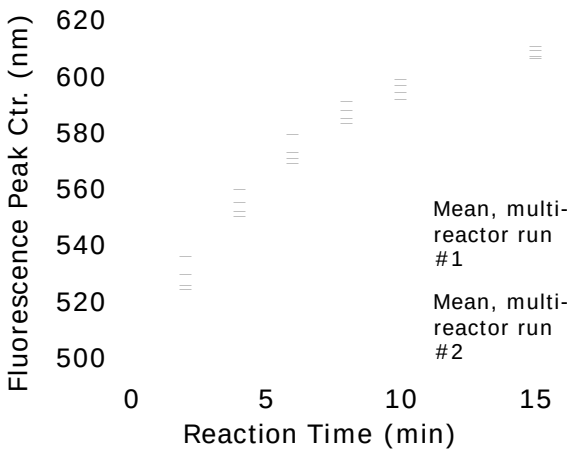

Critical to facilitating the diverse internal and user projects at the Molecular Foundry, WANDA's reactors are designed to switch instantly between different nanocrystals chemistries. For example, lanthanide-doped $NaYF_4$ nanocrystals are being developed as next-generation single-biomolecule probes. When co-doped with lanthanides which undergo efficient energy transfer, such as Yb^{3+} and Er^{3+}, these nanocrystals efficiently up-convert NIR excitation to visible emission, avoiding autofluorescence interference. Because up-conversion utilizes a real, long-lived intermediate state, the efficiency is orders of magnitude higher than two-photon excitation. We have recently investigated the single-particle photophysical properties of these materials to evaluate their potential as single-molecule probes. The ensemble of emitters in each particle eliminates the emission intermittency characteristic of organic probes and semiconductor nanocrystals alike, and they are extremely photostable. These attractive properties are maintained when an amphiphilic polymer coating is used to transfer the up-converting nanocrystals from organic to aqueous solution.

Future Work

Already, WANDA is synthesizing and characterizing nanocrystals of semiconductors (CdSe, CdTe, PbTe), metals (Co, Te), and up-converting materials, with new capabilities being developed to support internal and user projects. We plan also to implement synthetic methods in which previously synthesized nanocrystals are further modified in subsequent reactions. This will include the synthesis of nanocrystal heterostructures, whose nanoscale interfaces are the subject of a collaborative theoretical and spectroscopic investigation at the Foundry. Core/shell heterostructures with high luminescence quantum yield are of keen interest for optoelectronic and bio applications, yet are challenging to prepare reproducibly by conventional methods. Finally, post-synthetic ligand exchange will be carried out to investigate the role played by the organic-inorganic interface in determining nanocrystal properties and energetics.

Publications

S. Wu, G. Han, D.J. Milliron, S. Aloni, V. Altoe, D.V. Talapin, B.E. Cohen, P.J. Schuck, "Non-blinking and photostable upconverted luminescence from single lanthanide-doped nanocrystals," *PNAS*, in press.

Improved Hybrid Organic-Inorganic Photovoltaics via I*n Situ* UV-Polymerization in Nanotube Arrays

Sanja Tepavcevic[1], Seth B. Darling[2], Nada M. Dimitrijevic[2], Tijana Rajh[2], and Steven J. Sibener[1]

[1] James Franck Institute and Department of Chemistry, University of Chicago
[2] Center for Nanoscale Materials, Argonne National Laboratory

Research Achievement

Hybrid solar cells have been developed in the past decade as a promising alternative for traditional silicon-based solar cells. One approach for making inexpensive inorganic-organic hybrid photovoltaic (PV) cells is to fill nanostructured titania films with solid organic hole conductors such as conjugated polymers.[1] These compounds can function as light-absorbing species and inject electrons into the conduction band of the n-type semiconductor, while at the same time they conduct the holes to the cathode. Nanotube films offer a distinct advantage over nanoparticle films in that they facilitate charge carrier transport.

The infiltration of the polymer into the nanostructured metal oxide is of particular importance for optimizing the performance of these hybrid devices.[2] Most of the reports on solar cells using conjugated polymers have employed wet processing deposition techniques.[3-5] Since polymers suffer a loss of conformational entropy when they are confined in a channel whose radius is less than their radius of gyration, filling the pores with a polymer has been a challenge due to the possibility of the polymer chains clogging the pores of the nanotubular electrode.[1]

In this project we developed a new technique for deposition/infiltration of conjugated polymer into densely ordered TiO_2 nanotube arrays. In particular, we report the effects of *in situ* ultra-violet (UV) polymerization of polythiophene vs. infiltration of pre-synthesized P3HT on the performance of solar cell devices. In our simple and efficient photochemical approach, a nanotubular TiO_2 substrate is immersed in a 2,5-diiodothiophene monomer precursor solution and then irradiated with UV light in an argon environment. The selective UV photodissociation of the C–I bond (λ = 250–300 nm) in the precursor molecule produces monomer radicals with intact π-ring structure. Since the C–I bonds are present at the ends of the reaction coupling products, further photodissociation can take place forming oligomeric and polymer species that can couple to and self-assemble on the surface of TiO_2 nanotubes (Figure [d]).[6] The formation of polymeric semiconductor films by this method offers distinct advantages such as cost, uniformity, and scalability over other solution processing techniques. By polymerizing conjugated polymer inside an electron-accepting nanotube array, we have achieved significant improvements in optoelectronic device performance compared to those fabricated by infiltrating tubes with *ex situ*-synthesized polymer (Figure [c]). Our preparation leads to a strong coupling at the polymer-oxide interface, which is important for efficient exciton separation (Figure [b]), and fewer conformational defects (Figure [a]), which facilitates hole transport. The small molecule precursor also presumably achieves superior filling within the confined environment.

Future Work

One way to further improve performance of these hybrid cells is to maximize the light-harvesting capability through the construction of a rainbow solar cell.[7] An example would employ TiO_2 nanotubes packed with an ordered assembly of different-length oligothiophenes. As white light enters the cell, shorter oligothiophenes (larger band gap) will absorb the portion of the incident light with smaller wavelengths. Longer wavelength light, transmitted through the initial layer, will be absorbed by subsequent layers, and so on. By using *in situ* UV

polymerization, a gradient of different length oligothiophenes can be readily created by varying UV exposure time. By constructing an ordered gradient of conjugated oligomers/polymer, it should be possible to increase the effective capture of incident light.

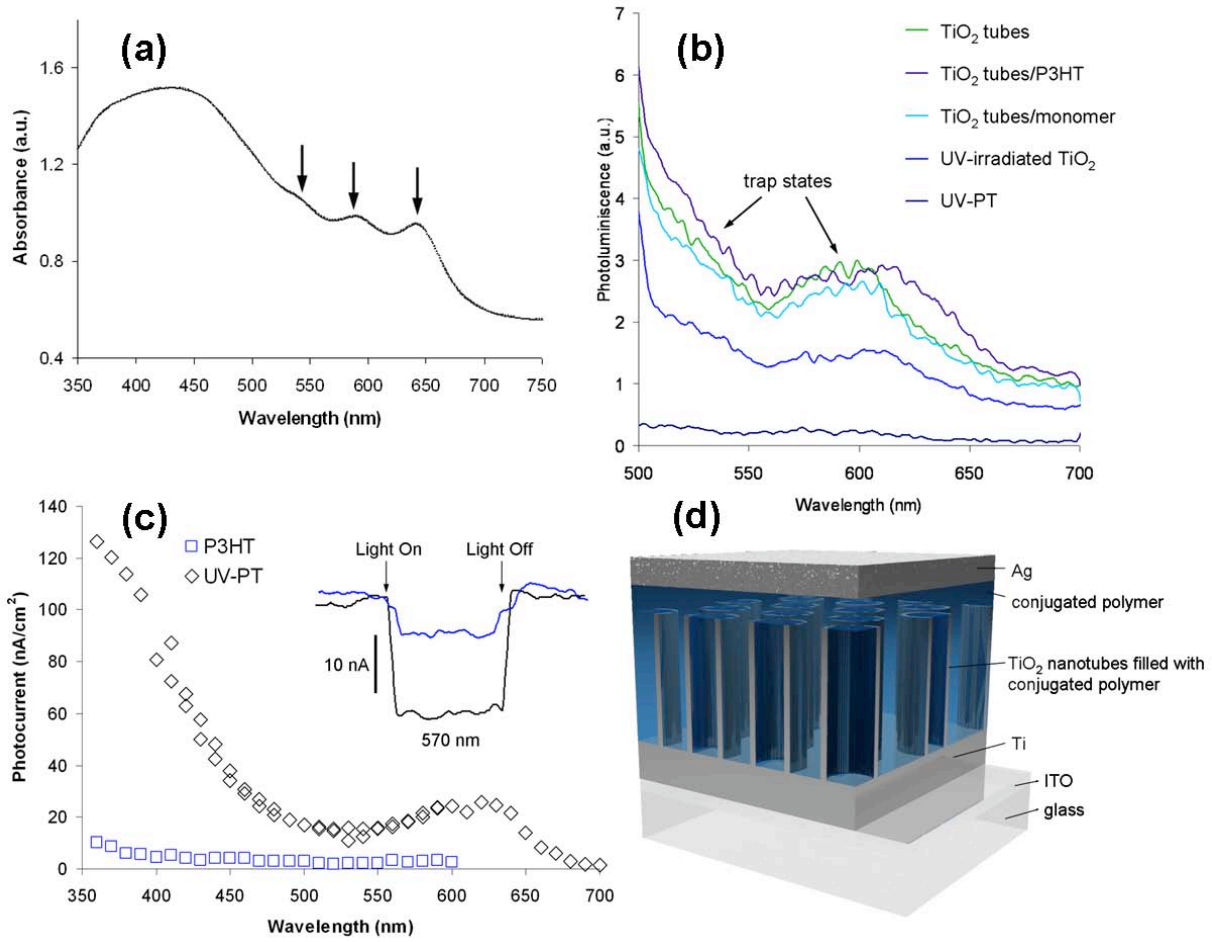

(a) UV-Vis absorption spectrum of polythiophene polymerized within TiO_2 nanotubes showing vibronic peaks; (b) photoluminescence spectra of TiO_2 nanotubes with various molecular fillers; (c) photoaction spectra of P3HT/TiO_2 and UV-PT/TiO_2 devices and time traces of photocurrent (inset); (d) schematic of hybrid solar cell construction

References

[1] K. Shankar, G. K. Mor, H. E. Prakasam, O. K. Varghese, C. A. Grimes, *Langmuir* **2007**, *23*, 12445.
[2] K. M. Coakley, Y. Liu, M. D. McGehee, K. L. Frindell, G. D. Stucky, *Adv. Func. Mater.* **2003**, *13*, 301.
[3] K. M. Coakley, M. D. McGehee, *Appl. Phys. Lett.* **2003**, *83*, 3380.
[4] A. C. Arango, L. R. Johnson, V. N. Bliznyuk, Z. Schlesinger, S. A. Carter, H.-H. Hörhold, *Adv. Mater.* **2000**, *12*, 1689.
[5] P. A. van Hal, M. P. T. Christiaans, M. M. Wienk, J. M. Kroon, R. A. J. Janssen, *J. Phys. Chem. B* **1999**, *102*, 4352.
[6] S. H. Kim, S. Natarajan, G. Liu, *Catal. Today* **2007**, *123*, 104.
[7] A. Kongkanand, K. Tvrdy, K. Takechi, M. Kuno, P. V. Kamat, *J. Am. Chem. Soc.* **2008**, *130*, 4007.

Publication

"Improved hybrid solar cells via in situ UV-polymerization," S. Tepavcevic, S.B. Darling, N.M. Dimitrijevic, T. Rajh, and S.J. Sibener, *Small* (2009). DOI: 10.1002/smll.200900093.

Visualizing 3-D Directed Assembly of Block-Copolymer Thin Films on Nanoparticle Substrates using Neutron Scattering

Alamgir Karim, Department of Polymer Engineering, University of Akron

Research Achievement

Self assembly of block-copolymers (BCPs) is one of the most promising of the emerging technologies for nanofabrication and photovoltaic applications such as polymer solar cells. BCP's can form ordered domains at the 10's of nanometer scale due to incompatibility between the two polymer blocks leading to a rich variety of structures such as cylinders, lamellae, bicontinuous and gyroids. Controlling and measuring the orientational order in 3-D in thin films is important for potential applications of these materials. In thin BCP films, the lamellae or cylinders orient parallel to the substrate interface as one of the blocks exhibits an energetic preference for the substrate, aided by the geometric constraint of the flat substrate. However, the effect of nanoscale roughness on BCP orientation has only been minimally investigated, yet most practical surfaces can be expected to exhibit such roughness.

We investigate the self-assembly of BCPs on nanoparticle roughened substrates as a novel strategy to obtain vertically oriented BCP lamellae. This approach relies on the premise that the interfacial bending energy of BCP lamellae oriented parallel to substrate is unfavorably high by conforming to the nanoscale topology and the system re-orients to a vertical assembly to minimize it. By using UV tunable modified silica nanoparticles, we additionally bias the self-assembly to form a surface neutral BCP condition to assist the vertical assembly. The nanoparticles have been modified with a propyl ligand, an organic coating that can be easily oxidized by exposure to UV. By controlling the exposure time, the surface energy of the nanoparticles can be controlled in a simple yet precise manner.

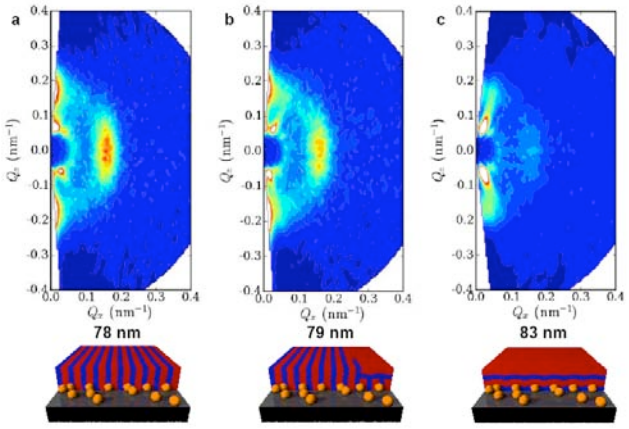

Fig. 1: Small-angle neutron scattering (SANS) data of dPS-PMMA block-copolymer films assembled on nanoparticle surfaces. The reciprocal-space maps were reconstructed by accumulating SANS data as a function of sample rotation angle. A schematic of the inferred lamellae orientation is provided beneath each map. **a**, A 78 nm film, which exhibits the vertical morphology by AFM, generates an intense peak at Q_x = 0.16 nm^{-1}, indicative of vertical order. **b**, A 79 nm film exhibits a slightly weaker vertical peak. **c**, The 83 nm film has effectively no peak in the SANS data, consistent with the horizontal morphology observed by AFM.

Using a combinatorial approach for modifying the surface energy and BCP film thickness, in the case of lamellar films, we observed that a theoretically-predicted, but previously unobserved, oscillation between horizontal and vertical orientations achieved in a single sample [1]. The fingerprint patterns observed by AFM can only confirm the surface orientation, *but in conjunction with rotational SANS enables us to set a bound on the orientation in 3-D as shown in Fig. 1.*

Although coating BCP on a non-periodic rough substrate seems to be an attractive and cheaper option, there is a paucity of knowledge about the mechanism and optimal surface features of a rough

substrate to obtain the vertical lamellae, and more detailed understanding of its dependence on the BCP thickness (L_0) and chemistry of the blocks. By developing a new sol-gel based xerogel substrates we have prepared fractally rough substrates to better understand factors controlling BCP orientation. Preliminary results indicate that the fractal dimension (D_f), which is a quantifiable measure of any rough substrate, irrespective of its periodic or non-periodic nature may be a critical determining factor in controlling the orientation of the BCP lamellae. As seen from Fig. 2, even though the roughness amplitude (R_{RMS}=30.4nm) for the xerogel substrate is much higher than the nanoparticle (R_{RMS}=5.2) substrate, vertically oriented lamellae were obtained over a large area for the slightly higher D_f value (~2.5) of the nanoparticles rather than xerogel substrate. Xerogels with D_f around 2.5 are able to vertically orient BCP as well, so fractal dimension of roughness rather than amplitude of roughness seems to be the controlling parameter. Finally, besides topography and surface energy, residual solvent effects are shown to produce interesting surface morphology maps as an added control variable [2].

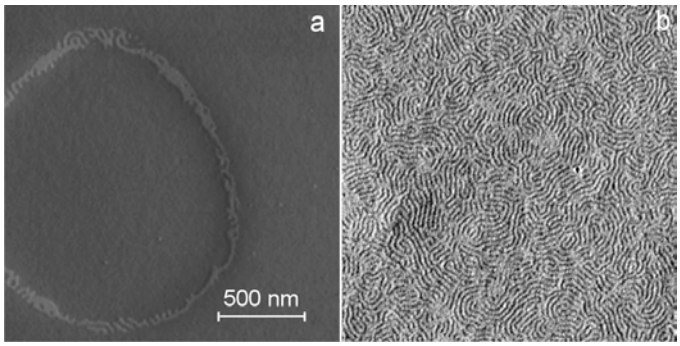

Figure 2. AFM phase images of surface of micro-phase separated lamellar dPS-PMMA BCP film (~65 nm thick) coated on (a) Xero-0.2M7m (D_f=2.4) and (b) SNP80 (D_f=2.5)substrates. The water contact angle for both the substrates was ~65^o

Future Work: In addition to silica xerogels, we will also explore the possibility of using resorcinol-formaldehyde (RF) based xerogels for preparing fractally rough substrates. The advantage of using RF-gel based substrates is that it can be converted to a conducting carbon substrate by pyrolysis, while preserving the fractal nanotopology needed for orientation control. This would be especially useful for solar cell applications, as the carbonized substrate can also work as a base electrode for conducting the holes/electrons through an external circuit for device testing. Due to the difference between the dense carbon-rich FPS phase and the hydrogen-rich P3HT phase, we expect a high contrast in neutron scattering with a scattering length density (SLD) of the order of $4.46x10^{-6}$ A-2. Neutron scattering would be a very useful tool to determine internal structure of these films. Recently we also submitted a proposal to CNMS for studying the directed self-assembly (orientation distribution, defects, long-range order, kinetics of ordering) of CNMS synthesized block copolymers with a [(polymer) – (semi-conducting NP)] or P-SNP architecture in thin films. One of the polymer phases incorporating percolating nanoparticles (PCBM) would act as an acceptor layer while the other polymeric phase (e.g. P3HT) as donor layer.

Publications

[1] K. G. Yager, B. C. Berry, K. Page, D. Patton, A. Karim, E. J. Amis, *Soft Matter* **2009**, 5, 622.

[2] Zhang X, Berry B.C., Yager K.G., Kim S., Jones R.L., Satija S., Pickel D. L., Douglas J.F., Karim A., *ACS Nano*, **2008**, 2, 2331. (***Using CNMS synthesized BCP***)

Solvent Vapor-Assisted Self-Assembly of Patternable Block Copolymers

Joan K. Bosworth,[1, 2, *] Charles T. Black,[3] and Christopher K. Ober[2]

1. Department of Chemistry & Chemical Biology, Cornell University, Ithaca, NY 14853
2. Department of Materials Science & Engineering, Cornell University, Ithaca, NY 14853
3. Center for Functional Nanomaterials, Brookhaven National Laboratory, Upton NY 11973
* Present address: Hitachi Global Storage Technologies, San Jose, CA, 95135

Proposal Title: Solvent Vapor Annealing of Block Copolymer Thin Films

Research Achievement

Block copolymer self-assembly presents a method for patterning and templating applications on the 10-50 nm length scale, smaller than is easily possible using photolithography. Here we investigate the use of polar-nonpolar block copolymers both as photopatternable self-assembling materials and also as vehicles for patterning by selective material infiltration into nanometer-scale polymer domains. Formation of block copolymer thin films with large areas of defect-free self-assembled morphologies, combined with careful control of the polymer domain orientation, are critical for patterning applications. The block copolymer self assembly process is facilitated by polymer chain mobility. The most common method for achieving this - thermal annealing - is a poor choice in our material systems due to thermal incompatibility of these polar-nonpolar block copolymers. Swelling the polymer in a solvent vapor (often termed solvent annealing) provides an alternate route to achieving sufficient chain mobility for self-assembly, and also has additional benefits not possible using a thermal annealing method.

We have used solvent annealing to promote self-assembly of a combined top-down/bottom-up block copolymer system comprised of poly(α-methylstyrene)-block-poly(4-hydroxystyrene), or PαMS-b-PHOST.[1] In this case, we designed photolithographic functionality into the block copolymers, allowing the majority component of the block copolymer to serve as a negative-tone photoresist. In this way we use lithography to control the precise location of the self-assembled block copolymer patterns. An added benefit of solvent vapor annealing is that we can reversibly change the self-assembled polymer film morphology by using the selectivity of different swelling solvents to the two blocks. The choice of solvent for annealing directs the formation of different morphologies in the dried film, demonstrated here to be either a spherical and cylindrical phase. This behavior is reversible and so therefore alternating annealing treatments results in repeatable pattern morphology changes within the film. Secondary ordering techniques applied in tandem with solvent vapor annealing can be used to

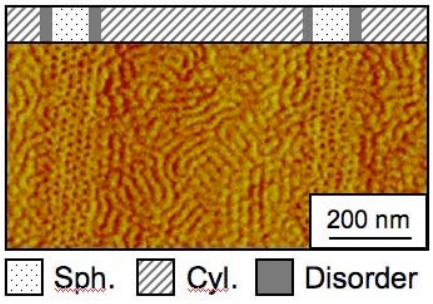

Figure 1. A single film of PαMS-b-PHOST displays two morphologies within high-resolution patterns in this atomic force microscopy height image. A spherical morphology is observed in 100 nm-wide stripes, surrounded by regions with parallel cylindrical morphology.

further control the self-assembly and give highly ordered block copolymer domains. For example, we have used surface topography (graphoepitaxy) to align these self-assembled block copolymer to patterns.

The combination of block copolymer self assembly with crosslinking by lithographic patterning was initially pursued to demonstrate an ability to control the precise location of the assembled patterns. We further combined solvent vapor annealing of PαMS-b-PHOST, used to reversibly tune the self-assembled morphology, with electron beam lithography, used to prevent switching in exposed regions.[2] This combined process has provided a method for selectively patterning 100 nm-wide domains of spherical morphology within regions of parallel-oriented cylindrical morphology, as seen in Figure 1. These results are achieved by first solvent vapor annealing in acetone to form a self-assembled spherical morphology in the entire film, and then patterning the film by expoure to an electron-beam. A second solvent anneal in tetrahydrofuran forms cylindrical morphology wherever the film had not been crosslinked by the electron beam.

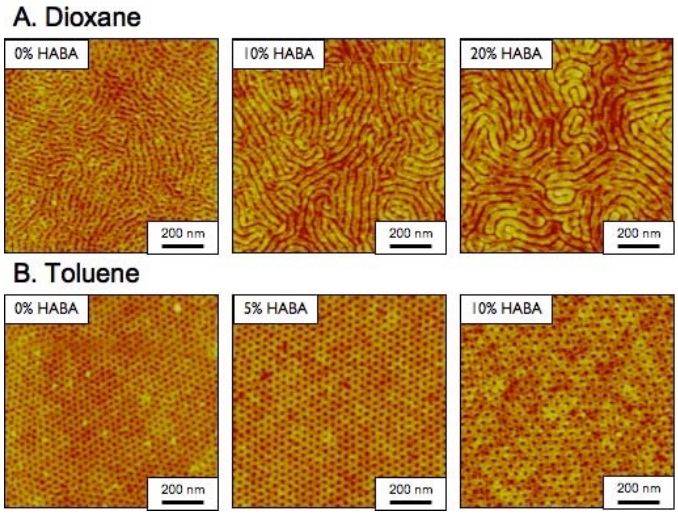

Figure 2. PS-b-P2VP solvent annealed in dioxane (A) display parallel cylinder morphology, while annealing in toluene (B) leads to spherical morphology. Varying the amount of 2-(4-hydroxyphenylazo)benzoic acid (HABA) blended with the PS-b-P2VP allows tuning of the morphology as well as formation of pores upon its extraction.

We have also investigated solvent vapor annealing of the block copolymer polystyrene-block-poly(2-vinylpyridine), PS-b-P2VP, blended with a hydrogen bonding material that selectively segregates into the polar block.[3] Blending the small molecule with the block copolymer provides a method of tuning the self-assembled domain periodicity upon solvent annealing, with morphology control again possible by choice of solvent and its associated block selectivity (Figure 2). Selective extraction of the blended material forms voids displaying the tunable periodicity, and such patterns can then be subsequently transferred by templating to inorganic materials.

Publications

1. Bosworth, J. K.; Paik, M. Y.; Ruiz, R.; Schwartz, E. L.; Huang, J. Q.; Ko, A. W.; Smilgies, D.-M.; Black, C. T.; Ober, C. K., Control of Self-Assembly of Lithographically Patternable Block Copolymer Films. *ACS Nano* **2008,** 2, 1396-1402.

2. Bosworth, J. K.; Black, C. T.; Ober, C. K., Selective Area Control of Self-Assembled Pattern Architecture Using a Lithographically Patternable Block Copolymer. *Submitted, ACS Nano*.

3. Bosworth, J. K.; Ober, C. K.; Black, C. T., Control of Self-Assembled Block Copolymer Film Morphology, Dimensions, and Packing Through Combined Selectve Molecule Blending and Solvent Vapor Annealing. *In preparation*.

Core-Shell particle restructuring during CO oxidation cycles: A DRIFTS investigation

Bryan Eichhorn, Anthony Dylla, Selim Alayoglu, Robert Walker, University of Maryland, College Park, Maryland 20742

Zili Wu CNMS - Oak Ridge National Labs

We show how oxidizing and reducing conditions restructure the surface of 5 nm Ru@Pt core/shell nanoparticle catalysts (Ru core, Pt shell). A combination of TEM line scans, in situ DRIFTS studies and catalytic evaluations show that the Ru atoms in the Ru core are brought to the surface to form a RuO/Pt alloy surface structure under oxidizing conditions and return to their sub-surface sites under reducing environments to re-generate an essentially pure Pt surface. Evaluation of the supported Ru@Pt catalysts for CO oxidation shows reactivity identical to that of the alloyed PtRu alloy, which is consistent with the in situ DRIFTS studies that show the same surface structure for both particles. Under reducing conditions, the DRIFTS studies show markedly different surface structures for the Ru@Pt vs. PtRu alloy particles. Evaluation of the preferential oxidation of CO in hydrogen feeds (PROX) reaction (i.e. CO oxidation under reducing conditions) shows significantly better activity for the core-shell catalysts relative to the alloy catalysts and are also in agreement with the DRIFTS experiments. Post catalysis TEM-EDS studies show that the core-shell structure is retained for the Ru@Pt NPs. The data show that the alloy NPs are essentially invariant in their surface and core structures under oxidizing and reducing conditions whereas the Ru@Pt core-shell particles undergo facile and reversible surface-to-subsurface migrations.

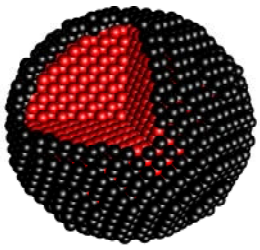

Core/Shell Ru@Pt

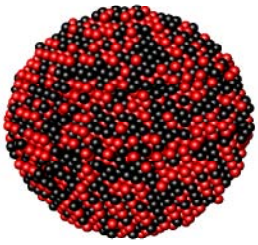

RuPt (1:1) alloy

Catalysis and Corrosion on Transition Metal Nanoclusters

Jeffrey P. Greeley
Center for Nanoscale Materials
Argonne National Laboratory
Argonne, IL 60439
jgreeley@anl.gov

Scientific Thrust Area
Nanoscale Theory and Modeling

Research Achievement
This effort involves comprehensive Density Functional Theory (DFT) simulations of a range of phenomena involving heterogeneous catalysis and corrosion on metal nanoparticles and clusters. It complements experimental catalysis and corrosion efforts at the Center for Nanoscale Materials, Argonne National Laboratory, and elsewhere.

Catalysis is the study and control of chemical transformations; a good catalyst will permit a given chemical reaction to proceed at high rates at modest temperatures ("activity") and will, at the same time, prevent the formation of unwanted byproducts ("selectivity") [1]. Typical catalysts are composed of either metal alloy or metal oxide nanoparticles and have been developed primarily by trial and error-based approaches. To fully optimize their properties, however, it is essential to develop fundamental understanding of the molecular-level properties that govern their operation. DFT analyses play an essential role in developing such understanding and will, ultimately, also facilitate the design and discovery of novel catalytic materials [2].

An emerging area of importance in theoretical nanocatalysis is the study of electrocatalytic systems [3]. Such systems, which are of first-order importance in the operation of fuel cells, batteries, and other electrochemical devices, are susceptible to all of the activity and selectivity-related problems of heterogeneous nanocatalysts, but they additionally suffer from significant corrosion and stability problems. Again, theory is poised to make an important contribution to the understanding, and ultimately suppression, of such nanocorrosive effects.

One application area in which we have been recently working is the use of subnanometer platinum clusters to catalyze chemical transformations in molecules needed for petrochemical processing. For example, we have recently completed a study of the properties of Pt_{8-10} nanoclusters for the oxidative dehydrogenation of propane to propylene (an important precursor for the production of polypropylene)[4]. Experimental results (S. Vadja et al., ANL/CNM-CSE) indicate that the nanoclusters catalyze this reaction with high selectivity and with an activity 40-100 times that of any existing catalyst. Our DFT-based investigations, in turn, provide a compelling explanation for this observation. The highly undercoordinated nature of the atoms in the Pt clusters permits them to rapidly cleave C-H bonds in propane, yielding propylene; the barriers for these critical steps are reduced by several tenths of an electron volt compared to the more

extended single-crystal surfaces that would be found on larger nanoparticles, resulting in substantially enhanced activity for the subnanometer catalysts.

A second thrust area that we have been studying is the catalytic activity and stability of metal nanoclusters supported on metal substrates in electrochemical environments. In collaboration with Nenad Markovic (ANL/MSD), we have found that Pt nanoparticles (0.5 -3 nm diameter) supported on Pt(111) or Pt(100) single crystal substrates have CO electrooxidation activities at least as high as that of the best known Pt-based alloy catalysts. Using extensive DFT calculations, we have traced the origin of this high activity to an enhanced competition of OH groups for highly undercoordinated sites on the particles' surfaces [5]. In addition, given the likelihood of corrosion of these small nanoparticles in electrochemical environments, we have studied the clusters' stability as a function of the electrode potential. We have found, among other results, that the stability of atoms in the clusters is directly proportional to their coordination number and that water dissociation, with concomittant oxide deposition, facilitates their dissolution.

Future Work

We will explore the catalytic properties of a broad array of subnanometer metal clusters for key heterogeneous catalytic reactions, including methanol dehydrogenation and propylene epoxidation. We will develop a database of key reactivity properties on these clusters that will ultimately permit us to make predictions about which clusters are likely to have promising properties for these reactions. In tandem, we will continue to explore the relationship between the oxidation state and the stability of metal clusters in electrochemical environments; our ultimate goal in this case will be to identify key features that will promote the stability of these clusters under realistic, fuel cell-like conditions.

References

[1] Somorjai, G. A., *Introduction to Surface Chemistry and Catalysis*. Wiley: New York, 1994.
[2] Hammer, B., Nørskov, J. K., *Adv. Catal.* 45, 71 (2000).
[3] J. Rossmeisl et al., in *Fuel Cell Catalysis*. Wiley: New York, 2009.
[4] S. Vajda et al., *Nature Materials.* **8**, 213 (2009).
[5] D. Strmcnik et al., *J. Am. Chem. Soc.* **130**, 15332 (2008).

Publications

C. Lucas et al., "Temperature-induced ordering and phase transitions in metal/adsorbate structures at electrochemical interfaces," *J. Am. Chem. Soc., in press.*

S. Vajda et al., "Subnanometre platinum clusters as highly active and selective catalysts for the oxidative dehydrogenation of propane," *Nature Materials.* 8, 213 (2009).

D. Strmcnik et al., "Unique activity of platinum ad-islands in the CO electrooxidation reaction," *J. Am. Chem. Soc.* 130, 15332 (2008).

P. Strasser et al., "Voltammetric surface dealloying of Pt bimetallic nanoparticles: an experimental and DFT computational analysis," *Phys. Chem. Chem. Phys.* **10**, 3670 (2008).

Tracking single quantum dots in three dimensions: Following receptor traffic and membrane topology

Nathan P. Wells[1], Diane S. Lidke[2], M. Lisa Phipps[1], Peter M. Goodwin[1], Bridget S. Wilson[2], and James H. Werner[*1]

[1]*Center for Integrated Nanotechnologies, Los Alamos National Laboratory, Los Alamos NM*
[2]*Cellular Pathology Department, University of New Mexico, Albuquerque NM*

Proposal Title: Probing the 3D nano-environment of live cells molecule by molecule (D. Lidke)

Research Achievement:

The detection of single molecules by laser induced fluorescence has become a powerful tool for the characterization and measurement of biological processes. For example, single molecule microscopy has been used to monitor individual enzymatic turnovers[1], directly observe the hand over hand motion of individual motor proteins with near nanometer precision[2], and has been used to visualize the diffusion and transport of individual lipids and receptors on live cells[3]. Much has been learned from these single-molecule studies that had been obscured in conventional ensemble microscopy, such as the direct observation of unexpected modes of travel around domain structure within live cell membranes[3].

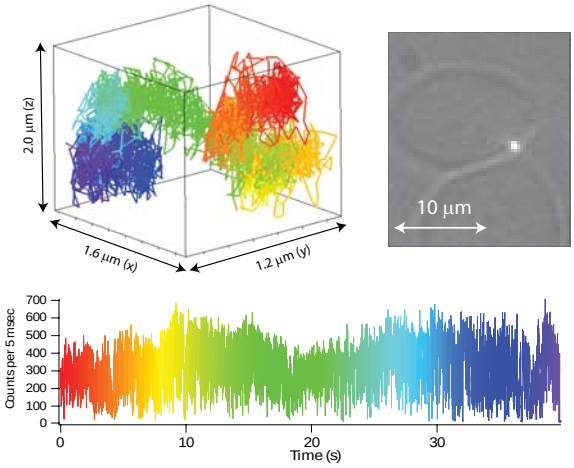

Figure 1 Top Left: 3D trajectory of a quantum dot labeled IgE-FcεRI on the side of a rat mast cell. **Top Right:** Image of this receptor on the cell obtained while 3D tracking. **Bottom:** Counts measured during the 40 second trajectory. Rainbow color scheme used to denote passage of time. Adapted from [7].

Note that in the examples cited above, the motion of the molecule under investigation was limited to zero[1], one[2], or two dimensions[3]. We point out perhaps the obvious: *most aspects of life, including intracellular signaling and trafficking, are inherently 3-dimensional.* However, tracking a single fluorescent molecule or a single quantum dot traveling through 3 dimensional space is a difficult (and until recently) unsolved technical problem. A small number of advanced 3D tracking methods based upon closed-loop feedback have been recently developed by a handful of research groups (Reviewed in[4]). Our approach[5-7] uses a unique spatial filter geometry and active feedback to always keep a molecule (or quantum dot) in the center of the field of view of a confocal microscope. This system can follow individual quantum dots over an extended X, Y, and Z range (tens of microns) at a spatial precision of ~50 nm obtained during 5 milliseconds of observation. We note our 3D tracking methods and algorithms are quite insensitive to a large homogeneous background, making them useful in "dirty" environments such as cells[6]. This microscope enables following the 3D transport and function of individual fluorescently labeled biomolecules (proteins, DNA, or RNA) inside living cells with near 100 picosecond temporal resolution for durations up to minutes.

* Contact: jwerner@lanl.gov (505)-667-8842

Here, facilitated with a CINT user proposal from experts in cellular signaling (Diane Lidke and Bridget Wilson, University of New Mexico), we are using our 3D tracking microscope to directly observe the three dimensional spatio-temporal dynamics of quantum dot labeled IgE-FcεRI, an important signaling molecule for the allergic response. Our 3D tracking results are consistent with prior observations of 2D diffusion of this receptor[8], and also capture dynamic z-motion on both the cell wall and on the apical membrane. Figure 1 shows one such trajectory of an individual IgE-FcεRI taken on the side of a rat mast cell. A rainbow color scheme has been applied to denote the passage of time. Both corralled diffusion and dynamic, directed motion (green period) are observed in this one 40 second trajectory.

We highlight the fact we record the arrival time of every photon detected during the trajectory with ~100 picosecond timing resolution.[6] This time-resolved photon stream can be used to determine changes in the emission lifetime as a function of position and positively identify single quantum dots via photon-pair correlations (photon anti-bunching)[6]. We further note that recording individual photon arrival times gives our microscope ~ 9 orders of magnitude superior temporal resolution than a conventional CCD-based microscope, bridging the decades of time between fast biomolecular conformational fluctuations[9] and cellular signaling processes[7].

Future Work: While our initial investigations have focused on membrane topology and dynamics, we are working towards following further steps in IgE-FcεRI signaling cascade, including its down-regulation via receptor-mediated endocytosis.

References:

1. Lu, H., L. Xun, and X. Xie, *Single-molecule enzymatic dynamics*. Science, 1998. **282**(5395): p. 1877-1882.
2. Yildiz, A., J.N. Forkey, S.A. Mckinney, T. Ha, Y.E. Goldman, and P.R. Selvin, *Myosin V walks hand-over-hand: Single fluorophore imaging with 1.5-nm localization.* Science, 2003. **27**(300): p. 2061-2065.
3. Fujiwara, T., K. Ritchie, H. Murakoshi, K. Jacobson, and A. Kusumi, *Phospholipids undergo hop diffusion in compartmentalized cell membrane.* J. Cell Biol., 2002. **157**(6): p. 1071-1081.
4. Cang, H., C.S. Xu, and H. Yang, *Progress in single-molecule tracking spectroscopy.* Chem. Phys. Lett., 2008. **457**(4-6): p. 285-291.
5. Lessard, G., P.M. Goodwin, and J.H. Werner, *Three dimensional tracking of individual quantum dots* Appl. Phys. Lett., 2007. **91**(22): p. 2224106.
6. Wells, N.P., G.A. Lessard, and J.H. Werner, *Confocal, 3-dimensional tracking of individual quantum-dots in high background environments.* Anal. Chem., 2008. **80**: p. 9830-9834.
7. Wells, N.P., G.A. Lessard, M.E. Phipps, P.M. Goodwin, D.S. Lidke, B.S. Wilson, and J.H. Werner, *Going beyond 2D: Following membrane diffusion and topography in the IgE–Fc[epsilon]RI system using 3-dimensional tracking microscopy.* Proc. of the SPIE, 2009. **7185**: p. 7185-1 to 7185-13.
8. Andrews, N.L., K.A. Lidke, J.R. Pfeiffer, A.R. Burns, B.S. Wilson, J.M. Oliver, and D.S. Lidke, *Actin restricts Fc epsilon RI diffusion and facilitates antigen-induced receptor immobilization.* Nature Cell Biology, 2008. **10**(8): p. 955-963.
9. Werner, J.H., R. Joggerst, R.B. Dyer, and P.M. Goodwin, *A two dimensional view of the folding energy landscape of cytochrome c.* PNAS, 2006. **103**(30): p. 11130-11135.

Publications:

Wells, N.P., G.A. Lessard, and J.H. Werner, *Confocal, 3-dimensional tracking of individual quantum-dots in high background environments.* Anal. Chem., 2008. **80**: p. 9830-9834.

Wells, N.P., G.A. Lessard, M.E. Phipps, P.M. Goodwin, D.S. Lidke, B.S. Wilson, and J.H. Werner, *Going beyond 2D: Following membrane diffusion and topography in the IgE–Fc[epsilon]RI system using 3-dimensional tracking microscopy.* Proc. of the SPIE, 2009. **7185**: p. 7185-1 to 7185-13 (Co-recipient, Best Paper Award, Single Molecule Session of Photonics West).

Werner, J.H., P.M. Goodwin, and G. Lessard, *Apparatus and method for tracking a molecule or particle in three dimensions*, in *US Patent 7,498,551*. 2009, Los Alamos National Laboratory: USA.

Werner, J.H., G.A. Lessard, N.P. Wells, and P.M. Goodwin, *3D tracking microscope.* R&D 100 Award, 2008.

Combinatorial Discovery of Biomimetic Atomically-Defined Soft Nanomaterials

Ki Tae Nam, Tammy K. Chu, Amanda B. Marciel, Sarah. A. Shelby, Philip H. Choi, Ritchie Chen, Byoung-Chul Lee, Michael D. Connolly, Ryan A. Mesch, and Ronald N. Zuckermann

Biological Nanostructures Facility, The Molecular Foundry, Lawrence Berkeley National Laboratory, 1 Cyclotron Rd., Berkeley, CA 94720
rnzuckermann@lbl.gov

Scientific Thrust Area: Biological Nanostructures

Research Achievement: A defining characteristic of most biomacromolecules is that they have precise 3-dimensional structures and very sophisticated functions, such as molecular recognition and catalysis. And yet the underlying architecture of protein and nucleic acid structure is relatively simple: a linear polymer chain of specific monomer sequence. We aim to apply the rules that govern the folding of these chains toward the construction of a new class of atomically-defined non-natural soft nanomaterials.

Peptoids are a novel class of non-natural biopolymer based on an N-substituted glycine backbone that are ideally suited for nanomaterials research[1] (Figure 1). This bio-inspired material has many unique properties that bridge the gap between proteins and bulk polymers[2]. Like proteins, they are a sequence-specific heteropolymer, capable of folding into specific shapes[3,4] and exhibiting potent biological activities[5]; and like bulk polymers they are chemically and biologically stable and relatively cheap to make. Peptoids are efficiently assembled via automated solid-phase synthesis from hundreds of chemically diverse building blocks[6], allowing the rapid generation of huge combinatorial libraries[7,8]. This provides an ideal platform to discover nanostructured materials capable of protein-like structure and function.

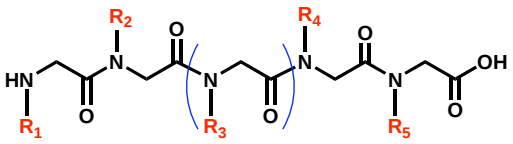

Figure 1. Peptoids are a sequence-specific bio-inspired polymer based on an N-substituted glycine backbone.

We will demonstrate that peptoids can be used to design precisely-structured nanomaterials. Because peptoids lack hydrogen bond donors and chiral centers in their backbone, simple designs emphasizing periodic hydrophobic and electrostatic interactions can be rapidly evaluated. We have designed a combinatorial library of amphiphilic peptoid 36mers of specific sequence, and discovered sequences that self assemble into extremely thin crystalline sheets in aqueous solution with no template. The sheets are only 3 nm thick, and yet extend in two dimensions up to hundreds of microns (Figure 2), creating one of the thinnest two-dimensional organic crystalline materials known. These materials have been characterized by fluorescence microscopy, atomic force microscopy, electron microscopy and x-ray diffraction, as well as their kinetics of formation and thermodynamic stabilities. The ability to spontaneously assemble two-dimensional crystalline materials in solution could have tremendous potential to enable the bottom-up fabrication of optical and electronic devices, template the patterning of inorganic or biological materials, or serve as biological membrane mimetics.

Future Work: In the short term, we plan to investigate the sequence and structural requirements of the peptoid chains to understand exactly what is necessary to form stable sheets. We plan to further engineer the sheet-forming interactions to create even more stable and more highly crystalline sheets. The ultimate goal is to create materials with atomically-precise control over the location of each atom in the material. Because the peptoid chemistry allows precise sequence control over every monomer, we can then begin to create tailored functional sheet structures.

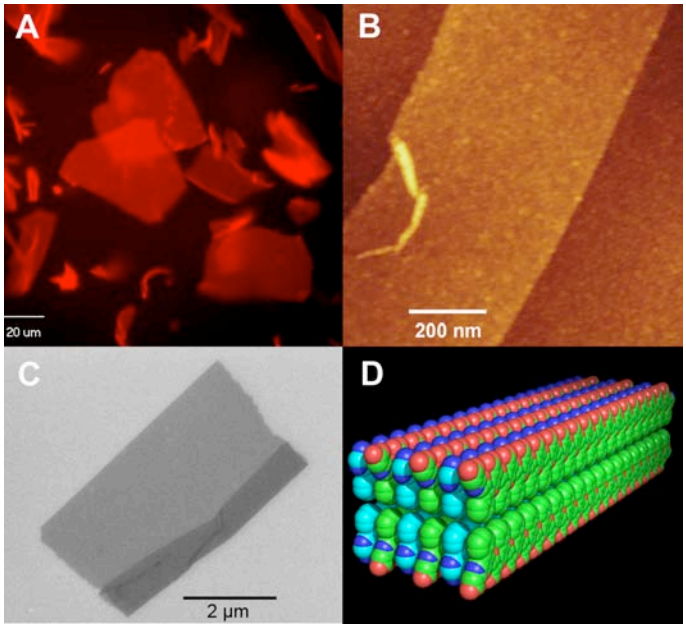

Figure 2. (A) Fluorescence microscopy image of sheets floating in aqueous solution stained with Nile Red, (B) AFM image of a single sheet, (C) SEM image of an isolated sheet, (D) molecular model showing proposed peptoid bilayer structure.

Our longer-term goals are to study the transport of ions and small organic molecules across the sheets, and to display proteins, peptides, small molecules, inorganic nanocrystals, cells and combinatorial libraries of ligands on the surface of the sheets. The freely-soluble 2D sheet motif can serve as a structural platform to segregate compartments or present attached materials in a soluble but highly correlated manner that should find a wide variety of applications.

References:

1. Lee, B.-C.; Zuckermann, R.N., Bio-inspired Polymers for Nanoscience Reseach. *Proc. NSTI Nanotech. Conf.* **2007**, *2*, 28-31.
2. Barron, A.E.; Zuckermann, R.N., Bioinspired Polymeric Materials: In-between Proteins and Plastics. *Curr. Op. Chem. Biol.* **1999**, *3*, 681-687.
3. Lee, B.-C.; Zuckermann, R.N.; Dill, K.A., Folding a Nonbiological Polymer into a Compact Multihelical Structure. *J. Am. Chem. Soc.* **2005**, *127*, 10999-11009.
6. Zuckermann, R.N.; Kerr, J.M.; Kent, S.B.H.; Moos, W.H., Efficient Method for the Preparation of Peptoids [Oligo(N-substituted glycines)] by Submonomer Solid Phase Synthesis. *J. Am. Chem. Soc.* **1992**, *114*, 10646-10647.
7. Figliozzi, G.M.; Goldsmith, R.; Ng, S.; Banville, S.C.; Zuckermann, R.N., Synthesis of N-(substituted)glycine Peptoid Libraries. *Methods Enzymol.* **1996**, *267*, 437-447.

Publications:

4. Lee, B.-C.; Chu, T.K.; Dill, K.A.; Zuckermann, R.N., Biomimetic Nanostructures: Creating a High-Affinity Zinc-Binding Site in a Folded Nonbiological Polymer. *J. Am. Chem. Soc.* **2008**, *130*, 8847-8855.
5. Chongsiriwatana, N.P.; Patch, J.A.; Czyzewski, A.M.; Dohm, M.T.; Ivankin, A.; Gidalevitz, D.; Zuckermann, R.N.; Barron, A.E., Peptoids that mimic the structure, function and mechanism of helical antimicrobial peptides. *Proc. Natl. Acad. Sci. U. S. A.* **2008**, *105*, 2794-2799.
8. Thakkar, A.; Cohen, A.S.; Connolly, M.D.; Zuckermann, R.N.; Pei, D., High-Throughput Sequencing of Peptoids and Peptide−Peptoid Hybrids by Partial Edman Degradation and Mass Spectrometry. *J. Comb. Chem.* **2009**, *11*, 294-302.

Multicomponent Nanoscale Systems Fabricated with a Macromolecular Toolbox

O. Gang, M. M. Maye, D. Nykypanchuk, D. van der Lelie*, W. Sherman, K. Mudalidge

Center for Functional Nanomaterials, *Biology Department
Brookhaven National Laboratory, Upton, NY 11973, USA

Scientific Thrust Area: Soft and Biological Nanomaterials

Research Achievement: Incorporation of biomolecules into nano-object design provides a unique opportunity to establish highly selective interactions between the components of nanosystems. The encoding and structural plasticity, provided by biomolecules, can allow for self-assembly of various nanoscale objects into well defined architectures. We are developing a range of strategies to use biomolecules as site-specific scaffolds, smart assembly guides and selective binding agents. These approaches are appealing as new effective ways for material fabrication and may produce new classes of engineered nanomaterials with potential use in novel optical and electrical devices as well as biomedical applications.

In my talk, I will describe our current progress in the fabrication of well-defined hybrid structures containing biomolecules and inorganic particles. Recently, we demonstrated that certain DNA motifs when attached to nanoparticles provide interaction that favors the formation of ordered superlattices. This opens a route to 3D fabrication of materials from a wide variety of nanoscale components - a task which is difficult to achieve using conventional lithographic techniques. We have also explored applications of DNA-based assembly approaches for fabrication 2D arrays, quasi-0D clusters, and on-demand reconfigurable systems.

Many unique phenomena emerge after arranging a few nanoscale objects into clusters, or so-called artificial molecules. The strategy of using biomolecules as linkers between nanoparticles has proven especially useful for construction of such nano-clusters. However, conventional solution-based reactions typically yield a broad population of multimers and require extensive purification, thus limiting the fabrication yields. We have developed a novel high-throughput method for producing clusters of DNA-encoded nanoparticles using stepwise assembly on a solid support (Fig. 1). This method efficiently bestows particles with anisotropy and generates remarkably high yields of well-defined dimer clusters and Janus (two-faced) nanoparticles. Using this approach we successfully fabricated, with yields exceeding 75%, dimer clusters that have well defined separation between cluster components determined by a designed linker. A similar approach was used for fabrication of anisotropic clusters using Janus particles with different, DNA-controlled binding properties on each Janus face. For example, we formed clusters containing about 5 small particles located on one hemisphere of a larger particle. The developed method was employed for assembly of homogenous (gold-gold) and heterogeneous (gold-silver) nanoparticle dimers. Using light and x-ray scattering methods and electron

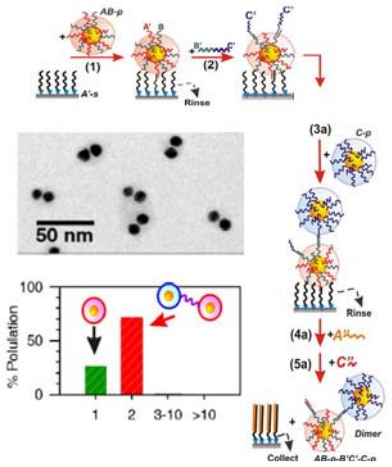

Fig. 1. Schematics of stepwise encoded assembly of dimer nanoclusters. TEM image of assembled structures. Histogram reveals ~75% assembly yield without additional purification.

microscopy, the details of cluster morphology were investigated. Additionally, optical studies showed that wavelength shift due to plasmonic coupling within gold-gold dimers depends exponentially on intra-dimer spacing. Recent work on the use of these clusters for real-time label-free sensing of nucleic acids will be also discussed.

Bio-inspired approaches for self-assembly of nanoscale components into static structures furnish a basis for the emerging paradigm in non-lithographical fabrication of designed nanomaterials. At the same time, the structural plasticity of biomolecules is auspicious for the creation of nanosystems that are dynamic, reconfigurable, and responsive. We have created and studied nanosystems that were assembled incorporating a reconfigurable DNA device into 3D superlattices or into clusters of two particles. The device allows for the post-assembly re-organization of the superlattices and clusters upon addition of molecular stimuli, simple DNA strands, while preserving the structural integrity of the systems. We investigated, using in-situ structural methods, the reconfiguration processes and observed two well defined and on-demand switchable states in the systems of superlattices and cluster assemblies.

Branched DNA nanostructures (scaffolds) offer design flexibility for precise placement of nanoparticles in 2D arrays. However, typically utilized methods rely on a single flexible chain to anchor a particle at a specific site. This results in some uncertainty in a particle position, and minimal control of nano-object orientation. We have designed scaffold motifs (Fig. 2) with spaced clusters of binding sites that allow multiple linkages to nanoparticles without introducing substantial disorder into the assembly. Additionally, we have developed a surface modification for DNA encoded particles that resolves a known problem of particle aggregation in the Mg-rich environment that is required for scaffold stabilization.

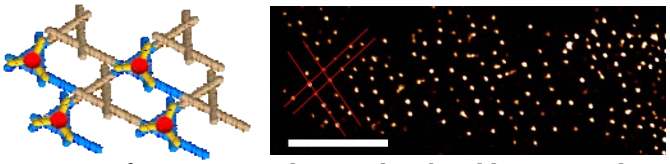

Fig. 2. Left: DNA array decorated with gold nanoparticles (red spheres). Right: A scanning electron micrograph of this system. Red lines mark a unit cell, scale bar is 200nm.

Future Work: We will use self-assembly fabrication methods as described above to create binary systems based on various types of nanoparticles and chromophores, in which DNA motifs and arrays control the inter-component distances and global system structure. Combining group expertise in assembly, structural characterization and single optical methods we will study distance-dependent light-driven interactions between different constituents of the system. In particular, we will construct systems composed of metallic and semiconductor particles to study energy harvesting and transfer, fluorescence quenching and enhancement processes arising from pair-wise and collective interactions in the designed nanosystems.

References: Y. Pinto *et al.*, *Nano Lett.* **5**, 2399 (2005); J. Zhang et al, *Nano Lett.* **6**, 248 (2006); F.A. Aldaye & H. F. Sleiman, *J. Am. Chem. Soc.* **129**, 4130 (2007); D. Nykypanchuk, M. Maye, D. van der Lelie & O. Gang, *Nature* **451**, 549 (2008); Park, S.Y. *et al.*, *Nature* **451**, 553 (2008); S.A. Claridge, H.Liang, S.R. Basu, J.M.J. Frechet & A.P. Alivisatos, *Nano Lett.* **8**, 1202 (2008).

Publication: M. M. Maye, D. Nykypanchuk, M. Cusiner, D. van der Lelie, & O. Gang, "Stepwise surface encoding for high-throughput assembly of nanoclusters", *Nature Materials*, **8**, 388 (2009)

Methods for the Synthesis of Defined Protein Nanotubes

Julie M. Silverman[1], James W. Wollack[2], Edward R. Ballister[3], Angela H. Lai[4], Yifan Cheng[4], Ronald N. Zuckermann[3], Tamir Gonen[5], Mark D. Distefano[2], and Joseph D. Mougous[1]

Departments of [1]Microbiology and [5]Biochemistry, University of Washington, Seattle, WA 98195; [2]Department of Chemistry, University of Minnesota, Minneapolis, MN 55455; [3]Molecular Foundry, Lawrence Berkeley National Laboratory, Berkeley, CA 94720; [4]W. M. Keck Advanced Microscopy Laboratory, Department of Biochemistry and Biophysics, University of California, San Francisco, CA 94158

Proposal Title:

Flexible Protein Building Blocks for Nanotechnology

Research Achievement:

Biological molecules fulfill a unique and important niche in nanoscale materials. Unlike synthetic inorganic and organic materials, biological molecules have evolved over eons to possess properties such as exquisite molecule recognition and highly efficient, selective catalysis. Proteins, arguably the most versatile natural polymers, are a particularly flexible nanoscale material – their templated synthesis makes them easily modified and many possess the ability to self-assemble into high-order arrays. We have developed a novel, flexible *in vitro* self-assembled protein nanotube system using the *Pseudomonas aeruginosa* secreted ring protein Hcp1. Hcp1 nanotubes differ from other protein nanotubes in that they are non-helical and are stabilized by covalent bonds (Figure 1). In addition, the nanotubes have an outer/inner diameter ratio of < 2.0, which is exceedingly small for protein nanotubes. We exploited these properties of the Hcp1 system in order to control nanotube length, specify terminating subunits, and to generate Hcp1 nanocapsules (Ballister 2008). Most recently, we have begun to develop methods that will allow for the synthesis of Hcp1 nanotubes of discrete length and composition. We have generated Hcp1 ring subunits site-specifically modified at their C-termini with assorted DNA oligonucleotides (Wollack 2009). These subunits will be brought together in a specified number and order using an appropriate

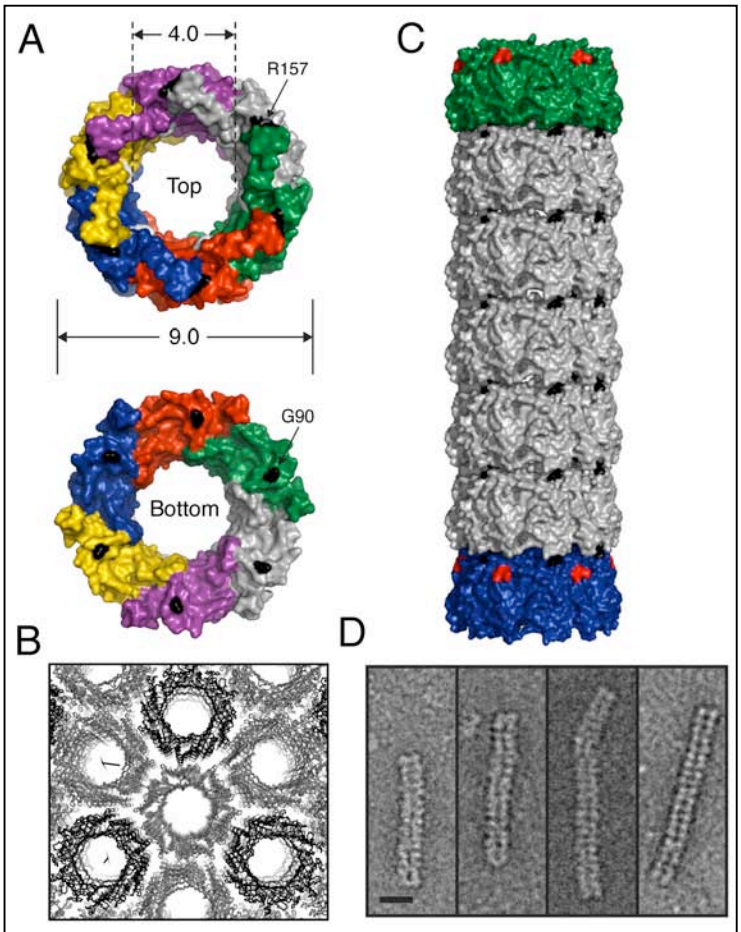

Figure 1. Overview of the Hcp1 nanotube system. (A) Molecular surface representation of the "top" and "bottom" faces of the Hcp1 hexamer. Monomers are colored for clarity. Cysteine mutation sites (black) and key dimensions (in nm) are provided. X-Y crossection of the honeycomb Hcp1 P6 crystal lattice. The two nanotube orientations are indicated with arrows (left) and gray shading. (C) Molecular model of a 7-mer Hcp1 nanotube (side and top view). Top and bottom "capping" subunits are green and blue, respectively. The position of the outer surface-exposed C-terminus of these subunits is colored red. (D) Transmission electron micrograph of Hcp1 nanotubes prepared from Hcp1 subunits containing double cysteine substitutions at R157 and G90. In the absence of these mutations, only Hcp1 rings are observed (Ballister and Mougous *PNAS* 2008).

complementary templating DNA strand (Figure 2). The ability to generate monodisperse populations of tailored Hcp1 nanotubes in high yield will represent an important step forward for realizing the potential of proteins in various nanotechnogical devices.

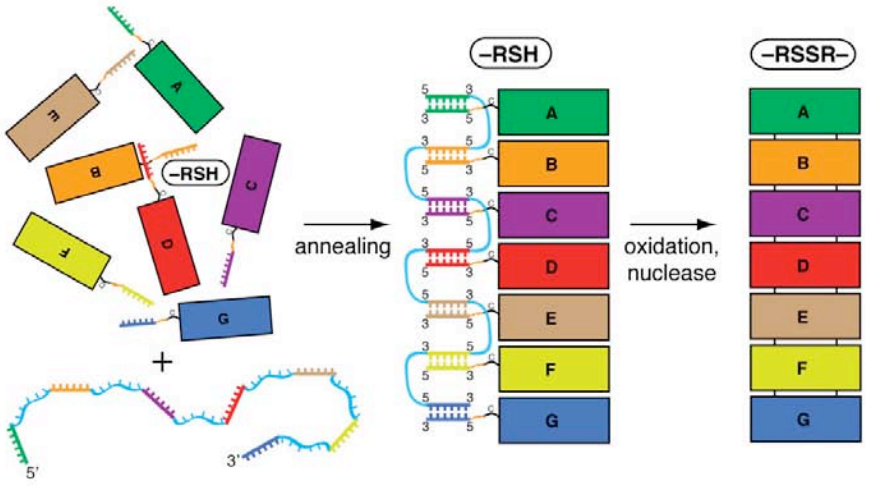

Figure 2. Schematic depiction of method for generating ordered, defined Hcp1 nanotubes by DNA templating. Hcp1 hexameric rings (rectangles) are labled A-G and are colored to indicate the uniqueness of each subunit and conjugated DNA oligo sequence (DNA covalently attached using "Click" chemistry following protein farnesyl transferase treatment). For clarity, we show only one conjugated DNA oligo and templating DNA strand. In actual experiments, each subunit of the hexamer will have the same DNA oligo attached and six templating DNA strands would be present on a single nanotube. This method will be the first to permanently trap the information from DNA-based assembly in a protein structure.

Future Work:

Following successful synthesis of second generation (DNA templated) Hcp1 nanotubes, we will adapt the scaffold for a diverse array of applications including targeted drug and DNA delivery. For cellular delivery applications, the nanotube exterior will be modified with molecules that target it to a specified cell type. For instance, we will use a poly-histidine-binding peptoid conjugated to folate in order to target nanotubes to folate receptor-expressing cancer cells. The interior of Hcp1 nanotubes will also be modified, such that terminal subunits of the nanotubes can be selectively "plugged" and middle subunits are loaded with covalently attached cargo.

Publications:

In vitro self-assembly of tailorable nanotubes from a simple protein building block.
Ballister E.R., Lai A.H., Zuckermann R.N., Cheng Y., and Mougous J.D.
Proc. Natl. Acad. Sci. U.S.A. 2008 Mar 11;105(10):3733-8.

A minimalist substrate for enzymatic peptide and protein conjugation.
Wollack J.W., Silverman J.M., Petzold C.J., Mougous J.D., and Distefano M.D.
ChemBioChem 2009 *in press*

Bioinspired Templates for the Growth of Semiconductor Nanowires

Yajaira Sierra[1], Leonardo Maestri[1], Aaron Strickland[1], Sukgeun G. Choi[2], S. Tom Picraux[2], and Carl A. Batt[1]

[1]*Cornell University, Ithaca NY*

[2]*Center for Integrated Nanotechnologies, Los Alamos National Laboratory, Los Alamos, NM*

Proposal Title: Bionanofabrication of Si Nanowire Array Using Bacterial Surface Layer Protein/Nanoparticle Templates

Research Achievement:

Biologically derived materials hold great promise as templates for a number of nanotechnological applications. They can self-assemble and have a long range order due to the complex inter and intramolecular interactions. In the case of proteins additional advantages lie in the ability to manipulate the amino acid sequence to introduce greater functionality. The use of biologically derived materials is becoming increasing in vogue as the search continues for novel material with enhanced functionality and the potential to make processes more environmentally friendly (*1*). Our group has been looking at different materials derived from biological sources (*2*).

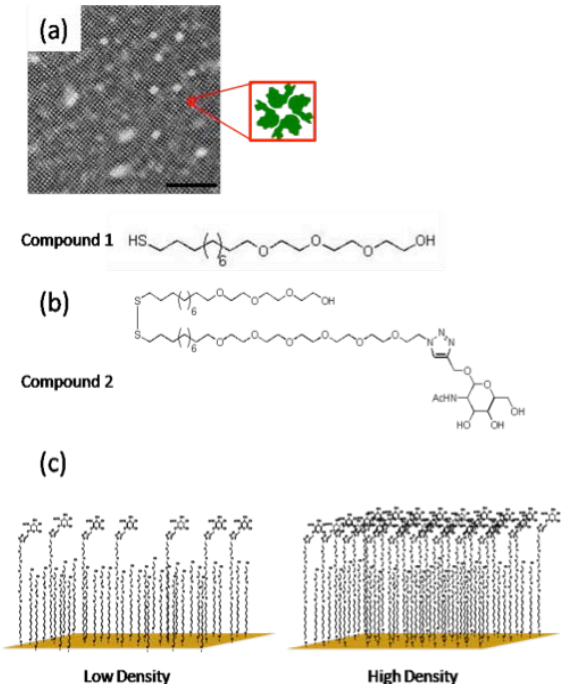

Figure 1. (a). Noise-filtered inverse FFT Brightfield TEM (negative-stain) images of native self-assembled SbpA, with a diagram illustrating the interaction of the protein monomers. (b). Compounds used for the formation of the mixed self-assembled monolayers (SAMs) (c). Diagrams illustrating SAMs with a low density, and a high density of compound 2.

The long range order that can be achieved with biologically derived materials is well known. As a result of this long range order, periodic arrays with nanometer precision over many microns can be achieved with biologically derived materials. One such material is S-layers, a two-dimensional protein crystal that is found as the 'surface layer' of many bacteria. It can be isolated and in many cases reassembled on planar surfaces. Our work on S-layers has focused on its application as a scaffold for the fabrication of nanometer-scale devices. Efforts have included the synthesis of a sugar-based foundation for crystallization of S-layer proteins and also the genetic engineering of mutations to these proteins to introduce site-specific functionality. S-layer from *Lysinibacillus sphaericus* (SbpA) forms an array with square symmetry (p4) (Fig. 1a), with a center-to-center spacing of the morphological units of 13.1 nm. It has been demonstrated that SbpA recognizes the Secondary Cell Wall Polymer (SCWP) of *L. sphaericus*, and can self-assembly *in vitro.*

We have synthesized mixed SAMs of carbohydrate-terminates disulfides (compound 2) and hydroxyl-terminated thiols (compound 1) (Figure 1b), and found that when lower densities of compound 2 are present in the Mixed SAMs (Figure 1c), SbpA had a stronger binding affinity to the SAM (Figure 2). By mimicking the SCWP on a gold surface with mixed SAMs, we anticipate the formation of larger monocrystal, which are essential for its use as scaffold for nanofabrication.

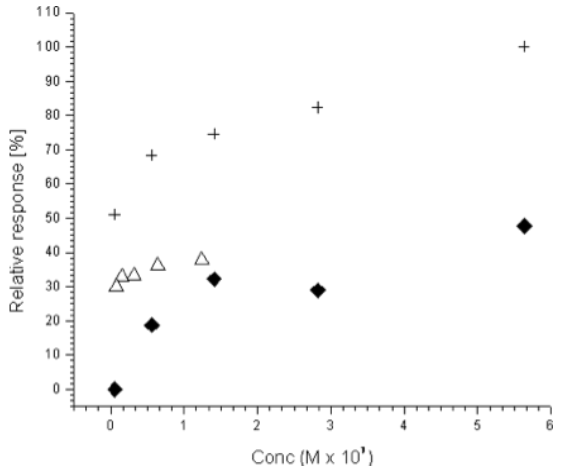

Figure.2. Dependence of the density of GlcNAc on the binding of SbpA to the SAMs formed on the sensor surface. Response levels reached after 240 s of protein injection. (+) 1% of GlcNAc, (Δ) 2.5% GlcNAc, (◆) 10% of GlcNAc.

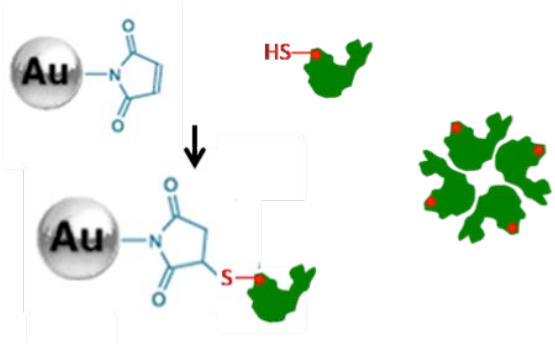

Figure.3. Diagram illustrating how a gold nanoparticle functionalized with maleimide can be covalently linked to the rSbpA-A1065C, and an illustration of how the single cysteine groups would be present in each monomer of the array.

In addition, we have engineered a recombinant SbpA, rSbpA-A1065C, in which 200 amino acids were truncated from the C-terminus of the protein to improve its surface accessibility, and a single cysteine residue incorporated. This recombinant SbpA allows for the potential covalent binding of inorganic materials to the protein array in a 1:1 ratio, as no other cysteine is found in each protein monomer (Figure 3).

Of note is the use of S-layers as scaffolds for patterning catalyst particles to grow semiconductor nanowires and other nanometer structures (*3*, *4*). Specifically very uniform vertical germanium nanowires have been grown from gold nanoparticle catalysts patterned using the S-layer proteins isolated from *Deinococcus radiodurans* (Figure 4a). Using this system Ge nanowires which are highly dense and nontapered with a strong preference for vertical growth were obtained on <111> germanium (Figure 4b-c). Recent work suggests that the substrate crystal along with the biotemplated catalyst can influence the orientation of the Ge nanowires. This observation can lead to a new processing scheme where not only the size and length but also the orientation of the nanowire relative to the substrate can be controlled. What functional properties these nanowires have yet to be fully explored.

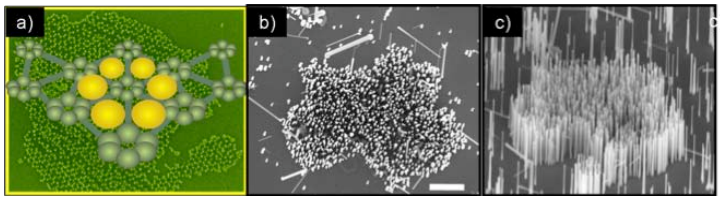

Figure 4. a) SEM image (background) of a honeycomb-like pattern of Au nanoparticles adsorbed on the hexagonal-closed packed intermediate (HPI) S-layer upon addition of 25 mM NaCl. The cartoon representation shows the hexagonal symmetry of HPI. b) top-view and c) 30º tilt view SEM images of vertical oriented Ge nanowires grown from

Acknowledgement: This work was supported in part by the National Science Foundation under a Nanoscale Interdisciplinary Research Team (NIRT) Grant (NSF-0403990). Y.S.S. would like to acknowledge additional funding support from Los Alamos National Laboratory.

References:

1. M. Bergkvist, S. S. Mark, X. Yang, E. R. Angert, C. A. Batt, *J. Phys. Chem B* **108**, 8241 (2004).
2. S. Sotiropoulou, Y. Sierra-Sastre, S. S. Mark, C. Batt, *Chem. Mater.* **20**, 821 (2008).
3. S. S. Mark *et al.*, *Colloids Surf B Biointerfaces* **57**, 161 (2007).
4. Y. Sierra-Sastre, S. Choi, S. T. Picraux, C. A. Batt, *J Am Chem Soc*, (2008).

Nanostructure characterization of resistive oxides

O. Heinonen[1], M. Siegert[1], A. Roelofs[1], A.K. Petford-Long[2], and M. Holt[3]

[1]Memory Products Group, Seagate Technology, Bloomington, MN 55435
[2]Materials Science Division, Argonne National Laboratory, 9700 S. Cass Ave, Argonne, IL 60439
[3]Center for Nanoscale Materials, Argonne National Laboratory, 9700 S. Cass Avenue, Argonne, IL 60439

Research Achievement

Ti-doped nickel oxide (Ti:NiO) is one material being considered for resistive random access memory applications. It has previously been demonstrated [1,2] that RRAM structures consisting of Pt/Ti:NiO/Pt can be switched between a high-resistance non-metallic state and a low-resistance metallic state with Ohmic conductance by applying unipolar voltage pulses in the range of a few volts. As deposited, a device is usually in a high-resistance state and has to be set into an initial low-resistance state by applying a moderately high voltage pulse of about 5 V (depending on the oxide layer thickness), a process call electroforming. A central question pertaining to this electroforming and switching mechanisms is whether or not ionic species (e.g. Ni vacancies or oxygen ions) or defects are actively migrating during electroforming and switching[3-6]. Such migration is certainly consistent with several of the proposed mechanisms, such as the formation of metallic filaments via oxidation and reduction of Ni.

There are a few possible mechanisms that relate the observed electronic response of these structures to microstructural changes of the constituent lattice. We have investigated changes in the NiO (111) diffraction intensity over a 10 μm × 10 μm Pt/Ti:NiO/Pt patterned structure, between the as-deposited and electroformed states using the Hard X-ray Nanoprobe beamline (HXN) facility and ~50nm spatial resolution. The HXN is part of the Center for Nanoscale Materials at the Advanced Photon Source at Argonne National Laboratory. We have correlated the change in resistance with structural changes.

The central result of our work is shown in the figure below, which displays the two-dimensional plots of the diffracted intensity (normalized to beam current) at the NiO(111) peak across the same Pt/Ti:NiO/Pt structure in the as-deposited state (left panel) and in the electroformed state (right panel). The solid-line (changed) regions are larger than the step size or the projected spot size, indicating that the regions in which structural changes have occurred are at least 400 nm in size, with several regions being considerably larger. This is also much larger than the grains size, which is about 15 nm as determined from TEM images. These changes in diffraction intensity are consistent with migration of ionic species or defects during electroforming. The structural changes that follow electroforming are rather subtle in that we observed changes in the NiO (111) diffraction amplitude, but we did not observe any loss complete loss of diffraction amplitude. Therefore, if metallic filaments are formed during electroforming, they are either much smaller than the resolution in the HXN, or consist of subtle structural changes over a larger region with a concomitant change in electronic structure. The former seems unlikely, since the observation of contiguous regions of the order of one micron implies that there would have to be many such filaments in one such contiguous region.

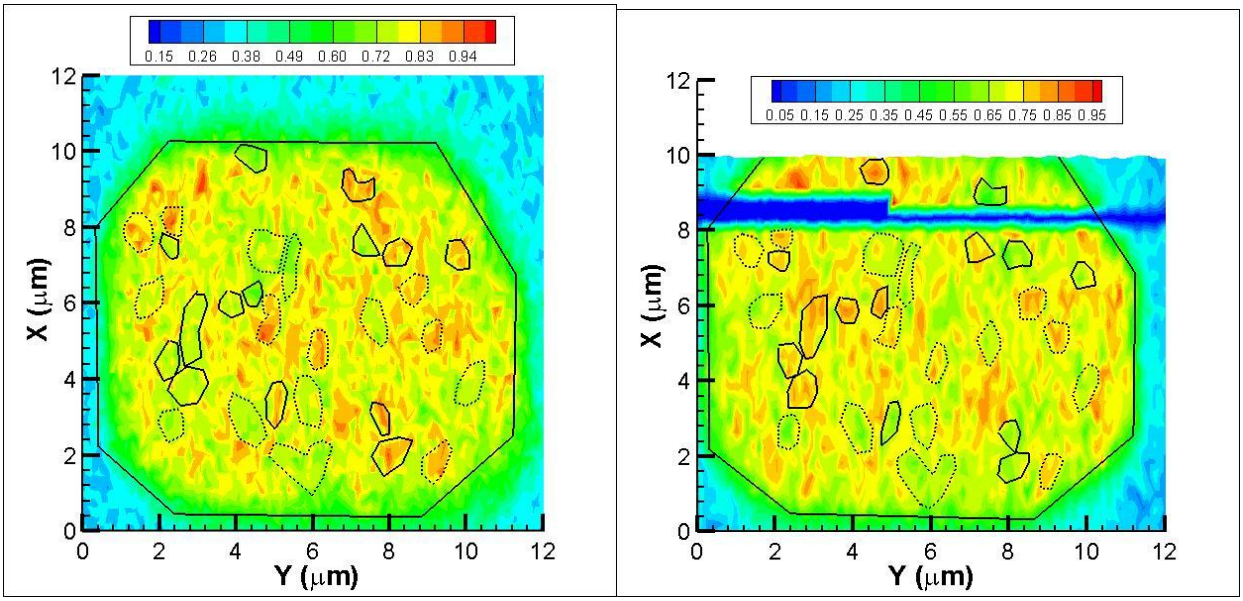

Normalized diffraction intensity in the as-deposited state (left panel) and electroformed state (right panel). In the figures are demarcated some of the regions that in which the diffraction intensity remained high or low after electroforming (dashed lines), as well as some of the regions in which the diffraction intensity changed from low to high, or from high to low upon electroforming. The color scales are indicated by the scale bars in the panels. The blue streak in the right panel is due to the beam current outage during the scan.

Future work

We plan to refine and expand the X-ray microscopy to include both as-deposited, electroformed, set and re-set devices. In addition, we plan to include rocking curves at selected locations of some devices to better quantify local stresses and lattice expansion/contractions. Finally, we intend to perform conducting AFM measurements to correlate local conductivity changes with local structural changes.

References

1. M.J. Lee, M.J. Lee, S.E. Ahn, B.S. Kang, C.B. Lee, K.H. Kim, W.X. Xianyu, I.K. Yoo, J.H. Lee, S.J. Chung, Y.H. Kim, C.S. Lee, K.N. Choi, and K.S. Chung, *J. Appl. Phys.* **103**, 013706 (2008).
2. S.E. Ahn, M.J. Lee, Y. Park, B.S. Kang, C.B. Lee, K.H. Kim, S. Seo, D. S. Suh, D.C. Kim, J. Hur, W.Xianyu, G. Stefanovich, H. Yin, I.K. Yoo, J.H. Lee, J.B. Park, I.G. Baek, and B.H. Park, *Adv. Mater.* **20**, 924 (2008).
3. K. Kinoshita, T. Tamura, M. Aoki, Y. Sugiyama, and H. Tanaka, *Appl. Phys. Lett.* **89**, 103509 (2006).
4. K. Jung, H. Seo, Y. Kim, H. Im, J.P. Hong, J.-W. Park, and J.-K. Lee, *Appl. Phys. Lett.* **90**, 052104 (2007).
5. C. Yoshida, K. Kinoshita, T. Yamasaki, and Y. Sugiyama, *Appl. Phys. Lett.* **93**, 042106 (2008).
6. J.W. Park, J.W. Park, K. Jung, M.K. Yang, and J.K. Lee, *J. Vac. Sci. Technol.* B **24**, 2205 (2006).

Publications

"Correlating structural and resisistive changes in Ti:NiO resistive memory elements", O. Heinonen, M. Siegert, A. Roelofs, A.K. Petford-Long, and M. Holt (to be submitted, Applied Physics Letters).

Linear and Nonlinear Properties of Large-Area Metamaterials

Zahyun Ku[1], Svyatoslav Smolev[1], Zingyu Zhang[1], S. R. J. Brueck[1], K. M. Dani[2], Prashanth C. Upadhya[2], Rohit P. Prasankumar[2], Antoinette J. Taylor[2], I. Brener[3], and M. Sinclair[3]

[1]*Center for High Technology Materials and Electrical and Computer Engineering Dept., Univ. of New Mexico*
[2]*Center for Integrated Nanotechnologies, Los Alamos National Laboratory,*
[3]*Center for Integrated Nanotechnologies , Sandia National Laboratories*

Scientific Thrust Area: Nanophotonics and Optical Nanomaterials

Research Achievement:

Optical lithography has long been the mainstay of the integrated circuit industry, and, despite many and frequent predictions to the contrary, is now widely accepted as the dominant volume manufacturing technology for the next several generations, accessing scales to less than 20 nm (with a 193-nm wavelength!). A major reason for the continued ascendency of optical lithography in manufacturing is its parallel writing capability that scales to large volumes at low cost. The issue with optical lithography for research applications is the extreme cost of modern lithography tools (approaching $40M) and masks which limits research accessibility. In contrast, much of the work in nanophotonics has been carried out with e-beam and related serial lithography techniques that inherently are not scalable. Interferometric lithography (IL) provides the bridge between these two trends [1]. IL uses the interference between a small number (usually two) of coherent beams to produce a maskless periodic pattern. Scales as small as 22-nm half-pitch have been demonstrated [2]. The restriction to periodic pattern arrays is not of major concern for many nanophotonic applications, mix-and-match with conventional, lower resolution, optical lithography techniques provides the additional customization needed for many device applications. Processing can provide more complex structures such as split ring resonators as shown in Fig. 1(a). At the University of New Mexico, we have used IL for a wide variety of nanophotonic structures including: 2D and 3D photonic crystals, metamaterials (Fig. 1(a) shows negative permeability split-rings with ~ 5 μm resonance wavelength) [3], negative index materials (Fig. 1(b)) [4], and plasmonic structures (Fig. 1(c)) [5]. Current efforts focus on inhomogeneous negative-index materials for lensing, active metamaterials for high speed modulators, higher-order nonlinearities in second harmonic generation in plasmonic structures and various approaches to 3D photonic crystals. Progress in these areas will be reviewed.

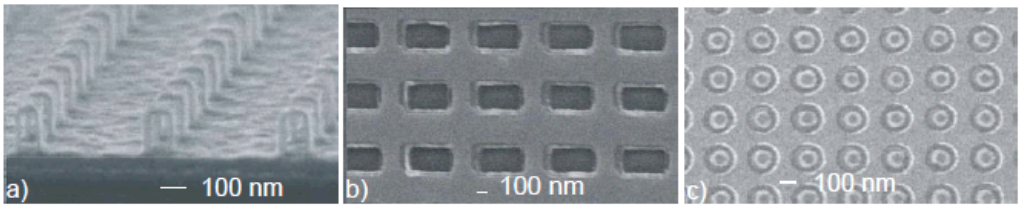

Fig. 1: Large area (> several cm2) nanophotonic arrays fabricated with interferometric lithography. A) Vertical split ring resonators (Au:MgO:Au) providing a negative permeability at ~ 5μm; b) Au:Al_2O_3:Au negative index metamaterial at ~ 2 μm; and c) GaAs-filled Au plasmonic structure for second harmonic generation. Note that all three structures exhibit complexity at the individual nanostructure level as a result of the integration of lithography and processing.

One example of these developments that has strongly benefited from a collaboration with CINT is the demonstration of ultrafast switching in metamaterial structures. Development of all-optical signal processing, eliminating the performance and cost penalties of optical-electrical-optical conversion, is important for continuing advances in Terabits/sec (Tb/s) communications [6]. Optical nonlinearities are generally weak, traditionally requiring long-path, large-area devices [7] or very high-Q, narrow-band resonator structures [8]. Optical metamaterials offer unique capabilities for optical-optical interactions. We have demonstrated 600-fs all-optical modulation at a broadband, negative-index resonance in a fishnet (2D-perforated metal/α-Si/metal film stack) metamaterial. We achieve this ultrafast response – two orders of magnitude faster than previously reported[9] – by accessing a previously unused regime of high-injection level, sub-ps carrier dynamics in α-Si [10-12]. A new, higher-order, shorter-wavelength resonance than previously reported in the fishnet structure is used [3,4], thereby extending device functionality (via structural tuning of device dimensions) over 1.0 – 2.0 μm. Over 20% modulation (experimentally limited) is achieved in a path length of only 116 nm. This device has the potential for Tb/s all-optical communication and will lead to other novel, compact, tunable, sub-picosecond (ps) photonic devices.

References

[1] S. R. J. Brueck, "Optical and Interferometric Lithography – Nanotechnology Enablers," Proc. IEEE **93**, 1704-1721 (2005).

[2]A. Raub, D. Li, A. Frauenglass and S. R. J. Brueck, "Fabrication of 22-nm Half-Pitch Silicon Lines by Single-Exposure Self-Aligned Spatial- Frequency Doubling," JVST. **B25**, 2224-2227 (2007)

[3] S. Zhang, W. Fan, A. Frauenglass, B. Minhas, K. J. Malloy and S. R. J. Brueck, "Mid-Infrared Resonant Magnetic Nanostructures Exhibiting a Negative Permeability," Phys. Rev. Lett. **94**, 037402 (2005)

[4] Z. Ku and S. R. J. Brueck, "Comparison of negative refractive index materials with circular, elliptical and rectangular holes," Opt. Exp. **15**, 4515-4522 (2007).

[5] W. Fan, S. Zhang, N.-C. Panoiu, A. Abdenour, S. Krisna, R. M. Osgood, Jr., K. J. Malloy and S. R. J. Brueck, "Second Harmonic Generation from a Nano-Patterned Isotropic Nonlinear Material," Nano Letters **6**, 1027-1030 (2006).

[6] Saruwatari, M. All-optical signal processing for terabit/second optical transmission. *IEEE Jour. Sel. Top. In Quant. Elec.* **6**, 1363-1374 (2000).

[7] Hochberg, M., et al. Terahertz all-optical modulation in a silicon-polymer hybrid system. *Nature Materials* **5**, 703-709 (2006).

[8] Manolatou, C. & Lipson, M. All-optical silicon modulators based on carrier injection by two-photon absorption. *Jour. Lightwave Tech.* **24**, 1433-1439 (2006).

[9] Kim, E. et al. Modulation of negative index metamaterials in the near-IR range. *Appl. Phys. Lett.* **91,** 17305 (2007)

[10] Fauchet, P. M., Hulin, D., Vanderhaghen, R., Mourchid, A. & Nighan, W. L. Jr. The properties of free carriers in amorphous silicon. *J. of Non-Cryst. Solids* **141,** 76-87 (1992)

[11] Mourchid, A., Vanderhaghen, R., Hulin, D., Tanguy, C. & Fauchet, P. M. Femtosecond optical spectroscopy in a-Si:H and its alloys. *J. of Non-Cryst. Solids* **114,** 582-584 (1989)

[12] Esser, A., et al. Ultrafast recombination and trapping in amorphous silicon. *Phys. Rev. B* **41,** 2879-2884 (1990)

Hybrid Plasmonics: New Routes to Imaging, Spectroscopy, and Efficient Energy Flow at the Nanoscale

G. P. Wiederrecht, S. K. Gray, Y. G. Sun, M. Pelton, D. J. Gosztola, J. Hranisavljevic,
Center for Nanoscale Materials, Argonne National Laboratory, Argonne, Illinois

R. Bachelot, J. Plain, M. Juan, P. Royer
Laboratory for Nanoscale Optical Instrumentation,
University of Technology at Troyes, Troyes, France

G. Wurtz
Nano Photonics and Surface Spectroscopies Laboratory
University of North Florida, Jacksonville, Florida

W. Dickson, D. O'Connor, P. Evans, W. Hendren, R. Atkinson, R. Pollard, and A. Zayats
Center for Nanostructured Media
The Queen's University of Belfast, United Kingdom

Scientific Thrust Area

Experimental nanophotonics.

Research Achievement

This work focuses on creating novel electronic and optical states in hybrid nanomaterials in order to provide new routes for the imaging and manipulation of optical energy at the nanoscale. The motivation for this work is that basic studies in nanophotonics can reveal optical phenomena that are useful for a range of critical technologies including energy collection and conversion, next generation optics, and ultrasensitive spectroscopies.

Plasmonic metal nanostructures are excellent systems in which to study nanophotonics processes, because they support evanescent optical fields with spatial features well below the diffraction limit of dielectric materials. The strong field confinement and field enhancement at the metal-dielectric interface, combined with strong tunability of the plasmonic properties with shape, size, composition, and environment, have produced a wealth of advances, particularly in enhanced spectroscopies (e.g. surface enhanced Raman scattering and fluorescence) and nanoscale optical circuitry. Plasmonic materials therefore serve as the "core" of our hybrid nanostructures.

The strongly localized fields that serve as the foundation of plasmonics research can be used to couple to, and modify, plasmonic, excitonic, and molecular excitations in hybrid materials. Due to the short-range nature of evanescent interactions in nanostructures, these coupling interactions can be strong and do not necessarily have analogs in bulk materials. In the research described here, we have utilized plasmonic coupling to both isolated molecular excitations and excitonic organic structures to realize (a) new routes to sub-wavelength imaging and (b) altered energy flow in nanostructures. One example for each is given here.

For the imaging example, plasmonic nanoparticles are covered with an azo-dye polymer film. The azo-dye is chosen to undergo a light-induced cis-trans isomerization when excited at the plasmon resonance energy. Repetitive isomerizations produce mass transport of the polymer out of the evanescent near-field zone, thereby producing holes in the polymer film that reflect the spatial features of the evanescent field. These can be

detected through atomic force microscopy with a resolution of approximately 20 nm. We have used this mass transport phenomenon to image optical near-fields of plasmonic bowtie antennae and nanorods. Theoretical work clarifies the light-molecule interactions that produce this effect.

For the second example, ultrafast relaxational processes in assemblies of strongly interacting nanorods are studied (Figure 1). Here, we characterize the modification of plasmon-mode relaxation processes when coupled to molecular excitonic materials placed within the interstices of the rods. We find that a mixed plasmon-exciton state is produced, and that variability in the plasmon-exciton coupling produces strong changes in the relaxation dynamics.

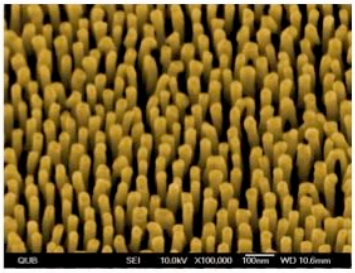

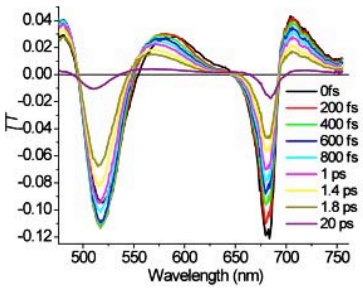

Figure 1. The plasmonic Au nanorod array and ultrafast transient absorption spectra are shown. Hybridizing with molecular excitonic materials strongly modifies the plasmonic modes.

Future Work

Future work will be to realize new hybrid materials and nanostructures with novel optical properties and altered energy flow phenomena, which also enable external control over that energy flow. Specific targets at this time are electronically responsive metal nanoparticle/liquid crystalline materials. Future work will be performed in continued collaboration with the theory and modeling group and will also use the advanced lithography capabilities at the CNM.

Publications

Plasmonic electromagnetic hot spots temporally addressed by photoinduced molecular displacement. M. L. Juan, J. Plain, R. Bachelot, A. Vial, P. Royer, S. K. Gray, G. P. Wiederrecht, *J. Phys. Chem. A* **113**, 4647 (2009).

Fabrication of metallic nano-slit waveguides with sharp bends. M. Lu, L. E. Ocola, S. K. Gray, G. P. Wiederrecht, *J. Vac. Sci. & Tech. B* **26**, 2151 (2008).

Stochastic model for photoinduced surface relief grating formation through molecular transport in polymer films. M. L. Juan, J. Plain, R. Bachelot, P. Royer, S. K. Gray, G. P. Wiederrecht, *Appl. Phys. Lett.* **93**, 153304 (2008).

Ultrafast hybrid plasmonics. G. P. Wiederrecht, G. A. Wurtz, A. Bouhelier, *Chem. Phys. Lett.* **461**, 171 (2008).

Comparative study on the growth of silver nanoplates on GaAs substrates by electron microscopy, synchrotron X-ray diffraction, and optical microscopy. Y. G. Sun, H. F. Yan, and G. P. Wiederrecht, *J. Phys. Chem. C* **112**, 8928 (2008).

Near-field polarization effects in molecular-motion-induced photochemical imaging. C. Hubert, R. Bachelot, J. Plain, S. Kostcheev, G. Lerondel, M. Juan, P. Royer, S. Zou, G. C. Schatz, G. P. Wiederrecht, and S. K. Gray. *J. Phys. Chem. C* **112**, 4111 (2008).

Surfactantless synthesis of silver nanoplates with rough surfaces and their application in SERS. Y. G. Sun and G. P. Wiederrecht, *Small* **3**, 1964 (2007). (cover article)

Surface plasmon interference excited by tightly focused laser beams. A. Bouhelier, F. Ignatovich, A. Bruyant, C. Huang, G.C. Francs, J. Weeber, A. Dereux, G.P. Wiederrecht, and L.Novotny, *Opt. Lett.* **32**, *2535* (2007).

Control of molecular energy redistribution pathways via surface plasmon gating. G. P. Wiederrecht, J.E. Hall, and A. Bouhelier, *Phys. Rev. Lett.* **98**, 083001 (2007).

Heterodyne method of apertureless near-field scanning optical microscopy on periodic gold nanowells. J. E. Hall, G.P. Wiederrecht, S.K. Gray, S. Chang, S. Jeon, J.A. Rogers, R. Bachelot, P. Royer, *Opt. Express* **15**, 4098 (2007).

Transition Metal Catalyzed Graphene

Peter Sutter, Eli Sutter, Mark Hybertsen, Jerzy Sadowski
Center for Functional Nanomaterials, Brookhaven National Laboratory, Upton NY 11973

Scientific Thrust Area

This research program is based in the CFN's scientific thrust on *Interface Science and Catalysis* (P.S., J.S.), and involves collaborators in *Electron Microscopy* (E.S.) and *Theory* (M.H.).

Research Achievement

Graphene, a two-dimensional honeycomb lattice of sp^2 bonded carbon, shows great promise for applications ranging from post-Moore's law electronics to transparent solar cell contacts. Assuming a continuation of "top-down" processing similar to today's microelectronics, the bottleneck to realizing this potential clearly lies in synthesizing the required starting material: structurally perfect, macroscopically large graphene sheets with uniform thickness, into which active device structures can be carved. Graphene growth on transition metals may provide a viable route toward large-scale graphene synthesis.

We have used *in-situ* experiments by low-energy electron microscopy (LEEM), synchrotron photoelectron microscopy, and scanning tunneling microscopy (STM), complemented by *ex-situ* measurements and density functional theory to study the growth and electronic structure of epitaxial graphene on Ru(0001). *In-situ* growth studies by LEEM have shown that epitaxy on Ru produces macroscopic single-crystalline graphene domains (fig. 1 A) with very low defect density in a controlled layer-by-layer mode.[1]

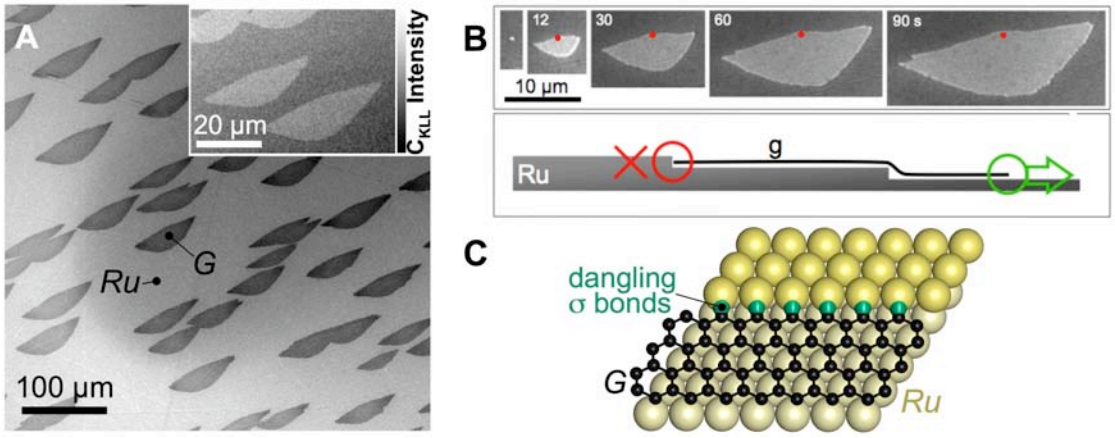

FIGURE 1: Macroscopic graphene growth on Ru(0001). A – Ultrahigh-vacuum scanning electron micrograph of ML graphene domains (G) on Ru. Inset: C_{KLL} scanning Auger map. **B –** Time-lapse LEEM sequence showing the nucleation and growth of a ML graphene domain on Ru at 850°C. Numbers indicate elapsed time in seconds following nucleation. Substrate steps, visible as faint dark lines, are aligned from lower left to upper right. Red dots mark the position of the nucleation site. **C –** Schematic sketch of the interaction of a zigzag graphene edge with an "uphill" Ru step.

The interaction with Ru substrate steps is key to the growth of monolayer (ML) graphene domains with size much larger than the step spacing. At high temperatures epitaxial graphene domains on Ru(0001) nucleate very sparsely and rapidly expand by carbon incorporation into graphene edge sites. *In-situ* microscopy during growth (fig. 1 B) shows a fast expansion of growing graphene domains parallel to substrate steps and across steps in the "downhill" direction, but an almost complete suppression of the crossing of "uphill" steps. Given that a graphene sheet projects a zigzag

edge with dangling σ bonds onto Ru steps (fig. 1 C), a boundary encountering an "uphill" step maximizes the orbital overlap and becomes immobilized at the step edge. Conversely, a graphene sheet growing in the "downhill" direction shows minimal overlap and can flow uninhibited in a carpet-like fashion across substrate steps.

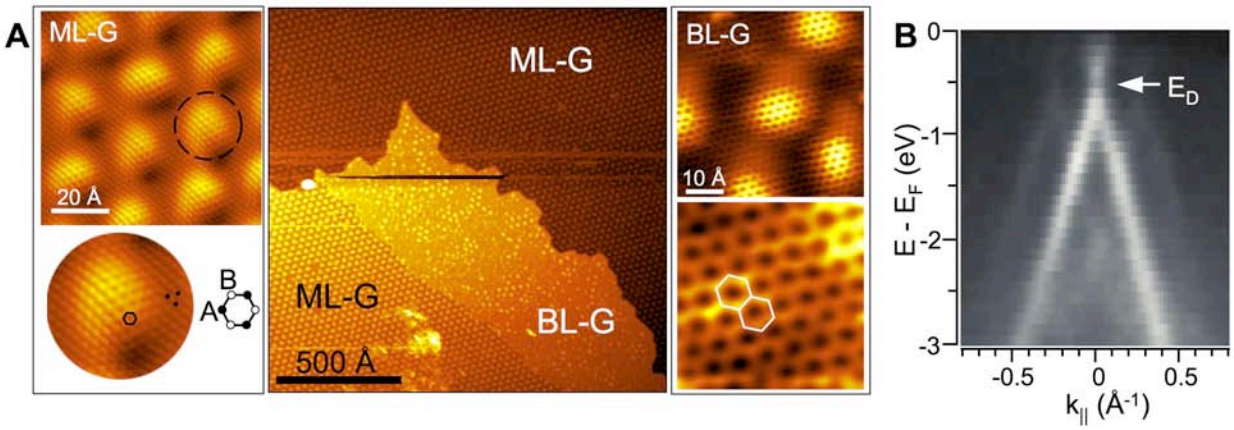

FIGURE 2: Structure and electronic properties of ML and BL graphene on Ru(0001). A – Scanning tunneling microscopy of epitaxial ML and BL graphene on Ru. Moiré structure of ML graphene; honeycomb structure with equivalent carbon sublattices on BL graphene. **B –** Micro-ARPES intensity map for BL graphene on Ru near the K-point of the two-dimensional Brillouin zone.

If sufficient carbon is supplied, ML graphene domains grow and ultimately coalesce to a complete layer. Additional growth can be used to produce bilayer (BL) or thicker few-layer graphene in a controlled layer-by-layer fashion. Measurements by Raman spectroscopy,[1] and more recently by STM and selected-area angle-resolved photoemission (micro-ARPES) in LEEM[2] have been used to determine how the proximity of the metal substrate affects the electronic structure of epitaxial graphene. For ML graphene, the coupling to Ru d-states strongly affects the graphene π-states near the Fermi energy. This strong coupling persists over almost the entire moiré unit cell of the ML graphene (fig. 2 A). The situation changes dramatically with the addition of one more layer. The top sheet of BL graphene is largely unperturbed by residual substrate interactions. Screened from the metal substrate by the interfacial graphene sheet, it shows the hallmarks of free-standing ML graphene: a honeycomb structure with equivalent carbon sublattices imaged in STM (fig. 2 A), and a linear dispersion of π-bands near the Dirac point (fig 2 B). These findings are relevant to graphene growth, and apply more generally to interfaces between graphene and transition metals, e.g., in device contacts.

Future Work

- Exploration of the chemical reactivity of epitaxial graphene on transition metals. Epitaxial graphene as a template for size-selected metal nanocluster catalysts.
- Isolation of epitaxial graphene from a transition metal substrate.

Publications

1. P. Sutter, J.I. Flege, and E. Sutter, "Epitaxial graphene on ruthenium", Nature Materials **7**, 406 (2008).
2. E. Sutter, D.P. Acharya, J.T. Sadowski, and P. Sutter, "Scanning tunneling microscopy on epitaxial bilayer graphene on ruthenium (0001)", Applied Physics Letters **94**, 133101 (2009).
3. P. Sutter "Epitaxial graphene: How silicon leaves the scene", Nature Materials **8**, 171 (2009).
4. BSA 08-37, "Monolayer or/and few-layer graphene on metals or metal-decorated semiconductors", patent pending.

Single Molecules Junctions: Conductance, Formation and Evolution Statistics

L. Venkataraman

Department of Applied Physics and Applied Mathematics, Columbia University, New York, NY

Proposal Title:

Physical Properties of Metal-Molecule Link Motifs in Single Molecule Electronic Circuits

Research Achievement:

Background: The size of electronic devices in commercially integrated circuits has been dropping exponentially over the past few decades, following a trend originally identified by Gordon Moore. This miniaturization of the building blocks of traditional Silicon devices, and the idea that single molecules could function as active electronic components have motivated the field of molecular electronics. The primary challenge in molecular electronics has been the ability to fabricate single molecule devices, a molecule attached to two metal electrodes to form a circuit reliably.

Prior Accomplishments: Over the past two years, we have very successfully implemented a point-contact technique to study electron transport through single molecule junctions in a modified scanning tunneling microscope (STM), a method which overcomes the major difficulties in single molecule transport measurements as it allows the measurements of molecules as small as 5 Å, and can be used to study thousands of junctions easily. We have implemented this method using amine chemical link groups rather than thiols to attach the molecules to gold metal electrodes [1,2]. The discovery of amine-gold link chemistry is a major breakthrough in the study of conductance through single molecule junctions, allowing reliable and reproducible measurements. This innovation has enabled the conductance measurements of over 50 different molecules in a short period of time, allowing the systematic studies of the impact of molecular structure on conductance [4]. We have shown, for example, that the conductance for alkanes and polyphenyls decreases exponentially with increasing length, decaying faster for the saturated molecules when compared to the conjugated molecules [1,2]. This has provided direct evidence that the transport mechanism through these junctions is through non-resonant tunneling. We have also shown, by measuring transport through a series of biphenyl derivatives that the conductance decreases as the twist angle between the two rings is increased. Our measurements are consistent with the cosine squared relationship expected from consideration of the conjugation in the pi-system [2]. For substituted benzenes, we have found that the conductance varies inversely with the calculated ionization potential of the molecules, providing evidence that the occupied states are closest to the gold Fermi energy [3].

Scientific Questions: In this work, we focused our experimental and theoretical research on answering fundamental questions regarding single molecule junction formation, link bond stability and junction evolution under stress. These were addressed both experimentally and theoretically, for single-molecule junctions bonded to gold electrodes using amine, methyl sulfide, and dimethyl phosphine link groups by measuring conductance as a function of junction elongation. Key questions addressed were: (1) How do single molecule junctions sustain elongation lengths comparable to the molecular length? (2) How does the conductance of a single molecule junction vary under stress? (3) How do the different binding strengths of the Amine and Phosphine link groups affect single molecule junction evolution.

Results: Our measurements showed that for each link, the maximum elongation and formation probability increase with molecular length, strongly suggesting that processes other than just metal-molecule bond breakage play a key role in junction evolution under stress. Density functional theory (DFT) based calculations, performed by Dr. Koentopp in my group at Columbia using CFN computing facilities and in collaboration with Dr. Mark Hybertsen through the CFN User Program, simulated the junction elongation process for the NH_2 and PMe_2 links. They show clearly that the long steps result from multiple processes including changes in the molecular binding site, changes in the gold electrode structure, and molecular rearrangements, as well as bond breakage. Bond breakage contributes only a small fraction of the total junction elongation distance. Furthermore, the zero-bias transmission does not change significantly upon changes in the molecular binding site or gold electrode structure, consistent with experiment [5].

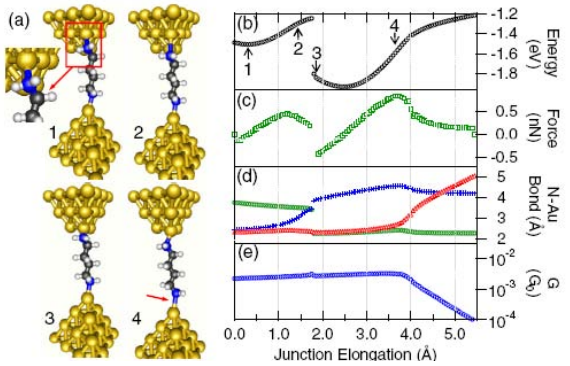

Future Work

We have recently developed and applied an approach to measure simultaneously, the conductance as well as the force applied across the molecular junction and we can now measure forces required to break gold point-contacts in the presence of different molecules, as well as the forces required to break gold-molecule bonds. Our preliminary results show that the gold-gold bond strength depends on the environment around the point contact. Specifically, we find that when amine terminated molecules are present around the gold point contact, the gold-gold bond strength decreases. We find a similar result when Methyl sulfide terminated molecules. Dr. Koentopp has done preliminary calculations modeling the influence of a nearby adsorbate on the physical evolution of gold point contacts. Under the new User proposal (Title: *Understanding the correlation between bond breaking forces and chemistry at the single molecule scale*), we plan to fully develop these calculations, closely tied to the developing experimental results.

Acknowledgements

This work was supported in part by the NSEC program of the NSF (Grant No. CHE-0641532), NYSTAR, and a NSF Career grant (No. CHE-07-44185). Part of this research was performed at the CFN at BNL and supported by DOE (Contract No. DE-AC02-98CH10886).

References:

[1] L. Venkataraman, J.E. Klare, I.W. Tam, C. Nuckolls, M.S Hybertsen and M. Steigerwald, Nano Lett. 6, 458 (2006).

[2] L. Venkataraman, J.E. Klare, C. Nuckolls, M.S Hybertsen and M. Steigerwald, Nature, 442, 904-907 (2006).

[3] L. Venkataraman, Y.S. Park, A.C. Whalley, C. Nuckolls, M.S Hybertsen and M.L. Steigerwald, Nano Letters, vol 7, pp 502-506.

[4] M.S.Hybertsen, L.Venkataraman, J.E. Klare, A.C. Whalley, M.L. Steigerwald and C.Nuckolls, J. Phys. Condens. Matter 20, 374115 (2008).

Publications:

[5] M. Kamenetska, M. Koentopp,A. C. Whalley, Y. S. Park, M. L. Steigerwald, C. Nuckolls, M. S. Hybertsen, and L. Venkataraman, Phys. Rev. Lett. 102, 126803 (2009)

Deciphering the Mechanisms of Bias-Induced Phase Transitions on a Single Defect Level

Sergei V. Kalinin, P. Maksymovych,[*] S. Jesse, and A.P. Baddorf
The Center for Nanophase Materials Sciences, Oak Ridge National Laboratory

Postdocs and students: N. Balke,[†] M. Nikiforov, S. Guo, A. Tselev, K. Seal, O. Ovchinnikov

Thrust area: Origins of Functionality in Nanoscale Systems

Research Achievement

The mechanisms of the phase transitions and electrochemical reactions in solids are determined by the atomistic and mesoscopic defects that act as nucleation centers for new phases and pinning sites for moving transformation fronts. In materials with several thermodynamically equivalent states (e.g. domains in ferroics or orientation variants in martensite) the defects can also select the transformation pathways and determine the final state of the system. The atomic and electronic structures of defects have become accessible with the advances in electron microscopy; however, the dynamic mechanisms of phase transitions on a single defect level until recently remained an enigma.

We aim to establish a set of scanning probe microscopy techniques for probing bias-induced phase transition locally on a level of a single defect and correlate the mechanisms with atomic and mesoscopic structure. Ferroelectric materials are used as prototypical systems in which bias-induced phase transition is (a) fully reversible and (b) can be studied *quantitatively* through the local electromechanical response. The classical Piezoresponse Force Microscopy does not allow efficient use of resonance enhancement methods, hence limiting energy resolution of spectroscopic methods. To address this limitation we have developed

- A family of novel SPM methods based on the excitation signal having finite density in a selected band in frequency domain, as compared to a single frequency in classical SPMs (R&D 100 award in 2008, licensed by Asylum Research)
- A spectroscopic imaging method based on PFM spectroscopy

Following demonstration of imaging capability [1], imaging within a single nanoparticle [2], and single defect resolution [3], these techniques were used to study polarization switching behavior on a number of well-defined systems, including

- 24° grain boundary in (100) rhombohedral ferroelectric (in-house research) [4]
- 180° domain wall in uniaxial ferroelectric (user proposal with V. Gopalan, Penn State)
- Ferroelastic 71° wall in (100) rhombohedral ferroelectric (user proposal by R. Ramesh, UC Berkeley) [5]
- Ferroelectric capacitors (user proposal by S. McKinstry, Penn State) [6]

Recently, the electromechanical detection was integrated with the current and resonance frequency measurements in the ultra-high vacuum environments, enabling

- Probing domain wall conductance in ferroelectrics (user proposal by R. Ramesh) [7]
- Controlling local metal-insulator transitions (user proposal by R. Ramesh) [8]

---

[*] Wigner fellow 2007 - 2009
[†] Humboldt fellow 2008-2010

- Implementation of polarization-controlled tunneling (in-house research) [9]
- Determination of intrinsic switching mechanisms (in-house research) [10,11]

We have shown that the SPM can be used to control the in-plane switching in ferroelectric materials, opening the pathway for controlling ferroelastic structures, magnetic ordering, and creation of long-thought vortex states [5]. The overarching achievement of this program is the demonstration that synergy between advance imaging capabilities and mesoscopic theory (L.Q. Chen, Penn State, A. Morozovska, Ukranian NAS) allows ***deterministic*** polarization reversal mechanisms to be determined on a single-defect level.

Future work:

In the future, we aim to extend the studies of local phase transitions to that in electrochemical systems and also thermal phase transition. To achieve this goal, we aim to:

- Develop dynamic thermal imaging and spectroscopy methods (Nikiforov)
- Develop microwave imaging capabilites (Tselev)
- Integrate the SPM and *in-situ* sample synthesis/controlled atmosphere

In collaboration with ORNL colleagues in electron microscopy, we expect to develop capacity for simultaneous SPM-STEM probing of local bias-induced dynamics on atomic level.

Publications: In total, ~50 peer-reviewed papers (3 Nature Mat., 1 PNAS, 3 Adv. Mat., 5 Phys. Rev. Lett., + 1 Science, 1 PNAS, and 1 Nature Nanotechnology under review), R&D 100 Award 2008 (SJ and SVK), AVS Peter Mark Award for Young Scientists (SVK), ACerS Robert L. Coble award (SVK), MicroBeam Society Cosslett award (SJ, APB, and SVK), BE technology licensed by Asylum Research.

1. S. Jesse, B.J. Rodriguez, A.P. Baddorf, I. Vrejoiu, D. Hesse, M. Alexe, E.A. Eliseev, A.N. Morozovska, and S.V. Kalinin, *Direct imaging of Spatial and Energy distribution of Nucleation Centers in Ferroelectric Materials*, Nature Materials **7**, 209 (2008).

2. B.J. Rodriguez, S. Jesse, M. Alexe, and S.V. Kalinin, *Spatially Resolved Mapping of Polarization Switching Behavior in Nanoscale Ferroelectrics*, Adv. Mat. **20**, 109 (2008).

3. S.V. Kalinin, S. Jesse, B.J. Rodriguez, Y.H. Chu, R. Ramesh, E.A. Eliseev and A.N. Morozovska, *Probing the role of single defects on the thermodynamics of electric-field induced phase transitions*, Phys. Rev. Lett. **100**, 155703 (2008).

4. B J. Rodriguez, Samrat Choudhury, Y.H. Chu, A. Bhattacharyya, S. Jesse, K. Seal, A.P. Baddorf, R. Ramesh, L.Q. Chen, and S.V. Kalinin, *Spatially Resolved Polarization Switching at an Engineered Defect: Bicrystal Grain Boundary in Bismuth Ferrite*, Adv. Func. Mat., in print

5. N. Balke, S. Choudhury, S. Jesse, M. Huijben, Y.H. Chu, A.P. Baddorf, L.Q. Chen, R. Ramesh, and S.V. Kalinin, *Deterministic control of ferroelastic switching in multiferroic materials*, submitted

6. P. Bintachitt, S. Trolier-McKinstry, K. Seal, S. Jesse, and S.V. Kalinin, *Switching Spectroscopy Piezoresponse Force Microscopy of Polycrystalline Capacitor Structures*, Applied. Phys. Lett. **94**, 042906 (2009).

7. J. Seidel, L. W. Martin, Q. He, Q. Zhan, Y.-H. Chu, A. Rother, M. Hawkridge, P. Maksymovych, S. Kalinin, S. Gemming, H. Lichte, P. Yu, F. Wang, G. Catalan, J. F. Scott, N. A. Spaldin, J. Orenstein, and R. Ramesh, *Conduction at domain walls in oxide multiferroics*, Nature Materials, NMAT2373

8. C.H. Yang, J. Seidel, S.Y. Kim, P. Rossen, P. Yu, M. Gajek, Y.H. Chu, L.W. Martin, M.B. Holcomb, Q. He, P. Maksymovych, N. Balke, S.V. Kalinin, A. P. Baddorf, S.R. Basu, M.L. Scullin, and R. Ramesh, *Electric modulation of conduction in multiferroic* Ca-*doped* BiFeO3 *films*, Nature Materials, accepted

9. P. Maksymovych, S. Jesse, P. Yu, R. Ramesh, A.P. Baddorf, and S.V. Kalinin, *Polarization Control of Electron Tunneling into Ferroelectric Surfaces*, submitted

10. S.V. Kalinin, B.J. Rodriguez, S. Jesse, Y.H. Chu, T. Zhao, R. Ramesh, E.A. Eliseev, and A.N. Morozovska, *Intrinsic Single Domain Switching in Ferroelectric Materials on a Nearly-Ideal Surface*, PNAS **104**, 20204 (2007).

11. P. Maksymovych, S. Jesse, M. Huijben, R. Ramesh, A. Morozovska, S. Choudhury, L.Q. Chen, A.P. Baddorf and Sergei V. Kalinin, *Intrinsic Nucleation Mechanism and Disorder in Polarization Switching on Ferroelectric Surfaces*, Phys. Rev. Lett. **102**, 017601 (2009).

Experimental and theoretical studies of molecular-scale quantum dots at carbon nanotube heterojunctions

Bhupesh Chandra[1], Joydeep Bhattacharjee[2], Young-Woo Son[2], Jeffrey. B. Neaton[2], James Hone[1]
[1]Columbia University, Department of Mechanical Engineering and NSEC
[2]Molecular Foundry, Lawrence Berkeley National Laboratory

Carbon nanotubes can be either semiconducting or metallic depending on their specific crystal structure, or chirality, and thus hold promise for electronics applications because most elements of integrated circuitry can be constructed from CNTs alone.

A related, but distinct and largely unexplored class of nanostructures are carbon nanotube heterojunctions- robust covalent nanoscale interfaces connecting tubes of different chiralities. There have been very few studies of these systems in the literature, and their structural and electronic properties still remain poorly understood, mainly because of their rare occurrences and the challenges associated with their synthesis, characterization and electrical measurements. In particular, there has been only one reported measurement of electrical transport in such a structure, and no study has (until now) provided independent confirmation of a chirality change. In addition to their clear relevance to nanoelectronics, these nanoscale covalent heterojunction interfaces also provide ideal test beds for fundamental studies of molecular-scale transport.

We used a combination of experimental measurements, atomistic modeling, and electronic structure calculations to study a well-characterized nanotube heterojunction. The chiralities of the nanotubes were indexed with Rayleigh scattering and confirmed by the transport measurements on both metal and semiconducting sides, making our device one of the most well characterized composite nanostructures that has ever been studied. Most interestingly, transport measurements through the heterojunction reveal for the first time an all-carbon molecular-scale quantum dot arising exclusively due to the arrangement of defects required to form the heterojunction interface. A detailed atomistic theory that complements our experimental measurements provides a general framework underlining guiding principles to make molecular-scale quantum dot devices from carbon nanotube heterojunctions.

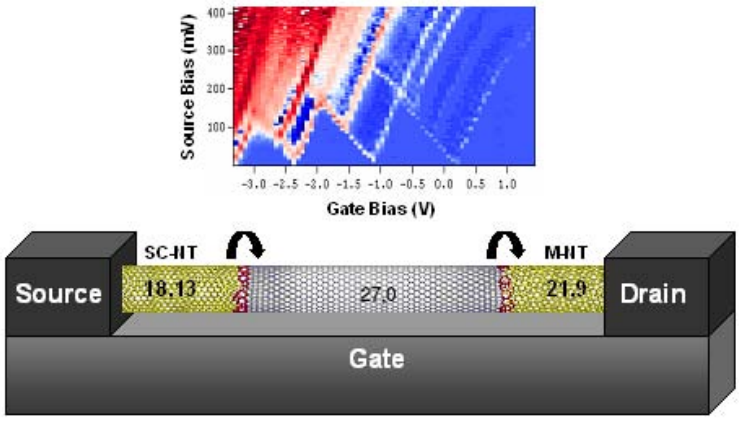

Chandra, B., et al., *Molecular-Scale Quantum Dots from Carbon Nanotube Heterojunctions.* Nano Letters, 2009. **9**(4): p. 1544-1548.

Discovery Platforms™ for Nanoscience

J. P. Sullivan[1], M. P. Lilly[1], A. Gin[1], M. J. Shaw[1], and S. T. Picraux[2]

[1]*Sandia National Laboratories, Albuquerque, NM*
[2]*Los Alamos National Laboratory, Los Alamos, NM*

Scientific Thrust Area: Nanoscale Electronics and Mechanics

Research Achievement:

The Center for Integrated NanoTechnologies (CINT) has a special focus topic in "chip-based nanoscience". We call these chips *Discovery Platforms™ (DPs)*, and they are designed to enable a CINT User to perform nanoscience experiments easily with little to no additional sample processing. In the first generation of DPs, two chips were mass-produced and widely used: (1) the Cantilever Array Discovery Platform (CADP) and (2) the Electrical Transport and Optical Spectroscopy Platform (ETOPS).

Cantilever Array Discovery Platform: The CADP is a multipurpose chip that is designed for experimenters wishing to perform research in the areas of nanomechanics, novel scanning probe technologies, chemical and biological sensing, magnetization studies, *in situ* TEM measurements, and physics of coupled mechanical systems. The platform is the same size as typical atomic force microscope (AFM) chips, and it can be mounted in most AFMs. Unlike an AFM chip, this platform has multiple cantilevers projecting from all edges, and it contains special microelectromechanical systems (MEMS) test structures in the center (see Fig. 1).

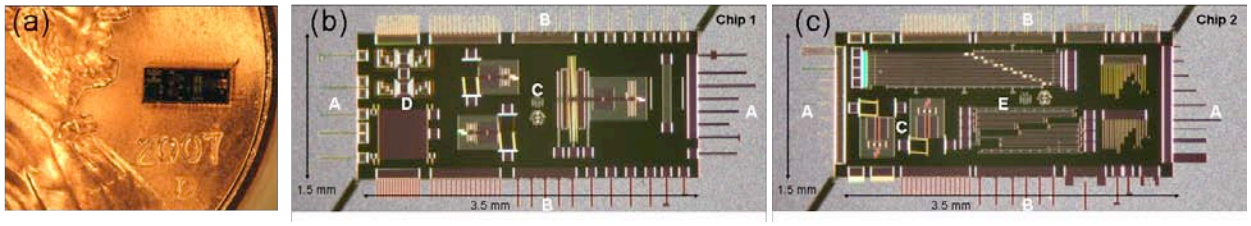

Figure 1. *(a) The CADP is the size of an AFM chip. There are two versions, chip 1 (b) and chip 2 (c). Separate experiments are performed in different regions of the chip: (A) beams for scanning probe microscopy studies, (B) beams for nanomechanics, cantilever-based sensing, coupled oscillators, (C) MEMS structures for mechanics testing of samples, (D) structures for magnetization studies, and (E) silicon beams for surface adhesion studies.*

Examples of experiments with the CADP performed by CINT Users are shown in Fig. 2. These include investigating the physics of high resolution sensing using arrays of mechanically-coupled oscillators *[A]*, measuring the mechanical behavior of metal nanowires under tension *[B]*, and developing techniques for precise local strain measurements in microscale samples *[C]*.

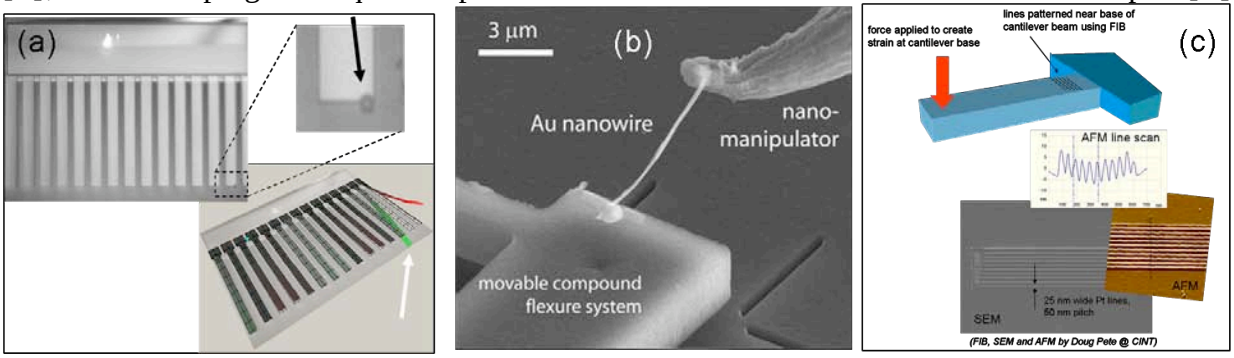

Figure 2. *(a) Sensing using coupled oscillators. Particle attachment (black arrow) leads to large changes in array eigenmodes (white arrow). (b) Nanomechanics testing of nanowires using the CADP load cells. (c) Patterning nanoscale line arrays at the base of CADP cantilevers for local strain measurement using an AFM moiré technique.*

Electrical Transport and Optical Spectroscopy Platform: The ETOPS has been designed to enable fundamental investigations of the optical, electronic, and transport properties of a wide variety of materials by providing a simple and well-characterized means of electrically or optically interfacing with nanoscale samples. The platform contains arrays of electrical contacts in a wide variety of geometries that thenfan out to contact pads, thus enabling electrical connection to a variety of samples (see Fig. 3).

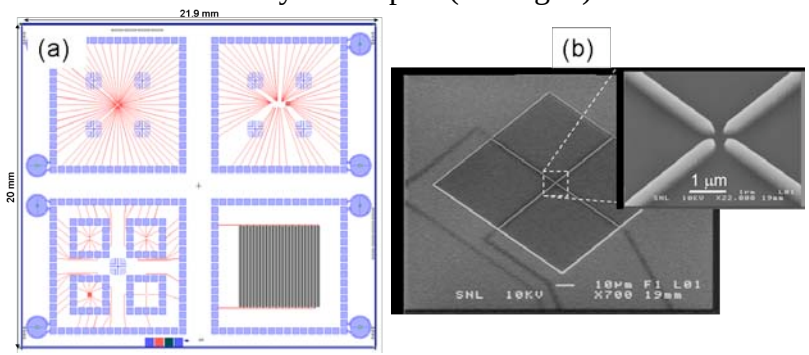

Figure 3*. ETOPS Platform showing overall view (a) and a close-up of one of several electrode patterns (b). In this pattern, 4 leads approach a central point with sub-micron spacing.*

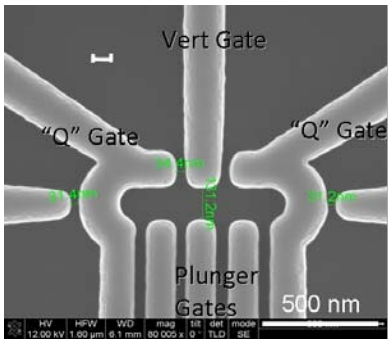

Figure 4*. SEM image of a coupled quantum dot structure on the modified ETOPS platform.*

Using a modified version of this Platform, CINT researchers have been investigating the physics of coupled quantum dots in silicon (see Fig. 4). These structures show great promise for creating practical qubits for quantum computing applications.

Future Work:

We have two new second-generation Discovery Platform chips that are in fabrication. The first platform is an update of our original CADP, called CADP 2.0. Given the success of the first version, we have kept most of the original structures, but we have added a number of additional features to permit the thermal, electrical, thermodynamic, and electromechanical characterization of nanoscale materials (see Fig. 5). This Platform is expected to be released in June 2009.

The second new Platform is called the Nanowire Discovery Platform. It is designed to promote the synthesis, integration, and electrical characterization of nanowire specimens. Some of the specific structures on this Platform include unique trench geometries to enable the growth and integration of vertical arrays of nanowires (see Fig. 6). This platform is expected to be released in late summer 2009.

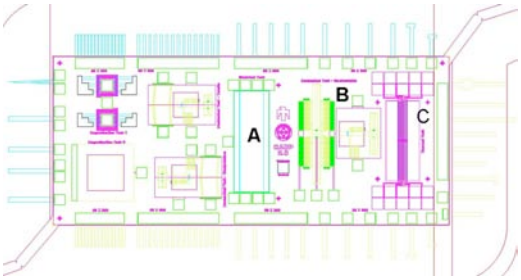

Figure 5*. Chip 1 of CADP 2.0 showing new structures for electrical (A), electromechanical (B), and thermal(C) property measurements of nanowires.*

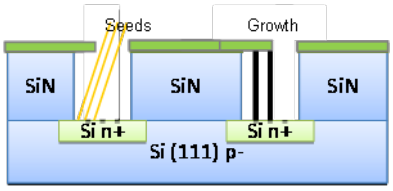

Figure 6*. Cross-section view of a portion of the Nanowire Discovery Platform showing the concept for growth and electrical integration of vertical nanowire arrays.*

Publications:

[A] M. Spletzer, A. Raman, H. Sumali, and J. P. Sullivan, Appl. Phys. Lett. **92**, 114102 (2008).
[B] C. Volkert, unpublished.
[C] H. Jin and W.-Y. Lu, unpublished.

Poster Extended Abstracts

Biomaterials

Temperature Compensation in Biomolecular Motor-Powered Nanomaterials and Devices

Robert Tucker,[1] Ajoy K. Saha,[1] Parag Katira,[1] Marlene Bachand,[2] George D. Bachand,[2] and Henry Hess[1]

[1]Department of Materials Science and Engineering, University of Florida, 160 Rhines Hall, Gainesville, FL 32611
[2] Center for Integrated Nanotechnologies (CINT), Sandia National Laboratories, PO Box 5800, MS 1303, Albuquerque, NM 87185-1303; gdbacha@sandia.gov

Proposal Title:
Temperature compensation of kinesin-powered molecular shuttle velocity (Henry Hess)

Research Achievement:

The use of kinesin motor proteins to transport synthetic nanomaterials[1-3] and assemble hybrid nanocomposites has been widely explored.[4-6] While these biomolecular machines offer unique functions, a number of fundamental challenges arise from this approach, particularly the stabilization of motor proteins against significant temperature changes. Two useful strategies for temperature compensation are common in biological systems: (1) feedback loops used in metabolic pathways, and (2) the ability to maintain constant enzymatic activity at subsaturating substrate concentrations. As an example of the latter, the Michaelis constant (K_m) of many enzymes has been shown to increase with temperature and compensate for the increased maximum turnover rate (v_{max}).[7,8] The goal of this User Project was to discern whether kinesin motor proteins use this temperature compensation strategy, and if so, to understand how this strategy applies to the integration of kinesin motors in hybrid nanomaterials and devices.

Methods

The temperature dependent, kinetic properties of two different kinesin motors (mesostable Drosophila kinesin-1 and thermostable Thermomcyes kinesin-3) were evaluated across a wide range of substrate concentrations using the gliding motility assay. These assays consisted of the adsorption of kinesin motors to the surface of microfluidic flow cells, followed by the introduction of fluorescently-labeled microtubule filaments and varying levels of ATP (i.e., kinesin motor substrate). Temperature of the flow cell was tightly controlled using a heated stage on an inverted microscope. Time-lapse images were captured and used to estimate microtubule transport velocities as a function of substrate concentration and temperature.

Results & Discussion

The ATP-dependent transport velocities for both the Drosophila and Thermomyces kinesins followed typical Michaelis-Menten kinetics (*not shown*), as expected. Curves fit to these data demonstrated a limited temperature dependence on the K_m across the temperature range tested (19-34ºC) for both kinesins (Figure 1A). The lack of temperature dependence was somewhat surprising as previous work with the Thermomcyes kinesin demonstrated a significant increase in the K_m at 50ºC (the thermal optimum for this kinesin).[9] The v_{max} for both kinesin displayed a relatively linear increase as a function of increasing temperature (Figure 1B), which is consistent with prior reports for kinesin and other enzymes.[7-10] Based on this relationship, the Q_{10} (temperature coefficient = increase in velocity per 10ºC change in temperature) for Drosophila and Thermomyces kinesin were estimated at 2.04 and 1.67, respectively. Overall, the incoherence between the temperature responses in the K_m and v_{max} parameters indicate that

temperature compensation in kinesin motor proteins is achieved by a different mechanism than has been observed in thermo- and psychro-stable enzymes.[7,8]

Future Work

The results of these experiments suggest that temperature compensation in kinesin motors does not occur through changes in the intrinsic kinetic properties of the enzyme. Thus, future work is focused on developing alternate strategies (e.g., feedback networks) to compensate for temperature-dependent effects on kinesin transport in hybrid materials and devices with applications in motor protein-powered biosensors.

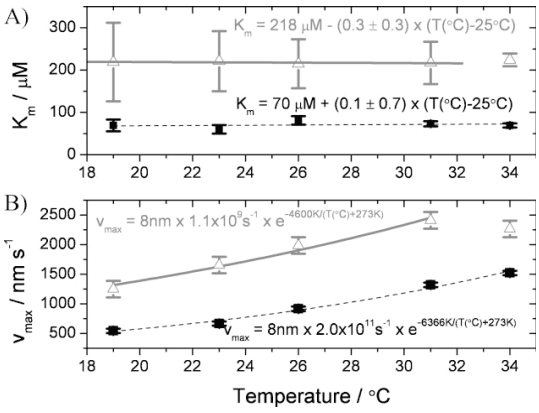

Figure 1. (**A**) K_m and (**B**) V_{max} of Drosophila kinesin-1 (black squares) and Thermomyces kinesin-3 (open grey triangles) as function of temperature. Figure taken from Tucker et al.[11]

References

1. Dinu, C.Z., Bale, S.S., Chrisey, D.B., and Dordick, J.S., Manipulation of individual carbon nanotubes by reconstructing the intracellular transport of a living cell. *Adv. Mater.* **21**, 1182 (2009).
2. Bachand, M., Trent, A.M., Bunker, B.C., and Bachand, G.D., Physical factors affecting kinesin-based transport of synthetic nanoparticle cargo. *J. Nanosci. Nanotechnol.* **5**, 718 (2005).
3. Bachand, G.D., Rivera, S.B., Boal, A.K., Gaudioso, J., Liu, J., and Bunker, B.C., Assembly and transport of nanocrystal cdse quantum dot nanocomposites using microtubules and kinesin motor proteins. *Nano Lett.* **4**, 817 (2004).
4. Liu, H.Q., Spoerke, E.D., Bachand, M., Koch, S.J., Bunker, B.C., and Bachand, G.D., Biomolecular motor-powered self-assembly of dissipative nanocomposite rings. *Adv. Mater.* **20**, 4476 (2008).
5. Hess, H., Self-assembly driven by molecular motors. *Soft Matter* **2**, 669 (2006).
6. Huang, T.J., Recent developments in artificial molecular-machine-based active nanomaterials and nanosystems. *MRS Bull.* **33**, 226 (2008).
7. Ruoff, P., Zakhartsev, M., and Westerhoff, H.V., Temperature compensation through systems biology. *Febs J.* **274**, 940 (2007).
8. Georlette, D., Jonsson, Z.O., Van Petegem, F., Chessa, J.P., Van Beeumen, J., Huscher, U., and Gerday, C., A DNA ligase from the psychrophile pseudoalteromonas haloplanktis gives insights into the adaptation of proteins to low temperatures. *Eur. J. Biochem.* **267**, 3502 (2000).
9. Rivera, S.B., Koch, S.J., Bauer, J.M., Edwards, J.M., and Bachand, G.D., Temperature dependent properties of a kinesin-3 motor protein from *thermomyces lanuginosus*. *Fungal Genet. Biol.* **44**, 1170 (2007).
10. Böhm, K.J., Stracke, R., Baum, M., Zieren, M., and Unger, E., Effect of temperature on kinesin-driven microtubule gliding and kinesin atpase activity. *FEBS Lett.* **466**, 59 (2000).
11. Tucker, R., Saha, A.K., Katira, P., Bachand, M., Bachand, G.D., and Hess, H., Temperature compensation for hybrid devices: Kinesin's K_m is temperature independent. *Small* **5**, DOI: 10.1002/smll.200801510 (2009).

Publications

Tucker, R., Saha, A.K., Katira, P., Bachand, M., Bachand, G.D., and Hess, H., Temperature compensation for hybrid devices: Kinesin's K_m is temperature independent. *Small* **5**, DOI: 10.1002/smll.200801510 (2009).

Smart Nanoparticles for Biological Imaging

Bruce E. Cohen
The Molecular Foundry
Lawrence Berkeley National Laboratory

Scientific Thrust Area: Biological Nanostructures

Research Achievement: Certain nanoparticles possess unusual optical properties that are highly desirable in biology, which relies heavily on imaging probes and microscopy. We have recently developed photoactivatable nanoparticles—called *caged quantum dots*—that are non-luminescent under typical microscopic illumination but can be activated with stronger pulses of UV light. These nanoparticles are hybrids of hard and soft materials, and their unique optical properties arise from the interaction between a classic organic caging group and a semiconducting quantum dot (QD). We have demonstrated that these QDs can be photoactivated within live cells and have begun to examine the physical basis of the interaction between caging group and QD.

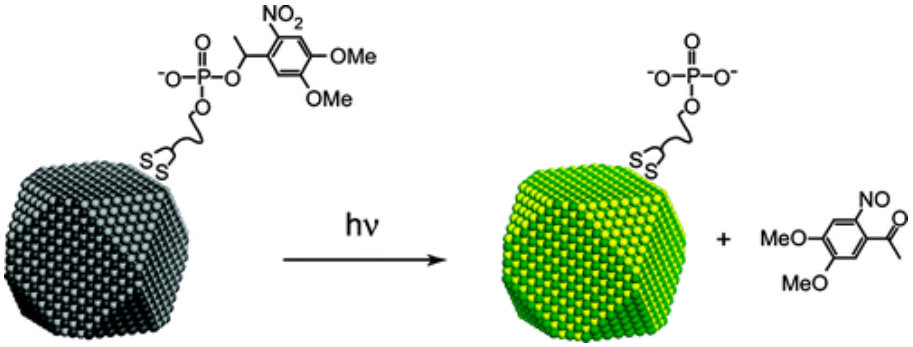

A second type of nanoparticle (developed in collaboration with Delia Milliron and James Schuck of the Molecular Foundry) with exceptional optical properties, the lanthanide-doped upconverting nanoparticle (UCNP), absorbs two photons in the nIR and emits one at shorter wavelengths in the visible or nIR. nIR excitation is exceptionally valuable for bioimaging: compared to the visible or UV, nIR radiation is less damaging to cells and scatters less, allowing deeper tissue penetration or even whole animal imaging. These particles emit "anti-Stokes" light, producing a higher-energy photon from multiple lower-energy photons, and because nothing in the cell emits anti-Stokes, there is no background autofluorescence with these nanoparticles. We have developed a synthesis of monodisperse UCNPs and a simple procedure for transferring them to water, and we have recorded the first single molecule images of UCNPs. We find that UCNPs do not blink, as QDs and organic probes do, and that they posses remarkable photostability, resisting photobleaching long after even QDs are extinguished.

Future Work: The two new particles described above will be further refined for work with cells. Caged QDs currently use UV-active caging groups as phototriggers, and while UV irradiation is commonly used to photoactivate proteins and organic probes, it is known to damage cells. We have synthesized a series of longer-wavelength caging

groups that can be photolyzed with the 488-nm source commonly found in imaging systems. These blue-light caging groups will also allow us to better understand the mechanism by which this class of compounds quench QDs so efficiently. We have previously found emission wavelength dependence of QD quenching; varying the caging group, along with computational efforts by Jeffery Neaton of the Molecular Foundry Theory Facility, should provide insight into the quenching mechanism.

Following our characterization of the single-molecule behaviors of lanthanide-doped upconverting nanoparticles, we have been pursuing several areas for improving their utility in cell imaging. We have developed a method of synthesizing smaller particles (< 10 nm) and are optimizing this synthesis using the WANDA robot in the Inorganic Facility. This smaller size regime is much more useful for bioimaging, with the larger particles more likely to perturb proteins being studied in tracking experiments. We are also pursuing other lanthanide combinations to vary the excitation wavelengths to avoid nIR water absorbances that may interfere with live cell imaging. The photostability and lack of blinking of UCNPs makes them ideal for tracking the motions of membrane proteins such as G-protein coupled receptors, which are critical in a variety of cellular functions. We have coated UCNPs with antibody-binding proteins and will pair these with antibodies to cellular receptors for long-term tracking experiments.

Publications:

C. Ajo-Franklin, G. Han, T. Mokari, B.E. Cohen. Caged Quantum Dots. *J. Am. Chem. Soc.* 130, 15811-15813 (2008).

S. Wu, G. Han, D.J. Milliron, S. Aloni, V. Altoe, D.V. Talapin, B.E. Cohen, P.J. Schuck. Non-blinking and photostable upconverted luminescence from single lanthanide-doped nanocrystals. *Proc. Nat. Acad. Sci.*, in press.

Dynamics of Phospholipid Membrane Composite Nanomaterials

Gabriel A. Montaño[1], James H. Werner[1], Gautam Gupta[2], Anthony L. Garcia[2], Andrew P. Shreve[1], Hsing-Lin Wang[1], & Gabriel P. Lopez[2]

[1]*Los Alamos National Laboratory, Los Alamos, NM*
[2] *University of New Mexico, Albuquerque, NM*

Scientific Thrust Area: Soft, Biological and Composite Nanomaterials Thrust

Proposal Title: Silica-Phospholipid Membrane Nanocomposites: Synthesis and Characterization of Robust Biological Transport Systems (G. P. Lopez)

Research Achievement:

Interactions at the bio-nano interface have exciting potential in the next generation of technological advances. At the cellular level, lipid membranes, composed mainly of lipids and proteins, create the barrier at which interaction between the biological and non-biological world take place. Membranes exist not only as barriers, but are also key components of cellular activity. For example, they allow for creation of potential gradients, allowing for processes such as energy production to occur, and also serve as sites for cellular target recognition. Lipid membrane model systems have become popular for investigating biological membrane structure and function. These assemblies have the advantage of compositional and environmental control, allowing for investigation of membrane properties that can often be difficult to assess in cellular systems. Interaction of these assemblies with synthetic substrates, including nanostructured materials, has already exhibited potential in creating new bio-synthetic architectures as well as in providing information on cellular responses to the non-biological world. Presented are examples from CINT user collaborations and CINT thrust efforts that utilize membrane assemblies to investigate biological phenomena and develop new methods towards understanding membrane properties and processes.

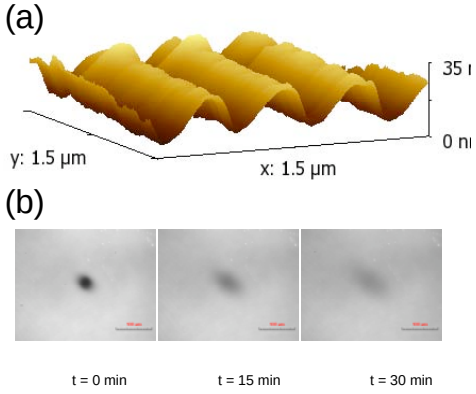

Figure 1. Lipid Membrane Assemblies (LMA) on nanostructured surface. (a) AFM of LMA on nanostructured surface. (b) Images of fluorescence recovery after photobleaching of LMAs on nanostructured surface.

Research that focuses on the morphology and dynamics of lipid bilayer assemblies on nanostructured surfaces will be shown. Using atomic force microscopy and quantitative fluorescence microscopy, we have shown that the bilayer assemblies conform to the underlying nanostructured substrate and display apparent anisotropic diffusion (Figure 1). Simulations indicate that lipid diffusion on the surfaces is homogeneous and consistent with isotropic diffusion along the periodic surface, however over macroscopic scales diffusion appears anisotropic due to the nanostructured surface.

Thus, we demonstrate how quantitative analysis of dynamics probed by larger-scale fluorescence imaging can yield information on nanoscale thin-film morphology.

Further, we will describe research focusing on mechanisms underlying biological and health effects of nanomaterials. Cellular lipid membranes represent the physical barrier between the cell and the external environment, and thus serve as a point of interaction of foreign particles, such as fullerenes, with the cell. In this study, we used in situ atomic force microscopy (AFM) and fluorescence spectroscopy to visualize the interaction of a systematically functionalized series of fullerenes with both THP-1 cellular membrane fragments and lipid bilayer assemblies (LBA) of various compositions. Results suggest various mechanisms in which fullerenes may interact with membrane architectures and elicit responses (Figure 2). Results were evaluated as a function of fullerene physical, chemical and electrical properties, providing input toward developing predictive models for biological effects of nanomaterials.

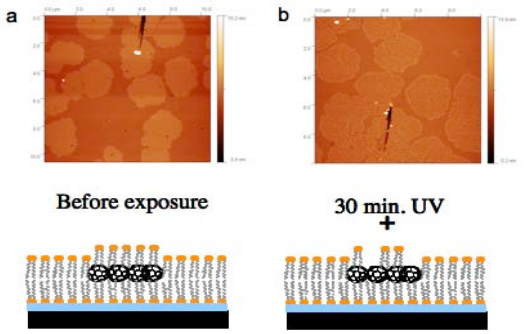

Figure 2. Fullerene incorporation into POPC LBA. (a) incorporation of fullerene into LBA interior with aggregation. (b) UV-exposed enhanced LBA damage localized to areas of fullerene incorporation.

Lastly, a novel strategy for silica encapsulation and stabilization of membrane components will be described. The described method is simple, controllable and non-toxic to biological structures. Various membrane components, both biological and bio-inspired that have been successfully encapsulated and exhibited stability over days to months will be described. This research represents a significant advancement in our ability to stabilize biological structures under various conditions and will have significant impact in biosensing, drug delivery and biophysical research.

Future Work:

Research will continue to explore dynamics of membrane composite nanomaterials. We will exploit the stability and maintenance of biological activity in robust materials to develop integrated composite systems that mimic biological activity such as active transport and signal propagation. Further, platforms will be developed for investigation of membrane dynamics and organization using a variety of biophysical techniques.

Associated Publications:

J. Werner, G.A. Montaño, A Zurek, A. Garcia, E. Akhadov, G.L Lopez, A.P. Shreve. (2009) *Formation and characterization of a supported phospholipid membrane on a periodic nanotextured substrate.* Langmuir 25(5):2986-2993.

R. Martin, H.-L. Wang, S. Iyer, G.A. Montaño, J.S. Martinez, A.P. Shreve, Y. Bao, C.-C. Wang, Z. Chang, Y. Gao, J. Gao, R. Iyer, . (2009) *Impact of physicochemical properties of engineered fullerenes on key biological responses* Toxicology and Appl. Pharmacology 234:58-67.

Nanobio Hybrids for Stimuli Transduction

Elena A. Rozhkova[1] , Ilya Ulasov[2], Maciej S. Lesniak[2] Nada M. Dimitrijevic [1], Barry Lai[3], Valker Rose[3], and Tijana Rajh[1]

[1] *Center for Nanoscale Materials, Argonne National Laboratory*
[2] *University of Chicago*
[3] *Advanced Photon Source, Argonne National Laboratory*

Scientific Trust Area: Design of functional materials at nanoscale

Research Achievements: Functional nanoscale materials that possess specific physical or chemical properties are able to leverage signal transduction *in vivo*. Once these hard materials integrated with biomolecules they combine properties of both inorganic and bioorganic moieties for successful interfacing with whole cells for direct manipulation and changing biochemical pathways via energy or information transmittance. These systems are appealing for wide range of application from the life sciences to advanced catalysis and clean energy production.

Semiconductor metal oxide particles such as TiO_2 have been of interest in a wide range of applications including dye-sensitized solar cells, gas sensors, photocatalytical degradation of organic substrates and deactivation of microorganisms. TiO_2 is a semiconductor with a bulk band gap of 3.2 eV that can induce reactive oxygen species (ROS) in aqueous medium under UV light exposure. Our strategy in construction of TiO_2 based nano-bio hybrids is based on application of natural dihydroxybenzenes (e.g. dopamine, DOPAC, L-Dopa) as linkers, which due to presence of two OH- groups in the ortho- position form a strong bidentate complex with coordinatively unsaturated Ti atoms at the surface of nanoparticles. When biomolecules, such as DNA or proteins are covalently bound to dopamine, this linker acts as a conductive bridge between TiO_2 nanocrystals and biomolecules allowing transport of photogenerated holes to biomolecules. Modification of TiO_2 nanoparticles with dopamine enables harvesting of visible light, and promotes spatial separation of charges. The formation of oxidative species (OH, $^1O_2$, O_2^-, HO_2, H_2O_2) upon illumination of TiO_2-dopamine was studied using complementary spin-trap EPR and radical-induced fluorescence techniques. The localization of holes on dopamine suppresses oxidation of adsorbed water molecules at the surface of nanoparticles, and thus formation of OH radicals. At the same time, dopamine does not affect electronic properties of photogenerated electrons and their reaction with dissolved oxygen to produce superoxide anions [1]. In experiments *in vivo* we demonstrated that under visible light illumination TiO_2-DOPAC-antibody system catalyses generation of superoxide, a relatively long-lived ROS; this ROS serves as a secondary messenger altering of cellular respiratory pathways for re-programming cancer cells intrinsic death agenda, Figure 1.

Of equal significance, for first time we report direct visualization of ligand-receptor interaction and mapping of a specific human GBM receptor through a single brain cancer cell using TiO_2 nanoparticles through XFM hard X-rays of the Advanced Photon Source, Figure 2.

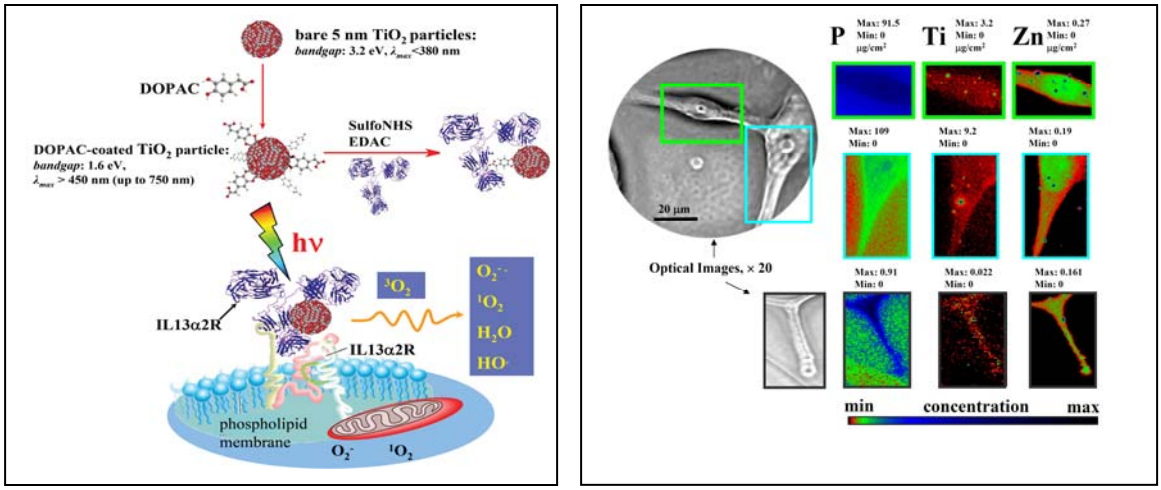

Figure1. General scheme
Nanobiocomposites consisted of 5 nm TiO_2 and IL13R recognizing antibody linked via DOPAC linker recognize and bind exclusively to surface IL13R. Visible light phoro-excitation of the nanobio hybrid in an aqueous solution results in formation of the various ROS. ROS, mainly superoxide cause cell membrane damage, permeability changes and cell death.

Figure2. X-ray fluorescence Microprobe-based visualization of the TiO_2-mAb binding to the single GBM cells (high antigen over-expressing A172 line). Elemental distribution of biogenic phosphorous and zinc are used to sketch cells and nucleus. Directed by the mAb exclusively to the surface of GB cells, TiO_2 nanoparticles are spread all through the GMB cell, including cells invadopodia (lower images). The intensity of the elemental images was displayed using a prism color table in logarithm scale which was shown to the bottom right. The max and minimum threshold values in micrograms per squared centimeter are given above each frame. Scans were obtained by using 10.0-keV incident energy with dwell times of 1 sec per pixel and 1-μm steps through the sample. Simultaneous appearance of intense "hot spots" in the Ti and Zn distribution images is possibly resulting of the titanium nanoparticles as well as other inorganic materials aggregation.

Future work: We will continue studies of TiO_2 nanobio hybrids interfacing with malignant mammalian cells using real-time PCR microarray analysis of the expression of key genes involved into ROS-based programmed cells death. Using novel advanced X-ray technique - Hard X-ray Nanoprobe we will study dynamics of important biochemical events following light-stimulus of photoreactive materials interfaced with mammalian cells. Furthermore, we will focus on development of other functional materials such as ferromagnetic particles with spin vortex ground state, for cellular signal transduction.

Publications:

N. M. Dimitrijevic, E. Rozhkova, T. Rajh, "Dynamics of Localized Charges in Dopamine-Modified TiO2 and their Effect on the Formation of Reactive Oxygen Species", *J. Am. Chem. Soc.*, 131, 2893-2899 (2009)

E. A. Rozhkova, V. Novosad, D.-H. Kim, J. Pearson, R. Divan, T. Rajh, and S. D. Bader "Ferromagnetic microdisks as carriers for biomedical applications" *J. Appl. Phys*., 105, 07B306 2009

Development of nanoparticle complexes as breast cancer imaging and therapy agent

Yan Zhao*†, Edwardine Labay§, Muriel Lainé†, Eugene R. DeSombre†,
Ralph R. Weichselbaum§, Jeffrey S. Souris‡, Xiao-Min Lin*, Geoffrey L. Greene†

†Ben May Department for Cancer Research, The University of Chicago,

‡Department of Radiology, The University of Chicago

§Department of Radiation and Cellular Oncology, University of Chicago Hospital

*Center for Nanoscale Materials, Argonne National Laboratory.

Scientific Thrust Area:

Among various forms of cancer that afflict women, breast cancer is the most prevalent. One of key prognostic and therapeutic markers for breast cancers is over expressed estrogen receptors (ERs). Although ERs are general considered to be nucleus transcription factor, they have recently been found to exist on cell membrane as well. However, the detailed functions of ERs in the cytoplasm and membrane remain unclear. The development of better fluorophores that have a higher binding specificity for ERs, with higher fluorescence quantum yield and lower photo-bleaching behavior, could help to elucidate the diverse ER functions in breast cancer and ultimately lead to a cure for breast cancer.

Research Achievement:

Utilizing resources at the Center for Nanoscale Materials, we have made several major breakthroughs in utilizing nanoparticles for breast cancer imaging.

(i) We have synthesized the first bio-conjugated CdSe/ZnS core-shell quantum dot system that contains estradiol (E2) moiety.

(ii) By pretreatment of cancer cells with a different size of QDs without E2 ligand, we are able to eliminate nonspecific binding sites and demonstrate E2-conjugated QDs bind only specifically to ERs. Figure 1a shows the coexistence of both types of QDs on the cell surface, namely the nonspecific binding of QDs without E2 (emits at 525 nm) and the E2-conjugatecd QDs (emits at 605 nm). The yellow color comes from overlap of the emission from both types of QDs. The predominant and slightly punctuate yellow color indicates that nonspecific binding sites are more or less evenly distributed on the cell surface, whereas the ER specific binding sites

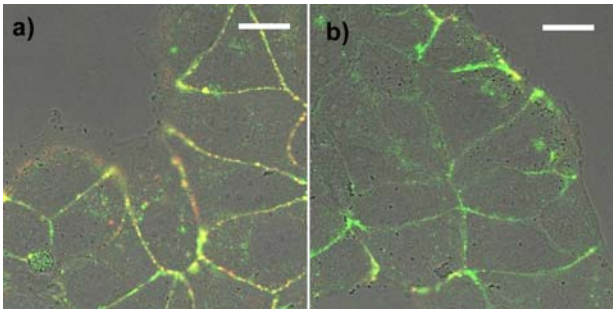

Figure 1 a) Fluorescence signals from both nonspecific-binding QDs (green) and specific binding QDs (red) in a cross section of MCF-7 K1 cells obtained by a confocal scanning optical microscope. b) shows non-specific binding QDs only.

are much more localized. Figure 1b shows the result of a control experiment performed with diethylstilbestrol (DES), a substance known to block ES binding sites. As a result, very little specific binding occurred, which is evident from a predominant green fluorescence from QDs without E2.

(iii) By measuring the amount of ligand conjugated on the QDs and the free ligand remained in solution, we are able to elucidate the effect of both parameters on nanoparticle cell binding process, as shown in Figure 2. These E2-conjugated QDs could be used as an optical marker to elucidate the functions of membrane associated ERs, help to deliver drugs locally to carcinoma cells, which could inhibit the molecular pathways that are critical for cell growth.

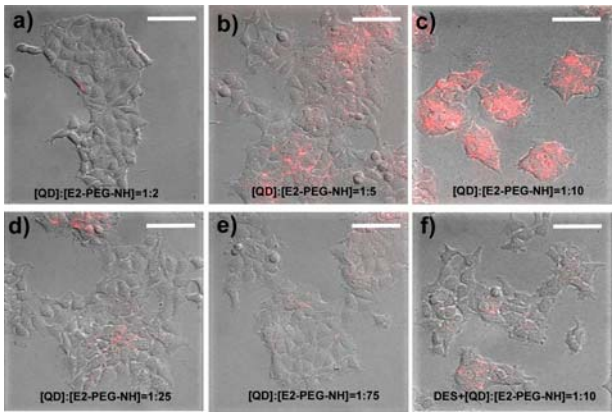

Figure 2. Fluorescence signals from E2-conjugated QDs or K1 cells. (a)-(e) are from different batches of conjugated Q solution, obtained by reacting 1μM of QD605 with varying of E2-PEG-NH ligand. In panel (f), DES was added prior t incubation the cell with E2-conjugated QDs.

Future work:

Our experiments also showed that the stability of the polymeric ligand shell on commercial QDs is still not robust enough for carrying out many experiments in physiological environment. We will further improve its stability. This could help us to carry out experiments to track bioconjugated QDs in cellular environment over an extended period of time, without concerns about the possible detachment of target ligand motifs from the QD surface. Besides targeting cancer cells, we will study various drug delivers strategies using conjugated nanoparticles as a platform.

References:

1. Anderson E. *Breast Cancer Res.* **2002**, 4, 197-201.
2. Clarke R.B. *Trends Endocrinol Metab.* **2004**, 15, 316-323
3. Bruchez, J. M.; Moronne, M.; Gin, P.; Weiss, S.; Alivisatos, A.P. *Science*, **1998**, 281, 2013-2015.
4. Harrington, W.R.; Kim, S.H.; Funk, C.C.; Madak-Erdogan, Z.; Schiff, R.; Katzenellenbogen, J.A. and Katezenellenbogen, B.S. *Mol. Endocrinol*, **2006**, 20, 491-502

Publication:

Zhao, Y., Labay, E., Lainé M., DeSombre, E.R., Weichselbaum, R.R., Souris, J.S., Lin, X.M., Greene, G.L., *Nano Letters*, under review.

Catalysis

Investigation of Structure and Photocatalytic Activity for Water Splitting at the Aqueous – $(Ga_{1-x}Zn_x)(N_{1-x}O_x)$ Alloy Interface

X. Shen[a,b], J. Wang[b], L. Li[b], Y. A. Small[a], P. B. Allen[b], M. V. Fernandez-Serra[b], M. S. Hybertsen[a] and J. T. Muckerman[a,c]

[a] *Center for Functional Nanomaterials, Brookhaven National Laboratory, Upton, NY*

[b] *Department of Physics and Astronomy, State University of New York, Stony Brook, NY*

[c] *Chemistry Department, Brookhaven National Laboratory, Upton, NY*

Scientific Thrust Area: Theory and Computation

This project is aligned to the CFN Interface and Catalysis theme.

Research Achievement

Background: Domen and coworkers have reported that a solid solution of GaN and ZnO is a stable photocatalyst, capable of splitting water under visible light [1, 2]. Of particular note is the high quantum efficiency for molecular oxygen evolution in the presence of a sacrificial electron acceptor (51% under 420-440 nm illumination) [2]. In prior work, Muckerman and coworkers explained the substantial bowing in the fundamental optical gap as a function of alloy composition using a modified Density Functional Theory (DFT) approach [3]. Meyer identified competing molecular and half dissociated phases for a water monolayer on the non-polar ZnO(10$\underline{1}$0) surface [4]. In the BNL Chemistry Department, a separate experimental program (Fujita, et al) is directed to synthesis of the alloy thin films as well as structural and catalytic characterization and we maintain close connection to this work.

Scientific Questions: We focus our theoretical research on the structure of the interface and identifying the pathway for the oxygen evolution reaction. Key questions include (1) What are the plausible local composition and bonding motifs at the interface? (2) Are there localized states for the photogenerated holes that are supported by these interface structures? (3) What are the critical steps whereby electrons transfer from water fragments near the interface to fill the photogenerated holes and what is the structure of the water fragments at each step?

Research Team and Methodology: We have formed an interdisciplinary theory team spanning Chemistry and CFN from BNL and Physics at Stony Brook to tackle these questions using DFT based approaches (GGA-PBE). We model the semiconductor with thin films or small clusters and consider one or a few monolayers of water. Minimum energy structures, minimum energy pathways and molecular dynamics simulations are used to establish structures and explore dynamical processes. DFT packages used include Quantum Espresso, Gaussian and Siesta.

Water – GaN Interface: In our initial study, we have determined the structure of an adsorbed monolayer of water on the non-polar GaN(10$\underline{1}$0) surface [publication below]. We find that water dissociates with a negligible energy barrier. Our analysis of the water-water interactions show that submonolayer water coverage will result in island formation due to substrate strain mediated and hydrogen bonding interactions. Because the results are very different from the ZnO case, this suggests that the surface composition of the semiconductor alloy will be a key factor determining active sites for catalytic activity.

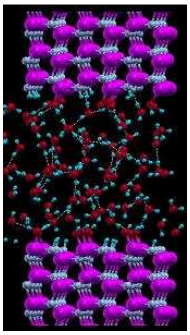

MD simulation snapshot.

We are now probing the water interactions at the full aqueous interface. First, we have performed static calculations with three additional monolayers of water on the GaN:H_20 surface, relaxing the

structures into local minima. Second MD simulations for a model system consisting of 96 H_2O molecules (equivalent to 8 monolayers of water) bounded by two GaN(10$\underline{1}$0) surfaces have been done. Initial results indicate a significant change in the hydrogen bonding network in the presence of additional water. In the single monolayer case, the OH species bound to Ga atoms form hydrogen-bonded chains parallel to the surface. However both the static multilayer calculations and the first-principles MD simulations of the GaN(10$\underline{1}$0) interface with bulk water indicate a stronger hydrogen-bonding interaction between bound OH species and water molecules in the overlayer or the bulk than with each other.

The initial step of the water oxidation process is being probed using a small cluster model consisting of a fragment of the GaN(10$\underline{1}$0) film that has two neighboring surface Ga atom active sites. A photo-hole near the surface is simulated by removing one electron from the cluster. Two possible products of the first step of oxidation of adsorbed $Ga{:}OH^-$ are identified: (a) a proton is transferred to the neighboring $Ga{:}OH^-$ resulting in $Ga{:}O^-$; (b) a Ga:OH* radical. Localization of the hole to the O p-state plays a key role.

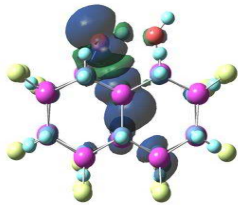

Cluster model, OH* with hole state illustrated.

Future Work

Key issues under investigation include dynamical processes revealed by the MD simulations, the role of solvation in the oxidation process, localization of the photogenerated hole near the interface (including the possible role of defects) and development of a full oxidation pathway.

Identification of active sites at the alloy surface is crucial. We are finishing a systematic study of the ZnO/GaN alloy properties which indicates that random alloys are relatively stable against phase separation. Our study of the (10$\underline{1}$0) surface shows that excess ZnO on this surface is likely. We are beginning to examine the interactions of water molecules with this surface. Alloy heterogeneity appears to make the interfacial water bonding and structure quite diverse.

With the Stony Brook part of the work developing independent funding in the past few months, a portion of the work will be performed under a newly accepted CFN User Project, "Water splitting at the surface of GaN nanoclusters and nanowires: computational modeling of the catalytic properties of GaN surfaces."

Acknowledgements

The work carried out at BNL was supported by the U.S. Department of Energy (DOE), Office of Basic Energy Sciences under contract DE-AC02-98CH10886. The work at Stony Brook was supported by DOE under contract DE-FG02-08ER46550 and by a grant from the Advanced Energy Research and Technology Center at Stony Brook Univeristy. Computing resources were provided by the New York Center for Computational Sciences (NYCCS) and the CFN at BNL.

References

[1] K. Maeda, et al., *J. Am. Chem. Soc.* **127**, 8286 (2005)

[2] K. Maeda, et al., *Nature* **440**, 295 (2006).

[3] L. L. Jensen, J. T. Muckerman, and M. D. Newton, *J. Phys. Chem. C* **112**, 3439 (2008).

[4] B. Meyer, et al., *Angew. Chem. Int. Ed.* **43**, 6642 (2004); O. Dulub, B. Meyer and U. Diebold, *Phys. Rev. Lett.* **95**, 136101 (2005).

Publications

X. Shen, P. B. Allen, M. S. Hybertsen, and J. T. Muckerman, "Water Adsorption on the GaN (10$\underline{1}$0) Nonpolar Surface," J. Phys. Chem. C **113**, 3365 (2009).

Nanoscale Heterogeneous Catalysis at the Center for Nanophase Materials Sciences

Multiscale Functionality Group
Center for Nanophase Materials Sciences
Oak Ridge National Laboratory, Oak Ridge, TN 37831-6201

CNMS-PIs: Chengdu Liang, Michelle Pawel, Adam Rondinone, Viviane Schwartz, Zili Wu, Ye Xu, Sheng Dai, Steven H. Overbury
Post-docs: Hong Xie, Shenghu Zhou
Collaborators: Bryan Eichhorn (university of Maryland), David Mullins, Jane Howe
Contact: Steven H. Overbury, overburysh@ornl.gov

Scientific Thrust Area

Functionality of "real world" nanomaterials is determined not only by their individual interfacial interactions, but also by the 3-D architectures that result from their assembly.. The goal of CNMS Catalytic Nanomaterials research is to explore these interactions and how they relate to catalytic functionality in nano-structured materials. Our approach integrates new methods of synthesis of nanostructured materials with techniques to probe the resulting catalytic performance and structure of these materials. We have focused on three types of materials, namely, bimetallic nanoparticles, synthetic carbon with tailored morphology, and isolated and interacting catalytic sites on mesoporous silica.

Research Achievement

We have explored the synthesis of isolatable NiAu alloy nanoparticles with tunable and relatively uniform sizes *via* a co-reduction method employing butyllithium as the reducing agent and trioctylphosphine as the protecting agent. NiAu alloy nanoparticles are obtained by these routes and these were then used as the precursor to prepare SiO_2 supported catalyst that can be highly active in low-temperature CO oxidation.[1,2] Pretreatment plays an important role in determining the final structure and activity for catalyzing CO oxidation, due to competing processes of removal of organics, oxidation of Ni, and growth of Au particles. XRD provides evidence that the initially synthesized NPs exist as a mixed reduced alloy. High temperature reductive treatments leads to a core-shell structure enriched in Ni on the outer surface. The combination of EXAFS, XANES and XRD indicates the formation of Au/NiO hetero-aggregate is generated through the oxidative phase separation of the Au@Ni core–shell intermediate. Pretreating the catalyst under optimal conditions, i.e., in H_2 at 600 or 720 °C followed by treating in O_2 at 300 °C, results in an Au-NiO/SiO_2 catalyst that is highly active in CO oxidation. For comparison, solely pre-treating the bimetallic NiAu/SiO_2 sample in H_2 does not lead to a reasonably active catalyst. The Ni/Au ratio in the precursor NPs is also important for determining the final structure and catalytic activity. The most active Au-NiO/SiO_2 catalyst was obtained by keeping the Ni/Au ratio at 1:1.

Figure 1. Schematic representation of the phase transformation from NiAu alloy to Au/NiO hetero-aggregate.

The effect of mesopores structure and surface functionalization has also been explored in synthetic carbon catalysts.[3] Carbon is catalytically active for oxidative dehydrogenation reactions, but little is know about the role of nanostructuring and surface functionalization upon the catalytic activity. High-temperature treatments on mesoporous amorphous carbon can convert it to a graphitized mesoporous carbon (GMC) with structure typical of glassy carbon, although the graphitic pore walls are only a few nanometers thick. Closed fullerene-like cavities were observed in this GMC. These cavities can be uniformly opened through air oxidation at 500 °C without affecting the graphitic structure of the glassy carbon. A secondary porosity of 2.5-nm size with complementary oxygenated functionalities was made accessible after oxidation. The oxygenated functionalities can be thermally removed by heating the carbon materials in helium at 1600 °C without affecting the openness of the cavities. Reheating of the oxidized GMC to 2600 °C caused the open fullerene-like cavities to close. Therefore, the fullerene-like cavities can be opened and closed reversibly through air oxidation and heat treatment. The GMCs showed obvious catalytic activities in the ODH reaction when the fullerene-like cavities were open, regardless of the existence of the surface-oxygenated functionalities. The GMC catalysts were deactivated after the fullerene-like cavities were closed by thermal treatment. Therefore, the catalytic activity is related to the openness of the fullerene-like cavities, and these open edges were most likely the active sites of the carbon catalysts in the ODH reactions. We anticipate that this synthesis approach could unravel an avenue for pursuing fundamental understanding of the unique catalytic properties of graphitic carbon nanostructures

Supported transition metal oxide represents an important class of heterogeneous catalyst and has been widely employed in a variety of redox reactions. The determination of the structure of surface metal oxide species is key in understanding the structure-catalysis relationship. Silica-supported vanadium oxide (VOx/SiO_2) is selected as a model catalytic system and its molecular and electronic structures have been probed with *in situ* multi-wavelength (244, 325, 442, 532, and 633 nm) Raman spectroscopy and UV-visible diffuse reflectance spectroscopy (DRS). An evident resonance Raman effect is observed when the sample is excited with UV wavelengths, as evidenced by (1) detection of overtones up to 5^{th} order of V=O band and combination bands of V-O and V=O, (2) clear detection of new bands related to V-O-Si mode; (3) extremely low detection limit of VO_x species at surface density at least 2 orders of magnitude lower than visible Raman. The observation of the interface modes (V-O-Si) is of catalytic significance since the interface bond is generally considered as the active site for redox reactions. Two different V=O bands are observed indicating at least two different types of isolated VO_x species are present, The new information obtained in this study clearly demonstrates the advantages of using multi-wavelength excitations in Raman characterization of supported metal oxide catalysts.

This research at Oak Ridge National Laboratory's Center for Nanophase Materials Sciences was sponsored by the Scientific User Facilities Division, Office of Basic Energy Sciences, U.S. Department of Energy.

Publications

[1] Zhou, S. H.; Yin, H. F.; Schwartz, V.; Wu, Z. L.; Mullins, D.; Eichhorn, B.; Overbury, S. H.; Dai, S. *Chemphyschem* 9, 2475 (2008).

[2] Zhou, S.; Ma, Z.; Yin, H.; Wu, Z.; Eichhorn, B.; Overbury, S. H.; Dai, S. *Journal of Physical Chemistry C* 113, 5758 (2009).

[3] Liang, C.; Xie, H.; Schwartz, V.; Howe, J.; Dai, S.; Overbury, S. H. *J. Am. Chem Soc.* in press, (2009).

X-ray Photoemission Spectroscopy and Scanning Tunneling Microscopy of Model Catalysts at Elevated Pressure Conditions

David E. Starr[1] and Hendrik Bluhm[2]
[1]*Center for Functional Nanomaterials, Brookhaven National Laboratory, Upton, NY 11973*
[2]*Chemical Sciences Division, Lawrence Berkeley National Laboratory, Berkeley, CA 94720*

Scientific Thrust Area

This work has been performed through the *Interface Science and Catalysis* research theme of the Center for Functional Nanomaterials at Brookhaven National Laboratory in collaboration with staff in the Chemical Sciences Division of Lawrence Berkeley National Laboratory.

Research Achievement

Ultra-high vacuum surface science techniques using single crystals have a long history of providing detailed molecular level information about the structure of model catalyst systems and the chemical state of adsorbates on their surfaces. However, such studies have two major limitations that hinder their direct application for the development of more effective catalysts. These are the materials gap and pressure gap. The materials gap arises from the inability of single crystal surfaces to fully capture the structural complexity of real catalysts. In addition, due to the approximately thirteen orders of magnitude pressure difference between ultra-high vacuum measurements and typical catalyst operating conditions, ultra-high vacuum experiments may not capture the chemical nature of the catalytically active phases. This is known as the pressure gap. Modern catalyst development continues to be largely via trial and error due to these pressure and materials gaps. Combining the use of more complex model systems and recently developed surface sensitive elevated pressure experimental techniques, this research aims to bridge the pressure and materials gaps to facilitate a more cognitive approach to catalyst design.

As a first step we have used ambient pressure photoemission spectroscopy to investigate the adsorption of carbon monoxide onto two model catalyst surfaces, Ru(0001) single crystal surfaces and PtRu/Ru(0001) near surface alloys, at pressures up to 1 Torr. CO adsorption on Ru(0001) is a model system for the Fischer-Tropsch synthesis of fuels which involves catalytically reacting CO and hydrogen (syn-gas) to form long chain hydrocarbons. A crucial step in the mechanism of fuel production on Ru is the dissociation of CO. PtRu alloys are currently used as the anode catalyst in proton exchange membrane fuel cells. Pure Pt catalysts are particularly susceptible to poisoning by CO when the concentration of CO in the hydrogen fuel stream approaches tens of ppm. Alloying Pt with Ru increases the CO tolerance of these catalysts. Despite this known property of the alloy simple questions such as the quantity and chemical nature of CO adsorbed on both Pt and Ru sites in the catalyst under realistic CO partial pressures are unknown. In this work we have addressed both the nature of CO adsorption and the onset of CO dissociation on Ru(0001) at pressures up to 1 Torr as well as the amount of CO adsorbed on Pt and Ru sites in model alloy catalyst surfaces at pressures corresponding to real CO partial pressures in PEMFC hydrogen fuel streams.

UHV studies of CO adsorption/desorption on Ru(0001) indicate that CO desorbs from the surface by ~ 500 K. This has led to the conclusion that the active sites for CO dissociation on Ru surfaces are under-coordinated Ru atoms such as those found at step sites. We have found that at room temperature the quantity of CO on the Ru(0001) surface at 1 Torr CO pressure is higher by ~ 1/3 than previously observed using UHV studies. The additional CO is adsorbed in a site on

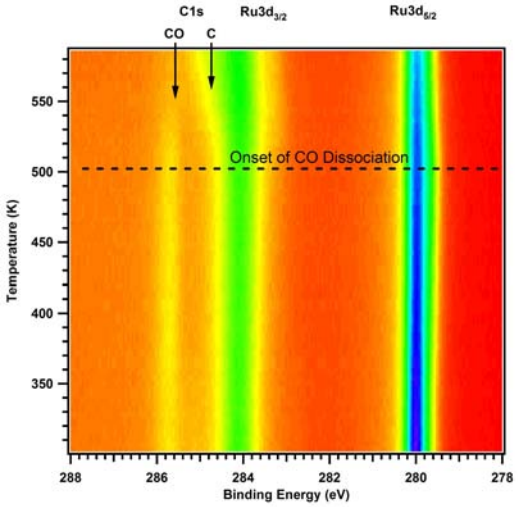

Temperature dependence of the C1s and Ru3d photoemission peaks during heating of a Ru(0001) single crystal in 0.04 torr CO

the Ru surface previously not observed under UHV conditions. Comparison of the O1s binding energy to those found for CO adsorption on other metal surfaces indicates that this site is most likely a bridge site between two Ru atoms. Upon heating the Ru(0001) single crystal in the presence of 0.04 Torr of CO, we have observed the dissociation of CO and formation of C on the surface beginning at ~ 500K. The amount of C on the surface far exceeds what would be expected for simple dissociation and formation of immobile species at step edges. This implies that either the flat Ru(0001) terraces are active for dissociation (counter to what has been previously thought) or more likely that the carbon species formed by CO dissociation at the steps are mobile on the surface at 500 K.

CO adsorption onto PtRu/Ru(0001) near surface alloy systems at pressures up to 0.04 Torr provide model studies of fuel cell catalysts under realistic partial pressures of CO in the hydrogen fuel stream. Using high pressure photoemission spectroscopy we have been able to quantify the amount of CO adsorbed on Pt sites and Ru sites at 300 K. UHV studies have indicated that Pt sites should be largely free of CO at this temperature. Our results not only show that under realistic partial pressures a certain fraction of Pt sites are covered by CO, but that this fraction depends on the relative concentrations of Pt and Ru in the surface. This may indicate that an optimum Pt:Ru ratio exists for these catalysts that provides both sufficient activity and CO tolerance and also lends support to the idea that the alloys increased CO tolerance is due to a decrease in the local binding strength of CO to Pt upon alloy formation.

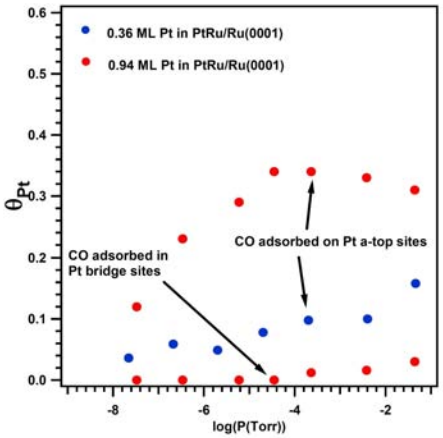

Fraction of Pt covered by CO as a function of CO pressure for PtRu near surface alloys with Pt concentrations of 0.94 (red) and 0.36 (blue).

Future Work

In the future we plan to more directly correlate the chemical nature of adsorbates on complex model catalysts with catalyst structure under elevated pressure conditions. Model catalysts produced by the growth of thin oxide films on single crystal metal surfaces (providing a model support) followed by vapor deposition of the catalytically active metal onto the oxide film will be studied using scanning tunneling microscopy at elevated pressures. We expect such studies to provide direct evidence for catalyst restructuring under near operating conditions. Correlating such restructuring with the chemical information from ambient pressure photoemission spectroscopy, as discussed above, will provide a detailed molecular level understanding of model catalysts near operating conditions.

Directional Etching of Graphene by Catalytic Silver Nanoparticles

Ariel Ismach, Ravisubhash Tangirala, Yuegang Zhang
The Molecular Foundry, Lawrence Berkeley National Lab
Scientific Area: Inorganic Nanostructure Facility in collaboration with Nanofabrication Facility

Graphene has a great potential for future high-speed and low-power electronics due to its unique transport properties.[1] The electron mobility is measured as high as 100,000 cm2/Vs at room temperature,[2,3] making ballistic transport possible at submicron scale. The zero-bandgap nature of 2D graphene,[1] however, cannot provide the high current on/off ratio in mainstream electronic switching devices. For field-effect transistors (FETs), a bandgap larger than 400 meV is normally required. Theoretical calculations showed that the quantum confinement effect in a quasi-1D graphene nanoribbon (GNR) could open a bandgap that is inversely proportional to the GNR width and strongly dependent on its edge atomic geometry (crystallographic orientation).[4,5] Current strategies are based on top-down lithographic processes, mainly electron-beam lithography followed by oxygen plasma etching to create narrow structures. The problem is that the resulting ribbon edges contain a mixture of different crystallographic directions which alters the electronic properties of the ribbon. Even when the edges looks atomic smooth by atomic force and scanning electron microscopes (AFM and SEM, respectively), it was shown by Raman spectroscopy that the samples contained disordered edges.[6] The lack of a methodology for the fabrication of atomic smooth graphene edges inhibits the study on such structures. The main goal of this project is to find an alternative method to create graphene nanoribbons with well-defined edge structures. We are studying three different ways for the guided catalytic etching:

1. Catalytic etching along crystallographic directions.

To achieve this, both, thin layer of silver (1-25 nm) was deposited by electron beam evaporation and silver nanoparticles were deposited on highly ordered pyrolytic graphite (HOPG). Then the samples were heated to 450-550ºC in air for few minutes to form nanoparticles that will etch the graphene layers catalytically (We chose silver rather than other metal nanoparticles[7] because of their low catalytic etching temperature). In contrast to previous report,[8] we have observed two etching modes: the etching along crystallographic directions and random etching. We found that the etching modes depend strongly on the nanoparticle diameters, since the trenches created by the etching along the crystallographic directions have a narrow wide distribution comparing to the random etching (Fig. 1).

2. Directional etching along nano-scale features.

In this case, silver lines were deposited by standard photolithography and electron beam evaporation on faceted surfaces, M-plane sapphire after annealing in air at 1200-1500 ºC, perpendicular to the facets (10-50 nm height depending on the annealing conditions). Then, the silver coated sapphire was placed on HOPG and heated as described above. As a result, three different etching modes were observed: random, along crystallographic directions and along the nanofacets. The trench lengths of the random and crystallographic etching are up to 3 μm (Fig. 2a), while the trenches in the direction of the nanofacets are up to 20 μm long (Fig. 2b). The parameters involved in the different etching modes are currently under research. As next steps, we plan to use lithographically defined features and nanowires to guide the etching directions.

3. Nanopatterning by self-assembled nanoparticle monolayers

We recently found that spin coating of colloidal phase silver nanoparticles on HOPG surface could lead to self-assembled monolayer (SAM) structures (Fig. 3). The edges of the SAM patterns were observed to align along some specific directions. We are now in the process to understanding the mechanism of this SAM pattern formation and investigate the correlation of the pattern orientation with the crystallographic directions of underneath graphene surface. We plan to use the SAM patterns to define graphene patterns through controlled local catalytic etching.

[1] Geim, A.; Novoselov, K. *Nature Materials* **2007**, *6*, 183-191.
[2] Bolotin, K. I.; Sikes, K. J.; Jiang, Z.; Klima, M.; Fudenberg, G.; Hone, J.; Kim, P.; Stormer, H. L. *Solid State Communications* **2008**, *146*, 351-355.
[3] Bolotin, K. I.; Sikes, K. J.; Hone, J.; Stormer, H. L.; Kim, P. *Physical Review Letters* **2008**, *101*, 096802.
[4] Son, Y. W.; Cohen, M. L.; Louie, S. G. *Physical Review Letters* **2006**, *97*, 216803.
[5] Yang, L.; Park, C. H.; Son, Y. W.; Cohen, M. L.; Louie, S. G. *Physical Review Letters* **2007**, *99*, 186801.
[6] Casiraghi, C. *et al*. *Nano Letters* **2009,** 9, 1433-1441.
[7] Tomita, A. and Tamai, Y. *J. Phys. Chem.*, **1974**, 78 (22), 2254-2258
[8] Severin, N. et al. *Nano Letters* **2009**, 9, 457-46.

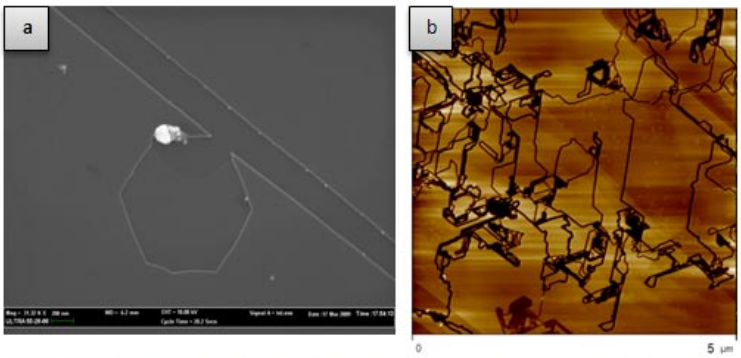

Fig. 1. SEM (a) and AFM (b) images of catalytic etching along the crystallographic directions on HOPG by Ag nanoparticles

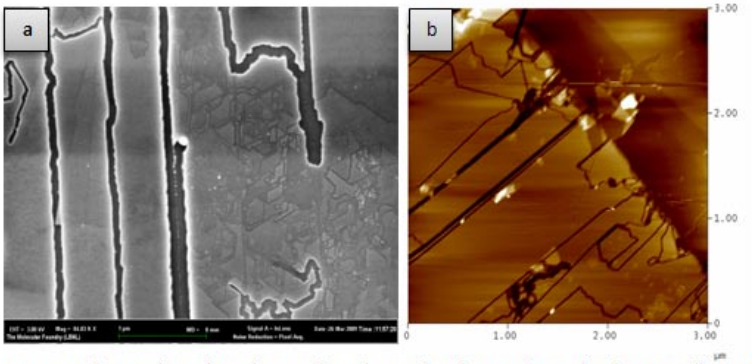

Fig. 2. Catalytic etching along the nanofacet (a, SEM) and crystallographic directions (b, AFM) on HOPG by Ag nanoparticles

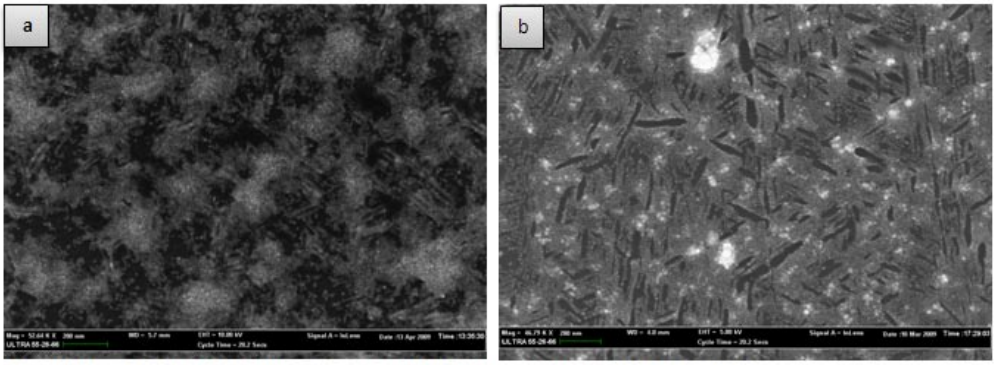

Fig. 3. SEM images of self-assembled Ag nanoparticle Monolayer patterns on HOPG surfaces

Electronic and Photonic Materials

Synthesis and Science of Correlated Complex Oxides at the Nanoscale

Tiffany Santos[1], Anand Bhattacharya[1,2]

[1] *Center for Nanoscale Materials, Argonne National Laboratory.*
[2] *Materials Science Division, Argonne National Laboratory.*

Scientific Thrust Area:

Complex oxide materials can host to a vast array of ordered collective states, including high temperature superconductivity, room temperature multiferroicity, half-metallic ferromagnetism, charge/orbital ordering, and stripe phases. These states arise out of the correlations between the spin, charge and lattice degrees of freedom unique to these materials. Our research program seeks to break new ground by exploring how these states behave on the nanoscale. We will create high quality epitaxial thin films and heterostructures of complex oxides that are known to have collective states of interest. Using the unique capabilities at the CNM to create and probe structures at the nanoscale, we will measure and understand fundamental electronic and optical properties of these materials at this length scale. The program will explore electronic phase-separation and competing ordered states that occur either intrinsically at the nanoscale or are promoted by confinement in nanoscale wires and constrictions. It includes studies of spin and charge dynamics, including correlation lengths and times to learn if these materials may be useful for information science and energy related applications.

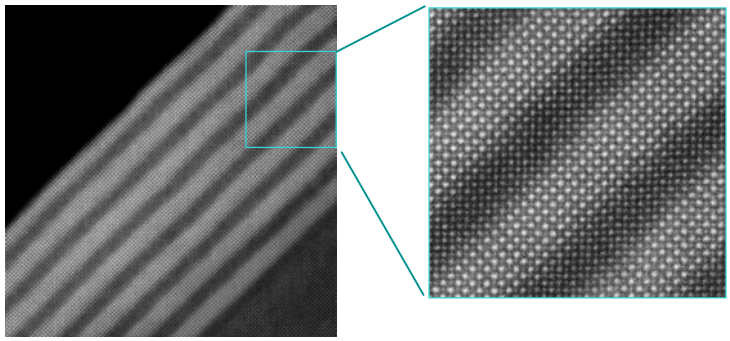

Fig. 1 Superlattice of $(LaMnO_3)_6/(SrMnO_3)_6$ synthesized by oxide MBE at the CNM, Argonne. Image: Amish Shah, Jian-Min Zuo,

Research Achievement:

The first step towards achieving our goals is to demonstrate the capability of creating complex oxide thin films and heterostructures (see Fig. 1) with fine control of stoichiometry, morphology (see Fig. 2) and thickness. To this end, we have commissioned a state-of-the-art oxide-MBE (Molecular Beam Epitaxy) synthesis tool. We have carried out careful calibration of the relative deposition rates of the various constituent elements to attain the correct sto ichiomery, and also an accurate measure of the total flux of atoms being deposited to attain the correct thickness. Annealing steps have been optimized to obtain atomically smooth films. Furthermore, the use of ozone at the appropriate pressure ensures that the materials are oxidized to their full extent to attain the desired properties. To demonstrate our capability, we have synthesized digital superlattices of $LaMnO_3/SrMnO_3$ where using x-ray scattering and reflectivity, we demonstrate that we have control at the level of a single atomic layer. We have also

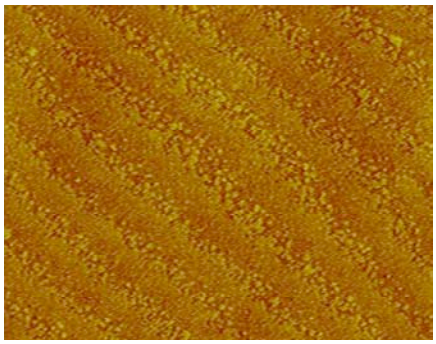

Fig. 2 AFM image of a surface of a superlattice of $(LaMnO_3)_1/(SrMnO_3)_1$ synthesized by oxide MBE at the CNM, Argonne. Image: Tiffany Santos

synthesized films and heterostructures of titanates, nickelates and cobaltates. Using these materials, we have begun a number of projects to explore nanoscale phenomena.

Nickelate/Manganite superlattices: Strained superlattices of $LaNiO_3$ sandwiched between insulating layers may be superconducting according to some theoretical predictions. This is because the under tensile strain, Ni^{3+} would mimic the Cuprate materials, having only one orbital participating at the Fermi level, and being quasi two-dimensional[1]. With Steve May (user, Materials Science Division, Argonne) we synthesized superlattices of $(SrMnO_3)_2/(LaNiO_3)_n$ (n = 1, 2, 4) using oxide MBE at the CNM. A metal-insulator transition was observed as n is decreased from 4 to 1. Analysis of the transport data suggests an evolution from gapped insulator (n = 1) to hopping conductor (n=2) to metal (n=4) with increasing LaNiO3 concentration.

Edge states in Manganite Nanowires: Any finite sized system with an energy gap, when pattened into a finite structure, is expected to have elementary excitations that are characteristic of the boundary. With Peter Abbamonte (user, UIUC) we seek to detect these edge states in patterned thin films of transition metal oxides such as the cuprates and manganites using transport and resonant (soft) x-ray scattering. Manganite films synthesized using oxide MBE at the CNM have been patterned into nanowire arrays in UIUC. Results of studies using resonant x-ray scattering and transport will be presented.

Future Work:

a. We have synthesized thin films of $(Sr,Ba)MnO_3$ which are predicted to allow off center distortions of the nominally Mn^{4+} ($3d^3$) cations. This prediction is remarkable in that typical of-center disortions in ferroelectrics involve d^0 cations (e.g. Ti^{4+}, Ta^{5+} and W^{6+}).[2]

b. Spin-polarized STM investigations of the Neel transition in A-type antiferromagnetic manganite films. This will seek analogs of the Griffiths phase, and antiferomagnetic domain formation in real space in an antiferromagnet.[3]

c. Systematic studies of nanoscale wires and dots, explore the effects of quantum confinement on phase separation with real space probes and transport/magnetic measurements.

d. Tool development: Development of *in-situ* real time rate measurement capabilities using atomic absorption spectroscopy.

References:

1. J. Chaloupka and G. Khaliullin, *Phys. Rev. Lett.* **100** 016404 (2008).

2. S. Bhattacharjee, E. Bousquet, P. Ghosez, "Engineering Multiferroism in $CaMnO_3$," *Phys. Rev. Lett.* **102** 117602 (2009).

3. M. Kleiber, M. Boder, R. Ravlić, R. Wiesendanger, "Topology-Induced Spin Frustrations at the Cr(001) Surface Studied by Spin-Polarized Scanning Tunneling Spectroscopy," *Phys. Rev. Lett.* **85** 4606 (2000).

Publications:

1. "Onset of metallic behavior in strained $(LaNiO_3)_n/(SrMnO_3)_2$ superlattices", S. J. May, T. S. Santos and A. Bhattacharya, *Phys. Rev.* B **79**, 115127 (2009).

Improving Electronic Transport in Nanostructured Organic Semiconductor Solar Cells

C. –Y. Nam, I. R. Gearba, and C. T. Black
Center for Functional Nanomaterials, Brookhaven National Laboratory

Scientific Thrust Area: CFN Electronic Nanomaterials group

Research Achievement:

The highest performing organic semiconductor solar cells employ device active layers of phase-separated blends of semiconducting polymers and fullerenes. This 'bulk heterojunction' architecture provides a highly nanostructured internal morphology that both decouples the photogenerated exciton diffusion length (<~10 nm) from the device active layer thickness and increases the heterojunction area available for exciton dissociation. State-of-the-art bulk heterojunction devices have demonstrated photovoltaic power conversion efficiencies between 4-5% using a single blend layer of regioregular poly(3-hexylthiophene) (P3HT) and [6,6]-phenyl-C_{61}-butyric acid methyl ester (PCBM).

The performance cost associated with the bulk heterojunction solar cell architecture comes from a significantly increased probability for deleterious interfacial charge recombination, an effect that places an upper limit on the device active layer thickness for effective charge collection and thereby constrains the amount of solar photon absorption. Our experimental efforts explore methods for improving electronic transport in bulk heterojunction device active layers in order to provide more effective charge collection and ultimately better performance.

We have demonstrated improvements in photovoltaic device performance of *ambient-air processed* bulk heterojunction solar cells having an active blend layer of organic P3HT:PCBM, with power conversion efficiencies reaching as high as 4.1% - comparable to state-of-the-art similar bulk heterojunction devices fabricated in *air-free environments* (Fig. 1a). We have combined high resolution transmission electron microscopy (Figs. 1b, 1c) with detailed analysis of electronic carrier transport in both the p-type P3HT and n-type PCBM in order to quantitatively understand the effects of oxygen exposure and different thermal treatments on electronic conduction through the highly nanostructured active blend semiconductor network. Improvement in photovoltaic device performance by suitable post-fabrication thermal processing results from a reduced oxygen charge trap density in the active blend layer and is consistent with a corresponding slight thickness increase in a ~4 nm Al_2O_3 hole-blocking layer present at the electron-collecting contact interface (Fig. 1c).

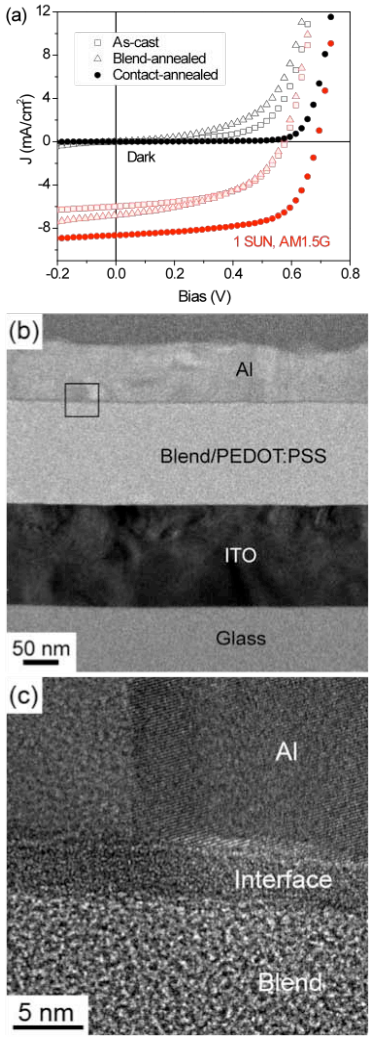

Fig. 1. (a) Dark and illuminated *J-V* of P3HT:PCBM blend solar cells with different anneals. (b) Bright-field TEM cross-section of a contact-annealed device. (c) High resolution image of blend-Al interface.

We can improve the transverse hole conductivity of p-type P3HT by as much as 5 times using a new experimental method for thermal crosslinking the semiconducting polymer using radical initiators (Fig. 2a). We achieve this improvement without any associated detrimental shift in the P3HT spectral light absorption to higher energies (i.e., blue shift) (Fig. 2b). Previous experimental methods to crosslink P3HT have improved mobility only at the expense of a blue shift in spectral absorption caused by a decrease in polymer chain conjugation length. Grazing incidence x-ray diffraction correlates P3HT film structural changes to measured electronic and optical properties and reveals polymer chain orientation changes responsible for increased pi-pi overlap in crosslinked P3HT. Model planar heterojunction PV devices having a crosslinked P3HT p-type active material show improved power conversion efficiency by three times as compared to otherwise identical devices having un-crosslinked P3HT active material (Fig. 2c).

We may introduce improvements in charge collection in the bulk heterojunction architecture by introducing nanostructured electrical contacts, which serve to shorten charge collection pathways in low-mobility organic semiconductor materials. We demonstrate the utility of this approach using a P3HT-fullerene blend device incorporating alkane-chain functionalized single wall carbon nanotubes into the active layer. Blend devices containing nanotubes show an 11% average increase in power conversion efficiency over control devices without nanotubes (from 3.2% to 3.5%) stemming largely from an increase in optimum device active layer thickness from ~90 nm to ~110 nm. Electrical characterization of model bi-layer devices reveals that carbon nanotube addition enhances carrier collection by effectively increasing P3HT hole mobility without an associated increase in charge recombination.

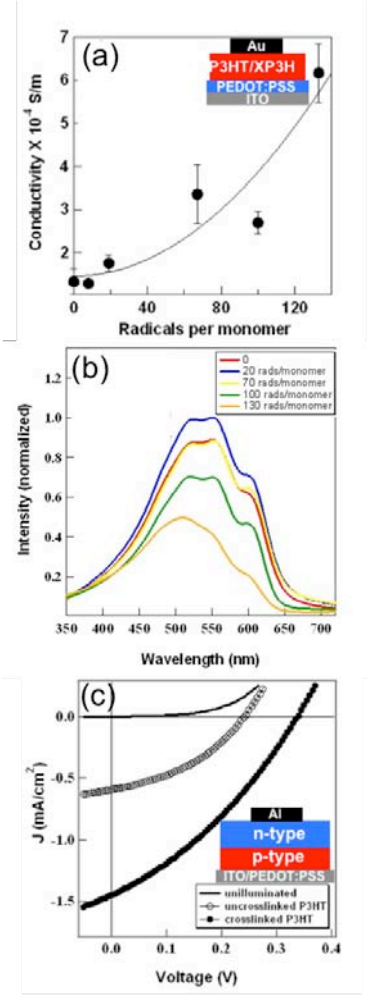

Fig. 2. (a) P3HT conductivity versus added crosslinker amount. Inset: Device schematic. (b) UV-VIS absorption spectra for P3HT films having increasing amounts of added crosslinker. (c) *J-V* for two planar heterojunction solar cells (1 SUN AMG). Inset: Device schematic.

Future Work:

Future work will further explore improvements to the bulk heterojunction solar cell architecture through introduction of nanostructured electrical contacts. We will employ methods of self assembly to precisely define and tune contact dimensions (e.g., pillar height, diameter, and pitch) for understanding the interplay between length scales for solar light absorption and charge collection.

Publications:

C. –Y. Nam, D. Su, and C. T. Black, *High-Performance All Air-Processed Polymer-Fullerene Bulk Heterojunction Solar Cells*, Advanced Functional Materials, submitted (2009).

R. I. Gearba, C. –Y. Nam, R. Pindak, and C. T. Black, *Improved Transverse Hole Conductivity in Organic Semiconducting Polythiophene by Thermal Crosslinking* , Applied Physics Letters, submitted (2009).

Active and Passive Metamaterials Research at CINT

Igal Brener[1], Hou-Tong Chen[2], Xomalin G. Peralta[3], Andrew Strikwerda[4], Richard D. Averitt[4], W. Padilla[5], Evgenya Smirnova[2], Abul K. Azad[2], Antoinette J. Taylor[2], John O'Hara[2], Steven Brueck[6], K. M. Dani[2], Zahyun Ku[6], Prashanth C. Upadhya[2], Rohit P. Prasankumar[2], Michael Cich[1], Clark Highstrete[1], Mark Lee[1], W. Liam[7], D. Mittleman[7], M. Wanke[1]

[1]*Center for Integrated Nanotechnologies , Sandia National Laboratories*
[2]*Center for Integrated Nanotechnologies, Los Alamos National Laborator,*
[3]*Department of Physics and Astronomy, The University of Texas at San Antonio*
[4]*Physics Department, Boston University*
5Department of Physics, Boston College
[6]*Center for High Technology Materials and Electrical and Computer Engineering Dept., Univ. of New Mexico*
[7]*Rice University, Houston*

Scientific Thrust Area: Nanophotonics and Optical Nanomaterials

Research Achievement:

The recent discovery of metamaterials has led to the demonstration of unique optical behavior such as a negative index of refraction [1] and cloaking [2]. Metamaterials provide a new scale-invariant design paradigm to create functional materials thereby enhancing our ability to manipulate, control, and detect electromagnetic radiation.

This poster highlights some of the activity at CINT in the area of active and passive metamaterials both as internal CINT science that reaches into both National Laboratories and in collaboration with a number of users at several universities.

Passive Metamaterials:

Composite metamaterial elements with sub-wavelength scale ($\sim\lambda_0/10$), such as split ring resonators (SRRs), can be patterned in a periodic array to form metamaterials. Thus metamaterials can be considered as an effective medium and are well described by magnetic permeability $\mu(\omega)$ and/or electric permittivity $\varepsilon(\omega)$, Our early work concentrated on fundamental aspects of planar metamaterials and at Terahertz frequencies such as electrical resonator designs [3], demonstrations of complementary designs (Babinet's principle) in metamaterials [4], etc. Metamaterials however, offer new degrees of freedom that are not easily attainable through other approaches, such as large optical phase shifts and tunable resonators that can be designed throughout much of the infrared spectra. Recently, we have used taken advantage of the latter properties to design polarimetric components at terahertz frequencies [5]. We explored the sensor aspects of metamaterials by taking advantage of the sensitivity of metamaterial resonances to local changes in the dielectric environment [6]. For example, using appropriate linker molecules, planar metamaterials can be turned into protein sensors. Also, we investigated a number of approaches to improve the sensitivity of such sensors, for example, by fabricating samples on free standing sub-wavelength membranes [7].

Active Metamaterials:

Intentional modifications to the local dielectric environment of the subwavelength constituents of metamaterials allow for dynamic control of their transmission and reflection. For example, direct photoexcitation of carriers in planar metamaterials can provide an AC shunt to the small capacitive gaps in planar metamaterial designs and thus

decrease the resonance strength. This effect was demonstrated at THz frequencies in Ref. [8]. More recently, this was demonstrated also in the near IR using fishnet metamaterials with an amorphous silicon dielectric spacer, and fabricated using nanolithography. Using the latter scheme, we achieved sub-picosecond modulation speeds corresponding to data rates of Terabits per second.

A similar dynamic change can be obtained by fabricating metallic metamaterial samples on a doped semiconductor layer and utilizing the top metal as a Schottky gate. Upon reverse bias, carriers are depleted from the capacitive gaps and the metamaterial resonances appear in transmission. Removal of that bias causes the capacitive gaps to be shunted and then the resonance features disappear. This effect has been used to design amplitude [9,] and phase [10] modulators, and more recently multi-pixel spatial light modulators for IR beams.

Future Work

We will push the operating wavelength of active metamaterials to the mid and near IR. This will necessitate the use of nanolithography and the exploration of other semiconductors, metals and other types of conductors. Additionally, research into new schemes for 3D lithography of metamaterials are under way.

Sandia is a multiprogram laboratory operated by Sandia Corporation, a Lockheed Martin Company, for the United States Department of Energy's National Nuclear Security Administration under Contract DE-AC04-94AL85000.

References and Publications

1. J. B. Pendry, and D. R. Smith, "Reversing light with negative refraction," Physics Today **57**, 37-43 (2004).
2. D. Schurig, J. J. Mock, B. J. Justice, S. A. Cummer, J. B. Pendry, A. F. Starr, and D. R. Smith, "Metamaterial electromagnetic cloak at microwave frequencies," Science **314**, 977-980 (2006).
3. W. J. Padilla, M. T. Aronsson, C. Highstrete, M. Lee, A. J. Taylor, and R. D. Averitt, "Electrically resonant terahertz metamaterials: Theoretical and experimental investigations," Physical Review B **75**, - (2007).
4. H. T. Chen, J. F. O'Hara, A. J. Taylor, R. D. Averitt, C. Highstrete, M. Lee, and W. J. Padilla, "Complementary planar terahertz metamaterials," Optics Express **15**, 1084-1095 (2007).
5. X. G. Peralta, E. I. Smirnova, A. K. Azad, H. T. Chen, A. J. Taylor, I. Brener, and J. F. O'Hara, "Metamaterials for THz polarimetric devices," Optics Express **17**, 773-783 (2009).
6. J. F. O'Hara, R. Singh, I. Brener, E. Smirnova, J. G. Han, A. J. Taylor, and W. L. Zhang, "Thin-film sensing with planar terahertz metamaterials: sensitivity and limitations," Optics Express **16**, 1786-1795 (2008).
7. X. G. Peralta, C. L. Arrington, M. C. Wanke, I. Brener, J. D. Williams, E. Smirnova, A. J. Taylor, J. F. O'Hara, A. Strikwerda, R. D. Averitt, and W. J. Padilla, "Flexible, Large-Area Metamaterials Fabricated on Thin Silicon Nitride Membranes," 2008 Conference on Lasers and Electro-Optics & Quantum Electronics and Laser Science Conference, Vols 1-9, 314-315, 3638 (2008).
8. W. J. Padilla, A. J. Taylor, C. Highstrete, M. Lee, and R. D. Averitt, "Dynamical electric and magnetic metamaterial response at terahertz frequencies," Physical Review Letters **96**, - (2006).
9. H. T. Chen, W. J. Padilla, J. M. O. Zide, A. C. Gossard, A. J. Taylor, and R. D. Averitt, "Active terahertz metamaterial devices," Nature **444**, 597-600 (2006).
10. H.T. Chen, W. J. Padilla, M. J. Cich, A. K. Azad, R. D. Averitt, and A. J. Taylor, "A metamaterial solid-state terahertz phase modulator," Nature Photonics **3**, 148-151 (2009).

Growth of Single-Crystalline $B_{12}As_2$ on m-plane (1-100) 15R-SiC

H. Chen, Y. Zhang, G. Wang and M. Dudley, Department of Materials Science and Engineering, Stony Brook University, Stony Brook, NY 11794-2275; Z. Xu and J.H. Edgar, Department of Chemical Engineering, Kansas State University, Manhattan, KS; T. Batten and M. Kuball, H.H. Wills Physics Laboratory, University of Bristol, Bristol, United Kingdom; L. Zhang, L. Wu and Y. Zhu, Center for Functional Nanomaterials, Brookhaven National Laboratory, Upton, NY

Research Achievement

Icosahedral boron arsenide $B_{12}As_2$ (IBA) is a wide band gap semiconductor (3.47eV) with the extraordinary ability to "self-heal" radiation damage. This makes it an attractive choice for devices exposed to radiation levels which can severely degrade the electrical properties of conventional semiconductors, causing devices to cease functioning. Among the particularly intriguing possible applications for IBA are Beta Cells, devices capable of producing electrical energy by coupling a radioactive beta emitter to a semiconductor junction, another space electronics [1-4]. IBA is based on twelve-boron-atom icosahedra, which reside at the corners of an α-rhombohedral unit cell, and two-atom As-As chains lying along the rhombohedral [111] axis [1]. In the absence of native substrates, IBA has been heteroepitaxially grown on substrates with compatible structural parameters. To date, this has been attempted on substrates with higher symmetry than IBA such as Si and 6H-SiC. Unfortunately, growth of a lower symmetry epilayer on a higher symmetry substrate often produces structural variants, a phenomenon known as degenerate epitaxy [5, 6]. These variants, which comprise both the rotational and translational variety, are expected to have a detrimental effect on device performance, and have severely hindered progress of this new material to date.

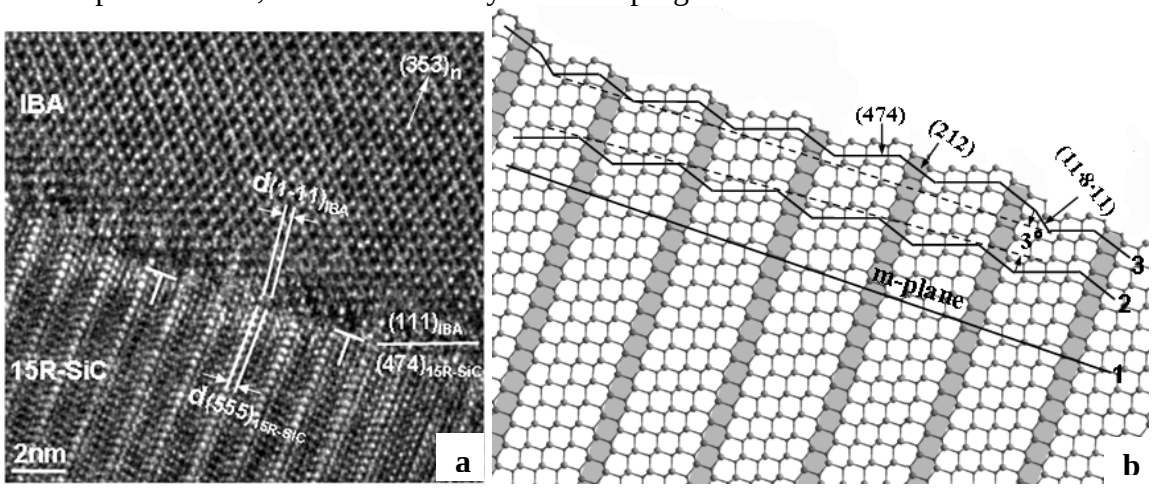

Fig. 1. (a) HRTEM image recorded along the [10-1] zone axis (equivalent to [11-20] in the hexagonal system) showing a sharp IBA/15R-SiC interface and the (353) surface orientation of IBA. The symbol ⊥ marks the location of interfacial dislocations with extra half-planes in the 15R-SiC substrate. (b) Cross-sectional visualization along [10-1] of the 15R-SiC structure. The uppermost black line indicates the on-axis, facet configuration comprising closed-packed (474) atomic terraces and coupled (212) and (11·8·11) step risers. The middle black line indicates the surface comprising only (474) and (212) facets which results in a 3° misorientation from m-plane and the lower line indicates the m-plane itself (unfaceted). Note the lamellar nano-domains of 3C-SiC structure bounded by the (474) facets and the shaded domain boundaries parallel to the (111) plane ((0001) in hexagonal system).

In this work, heteroepitaxial growth of untwinned single crystal IBA on m-plane 15R-SiC is demonstrated. Synchrotron white beam x-ray topography (SWBXT), Raman

spectroscopy and high resolution transmission electron microscopy (HRTEM) confirm the high quality of the films (see Fig 1(a). High quality growth is shown to be mediated by ordered nucleation of IBA on close packed (474) facets which dominate the m-plane surface. Such nucleation is shown to be possible for untwinned but not for twinned IBA (see Figs. 1(b) and 2). This work demonstrates that m-plane 15R-SiC is a good substrate choice for the growth of high-quality, untwinned IBA epilayers for future device applications.

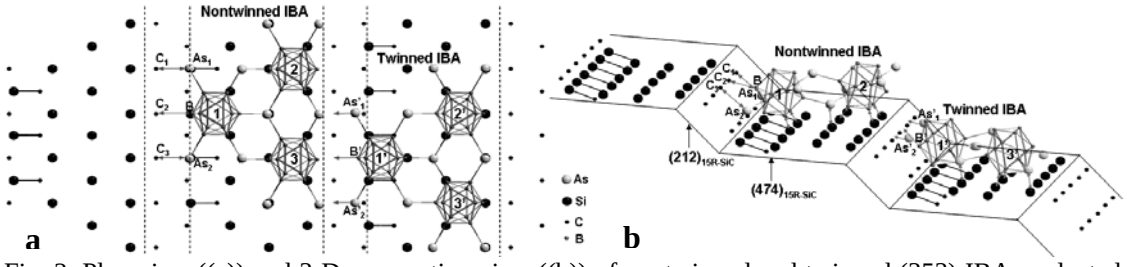

Fig. 2. Plan view ((a)) and 3-D perspective view ((b)) of nontwinned and twinned (353) IBA nucleated on m-plane 15R-SiC surface facets. For the non-twinned IBA, the triangular configuration of B atoms at the bottoms of icosahedra 1, 2 and 3 bond to the similarly oriented triangular configurations of Si atoms exposed on the (474) terrace (see (a) and (b)). In addition, atoms As1, B, and As2 can be well bonded to atoms C1, C2, and C3, respectively, on the neighboring (212)15R-SiC step riser. In contrast, while the triangular configuration of B atoms at the bottoms of icosahedra 1', 2' and 3' can similarly bond to the (474) terrace, atoms As'1, B', As'2 are not able to reasonably bond to the corresponding C atoms on the neighboring (212)15R-SiC step riser.

Future Work

Work is underway to grow IBA films on large area m-plane SiC substrates. Once completed, simple devices will be fabricated and tested to confirm improved performance.

Publications

H. Chen, G. Wang, M. Dudley, L. Zhang, Y. Zhu, and J. Edgar, ***Mater. Res. Soc. Symp. Proc.*, 994,** 0994-F03-01, Warrendale, PA, (2007).

H. Chen, G. Wang, M. Dudley, Z. Xu, J. H. Edgar, T. Batten, M. Kuball, L. Zhang, and Y. Zhu, **Appl. Phys. Lett.**, 92, 231917, (2008).

H. Chen, G. Wang, M. Dudley, L. Zhang, L. Wu, Y. Zhu, Z. Xu, J. H. Edgar, and M. Kuball , **J. Appl. Phys.**, 103, 123508-1 – 123508-9, (2008).

H. Chen, G. Wang, M. Dudley, L. Zhang, Y. Zhu, Z. Yu, Y. Zhang, J.H. Edgar, J. Gray, and M. Kuball, ***Mater. Res. Soc. Symp. Proc.***, Vol. **1069**, D08-03, Warrendale, PA, (2008).

References

1. D. Emin, Physics Today, 55, January (1987)
2. M. Carrard, D. Emin and L. Zuppiroli, Phys. Rev. B, 51(17), 11270 (1995).
3. D. Emin, J. Sol. Sta. Chem., 177, 1619 (2004)
4. D. Emin and T. L. Aselage, J. App. Phys., 97, 013529 (2005)
5. S.W. Chan, J. Phys. Chem. Solids, 55, 1137 (1994)
6. C. P. Flynn and J. A. Eades, Thin Soild Films, 389, 116 (2001)

Acknowledgements. Financial support from the National Science Foundation Materials World Network Program under Grant No.0602875 and by the Engineering and Physical Science Research Council (EPSRC) under Grant No. EP/D075033/1 under the NSF-EPSRC Joint Materials Program is acknowledged. SWBXT was carried out at Stony Brook Topography Facility (Beamline X19C) at the National Synchrotron Light Source (NSLS), Brookhaven National Laboratory (BNL), which is supported by the U.S. Department of Energy (D.O.E.) under Grant No. DE-AC02-76CH00016. Research carried out (in part) at the Center for Functional Nanomaterials, BNL, which is supported by the U.S. Department of Energy, Division of Materials Sciences and Division of Chemical Sciences, under Contract No. DE-AC02-98CH10886.

"Giant" Nanocrystal Quantum Dots: Suppressed Blinking and Auger Recombination Through Solution-Phase Physical and Electronic-Structure Engineering

Jennifer Hollingsworth[1,2], Han Htoon[1,2], Javier Vela[2], Yongfen Chen[2], Victor Klimov[1,2], Floren Garcia Santamaria[2], Donald Werder[2], Joanna Casson[2]

[1]Center for Integrated Nanotechnologies and [2]Chemistry Division, Los Alamos National Laboratory

Scientific Thrust Area: Nanophotonics and Optical Nanomaterials

Research Achievement:

In many respects, semiconductor nanocrystal quantum dots (NQDs) are near-ideal "building blocks" for light-emission applications. Their optically excited emission is efficient (quantum efficiencies can approach unity), narrow-band ("color-pure"), and particle-size-tunable, i.e., light-output colors are precisely tunable from the ultraviolet through the visible and into the mid-infrared depending on NQD composition and size. Furthermore, NQDs are synthesized using scalable and inexpensive solution-phase approaches, rendering NQDs with "molecule-like" properties and an ability to be chemically processed. Despite these enabling characteristics, conventional NQD optical properties are sensitive to NQD surface chemistry and chemical environment, which has three important results: (1) high NQD solution-phase photoluminescence quantum yields are not maintained in the solid state (e.g., 90% solution-phase QYs can drop to ~10% when the NQDs are deposited into thin-film form), (2) NQDs "bleach" (PL intensity degrades over time), and (3) NQDs at the single-particle level "blink" (exhibit fluorescence intermittency), all limiting total NQD "brightness."

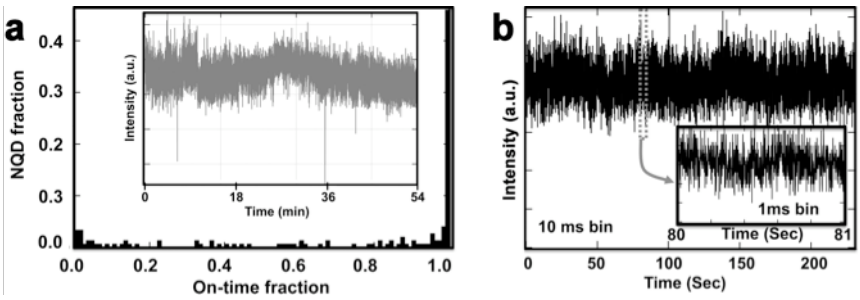

Figure 1. (a) On-time histogram for prototype (CdSe)19CdS g-NQDs. Inset shows fluorescence time trace for a representative g-NQD with an experimental temporal resolution of 200 ms. (b) Fluorescence time trace for representative individual g-NQD with temporal resolutions of 10 ms and 1 ms (inset), revealing that non-blinking behavior is evident at 'all' time-scales.

We recently reported that these key NQD optical properties—quantum yield, photobleaching and blinking—can be rendered independent of NQD surface chemistry and chemical environment by growth of a very thick, defect-free inorganic shell (Chen, et al. *J. Am. Chem. Soc.* 2008). Effectively, we isolated the wavefunction of the NQD core from its surface, creating a colloidal NQD that is structurally more akin to physically grown epitaxial QDs. We named this new functional "class" of NQD the "giant" NQD (g-NQD). Importantly, g-NQDs do not photobleach, are insensitive to changes in surface chemistry, and show markedly improved blinking behavior (Fig. 1). To date, for example, up to 50% of a given sample is "non-blinking," where non-blinking is defined as the NQD being "on" under continuous excitation for >99% of the long observation time of 54 minutes.

Suppressed blinking is a strong indicator of additional "new physics" that is afforded by this new class of NQD. Namely, suppressed blinking is an indicator of suppressed Auger recombination, where Auger recombination is a nonradiative carrier (electron-hole) recombination process that is active (and can outcompete radiative recombination processes) when an NQD is charged or populated with more than one electron-hole pair (Klimov et al. *Science* 2000). Through a random series of surface-related "charging" and "discharging" events, NQDs become alternatingly susceptible to nonradiative Auger recombination and, thus, successively turn "off" then "on," or blink. When Auger recombination is inactive, even a charged NQD should not blink. Therefore, the suppressed blinking behavior observed for g-NQDs is a possible indicator of suppressed Auger recombination.

Recently, we performed ensemble photoluminescence dynamical studies on g-NQDs that revealed more direct evidence for strong suppression of non-radiative Auger recombination – including biexciton lifetimes that are 50 times longer than those obtained for conventional NQDs. Also, we performed low-temperature single-g-NQD photoluminescence studies that revealed unprecedented emission from multiexciton states. In the case of conventional NQDs, multiexciton states cannot participate in emission, while for g-NQDs, multiexciton-state emission is in fact efficient. In this way, it is clear that g-NQDs can afford *new exciton→photon conversion pathways*.

Future Work:

Together, these novel properties have important implications for diverse applications from advanced bioimaging to room-temperature single-photon sources and efficient solid-state lighting. The observed enhanced environmental stability and novel photophysics go a long way toward solving the outstanding issues (e.g., sensitivity to chemical environment, blinking, and efficient nonradiative Auger recombination processes) that have to date limited the utility of these otherwise promising light-emitting nanomaterials. Further, the prototype g-NQDs provide a unique "test bed" for fundamental studies of the effect of nanoscale architecture in semiconductor systems on optical and electronic properties. Future work in the areas of nanomaterials synthesis, atomic-level structural characterization, and advanced spectroscopy will enable the fundamental understanding necessary to generalize these important early results to new g-NQD systems.

Publications

1. Chen, Y., Vela, J., Htoon, H., Casson, J. L., Werder, D. J., Bussian, D. A., Klimov, V. I., and Hollingsworth, J. A.,""Giant" multishell CdSe nanocrystal quantum dots with suppressed blinking," *J. Am. Chem. Soc.* **130**, 5026 (2008).
2. Hollingsworth, J. A., Vela, J., Chen, Y., Htoon, H., Klimov, V. I., and Casson, A. R., "Giant multishell CdSe nanocrystal quantum dots with suppressed blinking: novel fluorescent probes for real-time detection of single-molecule events," *Proc. SPIE* 7189, 718904 (2009).
3. Hollingsworth, J. A.; Chen, Y.; Vela, J.; Htoon, H.; Klimov, V. U.S. Patent Application No. 61/065,077 (Feb. 2009): "Thick-shell Nanocrystal Quantum Dots."

Tunable ferroelectric photonic crystals using epitaxial barium titanate thin films as the nonlinear medium

Pao Tai Lin[a], Alexandra Imre[b], Ralu Divan[b], Leonidas E. Ocola[b,*], B. W. Wessels[a,**]

[a] Department of Materials Science and Engineering, Northwestern University, 2220 Campus Dr, Evanston, IL 60208, USA

[b] Center for Nanoscale Materials, Argonne National Laboratory, Argonne, IL 60439, USA

[*,**] E-mail address: ocola@anl.gov, b-wessels@northwestern.edu

Proposal Title: CNM-292 Fabrication of nano electro-optic devices on epitaxial Barium Titanate thin films

Research Achievement: The optical properties of two dimensional photonic crystal (PhC) were investigated using ferroelectric barium titanate (BTO) thin films. BTO is a promising non-linear electro-optic (E-O) material with a high E-O coefficient and fast response time. Beyond its application in the optical communication, BTO has the potential to replace current semiconductor processors, which are limited by their speed and high energy consumption. To utilize BTO as a micron scale device for their enhancement of E-O coefficient is required. This can be achieved by using "slow light" effects observed in PhC structures. In this project the PhC structure was fabricated by ion milling using a dual beam focused ion beam (FIB). Because BTO is a chemically inert and mechanically hard material, conventional wet etching is not practicable for its nano patterning.

Highly uniformed PhC structures were fabricated and imaged by scanning electron microscopy (SEM). Fig. 1 (a) shows the top surface of a PhC consisting of a square array of air holes. The lattice constant is 450 nm. The black circles are the milled air holes and the gray area is the BTO dielectric stack. From the cross sectional view in Fig. 1 (b), the hole depth from is 450 nm where the hole diameter at the opening is 250 nm and 220 nm at the bottom. Hence an aspect ratio greater than two is achieved. The hole is slightly wider at the opening due to the ion beam having a Gaussian beam profile. Nevertheless there is minimal stigmatism in the focused ion beam optics since there is no distortion of the circular air hole. The photonic band structure of fabricated PhC shown in Fig. 1 (c) is calculated by 2-D finite difference time domain (FDTD) method. The vertical green lines indicate the photonic band gaps at X and M points. The calculation is along the Γ-X and M- Γ which are <1 0> and <1 1> directions in k space, respectively. From Fig. 1 (c) the gap is wider at the X point than the M point. The broad band gaps tell the BTO PhC has a broad bandwidth which is attributed to the high refractive index contrast between BTO and air.

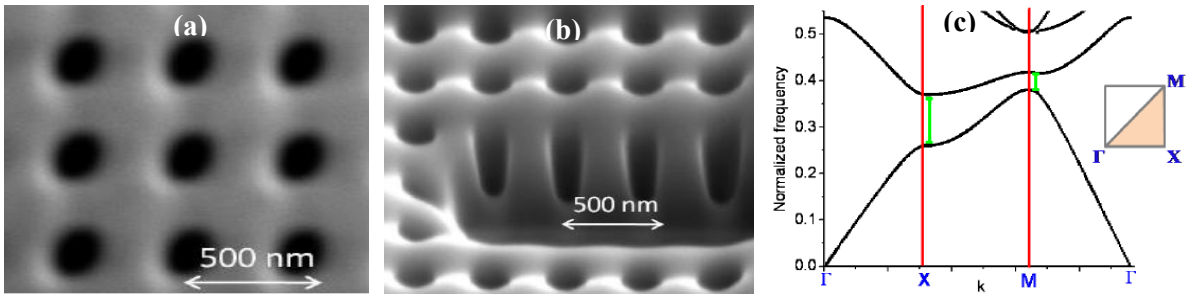

Figure 1

Optical diffraction patterns were analyzed to determine the symmetry of the PhC structure. A 3 dB modulation of light intensity is demonstrated from its thermo-optical response. Fig. 2 (a) shows the transmission diffraction pattern using a multiple wavelengths argon ion laser. The spots in Fig. 2 (a) represent 1st order diffraction. The pattern has diffraction along the [1 0] and [1 1] symmetry directions as would be expected for a PhC with square lattice symmetry. The bright

diffraction spots result from a very small patterned area. That indicates the PhC has a very high spatial uniformity. The thermo-optical response of the BTO PhC is shown in Fig. 2 (b). The normalized 1st order diffraction efficiency η decreases from 2.1 to 1 when temperature increases from 30°C to 150°C. No variation of the diffraction angle θ is found during the heating or cooling process. This indicates the thermal response is solely attributed to the temperature dependence of n_{BTO}; no thermal expansion of PhC lattice parameter is involved. The observed thermo-optical effect can be applied in the tuning of the photonic band gap. The PhC spectrum shifts if there is a change of n_{BTO}. From the FDTD calculation heating to 120°C leads to a 57 nm red shift of the band structure. Strong light scattering from the BTO PhC is also observed as shown in fig. 2 (c). The light is coupled to the PhC cavity through the waveguide edge. The bright rectangle at the right of the image is the scattering light from PhC and it indicates the light is highly localized within the PhC cavity. The scattering light intensity is proportional to the degree of light localization. The strong light confinement can significantly enhance the optical nonlinearity of the BTO thin films, potentially leading to ultra compact photonic devices.

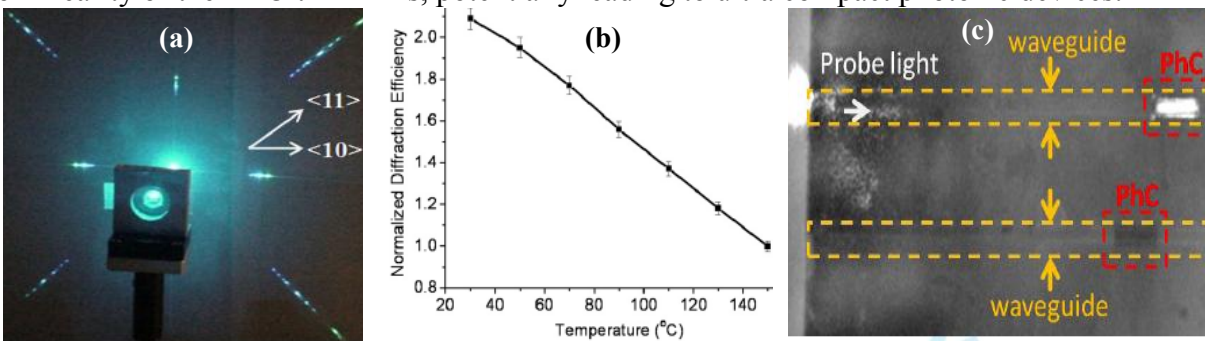

Figure 2

Future Work: CNM-827 Fabrication of integrated nano-photonic circuits on epitaxial barium titanate thin films

Further work is directed toward tunable 2-D photonic circuits. E-O devices having fabricated PhCs can be potentially used in a low V-pi waveguide modulator, slow light buffer, tunable filters, and high Q resonators. We are interested in photonic circuit fabrication using non-linear optical materials such as BTO thin films. BTO has low absorption constant in both IR and visible range. Furthermore BTO has a large E-O coefficient and exhibits broad band second harmonic generation.

The proposed nonlinear optic circuits are composed of micro-rings and photonic crystals which have a sharp transmission line and a well defined photonic band structure. The optic circuits can be generated by high resolution FIB and laser writing techniques. The device tunability is characterized by measuring the shifting of the resonant frequency with bias. The device performance is evaluated by comparing the experiments with the FDTD simulation. Successful completion of the project would lead to new generation of integrated and tunable non-linear photonic devices and circuits.

Acknowledgement: The author thanks Dr. Streiffer and Dr. Mancini for their strong support in this project. The arrangement provided by Dr. Gregar and Mrs. Clark from Center for Nanoscale Materials (CNM) user office is especially appreciated. This work was supported by the NSF through ECS Grant No. 0457610 and ECCS-0801684. FIB was done at the CNM at Argonne National Laboratory, supported by the US Department of Energy, Office of Science, Office of Basic Energy Sciences, under Contract No. DE-AC02-06CH11357.

Publications: **1.** **"**Two dimensional ferroelectric photonic crystal waveguides: simulation, fabrication, and optical characterization," *J. Lightwave Tech.* (2009) **2.** **"**Thin film ferroelectric photonic crystals and their application to thermo-optic switches," Opt. Commun. (2009) **3.** "Ferroelectric thin film photonic crystal waveguide and its electro-optic properties," *J. Opt. A: Pure Appl. Opt.* (2009) **4.** "Cascaded Bragg Reflectors for Barium titanate Thin Film Electro-optic Modulator," *J. Opt. A: Pure Appl. Opt.* 10 015302 (2008) **5.** "Non-linear Photonic Crystal Waveguide Structures Based on Barium Titanate Thin Films and their Optical Properties," *Appl. Phys. Lett.* 90, 201104 (2007)

Electron Donor-Acceptor Interactions Directed Self Assembly of Organic Nanostructures

Yi Liu, Organic Facility
The Molecular Foundry, Lawrence Berkeley National Laboratory

Scientific Thrust Area

The growing needs for miniaturization and better efficiency of electronic devices have inspired enormous interests in obtaining novel semiconductor nanostructures. One particular challenge is to obtain nanostructures with continuous interface between electron rich *p*-type materials and electron deficient *n*-type materials in order to facilitate charge separation and charge transport. This demands the understanding of organization principles of electroactive groups with molecular precision in multi-component systems, which also motivates the design and synthesis of new electron donors and acceptors. Our research focuses on utilizing the donor-acceptor interactions to direct the assembly of functional high-order nanostructures for the application in organic electronics.

Research Achievement

We have demonstrated the directed self-assembly of functional molecular and supramolecular assemblies, including interlocked molecular machines, highly ordered donor-acceptor stacks, and 1D organic nanowires.

High-fidelity Assemblies of Interlocked Molecules for Molecular Machinery

High-yield, one-pot synthesis of various interlocked structures have been developed to provide a convenient approach towards the development of sophisticated switchable molecular systems that are responsive towards electrochemical or photochemical stimuli. Examples include the expeditious formation of [2]rotaxanes[1] (Figure 1a) and dynamic switchable [2]catenanes[2,3] (Figure 1b) from multi-component reactions.

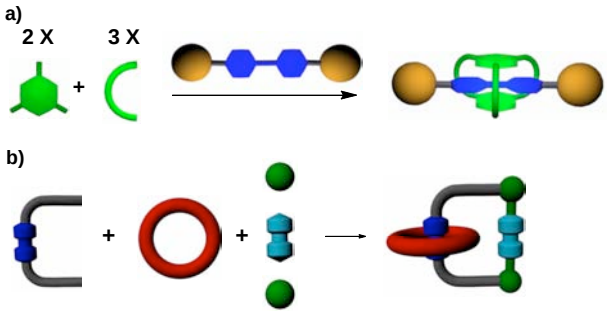

Figure 1. Cartoon representations of the one-pot assembly approach for the synthesis of a) [2]rotaxanes, and b) [2]catenanes.

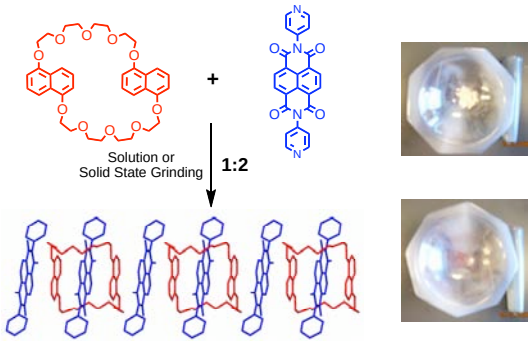

Figure 2. Assembly of alternative donor-acceptor stacks.

Supramolecular Aggregates as Novel Electronic Materials

We have shown a unique host-guest system that rapidly leads to extended 1D alternative donor-acceptor (ADA) stacks.[4] (Figure 2) The 1:2 complex can be obtained as a precipitate from solution within minutes or, more remarkably, from a solid-to-solid mechanical grinding process. The ADA stacking was confirmed by single crystal and powder XRD analysis and further characterized by solid

state CPMAS ^{13}C and ^{15}N NMR spectroscopy. Current findings not only provide a convenient way to a novel class of ADA stacks involving macrocyclic host, but also represent an important step in transferring electro-active host-guest systems from solution to the solid state. Investigations on their electronic and photophysical properties are currently underway.

1D Organic Nanoribbons Based on Liquid Crystaline Materials

Organic supramolecular aggregates with defined topology, such as 1D nanowires and nanotubes, represent attractive building blocks for electronic devices. We have obtained twisted organic nanoribbons with the width around 200 nm from the drop cast solution of a series of triphenylene derivatives, as indicated by scanning electron microscopy. (Figure 3) The nanoribbon formation is highly dependent on the nature of the solvent. The characterization of photoconductivity and electron transporting properties are currently underway.

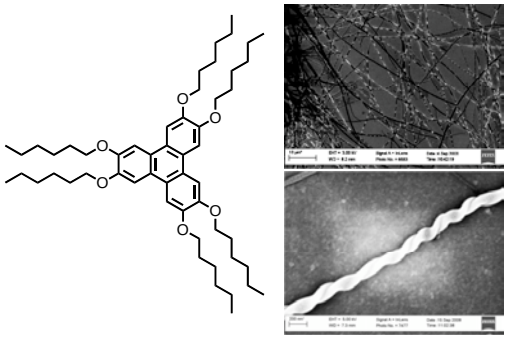

Figure 3. SEM images of organic nanoribbons based on a triphenylene derivative.

Future Work

Design and synthesis of molecular switches containing complementary donor-acceptor pairs is currently underway. Meanwhile, the knowledge obtained from the donor-acceptor systems will be applied on the exploration of small molecule-based *p*-type and *n*-type electronic materials for photovoltaic applications.

Publications

1.Klivansky, L. M.; Koshkakaryan, G.; Cao, D.; **Liu, Y.***, "Linear π-Acceptor Templated Dynamic Clipping to Macrobicycles and [2]Rotaxanes", *Angew. Chem. Int. Ed.* **2009**, *in press*. DOI: 10.1002/anie.200900716.

2. Koshkakaryan, G.; Parimal, K.; He, J.; Zhang, X.; Abliz, Z.; Flood, A. H.; **Liu, Y.***, "π-Stacking Enhanced Dynamic Self-Assembly of Donor-Acceptor Metallo-[2]Catenanes from Diimide Derivatives and Crown Ethers", *Chem. Eur. J.* **2008**, *14*, 10211-10218.

3. **Liu, Y.***; Bruneau, A.; He, J.; Abliz, Z., "Palldaium(II) Directed Self Assembly of Dynamic Donor-Acceptor [2]Catenanes", *Org. Lett.* **2008**, *10*, 765-768.

4. Koshkakaryan, G.; Klivansky, L. M.; Cao, D.; Snauko, M.; Teat, S. J.; Struppe, J. O.; **Liu, Y.***, "Alternative Donor-Acceptor Stacks from Crown Ethers and Naphthalene Diimide Derivatives: Rapid, Selective Formation from Solution and Solid State Grinding", *J. Am. Chem. Soc.* **2009**, *131*, 2078-2079.

5. Juluri, B. K.; Kumar, A. S.; **Liu, Y.**; Ye, T.; Yang, Y-W.; Flood, A. H.; Stoddart, J. F.; Weiss, P. S.; Huang, T. J., "A Nanomechanical Actuator Driven Electrochemically by Artificial Molecular Muscles", *ACS Nano* **2009**, *3*,291-300.

6. **Liu, Y.***; Zhang, X.; Klivansky, L. M.; Koshkakaryan, G., "Enhancing the Reactivity of 1,2,3-Triazoles in 'Click' Macrocycles by Face-to-Face Dibenzylammonium Ion Binding", *Chem. Commun.* **2007**, *45*, 4773-4775.

7. **Liu, Y.***; Klivansky, L. M.; Khan, S. I.; Zhang, X., "Templated Synthesis of Desymmetrized [2]Catenanes with Excellent Translational Selectivity", *Org. Lett.* **2007**, *9*, 2577-2580.

8. **Liu, Y.***, "Self-Assembled Ring-in-Ring Complexes from Metal-Ligand Coordination Macrocycles and β-Cyclodextrin", *Tetrahedron Lett.* **2007**, *48*, 3871-3874.

9. Nygaad, S.; **Liu, Y.**; Stein, P.; Flood, A. H.; Jeppesen, J. O., "Using Molecular Force to Overcome Steric Barriers in a Spring-Like Molecular Ouroborous", *Adv. Funct. Mater.* **2007**, *17*, 751-762.

Tracking Carrier Dynamics in Semiconductor Nanostructures Through Space and Time

Rohit P. Prasankumar[1], Prashanth C. Upadhya[1], George T. Wang[2], Samuel T. Picraux[1], Weng W. Chow[2], Sanjay Krishna[3], and A. J. Taylor[1]

[1]*Center for Integrated Nanotechnologies, Los Alamos National Laboratory*
[2]*Sandia National Laboratories*
[3]*Center for High Technology Materials, Electrical and Computer Engineering Department, University of New Mexico*

Scientific Thrust Area: Nanophotonics and Optical Nanomaterials

Proposal Titles: "Understanding Carrier Dynamics in a Novel Nanoscale System: Quantum Dots in a Well (DWELL) Heterostructure," PI: Sanjay Krishna; "Tracking Carrier Dynamics in Nitride-Based Nanowires," PI: George Wang.

Research Achievement: Semiconductor nanostructures have attracted much recent attention due to the unique size-dependent scaling of their physical properties, providing researchers an opportunity to tune these parameters for applications in areas ranging from medicine to solar energy. Many of these applications depend critically on a detailed knowledge of the response of these nanosystems to photoexcitation on a femtosecond time scale. Ultrafast optical spectroscopy (UOS) is the only technique capable of resolving dynamics in conventional metals and semiconductors at the fundamental time scales of electron and lattice motion.[1] Therefore, the application of UOS to probing the dynamic response of semiconductor nanostructures after femtosecond excitation will increase our understanding of their physics and enable their optimization for applications. In this work, we present ultrafast wavelength-and-time-resolved spectroscopic experiments on one-dimensional semiconductor nanowires (NWs) and quantum dots-in-a-well (DWELL) heterostructures, as well as the first demonstration of a new technique, ultrafast optical wide field microscopy, for performing space-and-time-resolved measurements.

Our density-dependent differential transmission (DT) experiments on a DWELL heterostructure, which consists of InAs quantum dot (QD) layers embedded in InGaAs quantum wells (QW) that are subsequently embedded in bulk GaAs, are particularly relevant to lasing applications.[2] The most unique feature of our data is the negative DT signal ($\Delta T/T<0$) observed at the QD excited state ($\lambda\sim1047$ nm) at high densities (Fig. 1); the low density dynamics have been previously described.[3] Comparison of the positive DT signal from the QW (not shown) with the negative part of the DT signal at the QD excited state reveals that the QW population strongly influences light absorption at the QD excited state through Coulomb interactions between the photoexcited carriers, which has not previously been observed.

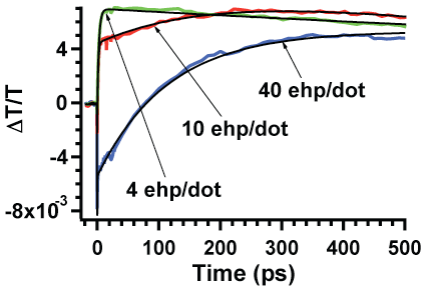

Fig. 1. Density-dependent 800 nm pump, 1047 probe measurements on a DWELL heterostructure.

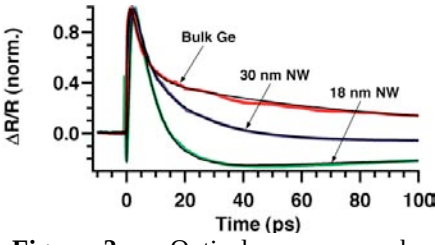

Fig. 2. Optical pump-probe measurements on Ge NWs as a function of NW diameter.[5]

Optical pump-probe experiments on semiconductor nanowires reveal novel effects resulting from the enhanced influence of surface and defect states. An example is shown in Figure 2, revealing that carrier lifetimes increase with diameter in Ge NWs due to trapping at surface states.[5]

Similar experiments performed on GaN NWs demonstrated the ability to tailor the influence of defect states on carrier relaxation through control of the growth temperature. Ultrafast optical spectroscopy thus enables us to shed light on carrier relaxation in these one-dimensional systems.

Finally, we have recently demonstrated an ultrafast optical microscope that combines the spatial resolution of wide field optical microscopy with the temporal resolution of ultrafast optical spectroscopy to rapidly and sensitively acquire images of nearly any sample with high sensitivity, temporal, and spatial resolution. This unique tool is based on a two-dimensional smart pixel array detector that separately demodulates the signal on each pixel, allowing us to detect transmission changes as small as $\Delta T/T \sim 10^{-5}$. We have acquired time-resolved images of a gold patterned Si film (Figure 3) to demonstrate this powerful concept for the first time.

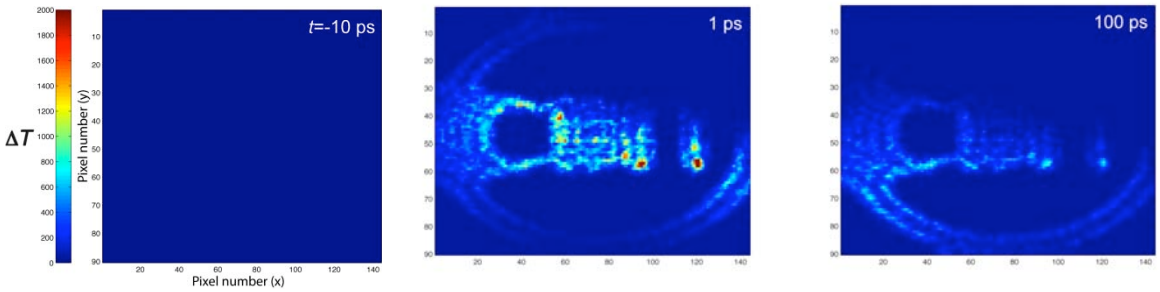

Fig. 3. Ultrafast optical wide field microscope images at different time delays between the pump and probe.

Future Work: We plan to extend our measurements of carrier dynamics in DWELL heterostructures to pump different quantized energy levels over a wide density and temperature range. In addition, we have recently developed a mid-infrared pump, terahertz (THz) probe system that will enable us to simulate photodetector operation with femtosecond time resolution. We will also perform optical-pump THz-probe experiments to measure the photoinduced conductivity in semiconductor NWs. Measurements on radially heterostructured NWs will also enable us to control the influence of surface states on the measured dynamics. Finally, we will apply ultrafast optical wide field microscopy to a number of materials, ranging from nanowires to neurons, to unravel coupled space-time dynamics in these complex systems.

References:

1 R. D. Averitt and A. J. Taylor, J. Phys. Condens. Matter **14**, R1357 (2002).

2 S. Krishna, J. Phys. D: Appl. Phys. **38**, 2142 (2005).

3 R. P. Prasankumar, R. S. Attaluri, R. D. Averitt, J. Urayama, N. Weisse-Bernstein, P. Rotella, A. Stintz, S. Krishna, and A. J. Taylor, Opt. Express **16**, 1165 (2008).

4 V. I. Klimov, J. Phys. Chem. B **104**, 6112 (2000).

5 R. P. Prasankumar, S. G. Choi, S. A. Trugman, S. T. Picraux, and A. J. Taylor, Nano Lett. **8**, 1619 (2008).

Publications:

1. R. P. Prasankumar, P. C. Upadhya, and A. J. Taylor, "Ultrafast dynamics in semiconductor nanowires," **invited review article,** submitted to *Physica Status Solidi (b)*, 2009.
2. R. P. Prasankumar, W. W. Chow, J. Urayama, R. S. Attaluri, R. V. Shenoi, S. Krishna, and A. J. Taylor, "Dynamic light-matter coupling across multiple spatial dimensions in a quantum dots-in-a-well heterostructure," submitted to *Applied Physics Letters.*
3. R. P. Prasankumar, S. G. Choi, S. A. Trugman, S. T. Picraux, and A. J. Taylor, "Ultrafast electron and hole dynamics in germanium nanowires," *Nano Letters* **8**, 1619 (2008).
4. R. P. Prasankumar, R. S. Attaluri, R. D. Averitt, J. Urayama, N. Weisse-Bernstein, P. Rotella, A. Stintz, S. Krishna, and A. J. Taylor, "Ultrafast carrier dynamics in an InAs/InGaAs quantum-dots-in-a-well heterostructure," *Optics Express*, **16**, 1165 (2008).

Synthesis of Plasmonic Nanoparticles for Hybrid Nanophotonic Materials

Yugang Sun and Gary Wiederrecht
Nanophotonics Group, Center for Nanoscale Materials, Argonne National Laboratory
9700 South Cass Avenue, Argonne, Illinois 60439

Scientific Thrust Area

The scientific thrust area of the research is to develop new routes to functional nanophotonic materials. In this thrust, we pursue the development of new optical materials via advanced colloidal synthesis to generate hybrid nanoscale structures over large areas.

Research Achievement

One of the most important successes is the direct growth of anisotropic metal nanoplates with clean surfaces on semiconductor substrates. In general, metal nanoparticles with varying shapes are synthesized through the well-developed solution-based approaches, which rely on surfactant molecules to direct the anisotropic growth of metal nanoparticles, followed by deposition of them on the desired semiconductor substrates with spin casting, Langmuir-Blogdett assembly and transfer, etc. The use of surfactant molecules may deleteriously influence the metal/semiconductor interfaces for applications. As a result, developing simple approaches to efficiently grow metal nanoparticles on semiconductor substrates with clean metal/semiconductor interfaces represents a challenge to synthesize hybrid materials with complex functionalities in nanophotonic applications, such as surface-enhanced Raman scattering (SERS), photoelectrochemical cells for solar energy conversion, and optoelectronics. We have tackled this challenge by combining colloid synthesis, surface chemistry, electrochemistry, and photoelectrochemistry in the last couple of years, leading to a promising progress in controllable growth of anisotropic nanoplates of various metals on semiconductor wafers of both n- and p-types. For example, silver nanoplates with uniform thickness (~25 nm) and different sizes (Figs. 1A and 1B) can be synthesized on highly doped n-type GaAs wafers through simple reactions between an aqueous solution of 1 M $AgNO_3$ and the wafers themselves at room temperature for

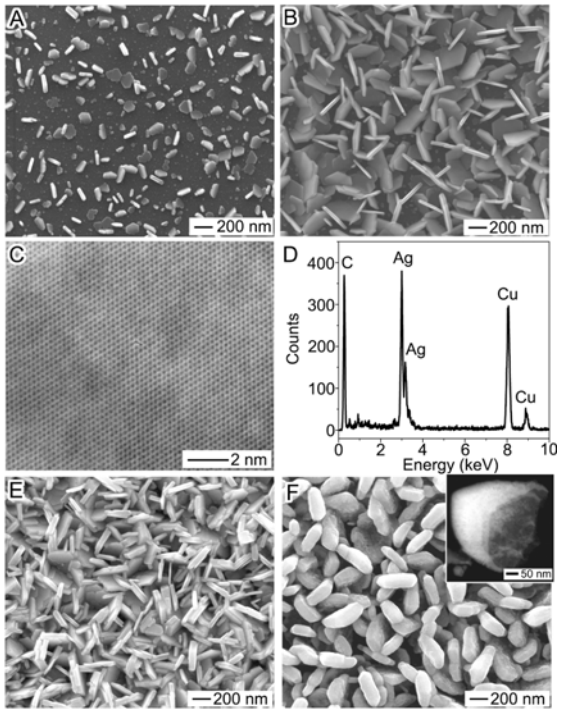

Figure 1. (A, B) SEM images of Ag nanoplates grown on n-GaAs wafers for (A) 0.5 and (B) 2 min. (C) High-resolution TEM image and (D) EDS spectrum of the individual Ag nanoplates shown in (B). (E) SEM image of Ag nanoplates grown on a p-type GaAs wafer. (D) Au/Ag alloy nanoplates converted from the Ag nanoplates shown in (B) through overgrowth.

different growth times. These Ag nanoplates have smooth surfaces and protrude out of the surfaces of the GaAs substrates. Structural (Fig. 1C) and elemental (Fig. 1D) analyses indicate that the as-grown Ag nanoplates are single crystals and are composed of pure silver without any contaminations from the GaAs substrates. With assistance of light illumination, Ag nanoplates can also be grown on p-type GaAs wafers (Fig. 1E). The as-grown Ag nanoplates can be converted to nanoplates made of other components, such as Au/Ag, Pt/Ag, Pd/Ag alloys, through a combination of overgrowth and alloying processes (Fig. 1F).

The Ag nanoplates exhibit interesting optical properties due to their strong surface plasmon resonance (SPR) under photo-illumination. Figure 2A presents extinction spectra of the Ag nanoplates with different sizes in the UV-visible-NIR regions, clearly showing that the major SPR peaks gradually shift to the red with increase of the sizes of the nanoplates. Due to the existence of sharp edges, the Ag nanoplates can serve as a kind of excellent SERS substrates for sensitive detection of molecules close to their surfaces (Fig. 2B).

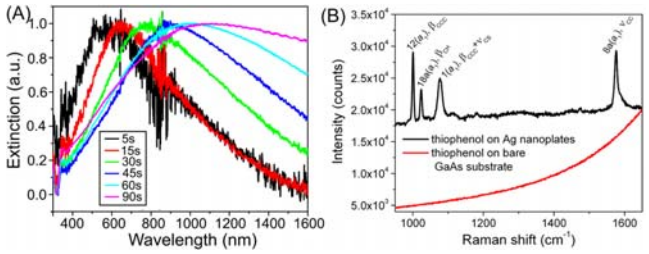

Figure 2. (A) Extinction spectra of the Ag nanoplates grown on n-GaAs wafers through reactions with 2 M $AgNO_3$ solutions for different times. (B) Raman spectra of thiophenol molecules self-assembled on (black) on Ag nanoplates and (red) bare GaAs surface.

Future Work

Future work includes the study of coupling behavior in terms of optical and electrical properties between the metal nanoplates and the semiconductor substrates as well as charge transfer processes at the metal/semiconductor interfaces under photo-excitation. The coupling behavior of these metal nanoplates/semiconductor hybrid materials and interesting dye molecules will also be studied for their photochemical and photoelectrochemical properties.

Publications

"Laser-Driven Growth of Silver Nanoplates on p-Type GaAs Substrates and Their SERS Activity", Sun, Y.; Pelton, M., *J. Phys. Chem. C*, **2009**, *113*, 6061-6067.

"Facile Tuning of Superhydrophobic States with Ag Nanoplates", Sun, Y.; Qiao, R., *Nano Research*, **2008**, *1(4)*, 292-302. (Highlighted as back cover article)

"Formation of Oxides and Their Role in the Growth of Ag Nanoplates on GaAs Substrates", Sun, Y.; Lei, C.; Gosztola, D.; Haasch, R., *Langmuir*, **2008**, *24(20)*, 11928-11934.

"Effects of Visible and Synchrotron X-Ray Radiation on the Growth of Silver Nanoplates on n-GaAs Wafers: A Comparative Study", Sun, Y.; Yan, H.; Wu, X., *Appl. Phys. Lett.* **2008**, *92*, 183109.

"Comparative Study on the Growth of Silver Nanoplates on GaAs Substrates by Electron Microscopy, Synchrotron X-Ray Diffraction, and Optical Spectroscopy", Sun, Y.; Yan, H.; Wiederrecht, G. P., *J. Phys. Chem. C* **2008**, *112*, 8928-8938.

"Direct Growth of Dense, Pristine Metal Nanoplates on Semiconductor Substrates", Sun, Y. *Chem. Mater.*, **2007**, *19*, 5845-5847.

"Surfactantless Synthesis of Silver Nanoplates with Rough Surfaces and Their Application in SERS", Sun, Y., Wiederecht, G. P. *Small*, **2007**, *3*, 1964-1975. (highlighted with cover illustration)

Electronic Conduction Mechanisms in Thin Wires and Nanoscale Contacts

B. S. Swartzentruber[1], A. A. Talin[2], F. Léonard[2], S. T. Picraux[3], and S. D. Hersee[4]

[1]*Sandia National Laboratories, Albuquerque, NM*
[2]*Sandia National Laboratories, Livermore, CA*
[3]*Los Alamos National Laboratory, Los Alamos, NM*
[4]*University of New Mexico, Albuquerque, NM*

Scientific Thrust Area: Nanoscale Electronics and Mechanics

Proposal Title: Characterization and Integration of Vertical GaN Nanorods (S. D. Hersee)

Research Achievement:

We report on the electrical transport characteristics of undoped, *n*-doped, and *pn*-junction GaN nanowires grown by selective epitaxy on GaN/sapphire substrates. The selective epitaxy is realized by a combination of a patterned Si_3N_4 mask, which defines the position and diameter of the nanowires, and appropriate growth conditions, which lead to a near one-dimensional growth along the *c*-direction. The current-voltage characteristics of thin wires are often observed to be nonlinear, and this behavior has been ascribed to Schottky barriers at the contacts. We present electronic transport measurements on nominally undoped GaN nanorods and demonstrate that the nonlinear behavior originates instead from space-charge-limited current (Fig. 1). A new theory of space-charge-limited current in thin wires corroborates the experiments and shows that poor screening in high-aspect ratio materials leads to a dramatic enhancement of space-charge limited current, resulting in new scaling in terms of the aspect ratio. We extract an electron mobility of ~400 cm^2 /V s and a free-carrier concentration of ~10^{15}–10^{16} cm^{-3}. By controlling the nanowire doping, we observe Ohmic transport for *n*-doped nanowires and rectifying characteristics for *pn*-junction, light-emitting diode, nanowires. For light-emitting diodes consisting of approximately 300 nanowire *pn*-homojunctions, operating in parallel (Fig. 2), the electroluminescence intensity grows superlinearly with current. For individual nanowire light-emitting diodes the forward and reverse leakage current is ~1 pA. The low leakage current of individual light-emitting nanowire diodes indicates that surface effects do not dominate the electrical behavior of these LEDs.

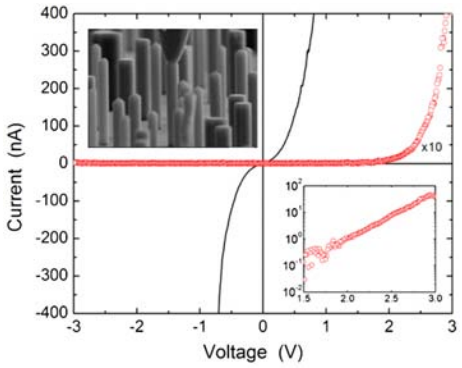

Fig. 1. Current-voltage characteristics before (symbols) and after (line) the tip is pressed into the nanowire. The bottom right inset shows the current before pressing on a log scale. The top left inset is a SEM image of the Au-coated W tip contacting a GaN nanowire.

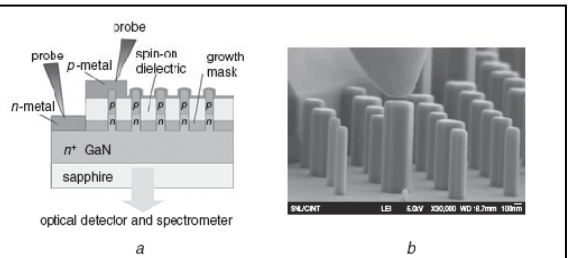

Fig. 2 (a) Schematic showing cross-section of nanowire array LED, and (b) SEM image showing electrical probing of individual pn-nanowire diode near edge of patterned growth template.

To study the electronic interface between Ge nanowires and the Au catalyst particles from

which they are grown, we measured the transport by contacting the Au catalyst particles directly. We present electronic transport measurements of the individual Au-catalyst–Ge-nanowire interfaces that demonstrate the presence of a Schottky barrier (Fig. 3). Surprisingly, the small-bias conductance density increases with decreasing diameter. Theoretical calculations suggest that this effect arises because electron-hole recombination in the depletion region is the dominant charge transport mechanism, with a diameter dependence of both the depletion width and the electron-hole recombination time. The recombination time is dominated by surface contributions and is found to depend linearly on the nanowire diameter.

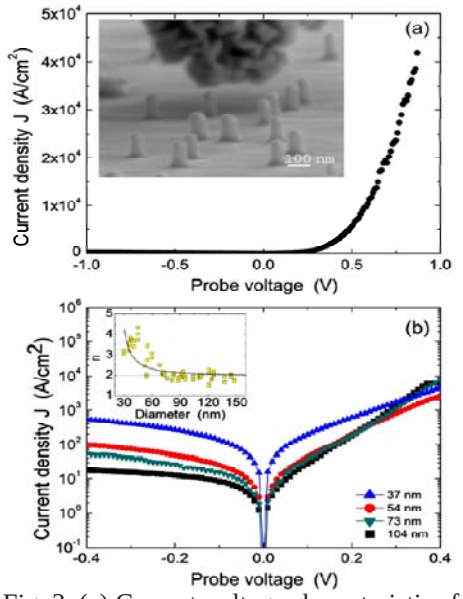

Fig. 3. (a) Current-voltage characteristics for a Ge nanowire of 54 nm diameter. The inset is a SEM image of the Au-coated W tip and several Ge nanowires. (b) Current-voltage curves on a log scale, for four nanowires of different diameters. The inset shows the ideality factor measured at forward bias as a function of nanowire diameter.

Future Work:

From the work on the Au/*n*-Ge NW/*n*-Ge substrate, above, we know that the Au/*n*-Ge NW interface has the Fermi level pinned near the valence band. Therefore, a *p*-type Ge nanowire should yield a relatively small Schottky barrier for hole injection at the Au contact, giving us a near-ohmic contact. We will probe the Au/*p*-Ge NW/*p*-Ge substrate configuration to test this. In addition, measuring the transport through a Au/*p*-Ge nanowire into an *n*-Ge substrate gives us the opportunity to study the transport properties of so-called "heterodimension" *pn*-junctions. That is, a *pn*-junction in which one side is a nanowire and the other side is the semi-infinite bulk substrate. This will enable us to measure how the transport scales as the dimensionality changes from ~1-d to ~3-d. Measuring the transport through Au dots directly on an *n*-Ge substrate should yield a barrier that is proportional to the Au dot diameter – opposite to the nanowire case. This should hold as long as the substrate is not too highly doped. A Ge substrate with a dopant concentration of 10^{17} cm^{-3} has a depletion width of about 100 nm. We expect to see a crossover from the nanocontact to the conventional contact regime by measuring Au dots with diameters from ~20 nm to ~150 nm.

Publications:

1. "Unusually Strong Space-Charge-Limited Current in Thin Wires", A. A. Talin, F. Léonard, B. S. Swartzentruber, X. Wang, and S. D. Hersee, Phys. Rev. Lett., **101**(7), 076802 (2008).
2. "GaN Nanowire Light Emitting Diodes Based on Templated and Scalable Nanowire Growth Process", S. D. Hersee, M. Fairchild, A. K. Rishinaramangalam, M. S. Ferdous, L. Zhang, P. M. Varangis, B. S. Swartzentruber, and A. A. Talin, Electronics Letters, **45**(1), 75 (2009).
3. "Diameter-Dependent Electronic Transport Properties of Au-Catalyst/Ge-Nanowire Schottky Diodes", F. Léonard, A. A. Talin, B. S. Swartzentruber, and S. T. Picraux, Phys. Rev. Lett., **102**(10), 106805 (2009).
4. "Electrical Transport in GaN Nanowires Grown by Selective Epitaxy", A. A. Talin, B. S. Swartzentruber, F. Léonard, X. Wang, and S. D. Hersee, J. Vac. Sci. Tech. B (in press).

Fabrication of carbon nanotube field-effect transistors with semiconductors as source and drain contact materials

Z. Xiao
Department of Electrical Engineering, Alabama A&M University, Normal, AL 35726
F. E. Camino
Center for Functional Nanomaterials, Brookhaven National Laboratory, Upton, NY 11973

Proposal Title

Fabrication of single-walled carbon nanotube field-effect transistors.

Research Achievement

Common problems in the fabrication of carbon nanotube field effect transistors (CNTFETs) include the positioning of tubes across electrodes and poor device electrical performance due to the presence of metallic nanotubes intermixed with semiconducting ones. To circumvent these problems, in this work dielectrophoresis has been used for tube alignment, while semiconducting electrodes have been employed to selectively turn off metallic nanotubes resulting in improved device electrical characteristics.

Research on how to achieve higher drain-source current (I_{DS}) on/off ratio and better I_{DS} saturation properties in CNTFETs is interesting due to the good prospect of these devices for nanoelectronic applications [1, 2]. However, the yield for good device performance is low because currently there is no effective way to separate metallic carbon nanotubes, which shunt FET characteristics, from semiconducting tubes, which are the active elements of the device. To solve this issue, semiconducting electrodes (Sb_2Te_3 or Bi_2Te_2Se) were used instead of metal electrodes in CNTFETs. This substitution allows to selectively isolate metallic nanotubes due to the current-blocking action produced by the back-to-back metal–semiconductor junctions formed at the interfaces between semiconducting electrodes and metallic nanotubes. Measurements indicate that this electrode material substitution results in improved device performance.

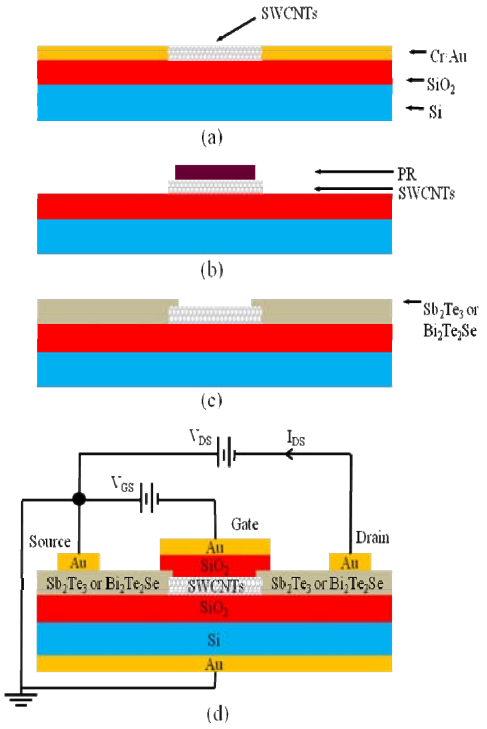

Fig. 1. Flow diagram of the main steps in the device fabrication process. (a) Alignment of SWCNTs to a pair of gold electrodes via dielectrophoresis. (b) Etching away of gold electrodes with the interelectrode region protected by photoresist (PR). (c) Deposition of Sb_2Te_3 or Bi_2Te_2Se layer followed by PR lift-off to define semiconducting contacts to SWCNTs. (d) Final device after the deposition of gate oxide and the formation of metal contacts.

In this research, ultra-purified SWCNTs from Carbon Nanotechnologies, Inc. were used for the fabrication of CNTFETs, and N-Methyl Pyrrolidone was used as the solvent for the dispersion of SWCNTs in solutions. Fig. 1 shows a flow diagram of the fabrication process of CNTFETs with Sb_2Te_3–SWCNT or Bi_2Te_2Se-SWCNT source/drain contacts.

Fig. 2 shows a scanning electron micrograph (SEM) of SWCNTs aligned onto a pair of gold electrodes using the dielectrophoresis process. Figs. 3 and 4 shows I_{DS}-V_{DS} curves at several gate voltages (V_{GS}) for a CNTFET fabricated using Sb_2Te_3 and Bi_2Te_2Se as source and drain contact material, respectively. CNTFETs have PMOS-like electrical properties. The CNTFET with Sb_2Te_3–SWCNT contacts has an I_{DS} ratio of about 5000 at V_{DS} = -3V. The CNTFET with Bi_2Te_2Se-SWCNT contacts has an I_{DS} ratio of about 2000 at V_{DS} = -1V. Both CNTFETs have higher V_{DS} starting the deviation from their switch-off status compared to CNTFETs fabricated with metal-SWCNT source/drain contacts [1]. The CNTFET with Sb_2Te_3–SWCNT source/drain contacts (Fig. 3) also shows a good saturation I_{DS} with increasing $V_{DS.}$ The fabrication processes developed in this research can be applied to other semiconductor electrode materials and could be employed in future wafer-scale CNTFET-based nanoelectronic circuits.

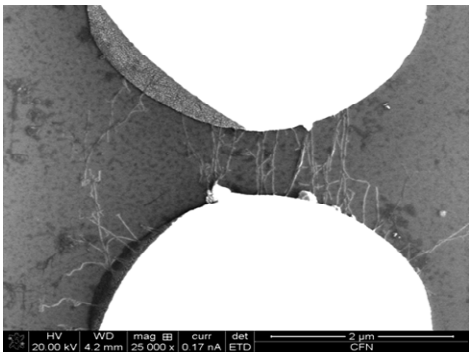

Fig. 2. SEM of SWNTs aligned onto a pair of gold electrodes via dielectrophoresis.

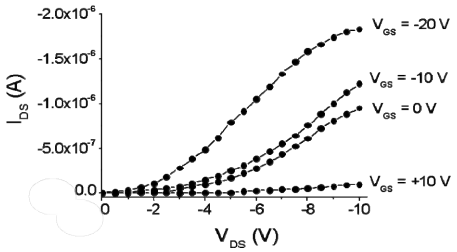

Fig. 3. Drain-source current (I_{DS}) versus drain-source voltage (V_{DS}) and gate voltage (V_{GS}) for the CNTFET fabricated with Sb_2Te_3–SWCNT source/drain contacts.

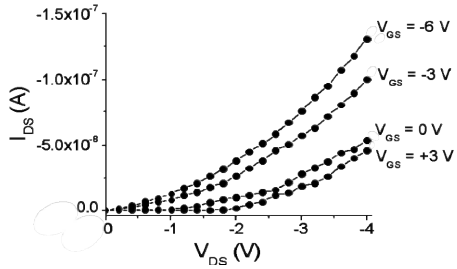

Fig. 4. Drain-source current (I_{DS}) versus drain-source voltage (V_{DS}) and gate voltage (V_{GS}) for the CNTFET fabricated with Bi_2Te_2Se-SWCNT source/drain contacts.

Future Work

As a continuation of this work, we plan to define submicron gates within the interelectrode region using the ion beam assisted deposition capability of the dual electron/ion beam system at the Center for Functional Nanomaterials. We also plan to use this tool for the fabrication of single-tube CNTFETs. In addition, wafer-scale fabrication of CNTFET-based nanoelectronic circuits with semiconductor contact materials using the dielectrophoresis technique will be explored.

References

[1] Kang S J, Kocabas C, Ozel T, Shimi M, Pimparkar N, Alam M, Rotkin S and Rodger J A , **Nature** 2, 230 (2007).
[2] LeMieux M C, Roberts M, Barman S, Jin Y W, Kim J M and Bao Z, **Science** 321, 101 (2008).

Publications

This work has been published in **Nanotechnology** 20 (2009) 135205.

Acknowledgements

This research was carried out in part at the Center for Functional Nanomaterials, Brookhaven National Laboratory, which is supported by the U.S. Department of Energy, Office of Basic Energy Sciences, under Contract No. DE-AC02-98CH10886; Zhigang Xiao is grateful for National Security Agency (NSA) and National Science Foundation (NSF) for financial support for this research (Grant No.: H98230-07-1-0113 and EPS-0814103).

Electrodeposition of Patterned Metal and Semiconductor Micro- and Nanowires on Ultrananocrystalline Diamond Electrodes

Daniel A. Dissing[1], Eric A. Terrell[1], David B. Seley[1], Anirudha V. Sumant[2], Ralu Divan[2], Suzanne Miller,[2] Orlando Auciello[2,3], Michael P. Zach*[1] [1]Department of Chemistry, University of Wisconsin – Stevens Point, Stevens Point, WI 54481, [2]Center for Nanoscale Materials, Argonne National Laboratory, Argonne, IL 60439, [3]Materials Science Division, Argonne National Laboratory, Argonne, IL 60439 *MZach@uwsp.edu

Research Achievement: A new layered electrode composed of conductive and non-conductive ultrananocrystalline diamond (UNCD) has been proven to produce consistent, patterned micro- and nanostructures. These structures can be electrodeposited with uniformity (Figure 1A). The technique is not material specific allowing wires to be made from nearly any material that can be electrodeposited out of aqueous or non-aqueous solutions. Electrically-conductive nitrogen-doped UNCD serves as an efficient electrode with an extremely large electrochemical window due to its chemically inert nature. A layer of insulating undoped UNCD prevents deposition on the top surface so that electrodeposition occurs only at the thin exposed edge of the underlying nitrogen doped UNCD layer.

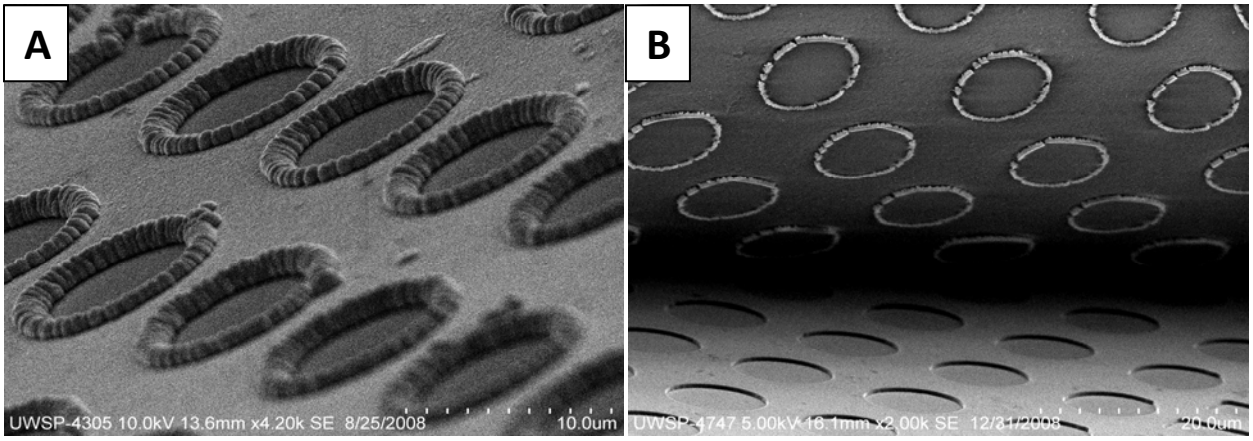

Figure 1 – A Scanning electron microscope (SEM) image of cadmium telluride microwires electrodeposited onto ultrananocrystalline diamond electrodes. **B** SEM image of platinum microwires embedded in a polymer film (upper) that is being peeled away from the diamond template (lower). The extremely sharp angle for pulling and stretching of the polymer film needed to show the interface where wires were being lifted from the template has fractured these wires, but the normal method for peeling is gentle and leaves the wires intact and continuous.

While the initial synthesis of this electrode requires numerous clean room techniques and expensive instrumentation, once the electrode has been made, it is a permanent template for synthesis of micro- and nanowires. Subsequent manufacture of nanowires becomes almost as simple as using a rubber stamp and ink. The multilayer diamond electrode is low in adhesion to the deposited materials, thus allowing easy transfer of the resulting deposited micro- or nanostructures onto an adhesive polymer (Figure 1B). The polymer also strips contamination

from the electrode leaving a pristine electrode surface for repeated use. Duplicate copies of the original electrodeposited wires were made without repeating the difficult lithography steps for each batch of wires made. The combination of unique electrical, chemical and physical properties of UNCD is promising to allow mass production of uniform patterned nanostructures. Materials electrodeposited include: Pb, Au, Cu, Pd, Pt, Ag, Zn, Co (from an ionic liquid electrolyte), Te, CdTe, and CdS. The most recent work has proved that this technique can make patterned nanowires as small as 70 nm in diameter. Figure 2 shows an electrode schematic.

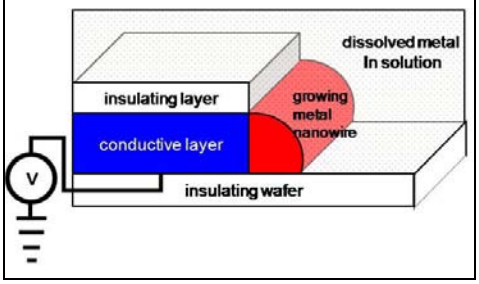

Figure 2 – Schematic of a layered UNCD electrode. Nitrogen doped UNCD forms a thin electrode that is protected on the surface by a capping layer of undoped (insulating) UNCD. Electrodeposition can occur only at the exposed edge of the doped layer.

Future Work: The UNCD nanowire templates are a fundamental and novel advance in methods for making patterned nanowires. Since the templates are extremely robust and not sacrificial, this innovation may help bring nanomanufacturing to “main street” American businesses. Future research will focus in three major areas. The first research thrust is extending the range of nanowire materials. The UNCD templates are extremely robust because diamond is inert under many extreme conditions. This will likely allow electrodeposition of extremely reactive alkali metals, refractory metals such as Ti, Nb, Ta and Zr; and expanding the range of semiconductor nanowires. The second goal is making proof-of-concept heterostructure-type devices containing two or more materials. Examples include solar cells, thermocouples, semiconductor devices or even complex circuitry. The third area is developing scalable production methods that will allow for synthesis of gram to kilogram quantities of patterned nanowires or complex circuits on a continuous basis. Because the template is permanent, once an electrode has been made, all of the extremely tedious steps of nanopatterning surfaces typically used such as electron beam patterning can be eliminated. A continuous production method for patterned nanowires would enable inexpensive manufacturing of such diverse products as nanowires for powdered metallurgy applications, plate and peel circuits as an alternative to traditional electronics manufacturing, and RFID tags for smart-dust type applications.

Publications: This work has not been published yet, but two manuscripts are being prepared for submission later this spring and summer. This conference represents one of the first public displays of this work.

Acknowledgments: Part of this work was carried out at the Center for Nanoscale Materials and the Materials Science Division, Argonne National Laboratory. Argonne is operated by UChicago Argonne, LLC, for the U.S. Department of Energy, Office of Science, Office of Basic Energy Sciences, under contract No. DE-AC02-06CH11357. Additional support was provided by UPDC Fund (UWSP), WiTAG and UW-System.

Nanofabrication and Other Nanosynthesis

Nanoimprint and Nanoprint – Based Routes for Producing Organized Few-Layer-Graphene Nano/Microstructures

Xiaogan Liang, Yuegang Zhang, Deirdre L. Olynick, and Stefano Cabrini
Molecular Foundry, Lawrence Berkeley National Laboratory, 1 Cyclotron Road,
Berkeley, California 94720

Scientific Thrust Area

Nanoimprint and nanoprint technology (NNT) appeared as a newly efficient and economical nanoscale pattern formation technology.[1] It also provided new routes for engineering and integrating nanomaterials into complex functional structures. One of the nanomaterials we have been working on is graphene. Graphene is of great interest as a material for next-generation electronics and energy storage media because of its superior electronic properties.[2] Two of important challenges for scale-up applications are incorporating graphene over large areas and patterning nanostructures to achieve desirable electronic characteristics. Obviously, a nanofabrication-based approach to simultaneously achieve graphene micro- and nanostructures over large areas would be a benefit to the practical applications of graphene.

Research Achievements

We explore novel nanoimprint/nanoprint technologies (NNTs) for producing organized graphene nanostructures. In general, such approaches consist of two steps: (1) prepatterning of nanostructures onto a high-quality graphite substrate, which serves as a template; (2) exfoliation and printing of prepatterned graphene nanofeatures onto device substrates.

To prepattern graphite templates, we not only exploited standard nano/microlithographic techniques such as photolithography (Fig. 1a), electron-beam induced deposition (EBID) (Fig. 1b), and focused ion beam (FIB), but also developed a new chemical approach, named as catalytic-assisted nanoimprint lithography (CANIL) (Fig. 1c).[3] In CANIL, an imprinting template bearing catalytic metal nanofeatures is brought into contact with a graphite substrate. At elevated temperature, the metal nanofeatures (e.g. Ag) can catalytically induce gasification of carbon material and therefore produce nanostructures in graphite. CANIL enables the direct parallel patterning of densely arranged ultrasmooth nanofeatures over large areas (Fig. 1c).

In order to exfoliate/print prepatterned graphene features, we developed a new nanoprinting approach, which uses a combination of electrostatic exfoliation with lithographically patterned highly oriented pyrolytic graphite (HOPG) to produce organized pristine graphene features.[4] With this method, we have successfully demonstrated the exfoliation/printing of few-layer-graphene (FLG) features ranging from 18 nm to 10s μm (Fig. 2). Furthermore, we have fabricated field-effect transistors (FETs) using patterned graphene nanolines, which exhibit excellent transport properties (Fig. 3).

Future Works

Our future works will be focused on (1) understanding the physical and chemical mechanisms underlying the catalytic nanoimprinting and building model for describing the dynamic process of the pattern formation; (2) fabricating well-defined graphene-based devices for studying the electrical and optical properties of graphene nanostructures, such as the effect of the edge states and quantum confinement on the electronic structures of graphene nanolines as well as evolution of Raman and two-photon-photoluminescence (TPPL) peaks as a function of graphene feature size.

References

1. Guo, L. J. J. Phys. D: Appl. Phys. 37 R123-R141 (**2004**)
2. Novoselov, K. S.; Geim, A. K.; Morozov, S. V.; Jiang, D.; Zhang, Y.; Dubonos, S. V.; Grigorieva, I. V.; Firsov, A. A. Science **2004**, 306, (5696), 666-669.

* Email: xliang@lbl.gov

3. Liang, X. G. et al, To be submitted to Advanced Materials (**2009**).
4. Liang, X. G.; Chang, A. S. P.; Zhang, Y. G.; Harteneck, B. D.; Choo, H.; Olynick, D. L.; and Cabrini. S, Nano Lett. 9(1), 467-472 (**2009**).

Publications

1. Liang, X. G.; Chang, A. S. P.; Zhang, Y. G.; Harteneck, B. D.; Choo, H.; Olynick, D. L.; and Cabrini. S, Nano Lett. 9(1), 467-472 (**2009**).
2. Liang, X. G.; Chang, A. S. P.; Zhang, Y. G.; Harteneck, B. D.; Choo, H.; Olynick, D. L.; and Cabrini. S, The 53rd International Conference on Electron, Ion, Photon Beams and Nanolithography (EIPBN 2008) May 26 – 29, **2009**, Marco Island, Florida.

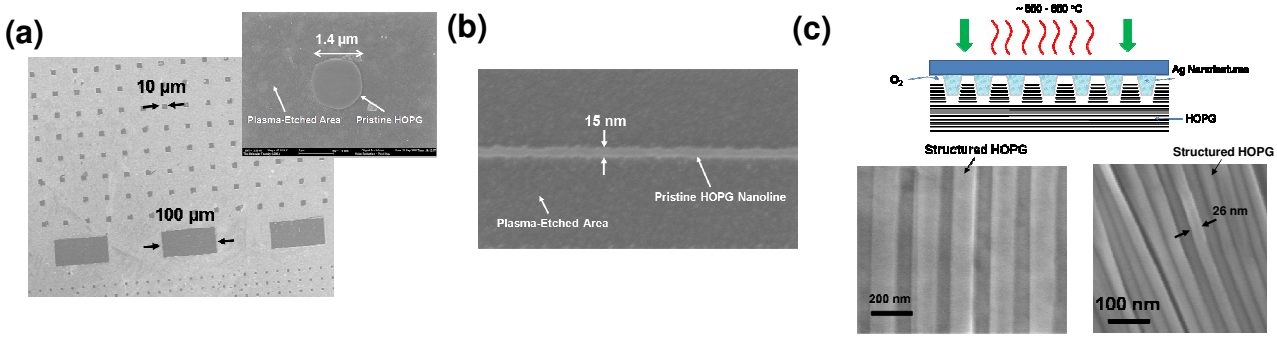

Fig. 1 SEM images of features prepatterned on graphite templates, which includes (a) 5 x 5 μm, 10 x 10 μm, and 100 x 50 μm rectangles and 1.4 μm size pillars, fabricated by photolithography, (b) 15 nm nanolines fabricated by electron beam induced deposition, and (c) 200 nm and 26 nm pitch smooth nanolines fabricated via catalytic-assisted nanoimprint lithography (CANIL) (the inset schematically illustrates the CANIL process).

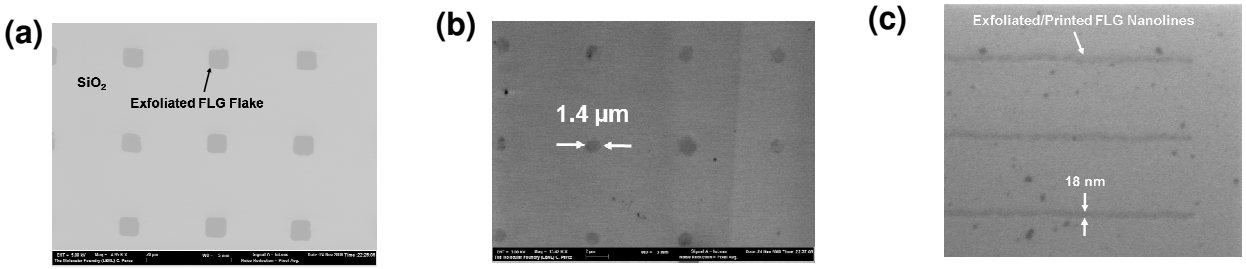

Fig. 2 Representative SEMs of electrically exfoliated/printed few-layer-graphene (FLG) features, which includes (a) 5 x 5 μm squares, (b) 1.4 μm size periodic pillars, and (c) 18 nm wide nanolines.

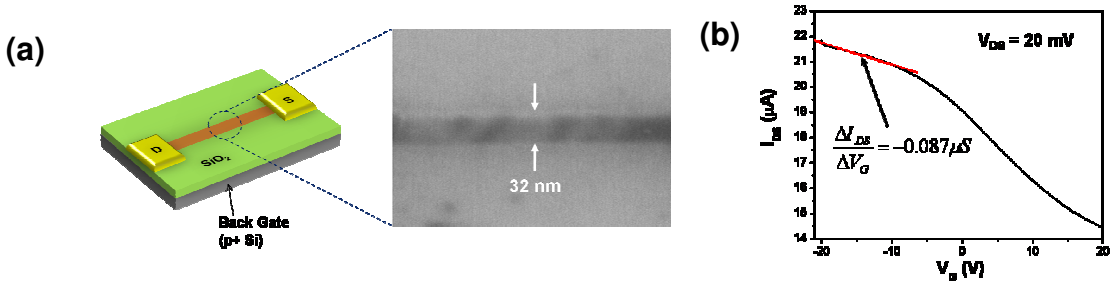

Fig. 3 (a) A back-gated graphene field-effect transistor (GFET) with a 32 nm wide, 0.53 μm long as-exfoliated FLG line as the channel. (b) I_{DS} - V_G of the GFET, from which the hole mobility is extracted to be μ_h = 1,050 cm^2/Vs.

* Email: xliang@lbl.gov

"Resolving" the Mysteries of Electron Beam Resist Exposure and Development

Deirdre L. Olynick [a], Paul Ashby [a], Jim Schuck [a], Frank Ogletree [a], Weilun Chao [b], Mark Lewis [a], Timothy Jen [a], Andreas Shipotinin [c], Xiaogan Liang [a], Stefano Cabrini [a]

[a] *Molecular Foundry, Lawrence Berkeley National Laboratory, Berkeley, CA*

[b] *Center for X-ray Optics, Lawrence Berkeley National Laboratory, Berkeley, CA*

[c] *Helmut Schmidt University, Hamburg, Germany*

Scientific Thrust Area

In the Nanofabrication Facility at the Molecular Foundry, one of the main thrusts is to enable new nanoscience with single digit nanofabrication (sub-10 nm patterning). Despite considerable efforts, patterning sub-10 nm features is still not routine. In electron beam lithography, there is substantial evidence that electron beam resist resolution is often limited by the development conditions (due to contrast, swelling, and collapse) and not beam size. For instance, Fujita et. al.[1] demonstrated the minimum resolvable feature of 10 nm in calixarene was independent of e-beam energy (varied from 10 to 50 keV) and found collapse was dose dependent. Yasin, et. al.[2] showed better line acuity is achieved with ultrasonic development. Furthermore, chemical reactions induced by the beam during exposure can extend far beyond the electron scattering range and limit resolution.[3]

Research Achievements

We have combined numerous techniques to study the exposure and development chemistry of electron beam resists. We begin to reveal mechanisms responsible for resolution, where the limits lie, and how to best utilize e-beam resists for directed self assembly. In our studies of hexaacetate p-methyl-calix[6]arene, a high resolution negative molecular resist (6 nm isolated lines have been demonstrated[2]), we investigate the interplay between thermodynamics and kinetics during development and the effects on nanoresolution. Using solubility parameters and measuring the Hansen Solubility Sphere (HSS) for calixarene, we have estimated the Flory-Huggins interaction parameter, χ, for calixarene and numerous developers (Fig. 1). Using this, we unravel how development contrast evolves and the contributions to pattern swelling and collapse (two of the biggest resolution limiters). Long development times were investigated to elucidate kinetically versus thermodynamically driven behavior. Contrast is higher at lower development times because low molecular weight material is trapped in the beam networked matrix. Using atomic formic microscopy (AFM), we probe calixarene immersed in solvent developers (Fig. 2). One of the crucial findings is that the low molecular weight material trapped in the matrix contributes significantly to swelling and limits resolution (this is driven by lowering of the Gibbs free energy through the entropic term).

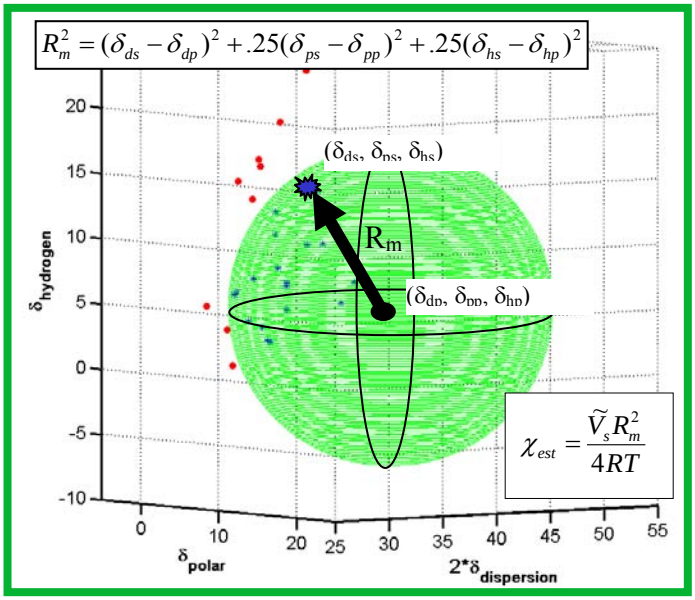

Fig. 1. Hansen Solubility Sphere for calixarene. Determined empirically by looking at calixarene solubility in several solvents (red dots, insoluble, blue dots, soluble). Any solvent with a solubility parameter inside the sphere will dissolve calixarene. Allows estimation of the Flory-Huggins parameter, χ, for all solvents.

In studies of Hydrogen Silsesquioxane (HSQ), an inorganic resist system, we have investigated chemistry induced by the exposing beam. With Raman spectroscopy and electron-beam induced desorption, we identified a beam exposure mechanism. The $Si-H_2$ peak present in the Raman spectra in combination with the e-beam induced desorption of silane, reveal that cross-linking of HSQ occurs via a rearrangement reaction (Fig. 3). In this reaction, hydrogen removed from an HSQ cage bonds with silicon on a nearby cage. This breaks a Si-O bond. The oxygen dangling bond then bridges to the neighboring cage where the hydrogen was lost from a silicon atom. This cross-links the two cages and contributes to the formation of a network. As the system becomes more cross-linked, it becomes more resistant to attack by the aqueous base developer. Currently, we are studying the mechanism of aqueous base development of HSQ.

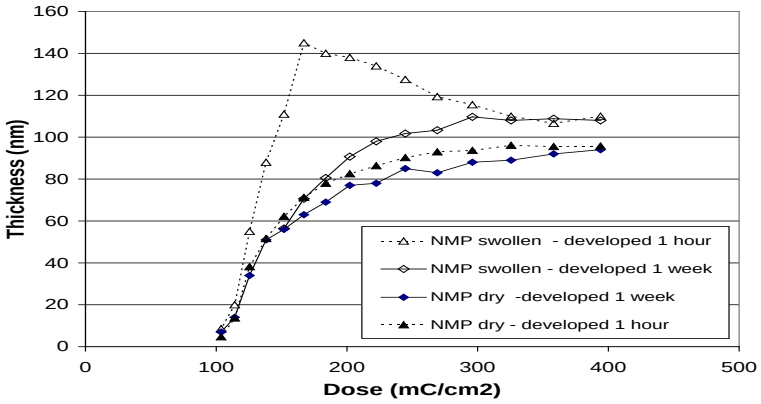

Fig. 2. Chart showing AFM measured thickness of exposed calixarene during development (swollen) and after removing the solvent (dry). The small amount of un-networked material (we know it is un-networked because it is removed with long development times) present in the 1 hour development versus the 1 week development contributes significantly to the resist swelling.

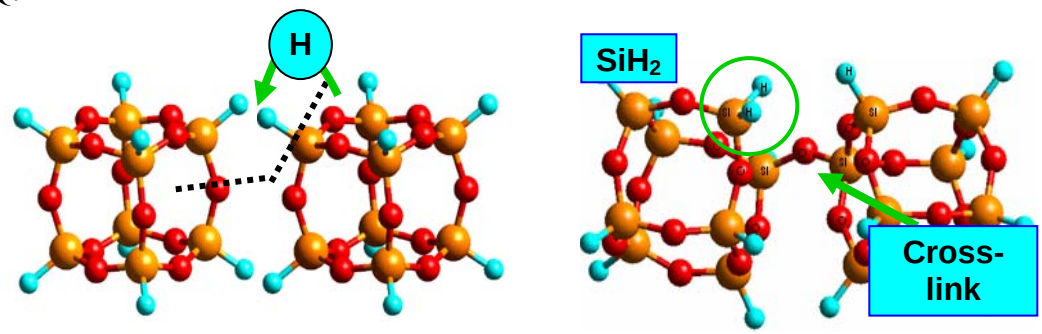

Fig. 3. Networking of HSQ through the redistribution reaction.

Future work

Using these findings, techniques, and our developed expertise, we will investigate new resist materials for single digit nanoresolution, improved process integration (i.e. etching resistance), directed self-assembly, and as active materials. For instance, a user project is underway which uses the techniques developed at the Molecular Foundry to probe new inorganic resists based on ZrO_2 and HfO_2. An internal project is starting to study patterning of nanoparticle embedded calixarenes.

References

1 J. Fujita, Y. Ohnishi, S. Manako et al., Microelectronic Engineering **41/42**, 323 (1998).

2 Shazia Yasin, D. G. Hasko, and F. Carecenac, J. Vac. Sci. Technol. B **19** (1), 311 (2001).

3 Deirdre L. Olynick, J. Alexander Liddle, Alexei V. Tivanski et al., Journal of Vacuum Science and Technology B : Microelectronics and Nanometer Structures **24** (6), 3048 (2006).

Publications

Deirdre L. Olynick, Paul Ashby, Mark D. Lewis, Haoren Lu, J. Alexander Liddle and Weilun L. Chao, *"The link between nanoscale feature development in a negative resist and the Hansen Solubility Sphere"* Accepted Journal of Polymer Physics 2009

Nanoparticles with different functionalities and their periodic structures

Elena V. Shevchenko[1], Paul Podsiadlo[1], Galyna Krylova[1], Dmitri Talapin[1,2], Byeongdu Lee[3] and Tijana Rajh[1]

[1] *Center for Nanoscale Materials, Argonne National Laboratory*
[2] *University of Chicago*
[3] *Advanced Photon Source, Argonne National Laboratory*

Scientific Trust Area: Design of functional materials at nanoscale

Research Achievements: We work on synthesis of different types of nanoparticles with controllable size, shape and composition and understanding their fundamental properties. Nanoparticles display size-dependent electronic structure and could be used as the building blocks for electronic and optoelectronic devices including solar cells, photodetectors, and field-effect transistors; as well as in catalysis and biomedicine. Organization of uniform objects into periodic structures is found in many natural systems, such as atomic and molecular solids, opals, bacterial colonies, etc. In contrast to random mixtures, the ordered nanoparticle arrays provide precise uniformity of packing and rigorous control of the interparticle distances. The ability to assemble "artificial atoms" into ordered structures is expected to create novel class of "artificial solids", that are, nowadays, one of the most exciting materials. The interparticle spacing in nanoparticle superlattices is determined by the length of capping ligands and the type of superlattice. Interparticle spacing is a crucial parameter that dramatically affects electronic and optical properties of nanoparticle solids. Periodic structures can be obtained in a form of films by evaporation of colloidal solution or in a form of perfectly faceted colloidal crystals by technique called "controllable oversaturation" (Figure 1, inset). To date there was no clear understanding in the difference between three-dimensional films and colloidal crystals in terms of their lattice structure and interparticle spacing and how different the behavior of highly organized superlattices from their glassy analogues. We have performed systematic study on nanoparticles solids with no long range order, periodic nanoparticle films and colloidal crystals by time resolved small angle X-Ray scattering (SAXS). At the example of 7 nm PbS nanoparticles we have shown that both periodic films and colloidal crystals have the same face centered cubic structures, however they differ in terms of degree of ordering and interparticle spacing (Figure 1). Thus colloidal crystals demonstrated ~28% smaller interparticle spacing and almost no variation in sample to sample in degree of ordering as compared to periodic films. Moderate thermal annealing of both periodic structures at temperatures below the boiling temperature of capping ligands has let further irreversible shrinkage of crystalline lattice from 1.4 nm up to 0.9 nm without sintering of individual PbS nanoparticles. SAXS study performed for structures assembled from a variety of other nanoparticles (eg CdSe, Fe_xO_y, PbSe, etc) confirmed the better ordering and smaller interparticle spacing for colloidal crystals. In addition to that we have studied mechanical properties of colloidal crystals and effect of different capping ligands on the mechanical stability.

Electronic properties of semiconductor nanoparticles can be also altered by creation of hybrid structures at the level of individual nanoparticles. We explore the synthesis,

optical and electronic properties of hybrid Au/PbS nanoparticles. We synthesized multicomponent nanostructures with metallic Au core and semiconducting PbS shells. In Au-PbS core-shells, we observed enhancement of the absorption cross section due to synergistic coupling between plasmon and exciton in the core and shell, correspondingly. Field-effect devices with channels assembled from arrays of Au-PbS core-shell nanostructures demonstrate strong p-type doping that we attributed to the formation of an intra-particle charge transfer complex.

Another example of hybrid structures at nanoscale is self-assembly of different types of nanoparticles that is amazingly simple and powerful technique in material design. In addition to periodic lattices isostructural to crystalline lattices we have found quasi-crystalline phase assembled from gold and iron oxide nanoparticles.

The surface of nanoparticles is extremely important for any type of applications, especially for catalysis and biomedicine. At the example of magnetic nanoparticles we have developed an approach based on chemiluminesence catalyzed by surface atoms to characterize the chemical activity of surface atoms and total stability of nanoparticles in aqueous media. Hybrid dumbbell-like structures (eg $CoPt_3$/Au) were found to reveal very different catalytic behavior.

Future work: We will focus on manipulation of interpaticle spacing in self-assembled structures in order to create mini-bands that are very important for electronic and optoelectronic properties. We will explore in more details the possibility of formation of nanoparticle quiasicrsytals from different types of nanoparticles. We will try to achieve better control over nanoparticle crystallization in terms of localization of crystallization event, control over type and dimensions of periodic structures. Also we will further study catalytic and electrocatalitic properties of nanoparticles, including complex multicomponent hybrid particles, hollow nanoparticles and multicomponent arrays.

Publications:

E.V. Shevchenko, M.I. Bodnarchuk, M.V. Kovalenko, D.V. Talapin, R.K. Smith, S. Aloni, W. Heiss, A.P. Alivisatos, „Gold (Core) – Iron Oxide (Hollow Shell) Nanoparticles“, *Adv. Mater.* 20, 4323-4329, (2008).

J.-S. Lee, E.V. Shevchenko, D.V.Talapin. Au-PbS Core-Shell Nanocrystals: Plasmonic Absorption Enhancement and Electrical Doping via Intraparticle Charge Transfer. J. Am. Chem. Soc., 130, 9673-9675, (2008).

E.V.Shevchenko, D.V. Talapin. „Self-assebly of semiconductor nanocrystals into ordered superstructures” pp. 118-169 in “Semicondcutor Nanocrystal Quantum Dots. Synthetsis, Assembly, Spectroscopy and Applications”. Ed.: A.L. Rogach. SpringlerWienNewYork. 2008 .

Synthesis, Characterization, and Fabrication of Ultrananocrystalline Diamond Based NEMS

A. V. Sumant, O. Auciello, and D. C. Mancini
Center for Nanoscale Materials, Argonne National Laboratory, Argonne, IL

Scientific Thrust Area: Nanofabrication and Devices

Research Achievement:

We have studied the fundamental electrical and mechanical properties of ultrananocrystalline diamond (UNCD) films, which will enable fabrication of new generation of nanoelectromechanical systems (NEMS) integrated with complementary-metal-oxide-semiconductor (CMOS) devices to enable the development of nanodevices with advanced functionalities.

a) Synthesis and characterization of large-area, low-temperature UNCD films and integration with CMOS:

The first important step in developing diamond based NEMS is the ability to synthesize diamond thin films on a wafer scale with thickness and nanostructure uniformity acceptable for nanodevices. The new 915 MHz microwave plasma chemical vapor deposition (MPCVD) system from Lambda Technologies installed in the clean room at CNM enabled the development of a process to synthesize UNCD at 400 ^{o}C and demonstrated film thickness uniformity in the range of 5-11% on 150-200 mm diameter silicon wafers respectively (fig. 1(a-c)) with excellent nanostructure uniformity as characterized by Raman spectroscopy and near edge x-ray absorption fine structure spectroscopy. The level of uniformity achieved is unmatched with any other diamond MPCVD process. More importantly, we have developed scheme to monolithically integrate low temperature UNCD with CMOS. The ability to preserve the functionality of CMOS devices was demonstrated by depositing UNCD directly on the CMOS wafer at 400^{o}C (fig. 1(b)) and measuring I-V characteristics before and after UNCD deposition (fig. 1(c)). This process enabled later development of monolithically integrated CMOS with RF-MEMS switches based on diamond as a dielectric. This first successful demonstration of integration of UNCD with CMOS devices is a major breakthrough that opens new pathways for fabricating CMOS-driven NEMS based on UNCD.

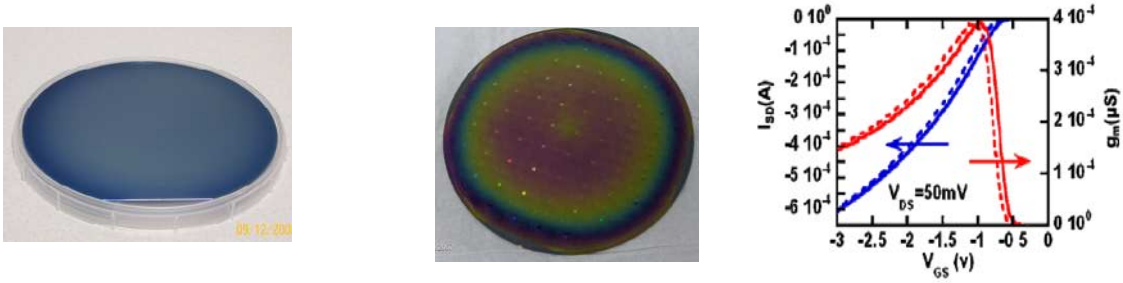

(a) (b) (c)

Figure 1. Photographs of uniform UNCD film deposited on (a)150 mm diameter si wafer and (b) 200 mm diameter Si-CMOS wafer respectively and(c) I-V measurements on CMOS before (solid lines) and after (dashed lines) UNCD deposition demonstrating no appreciable change in CMOS device performance.

b) Integration of UNCD films with piezoelectric films for high-frequency resonators:

The integration of piezoelectric $Pb(Zr_xTi_{1-x})O_3$ (PZT) thin films with the UNCD opens up the possibility of advanced piezo-actuated devices, which can be actuated at lower voltages (< 5 V) compared to typical electrostatic actuation requiring higher voltages (30-

50V). The integration is challenging, because PZT films are grown in an oxygen-rich environment and oxygen reacts with carbon, resulting in the chemical etching of the UNCD and thus degrading the PZT/UNCD interface. We developed Ti-Al as an oxygen diffusion barrier layer and demonstrated PZT/UNCD piezo-actuated resonator structures with actuation voltage as low as 1 volt, enabling a new class of piezo-actuated high frequency UNCD resonators.

c) Mechanical dissipation in UNCD microresonators:

We have carried out fundamental studies to investigate the origin of dissipative losses in diamond. Dissipation in the UNCD cantilevers is determined using ring-down measurement under UHV conditions and the quality factor Q was measured to be in the range of 5000–16,000 at kHz resonance frequencies. The UNCD cantilever resonators exhibited higher dissipation compared to microcrystalline diamond cantilevers with comparable resonant frequencies, but less dissipation than amorphous carbon cantilever resonators. We attribute higher dissipation in the UNCD resonators mainly to the presence of defects such as carbon bonding at grain boundaries and surfaces.

Future Work:

(a)UNCD nanowire: A new platform for developing next generation diamond based nanoelectronic devices:

UNCD nanowires are quasi 1-dimensional sp^3 nanostructures and are predicted to have exceptional electronic and mechanical properties. We used e-beam lithography and reactive ion etching of UNCD, to fabricate nanowires with diameter as small as 20 nm. The effective surface area of the grains and grain boundary in nanowire is large and any small chemical changes on the surface could greatly affect electrical transport properties of these nanowires. We will fabricate UNCD nanowires and perform detailed studies on their electronic, mechanical and thermal properties. This may enable fabrication of new functional nanoelectronic devices for a variety of applications.

(b) Dielectric properties of nitrogen doped UNCD:

We have made preliminary measurements of optical dielectric properties of undoped and nitrogen doped UNCD films. We will make detailed measurements across the entire electromagnetic spectrum from DC to RF to UV correlating these electro-optic properties as a function of nitrogen content in UNCD in order to understand the role of nitrogen in determining the dielectric properties of UNCD.

Publications:

1. V. P. Adiga, A. V. Sumant, S. Suresh, C. Gudeman, O. Auciello, J. A. Carlisle, R. W. Carpick, Mechanical stiffness and dissipation in ultrananocrystalline diamond microresonators", *Physical Review B* 79, 1 (2009).
2. J. E. Butler and A. V. Sumant, "The CVD of nanodiamond materials," *Chem. Vap. Deposition*. 14, 145 (2008). Invited Review Article.
3. A.V. Sumant, D. S. Grierson, J. E. Gerbi, J. Carlisle, O. Auciello, R. W. Carpick, "The surface chemistry and bonding configuration of ultrananocrystalline diamond surfaces, and their effects on nanotribological properties," *Physical Review B* 76 235429 (2007).
4. O. Auciello, S. Pacheco, A. V. Sumant, C. Gudeman, S. Sampath, A. Dutta, R. W. Carpick, V. Adiga, P. Zurcher, Z. Ma, H. Yuan, J. A. Carlisle, B. Kabuis, J. Hiller, S. Srinivasan, "Are diamonds MEMS' best friend?" *IEEE Microwave Mag.* 8(7), 61 (2007).
5. S. Srinivasan, J. Hiller, B. Kabius, O. Auciello, "Piezoelectric/ultrananocrystalline diamond heterostructures for high-performance multifunctional micro/nanoelectromechanical systems", Appl. Phys. Lett., 90, 134101 (2007).

Use of the Center for Nanoscale Materials was supported by the U. S. Department of Energy, Office of Science, Office of Basic Energy Sciences, under Contract No. DE-AC02-06CH11357.

Tailored Nanopost Arrays for Nanophotonic Ion Production

Jessica A. Stolee[1], Bennett N. Walker[1], Deanna L. Pickel[2], Scott T. Retterer[2], and Akos Vertes[1*]

[1]*Department of Chemistry, George Washington University, Washington, DC 20052*
[2]*Center for Nanophase Materials Sciences, Oak Ridge National Laboratory, Oak Ridge, TN 37831*

Proposal Title
Laser Desorption Ionization of Biomolecules from Silicon Microcolumn and Nanopost Arrays

Research Achievement
Recently we have demonstrated that quasi-periodic nanostructures with features commensurate with the wavelength of the radiation, such as laser-induced silicon microcolumn arrays (LISMA), can serve as nanophotonic ion sources for the mass spectrometry of organic and biomolecules.[1,2] In contrast to conventional laser desorption ionization, nanophotonic ion production relies on antenna-like harvesting of energy from the electromagnetic radiation by the nanostructure, confinement of the deposited energy within the nanostructure and confinement of the desorbed plume in the troughs of the surface. Recently we found a dramatic dependence of the ion yield on the polarization and incidence angle of the desorption laser beam.[2] As the LISMA periodicity is commensurate with the wavelength of the desorption laser, interference effects are also anticipated. This might be combined with local field enhancement due to near field effects. LISMA, however, can only be produced with a limited range of surface morphologies. This hinders mechanistic studies and the optimization of ion production properties.

Silicon nanopost arrays (NAPA) exhibit the essential geometrical features of LISMA and can be produced by nanofabrication with a broad range of morphologies. Tailoring the NAPA dimensions, such as post diameter, post height and periodicity, enable both studying the ion production mechanism and finding the geometry with optimum ion yield. NAPA were produced from high conductivity silicon at the Center for Nanophase Materials Sciences of the Oak Ridge National Laboratory. Initially NAPA patterns with a range of diameters (50 nm to 600 nm) and periodicities (100 nm to 1100 nm) were created with electron beam lithography. The various post heights (200 nm to 1600 nm) were achieved with deep reactive ion etching. An example of such a tailored NAPA is shown in Figure 1.

Similar to LISMA, NAPA structures also exhibited a strong orientation dependence, where the p-polarized beam produced efficient ionization in contrast to the s-polarized beam, which produced minimal or no ions. This behavior confirmed that NAPA could also be viewed as optical antenna arrays for energy deposition.

To gain insight into the energy transfer to the ions, their internal energy was probed by taking survival yield measurements (SY) at various fluences using a set of benzyl-substituted benzylpyridinium cations as thermometer ions. These studies as a function of NAPA geometries showed that NAPA with 100 nm post diameters had

decreasing SYs as laser fluence was increased, whereas larger post diameters (200 nm to 500 nm) exhibited stable survival yields at low to medium fluences and increasing SYs at higher laser intensities (see Figure 2). This dramatic disparity may be attributed to the confinement of the deposited energy in the 100 nm diameter posts resulting in significantly higher surface temperatures.

Preliminary optimization studies indicated that NAPA with post diameters of 200 nm and post heights of 1200 nm resulted in the highest ionization efficiencies and that NAPA with periodicities comparable to the wavelength of irradiation produced elevated ion yields.

Future Work

NAPA are novel ion sources for mass spectrometry with high sensitivity and mass resolution. Similar to LISMA, but in contrast to other soft laser desorption ionization methods, NAPA enables fine control over ion yields and fragmentation, where intact molecular ions are observed at low laser fluences, and at higher fluences structure specific fragmentation occurs.

Further studies are needed to understand the mechanism of nanophotonic interactions through studying NAPA with modified geometries and material parameters. We intend to explore the effect of nanopost shape and electrical conductivity on ion yields. Detailed optical characterization will also be conducted using spectroscopic reflectometry, polarization dependent reflectivity and UV-VIS spectroscopy of the NAPA.

Figures

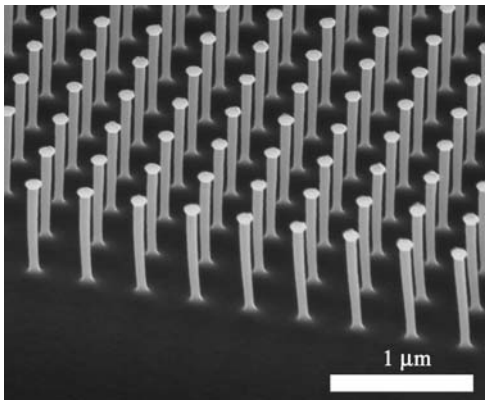

Figure 1. SEM image of NAPA with 1000 nm post height, 100 nm post diameter, and 350 nm periodicity.

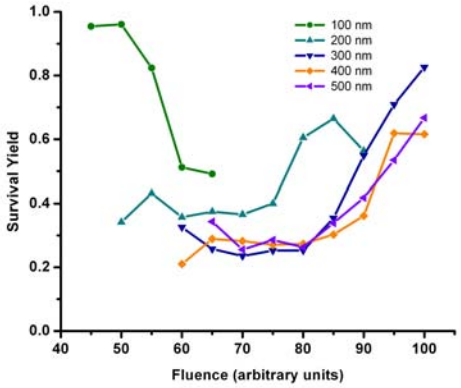

Figure 2. Survival yields of 4methyl-benzylpyridinium ions desorbed from NAPA of varying diameters and a post height of 1000 nm.

References

(1) Chen, Y.; Vertes, A. *Analytical Chemistry* **2006**, *78*, 5835-5844.

(2) Walker, B. N.; Razunguzwa, T.; Powell, M.; Knochenmuss, R.; Vertes, A. *Angewandte Chemie-International Edition* **2009**, *48*, 1669-1672.

Polymer / Macromolecular Materials

Thermochromism of poly(phenylene) vinylene: untangling the role of polymer aggregate and chain conformation

Mircea Cotlet[1*], Hsing-Lin Wang[2], Andrew P. Shreve[3]

[1]Center for Functional Nanomaterials, Brookhaven National Laboratory, Upton NY

[2]Chemistry Division, Los Alamos National Laboratory, Los Alamos NM

[3]Center for Integrated Nanotechnologies, Los Alamos National Laboratory, Los Alamos NM

[*]e-mail: cotlet@bnl.gov

Scientific thrust area: Soft and biological nanomaterials

Research achievements:

Conjugated polymers with reversible thermochromic properties have potential applications toward smart windows, colorimetric sensors, and light emitting diodes.[1,2] Thermochromic behavior for conjugated polymers has been reported for substituted polythiophenes, polyaniline, polydiacetylene and poly(phenylene vinylene) (PPV). For substituted polythiophenes, the thermochromism has been attributed to thermal vibrations imposing twisting of benzene rings resulting in a less coplanar polymer conformation[1]. For MEH-PPV, thermochromic behavior has been related to conformational changes in the polymer chain leading to changes in the energetics of the HOMO and LUMO[2], and, alternatively, to enhanced solubility minimizing interchain interactions by untangling polymer aggregate into single polymer chains[3].

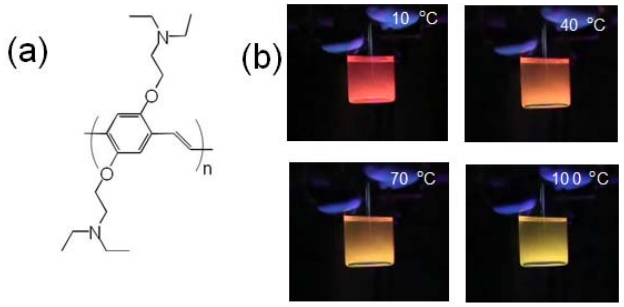

Figure 1. a). DAAO-PPV, b) temperature-induced color changes of DAAO-PPV diluted in toluene.

We have investigated the temperature dependent photophysical properties of a conjugated polymer, poly{2,5-bis[3-(N,N-diethylammonium acetate)-1-oxapropyl]-1,4-phenylenevinylene} (DAAO-PPV, Figure 1a), in diluted solutions of toluene and 1,2-dichlorobenzene. We found DAAO-PPV to exhibit a reversible thermochromic behavior with color changes from red to green as the temperature raises from 278K to 373K (Fig.1b). This thermochromism is the result of untangling/formation of polymer aggregates due to varying solubility and conformational changes of single polymer chains within aggregate. By means of temperature-dependent UV-VIS spectroscopy, time-resolved fluorescence spectroscopy and dynamic light scattering spectroscopy we show how aggregation and polymer chain conformational changes manifest in the photophysics of DAAO-PPV. We find aggregates to dominate the spectroscopy of DAAO-PPVs at low temperatures, with absorption and emission bands peaking at red visible wavelengths. Time-resolved photoluminescence experiments demonstrate that within the aggregate, the energy is funneled from interchain excitons to single

(or few) chromophoric sites, from which final luminescence occurs. By increasing the temperature, DAAO-PPV aggregates are driven into single polymer chains with absorption and emission bands peaking in the green visible wavelengths. The transition from polymer aggregate to single chain species involves an intermediate species, a loose aggregate whose size and conjugation length changes as a function of temperature due to weaker interchain interactions. By monitoring the hydrodynamic volume and the photophysics as a function of temperature and solvent viscosity, we offer unequivocal evidence of how aggregates impact the optical and photophysical properties of the conjugated polymers. The model we propose to explain the thermochromism DAAO-PPV is shown in Figure 2. In this model, temperature untangles polymer aggregates into single chains by increasing polymer-solvent interactions, leading to solvent molecules to protrude inside the aggregate and to diminish interchain interactions. This makes the aggregate to swollen and to break apart in loose aggregates. Further increase in temperature leads to detachment of loose aggregates into isolated chains. Untangling of a dense aggregate into isolated chains seems to be a complex process, with no clear singular states at any of the temperatures points employed in this study. That is, over the temperature range investigated here, the sample is a blend of dense aggregate, loose aggregate and isolated chains with the temperature only biasing the contribution of each of these species.

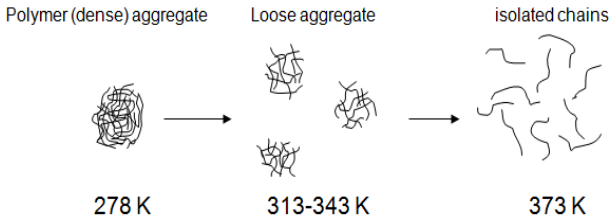

Figure 2. Model explaining thermochromism in DAAO-PPV: temperature increases polymer-solvent interactions untangling polymer aggregate into isolated chains via a loose aggregate state.

Future work:

We are investigating the structure-optical properties in conjugated polymers, in particular the role of aggregate and chain conformation in defining the heterogenic optical properties of PPVs when dispersed in thin films. This particular study is addressed with time-resolved confocal fluorescence microscopy and it aims at understanding and controlling the heterogenic optical response of conjugated polymers for improved performance in devices such as organic solar cells or light emitting diodes.

Publications:

Chun-Chih Wang, Yuan Gao, Andrew P. Shreve, Hsing-Lin Wang* and Mircea Cotlet, "Thermochromism of poly(phenylene vinylene): untangling the roles of polymer aggregate and chain conformation", *, submitted *to J.Amer.Chem.Soc.*

References:

1. Song, J.; Cisar, J. S.; Bertozzi, C. R., *Journal of the American Chemical Society* **2004,** 126, (27), 8459-8465. 2.Leclerc, M., *Advanced Materials* **1999,** 11, (18), 1491-8. 3. Lebouch, N.; Garreau, S.; Louarn, G.; Belletete, M.; Durocher, G.; Leclerc, M. *MACROMOLECULES* **2005,** 38, (23), 9631-9637.

Functional Soft Interfaces Based on Reactive Polymer Scaffolds

Jamie M. Messman[1], Bradley S. Lokitz[2], Juan Pablo Hinestrosa[1],
John F. Ankner[2] and S. Michael Kilbey II[1]
[1] Center for Nanophase Materials Sciences, Oak Ridge, TN 37831
[2] Spallation Neutron Source, Oak Ridge, TN 37831

Scientific Thrust Area: Polymer science, thin films

Research Achievements

Materials interact with their environment via their interfaces, and as the volume of materials decreases to the nanoscale, surface-to-volume ratios increase dramatically. For these reasons, modification of surfaces with thin polymer films is commonly used to tailor a range of properties, including wettability and antifouling characteristics, adhesion and lubricious behavior, and abrasion and corrosion resistance. The ability to alter interfacial structure and confer desirable properties to the substrate enables application across a broad array of technologies. Underlying such applications is the need to understand the interconnected assembly-structure-property relationships.

In this regard we have been studying polymers based on the reactive monomer, 2-vinyl-4,4-dimethylazlactone (VDMA), which offers compelling potential for creating functional polymers due to its ability to readily react with nucleophiles, such as alcohols and primary amines, as well as its intrinsic hydrolytic stability. The robustness of these transformations provides a convenient way to alter polymer structure and properties. A series of well-defined polymers based on VDMA were synthesized using reversible addition fragmentation-chain transfer (RAFT) polymerization. Linear pseudo first order kinetics are observed for the RAFT polymerization of VDMA in benzene at 65 °C, with differences in polymerization rate most likely due to the higher rate of fragmentation of the two chain transfer agents (CTAs) used to mediate the polymerization.

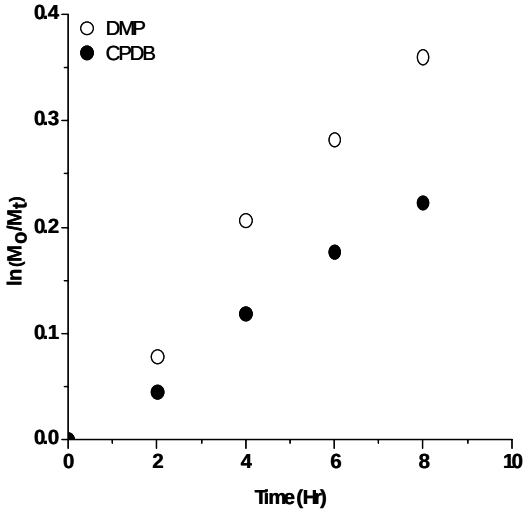

The ability to modify the chemical structure and properties of these polymers has been demonstrated using a variety of nucleophiles that transform these polymers into weak polyelectrolytes, decorate the chains with pendant biomolecules or fluorescent tags, or provide specific motifs used for site-specific immobilization of tagged proteins. An example of such a transformation is shown below, where gel permeation chromatography (GPC) is used to confirm

functionalization of the parent polymer. In this case, a copolymer consisting of VDMA and vinylpyrrolidone was functionalized with dansylcadaverine, which has a single primary amine and is fluorescent. The images shown at the right overlay the outputs from the refractive index and UV detectors of the GPC system for the parent copolymer (top) and dansylcadaverine-modified copolymer (bottom). The UV chromatogram of the modified copolymer reveals distinct peaks at 253.5 nm and 337.8 nm. These new peaks, which are absent in the parent material, confirm modification of the copolymer by ring opening and attachment of the biomarker dansylcadaverine.

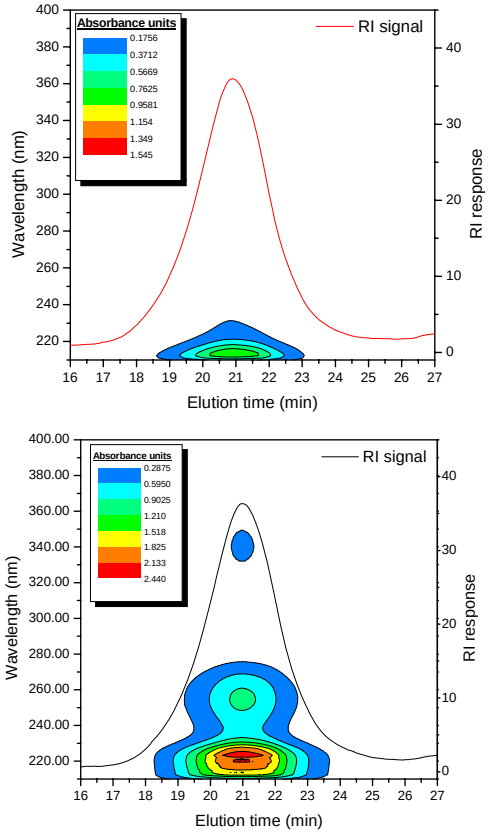

In addition to successful modification of polymers based on VDMA, we have demonstrated robust functionalization of monomers, the ability to create block copolymers, and new strategies for tethering these polymers at solid-fluid interfaces. Coupled with the success RAFT-mediated polymerization of these materials, this work engenders opportunities for designing tailored polymers and polymer-modified interfaces, thereby enhancing our ability to tease apart the links between arrangement, structure, and function of functional polymeric materials.

Future Work

Our interests reside in exploring how the chemical information encoded through precision synthesis and subsequent modification influences structure and properties. One aspect of this endeavor requires developing strategies for creating well-defined, end-tethered polymers based on VDMA, and using neutron reflectivity to investigate the nanoscale structure of the surface-tethered layers as well as structural changes and responsiveness when the pVDMA-based chains are subjected to base-catalyzed hydrolysis to yield a polyelectrolyte. Polyelectrolytes remain one of the least-understood classes of soft materials due to the intimate and intertwined connections between charge and structure. In this pursuit, co-location and partnership with the Spallation Neutron Source offers near-unique capabilities for investigating these novel materials.

References

Barringer, J. E.; Messman, J. M.; Banaszek, A L,.; Meyer, H. M. III; Kilbey, S. M. II *Langmuir* **2009**, *25*, 262-268.

Messman, J. M.; Lokitz, B. S.; Pickell, J. M.; Kilbey, S. M. II *Macromolecules* **2009**, published on-line (ASAP article) May 11, 2009.

Collaborative Partnerships with Oak Ridge National Laboratory for the Discovery of Functional Charged Macromolecules

Rebecca H. Brown, John M. Layman, Sharlene R. Williams, Sean M. Ramirez,
and Timothy E. Long
Virginia Tech, Department of Chemistry and the Macromolecules and Interfaces Institute,
Blacksburg, VA 24061-0344

User Proposal Titles

(1) Hydrogen bonding influence of urea-functionalized carbon nanotubes with complementary polymer matrices (Sean M. Ramirez), **(2)** Aqueous size exclusion chromatography for the characterization of ion containing polymers for gene delivery (John M. Layman), **(3)** RAFT polymerization of acrylic monomers for block copolymer architectures (summer internship for Rebecca H. Brown), and **(4)** Synthesis of ionenes in the presence of ionic liquids (Sharlene R. Williams)

Research Achievements

Non-viral gene delivery agents, such as cationic polyelectrolytes, are attractive replacements to viruses due to the absence of potential immunogenic risk and the ability to tune their macromolecular structure. Although non-viral vectors possess numerous design advantages, several investigators have shown that transfer efficiencies are considerably lower when compared to viral vectors. Our work aims to fundamentally understand the underlying structure-property relationships involved in polycation-mediated gene delivery. The molecular weight was determined using absolute molecular weight detection, and the control of molecular weight over a broad range is depicted. The molecular weight of PDMAEMA was found to have a dramatic influence on transfection efficiency, and luciferase reporter gene expression increased as a function of increasing molecular weight. However, cellular uptake of polyplexes was determined to be insensitive to molecular weight. Collectively, our data suggested that the intracellular fate of the polyplexes, which involves endosomal release and DNase resistance, is more important to overall transfection efficiency than barriers to entry, such as polyplex size. User collaborations with ORNL CNMS provided key experimental parameters to the determination of the absolute molecular weight measurements of these vectors, and the following figure depicts the role of molecular weight on the transfection efficiency for a series of cationic polyelectrolytes.

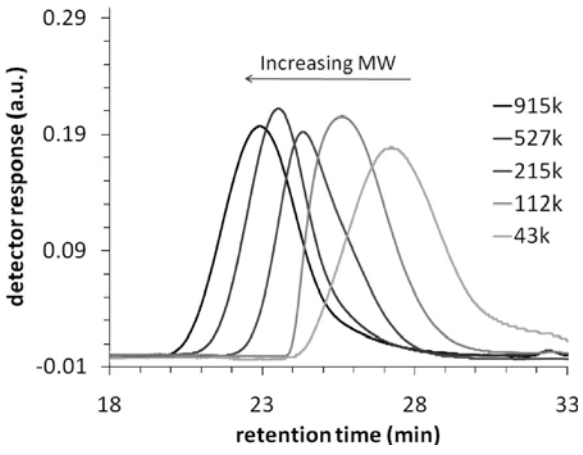

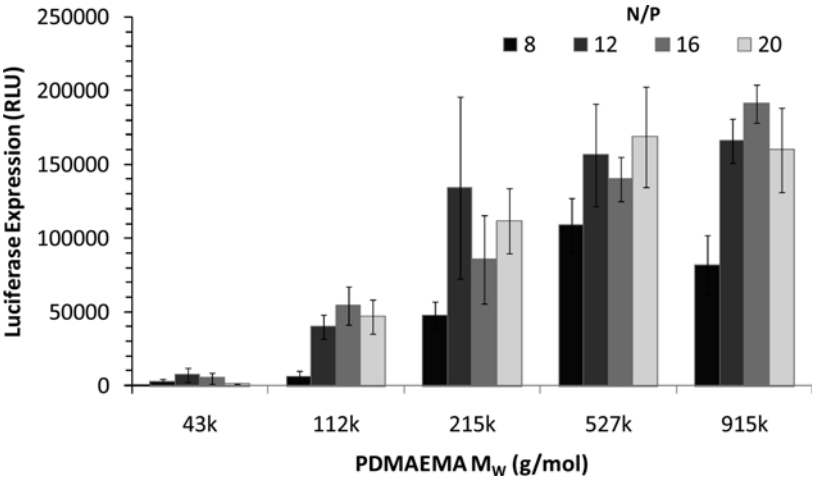

ORNL CNMS collaborations also involved investigations of the polymerization of cationic ionenes in ionic liquid monomers. The use of ionic liquids offers versatility in the solubility and ultimate performance in electro-active devices. Ionenes consist of cations within the polymer backbone as opposed to pendant as described above for gene therapy vectors. The following synthetic scheme illustrates the synthesis of functional ionenes, and the preparation of these novel monomer families in ionic liquid solvents will be described in more detail.

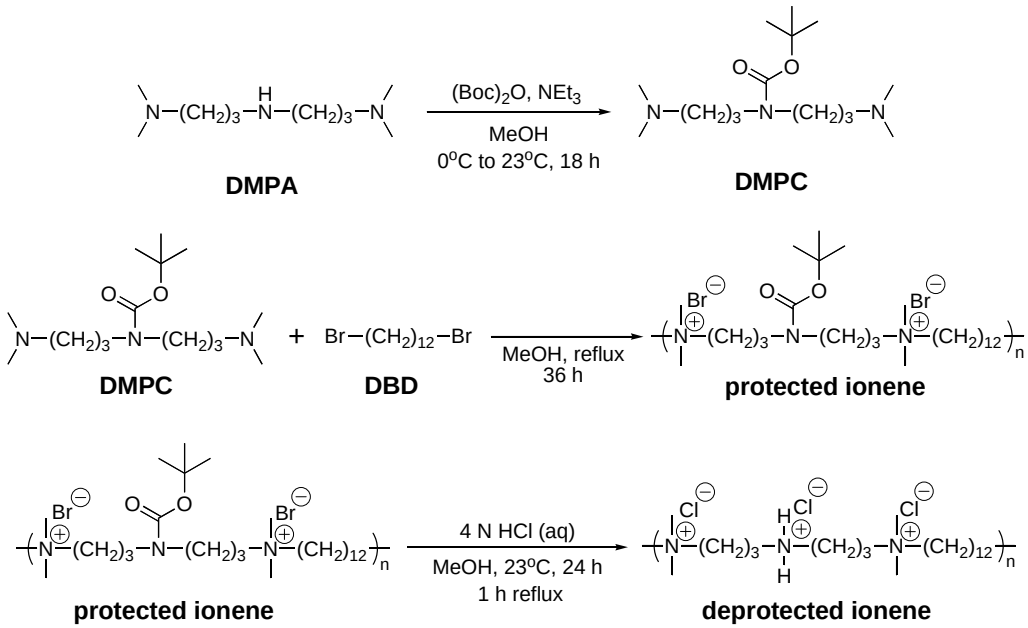

Future Work

Our current collaborative efforts are focused on the introduction of nucleobase intermolecular interactions between MWCNTs and various polymer matrices, and collaborations involve the characterization of functionalization efficiency. In addition, ionene synthesis continues with a focus on the introduction of imidazolium cations to the ionene architecture in an attempt to provide favorable interactions with complementary ionic liquids.

References

Layman, J. M., Long, T.E., et al. *Biomacromolecules* **2009,** *in press.*

Nanoporous Polymer Networks: Potential Adsorbents for Hydrogen Storage

Frantisek Svec, Jonathan Germain, Jean M.J. Fréchet
The Molecular Foundry, Lawrence Berkeley National Laboratory, Berkeley CA 94720

Scientific Thrust Area. The use of hydrogen as a fuel and the development of a hydrogen economy have been suggested as means to decrease our dependency on petroleum products worldwide. However, before this vision can be realized, a number of very significant technological hurdles need to be overcome such as the development of safe, compact, and high capacity storage systems for molecular hydrogen. A wide variety of approaches including carbon nanostructures [1], carbon/metal nanostructures [2], carbon aerogels [3], metal-organic frameworks [4], and numerous metal hydrides [5] have been tested to achieve this goal. The first generation of porous polymers found suitable for this application included hypercrosslinked polystyrene-based copolymers with high surface areas exceeding 2000 m^2/g [6-10]. For example, our material of this type enabled storage of up to 5.5 wt.% hydrogen [6]. However, this high capacity was only achieved at a temperature of 77 K and a pressure of 80 bar, i.e. at conditions that are difficult to manage in a car. These conditions are necessary though since the enthalpy of adsorption (ΔH) was only 4-6 kJ/mol. Theoretical calculations indicate that ΔH in the range of 15-20 kJ/mol is needed to achieve hydrogen adsorption at room temperature [11]. One option to reach this level is to develop polymeric materials with new chemistries.

Research Achievement. In this study, we targeted networks consisting of aromatic rings held in a porous framework by the smallest possible linking groups. The simplest approach to forming networks consisting of aromatic rings starts with precursors containing reactive groups directly attached to the aromatic ring such as aryl halides and amines, which can be coupled using a variety of synthetic routes. For example, the Ullman (A, B) and the Buchwald reaction (C) can be used to perform such couplings. As shown in scheme below, we applied both of these syntheses to the crosslinking of aryl amines with polyhalogenobenzenes to form amine-linked networks of aromatic rings.

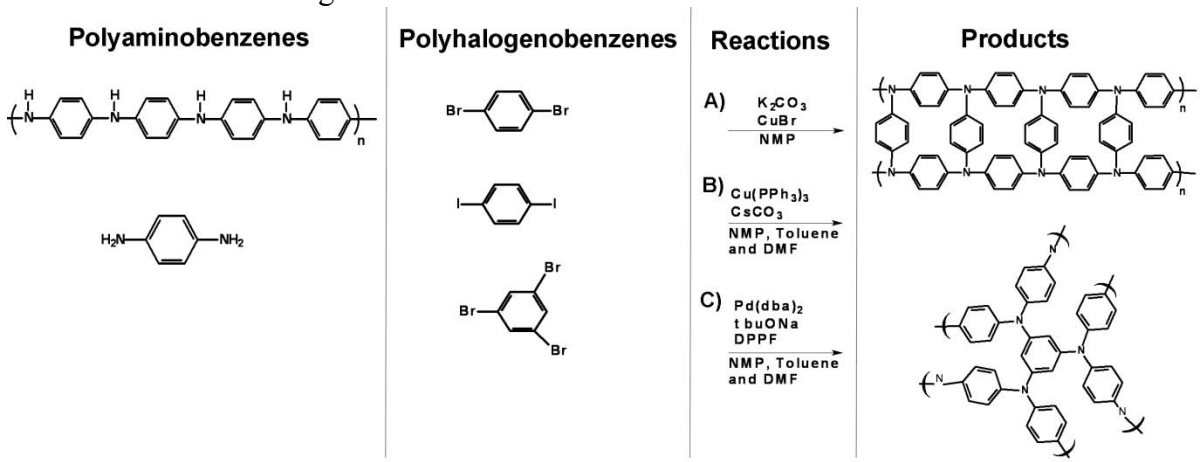

Low pressure hydrogen adsorption isotherms demonstrate that our new network of aromatic rings with a BET surface area of about 250 m^2/g adsorb more hydrogen at low pressures of up to 1.2 bar than hypercrosslinked polystyrenes with surface areas more than seven times as large. In addition, these materials exhibit Langmuir surface areas calculated using H_2 adsorption isotherms larger than those calculated using the BET equation and nitrogen adsorption isotherms.

This unexpected observation and the high hydrogen adsorption at low pressures suggest high H_2-polymer interaction energies in our networks of aromatic rings. Indeed, the enthalpy of adsorption of hydrogen found for most of our polymers is 14 kJ/mol. However, polymer prepared from 1,4-diaminobenzene crosslinked with tribromobenzene features a ΔH of hydrogen adsorption as high as -18 kJ/mol. This value is promising for the adsorption even at room temperature. Another interesting feature of these polymers is that the actual hydrogen storage capacity for most of the networks of aromatic rings in this study exceeds the capacity that could be realized in nitrogen-accessible nanopores. This finding indicates that our networks of aromatic rings include pores that are too small to allow penetration of nitrogen but large enough for hydrogen adsorption.

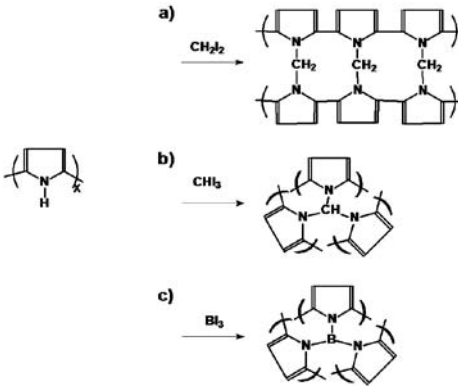

Using reactions shown in the scheme that are similar to those depicted above, we also prepared nanoporous polypyrrols. The diiodomethane-crosslinked polypyrrole, which exhibits very small pores and remarkably high surface areas of 732 m^2/g, reversibly adsorbs 1.6 wt% hydrogen at 77 K and 4 bar. In order to explore the effect of the number of bonds linking the crosslinker with polypyrrole on the porous properties of our materials, we used iodoform. This reaction produced material which reversibly adsorbs 1.3 wt% H_2 at 77K and 4 bar and exhibited surface area of 436 m^2/g. A complete novelty is crosslinking of polypyrrole with boron atoms. This process required significant experimentation in order to optimize the choice of both solvent and base. We again prepared polymer with nanoporosity enabling exclusion of gas molecules larger than hydrogen based on their size. This result is important since it may enable selective adsorption of pure H_2 from its mixtures with other gases that are typically present in the industrially produced hydrogen.

Future Work. While we have now available nanoporous polymers with chemistries providing high enthalpy of hydrogen adsorption, their surface areas need to be increased significantly. Optimization of the reaction conditions using methods of combinatorial chemistry and new catalysts to accelerate the crosslinking are expected to provide the high surface area polymers.

References. [1] B. Panella, M. Hirscher, S. Roth, *Carbon* 2005, *43*, 2209. [2] L. Zhou, Y.P. Zhou, *Int. J. Hydrogen Energy* 2004, *29*, 319. [3] Z.Y. Zhong, Z.T. Xiong, L.F. Sun, J.Z. Luo, P. Chen, X. Wu, J. Lin, K.L. Tan, *J. Phys. Chem. B* 2002, *106*, 9507. [4] S.S. Kaye, A. Dailly, O.M. Yaghi, J.R. Long, *J. Am. Chem. Soc.* 2007, *129*, 14176. [5] F. Schuth, B. Bogdanovic, M. Felderhoff, *Chem. Comm.* 2004, 2249-2258. [6] J. Germain, J. Hradil, F. Svec, J.M.J. Fréchet , *Chem. Mater.* 2006, *18*, 4430. [7] J.Y. Lee, C.D. Wood, D. Bradshaw, M.J. Rosseinsky, A.I. Cooper, *Chem. Comm.* 2006, 2670-2672. [8] N.B. McKeown, P.M. Budd, D. Book, *Macromol. Rapid Commun.* 2007, *28*, 995. [9] P. M. Budd, A. Butler, J. Selbie, K. Mahmood, N.B. McKeown, B. Ghanem, K. Msayib, D. Book, A. Walton. Phys. Chem. Chem. Phys. 2007, 9, 1802. [10] J.X. Jiang, F. Su, A. Trewin, C.D. Wood, H. Niu, J.T.A. Jones, Y.Z. Khimyak, A.I. Cooper, *J. Am. Chem. Soc.* 2008, *130*, 7710-7720. [11] S.K. Bhatia, *Langmuir* 2006, *22*, 1688-1700.

Publications. [1] J. Germain, J. Hradil, F. Svec, J.M.J. Fréchet , *Chem. Mater.* 2006, *18*, 4430. [2] J. Germain, F. Svec, J.M.J. Fréchet , *Polym. Mat., Sci. Eng.* 2007, 97, 272. [3] J. Germain, F. Svec, J.M.J. Fréchet , *J. Mater. Chem.* 2007, 17, 4989. [4] J. Germain, F. Svec, J.M.J. Fréchet , *Chem. Mater.* 2008, 20, 7069. [5] J. Germain, J.M.J. Fréchet , F. Svec, *Chem. Com.* 2009, 1526. [6] J. Germain, J.M.J. Fréchet , F. Svec, *Small*, 2009 (Published online April 22, 2009; DOI: 10.1002/smll.200801762).

Scanning Probes

Deterministic control of polarization switching in multiferroic materials using scanning probe microscopy

N. Balke,[1] S. Choudhury,[2] S. Jesse,[1] M. Huijben,[3,4] Y.H. Chu,[3,5] A.P. Baddorf,[1] L.Q. Chen,[2] R. Ramesh,[3] and S.V. Kalinin[1]

[1] Oak Ridge National Laboratory, Oak Ridge, Tennessee 37831

[2] Dept. of Mat. Sci. Eng., Pennsylvania State University, University Park, PA 16802

[3] Department of Materials Science and Engineering and Department of Physics, University of California, Berkeley, California, 94720

[4] Faculty of Science and Technology, MESA$^+$ Institute for Nanotechnology, University of Twente, P.O. BOX 217, 7500 AE, Enschede, The Netherlands

[5] Dept. of Materials Science and Engineering, National Chiao Tung University, Hsinchu 30010, Taiwan

Proposal Title

Polarization measurements and switching spectroscopy on ferroelectric thin films as function of film thickness (CNMS2008-R07)

Research Achievement

Bias induced phase transitions in ferroelectric oxide materials are used as a functional basis for information storage. Realization of the next generation of magnetoelectric, strain-coupled, and domain-wall based devices necessitates the deterministic control of polarization switching in multiaxial multiferroics. In rhombohedral ferroelectrics, application of an electric field in the pseudocubic (001) direction can lead to 180° ferroelectric switching and 71° and 109° ferroelastic switching. While the electrostatic energy gain is equivalent, the properties of the final structures are remarkably different. In materials such as $BiFeO_3$ (BFO) enhanced conduction at 180° and 109° domain walls has been reported [1], raising the possibility for novel electronic and memory devices. Finally, given that magnetic ordering in BFO is ferromagnetic in (111) planes and antiferromagnetic between these planes, control of non-180° switching is crucial for the development of exchange-coupled magnetoelectric devices.

The goal of this proposal was to investigate and understand the domain switching process on the nanoscale using Scanning Probe Microscopy (SPM). It was found that ferroelectric switching underneath a SPM tip creates a flower like pattern of different domains with different sizes and penetration depths. Most domains were not stable and were not observed experimentally. In order to stabilize certain domains which form underneath a biased SPM tip, the symmetry of the rotationally invariant electric field

around the tip has to be broken. Broken symmetry was created by moving the probe during the switching process. This enabled us to fabricate predefined domain patterns demonstrated through the creation of artificial ferroelectric closure domains which are believed to be the precursors to vortex domains (see Fig. 1). Vortex domains are highly discussed in the literature [2] although not yet observed in ferroelectric materials.

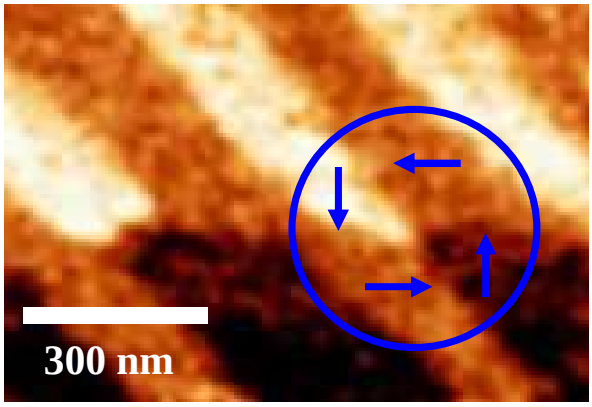

Figure 1 | Closure domains consisting of in-plane domains formed by motion of a scanning SPM tip.

In summary, the deterministic control of ferroelectric switching enables a reliable pathway for local control of non-ferroelectric order parameters, probing local strain and magnetic orderings, and design and creation of domain engineered magnetoelectric, domain-wall based and strain coupled devices.

Future Work

Future work will focus on two directions. The first is to explore the possibilities of local control of the ferroelectric switching at expanded length scales ranging from 20 nm to several μm. The goal is to understand and manipulate switching of macroscopic devices and to find new concepts for device structuring. The second direction will focus on the detailed investigation of artificially created closure domains. These measurements will show if a ferroelectric vortex state forms in the core of the closure domain and will clarify the coupling of this toroidal compared to the classical ferroid order parameters.

References

[1] J. Seidel, L. W. Martin, Q. He, Q. Zhan, Y.-H. Chu, A. Rother, M. E. Hawkridge, P. Maksymovych, P. Yu, M. Gajek, N. Balke, S. V. Kalinin, S. Gemming, F. Wang, G. Catalan, J. F. Scott, N. A. Spaldin, J. Orenstein, and R. Ramesh, Nat Mater. 8, 229 (2009).

[2] I. I. Naumov, L. Bellaiche, and H. Fu, Nature **432**, 7028 (2004).

Publications

[1] N. Balke, S. Choudhury, S. Jesse, M. Huijben, Y.H. Chu, A.P. Baddorf, L.Q. Chen, R. Ramesh, and S.V. Kalinin, “Deterministic control of ferroelastic switching in multiferroic materials”, Nature Nanotechnology, *under review*

Recent progress in scanning probe microscopy at Argonne's CNM

Nathan P. Guisinger[*], Jeffrey R. Guest[*], Paolo Sessi[*,§], and Matthias Bode[*]

[*] Center for Nanoscale Materials, Argonne National Laboratory
§ Politecnico di Milano, Italy

Scientific Thrust Area:

The static and dynamic properties of magnetic nanostructures and strongly correlated materials are of intense current interest in both basic and applied research. Argonne's Center for Nanoscale Materials has science thrusts in the spin dynamics of nanostructures as well as in the atomic-scale characterization of complex oxides and their emerging electronic and magnetic material properties. Significant progress has recently been achieved in both areas.

Research Achievements:

One important pre-condition for cross-sectional STM on complex-oxide heterostructures is that the substrate, single crystalline $SrTiO_3$, can be cleaved/fractured resulting in high quality surfaces. We have successfully achieved the following milestones (see Fig. 1):

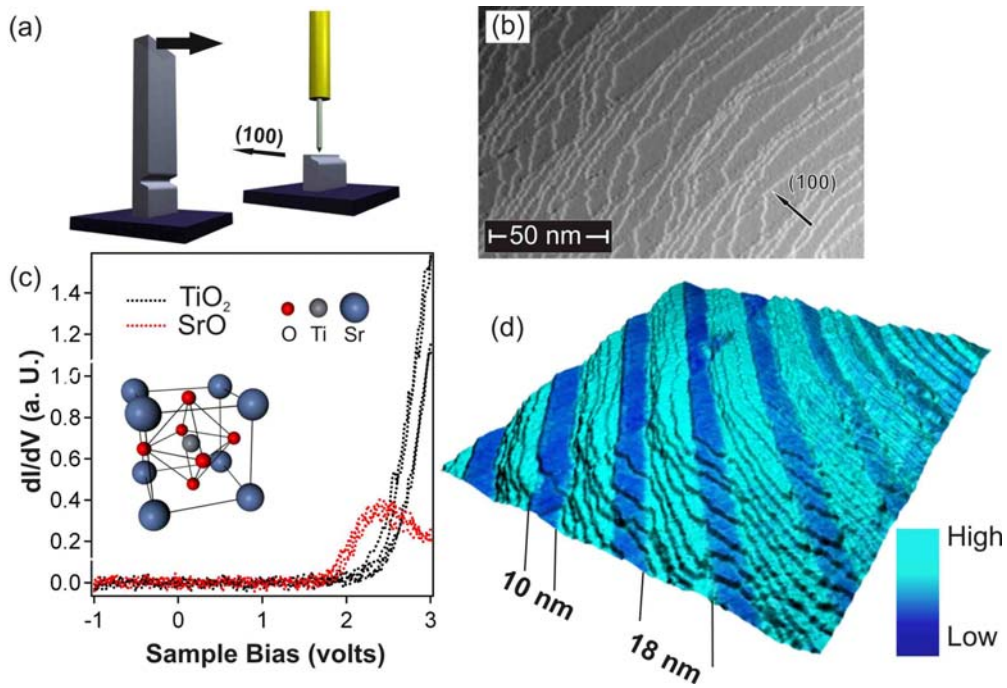

Figure 1(a): Schematic representation of the cleavage process of STO substrates. (b) Topography of the cleaved $SrTiO_3$(001) surface. (c) Tunneling spectra taken on TiO_2 and SrO terminated terraces revealing a strikingly different LDOS in the empty electronic states. (d) Rendered 3-dimensional representation of the surface topography shown in (b) color-coded with the simultaneously measured dI/dV conductance map.

(i) For the first time the cleavage/frature of $SrTiO_3$ has been investigated with the STM revealing large facets of (001) surfaces.

(ii) STM and STS measurements studying the correlation of structural and electronic properties by differential conductance mapping.

Also, we have performed temperature-dependent measurements of the Mn monolayer on W(110) which is known to exhibit a rather complex magnetic structure [1], i.e. a cycloidal antiferromagnetic spin spiral [see inset of Fig. 2(b)]. In this spin spiral in-plane and out-of-plane antiferromagnetic order alternate with a 6 nm period can be visualized because of their different electronic properties [Fig. 2(b)]. Our results suggest that the Néel temperature (long range magnetic order) depends on terrace width.

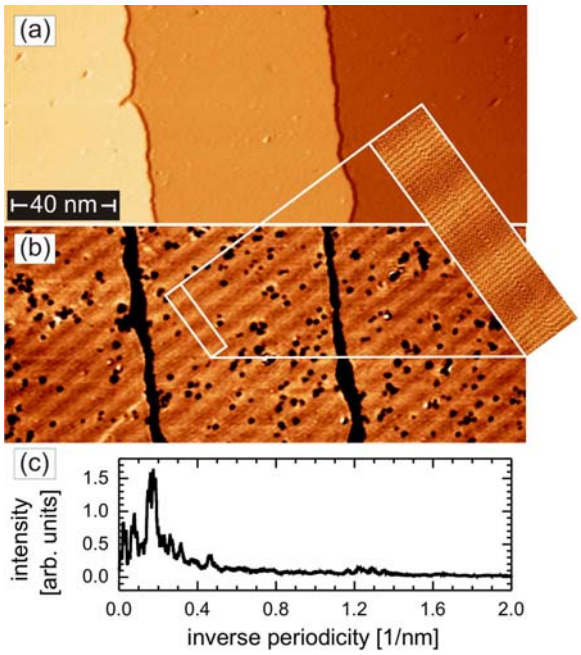

Figure 2. (a) Constant-current STM image of 0.95 AL Mn/W(110). The Mn monolayer is known to form a cycloidal antiferromagnetic spin spiral. (b) Differential conductance maps obtained with a magnetic Fe-coated probe tip. The large scale image shows a modulated intensity originating from spin-orbit coupling with in-plane and out-of-plane magnetized regions exhibiting slightly different spin-averaged electronic properties. The atomic-scale antiferromagnetic order becomes visible at higher resolution (inset). (c) Fourier-spectrum of line sections taken along the [1$\underline{1}$0] direction, i.e. perpendicular to the stripes in (b).

Future work:

The next step in our experiments on complex-oxide superlattices will be to reliably locate the edge of the sample. After this is accomplished we will investigate structural, electronic, and magnetic properties of the superlattices. Key questions will be:

(i) Can we distinguish the compounds based on their different structural electronic properties?

(ii) Does the interface exhibit extraordinary electronic properties?

(iii)How do the interfaces order on the atomic-scale?

In the case of antiferromagnetic nanostructures we will focus on the following questions:

(i) What is the relation between short- and long-range magnetic order?

(ii) How do single antiferromagnetic particles behave when thermally activated magnetization reversal processes kick in?

References:

[1] M. Bode et al., *Chiral magnetic order at surfaces driven by inversion asymmetry*, Nature 447, 190 (2007)

New Ways of Seeing: Developing and Understanding Sensors for Scanning Probe Microscopy

Babak Sanii [a], Paul D. Ashby [a], Virginia P. Altoe [a] , Miquel Salmeron[a], Alex Weber-Bargioni[a,b] , Bruce Hartneck[b], Stefano Cabrini[b], James P. Schuck[a], Ivo W. Rangelow[c] and D. Frank Ogletree [a].
[a]*Imaging and Manipulation Facility, Molecular Foundry, Lawrence Berkeley National Laboratory, Berkeley, CA*
[b]*Nanofabrication Facility, Molecular Foundry, Lawrence Berkeley National Laboratory, Berkeley, CA*
[c] *Technische Universität Ilmenau, Germany*

Scientific Thrust Area

A main thrust of the Imaging and Manipulation Facility of the Molecular Foundry is to develop novel probes and extend the power of scanning probe microscopy to new areas.

- AFM studies of biological samples in fluid environments are limited by cantilever dissipation and noise. A novel "fiber force probe" is being developed to reduce the imaging noise floor by several orders of magnitude.
- A novel technique has been developed to fabricate optically-resonant plasmonic nano-antennas on AFM cantilever tips to perform near-field optical spectroscopy with ~ 20 nm resolution.
- Analytical transmission electron microscopy is being applied to study wear and failure mechanisms of AFM tips, and to explain the fundamental tribochemical wear processes that take place.
- Self-actuating self-sensing AFM cantilevers developed at the Technical University of Ilmenau are being applied to in-situ electron microscopy studies.

Research Achievements

Fiber Force Probe

Imaging soft materials such as cell membranes and protein structures requires low forces to avoid sample deformation or damage. Cantilever thermal noise caused by coupling to the fluid environment (dissipation) places a fundamental lower limit on the forces that can be measured. Reducing the cross-section of the cantilever decreases the noise, but size reduction is limited by the AFM optical detection mechanisms. In the "fiber force probe" concept, shown at right, the deflection of a sub-wavelength nanowire cantilever is measured by forward scattering, similar to the methods used in "optical tweezers" experiments.

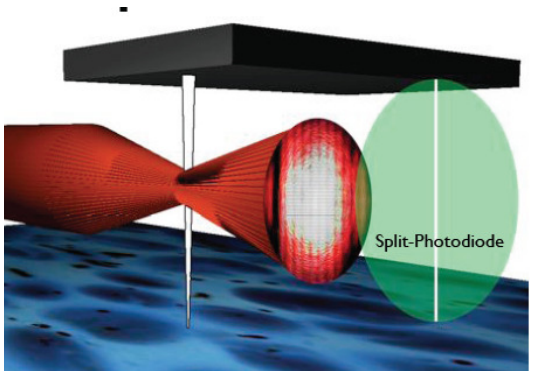

The "fiber force probe" concept

Detailed Mie-scattering calculations predict high force resolution for the fiber force probe, as shown in the simulated images at right. These predictions have been experimentally verified using 100 nm diameter $AgGa_2$ single-crystal nanowires and red laser light.

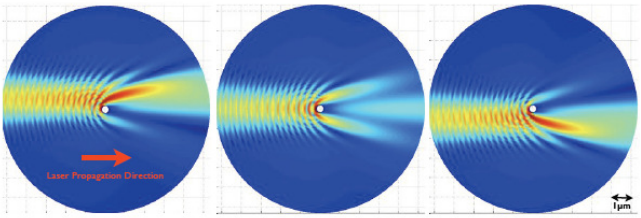

Mie scattering calculations showing nanometer displacement sensitivity for the fiber probe

Plasmonic Antenna Tips

Optical spectroscopy is normally limited by the wave-length of light, however scanning optical microscopy based on near-field scattering from metallic tip structures has demonstrated spatial resolution better than 20 nm. Resonant scattering from gold "bowtie" antennas[1] can generate significantly stronger optical fields than sharp metallic tips. We are constructing AFM cantilevers

with plasmonic antennas fabricated at the tip apex in order to perform scanning near-field optical spectroscopy using Raman scattering or non-linear photoluminescence.

High-quality bowtie antennas can be produced on flat substrates by electron-beam lithography, but this method is not practical for cantilever tips, since it is difficult to align antennas with the required ~ 50 nm precision, and resist spin-coating is problematic. Antennas can also be produced with focused ion beam milling, but Ga ion contamination changes the Au plasmonic properties. A novel fabrication[2] method has been developed in the Nanofabrication facility to deposit a continuous 40 nm Au film, then use electron beam induced deposition (EBID) to make a high-resolution W mask, followed by low-energy Ar sputtering to remove the unmasked gold and the W mask, leaving a precision-aligned bowtie on the cantilever tip. Antenna tips have been successfully fabricated that show significant near-field Raman enhancement.

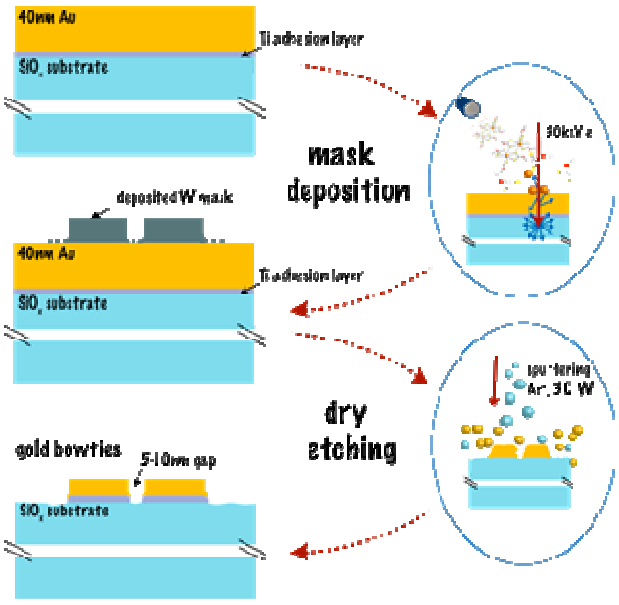

Fabrication Process for Bowtie Cantilever Tips

TEM investigation of AFM tip

As an AFM tip moves across a sample surface wear processes take place at the tip apex. This can change resolution in imaging experiments, and cause loss of signal in measurements such as local conductivity or work function. Analytical TEM studies reveal that the wear processes depend on the specific tribochemical system under study. In studies of organic monolayers on Si, the tips, terminated by single-crystal grains of Pt, showed atomic-scale wear without plastic deformation or dislocation formation. Once a flat facet was formed, an transfer film containing C, Si and Pt formed on the end of the tip, modifying the electrical properties.

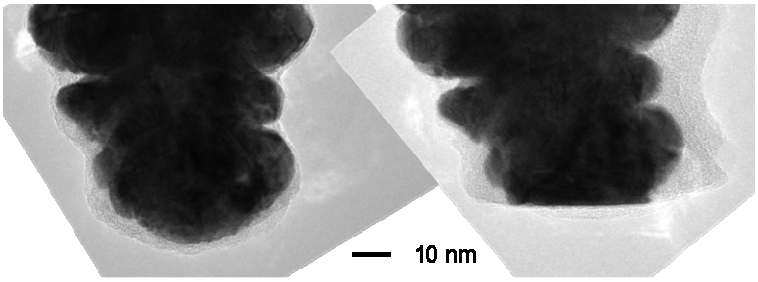

Pt-coated AFM tip before and after imaging organic monolayers on Silicon substrates.

Future work

The fiber force probe, which has been validated in simulation and sensor tests, will be applied to biological systems for *in-situ* imaging of soft matter systems.

The plasmonic antenna tips will be used for near-field spectroscopic imaging of nanoscale samples.

Additional investigations are underway to determine the exact mechanisms of AFM tip wear as a function of substrate composition and imaging conditions.

References

1 P. J. Schuck**,** *et al*., "Improving the mismatch between light and nanoscale objects with gold bowtie nanoantennas." *Phys. Rev. Lett.* 94, 017402 (2005).

2 A. Weber-Bargioni et al.*, in preparation.*

Toward Complete Control of Localized Light and its Interactions with Matter

P. J. Schuck[1], S. Wu[1], A. Weber-Bargioni[1], Z. Zhang[1], M. Schmidt[1], D. F. Ogletree[1], P. Ashby[1], H. Choo[1], J. Bokor[1], S. Cabrini[1], A. Schwartzberg[1], J. Urban[1], P. Adams[2], M. Salmeron[1]
[1] Molecular Foundry, [2] Physical Biosciences Division; Lawrence Berkeley National Lab

Scientific Thrust Areas: (1) Plasmonic optical antennas and optical transformers, **(2)** Chemical imaging of plant biomass with μ-Raman spectroscopy for biofuel applications

Research Achievements

Plasmonic optical antennas and optical transformers - The recent invention of single metallic optical nanoantennas has greatly improved the mismatch between light and nanometer-scale objects[1]. Optical nanoantennas are specifically engineered to enhance fields at visible and near-infrared (NIR) wavelengths and confine them to nanoscale regions in size, significantly defeating conventional diffraction-limited resolution (~ 300 nm). By *efficiently* coupling light with localized plasmon modes, optical nanoantennas harness the short wavelength excitations to create extremely intense, ultra-confined optical fields.

One major thrust has been the fabrication and characterization of nanoantenna-based scanning probes that we will use for high-spatial resolution (nm-scale) imaging spectroscopy [fig. 1c]. Nanoantennas comprised of plasmonically-coupled metallic nanoparticles offer appreciable advantages over other near-field optical devices, most notably aperture-based and apertureless near-field scanning optical microscope probes. In particular, nanoantennas present much greater near-field coupling efficiency than NSOM probes (efficiency > 10% for a bowtie versus ~10^{-5} for a typical metal-coated pulled fiber probe) and significantly higher field enhancement than has been measured for apertureless tips.

Another related research thrust has been the experimental and theoretical study of a device, termed the Plasmonic Color Nanosorter (PCoN), which demonstrates both the ability to efficiently capture and strongly confine broadband optical fields, as well as to spectrally filter and steer them while maintaining nanoscale field distributions [fig. 1a-b]. A central goal of plasmonics is complete control over optical signals at deeply sub-wavelength scales. The recent invention of optical nanoantennas has led to a number of device designs that provide confinement of optical fields at nanometer length scales. For photonic applications, however, the effectiveness of these structures would be *significantly improved* by the added ability to spatially sort the optical signals based on energy/color. Because of the capability to localize *and* steer photons, color nanosorters are expected to have profound impact on a wide range of optoelectronic and plasmonic applications including ultrafast color-sensitive photodetection, solar power light harvesting, and multiplexed chemical sensing.

In addition to the nanoantenna tips and the PCoN, we have undertaken a number of other plasmonics-related projects in our lab, including the study of novel tapered 3-dimensional nano-optical transformers/antennas specifically engineered for SERS detection (with users M. Wu and E. Yablonovitch, UCB), nonlinear optical imaging spectroscopy of plasmonic nanostructures [fig. 1d], and the demonstration of a MEMS-based tunable-gap nanoantenna fabricated with Au-coated TiOx nanoswords (with users B. Sosnowchik and L. Lin, UCB).

Chemical imaging of plant biomass with μ-Raman spectroscopy - A detailed knowledge of the plant cell wall will allow researchers to visualize the chemical and physical obstacles to biomass breakdown. This will be vital in developing better pretreatment procedures, and identifying plant material that may naturally be better suited to use in such processes. We demonstrate, for the first time, the label-free *in situ* study of wild type and low lignin transgenic poplar wood by confocal Raman microscopy aimed at the characterization and comparison of local compositional and structural traits. Accurate investigation of these samples will have significant impact on biofuel technology since low lignin wood offers potentials for improved biomass conversion into fermentable sugars. Importantly, lignin was found to be significantly reduced in the S2 wall layers of the transgenic poplar fibers, suggesting that such transgenic approach may help overcome cell wall recalcitrance to wood saccharification [fig. 1e-f]. Also, spatial heterogeneities in the lignin composition, particularly with regard to coniferaldehyde moieties, were found in both the wild type and the transgenic samples.

Future work: Our future goals include the use of nanoantenna scanning probes for nanoscale optical imaging spectroscopy of novel nanomaterial-based light-harvesting devices, non-invasive imaging of fundamental nanoscale mode volumes/field distributions created by plasmonic devices/structures, nano-Raman chemical mapping of plant cell walls, and the use of a novel background fluorescence-suppressing method for the first ever Raman chemical imaging studies of *Arabidopsis*.

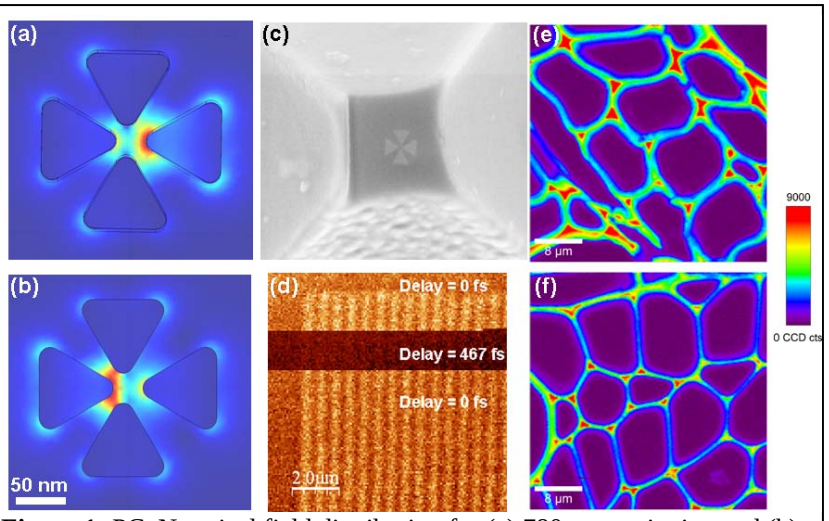

Figure 1: PCoN optical field distribution for (a) 780 nm excitation and (b) 820 nm excitation; (c) SEM image of a double-bowtie "cross" nanoantenna fabricated at the end of an AFM tip; (d) image of enhanced four-wave-mixing signal originating from a Au plasmonic grating. Note the disappearance of signal when pump and probe pulses are separated by a non-zero delay; chemical map of lignin distribution in wood from (e) wild-type poplar and (f) transgenic low-lignin poplar.

References:

[1] P. J. Schuck**,** *et al*., "Improving the mismatch between light and nanoscale objects with gold bowtie nanoantennas." *Phys. Rev. Lett.* 94, 017402 (2005).

Publications:

- S. Wu[†], Gang Han[†], *et al*, "Non-blinking and photostable upconverted luminescence from single lanthanide-doped nanocrystals," *PNAS*, in press (2009)
- M. Schmidt, *et al*., "Label-free *in situ* imaging of lignification in the cell wall of low lignin transgenic *Populus trichocarpa*," *Planta Rapid Comm*., submitted (2009)
- B. D. Sosnowchik, *et al*, "Tunable Optical Enhancement from a MEMS-Integrated TiO2 Nanosword Plasmonic Antenna," *Proceedings of 22th IEEE Micro Electro Mechanical Systems Conference*, pp. 128-131, Sorrento, Italy, Jan. 2009.
- C. Nobile, *et al*, "Probe tips functionalized with nanocrystal tetrapods for high resolution atomic force microscopy imaging," *Small* 4, 2123 (2008)
- A. Jamshidi, *et al*, "Dynamic manipulation and separation of individual semiconducting and metallic nanowires," *Nature Photonics* 2, 85 (2008), **Cover Article**
- F. Wang, *et al*, "Observation of excitons in one-dimensional metals," *Phys. Rev. Lett.* 99, 227401 (2007)

An STM Study of Atomic Co Wires

Nader Zaki[1], Denis Potapenko[1], Peter Johnson[2], Percy Zahl[3], Danda Acharya[3]
Peter Sutter[3], Richard Osgood[1]

[1] *Columbia University, New York, NY 10027*
[2] *Brookhaven National Lab, Upton, NY 11973*
[3] *Brookhaven National Lab, Center for Functional Nanomaterials, Upton, NY 11973*

Proposal Title: STS Study of One-Atom Wide Co Wires

Research Achievement:
Due to stronger electron-electron interactions, 1-D systems are predicted and, in some cases, have been shown to exhibit unique and exotic electronic properties. One route to the formation of 1-D systems is by self-assembly using low-index vicinal crystal surfaces. In this regard, we have successfully formed 1-atom wide Co wires using Cu(775), a 7-atom wide stepped array with (111) terraces. For our particular morphology, the Co wires are not laterally encapsulated but are positioned exactly at the step edge. We have performed STM studies of this system at room temperature (RT) and have made STS measurements at low temperature (LT), ~5K. While vicinal Cu(111) does exhibit

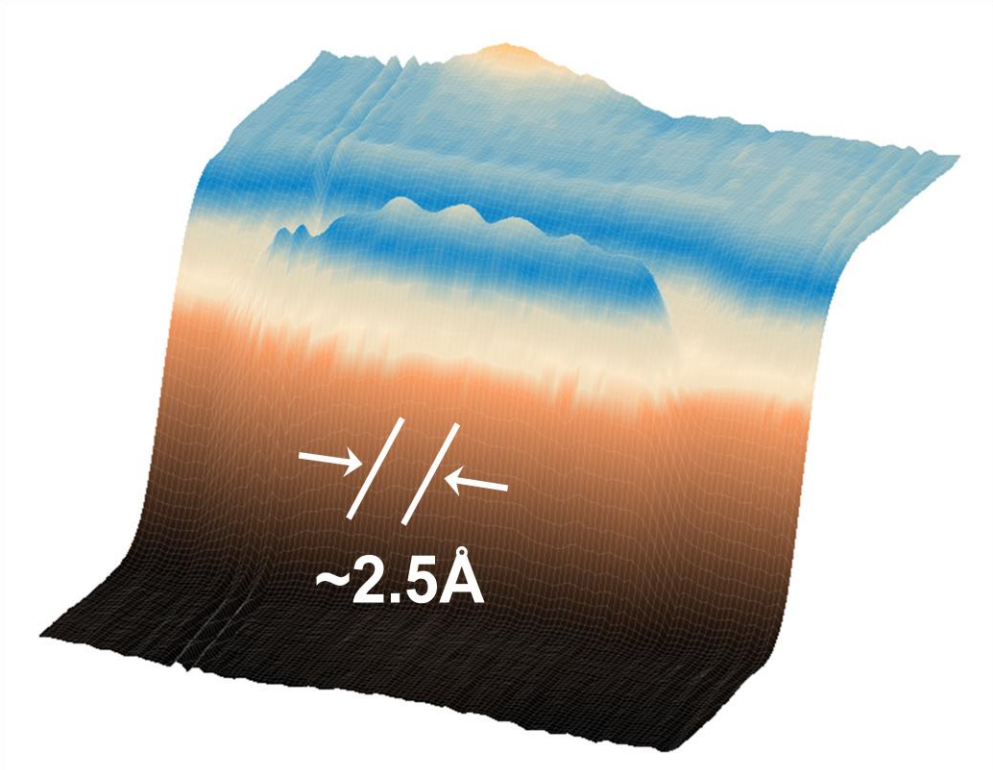

Figure 1: *A 7-atom Co chain that self-assembled at a Cu step edge. This image was obtained using a low-temperature STM at the Center for Functional Nanomaterials, Brookhaven National Labs.*

"frizz" at the steps when scanning above cryogenic temperatures, the Co wires pin the edges, visually accentuating their presence under STM. Furthermore, we observe a lower local density of states for the Co wires as compared with the Cu steps at RT, which also serves to differentiate the two metals. At LT, a Co chain at the step edge induces a Friedel-like oscillation (as shown in Fig.1) that is not present at a bare Cu step. Cu(111) possess a surface projected bandgap which may electronically decouple the wire electrons that reside in this gap. However, we also see resonances at the Fermi level which suggests electronic coupling between the vicinal Cu surface and the Co electrons.

Future Work:

We have obtained interesting scanning tunneling spectra and are currently trying to understand them more theoretically. To facilitate our understanding, we intend to perform more tunneling spectroscopy measurements to rule out tip effects and other sources of spectra variability. This would, for example, involve using a different type of tip, such as Pt-Ir, instead of W. Furthermore, we would like to attempt the spectral mapping of a Co chain region. This would add greatly to our limited point-based measurements that have been made so far.

Theory and Simulation

Unconventional Donor–Acceptor Molecules for Supramolecular Assembly and Electronics

Bobby G. Sumpter[1], Vincent Meunier[1], Edward F. Valeev[2], Álvaro Vázquez-Mayagoitia[3], Ling Yuan[4], Andrew J. Lampkins[4], Hengfeng Li[4], and Ronald K. Castellano[4]

[1]*Computer Science and Mathematics Division and Center for Nanophase Materials Sciences, Oak Ridge National Laboratory, Oak Ridge, TN 37831*; [2]*Dept. of Chemistry, Virginia Tech, Blacksburg, VA 24061*; [3]*Universidad Autónoma Metropolitana Iztapalapa, Dept. de Química, San Rafael Atlixco 186, Col Vicentina, Iztaplapa, Mexico City, DF 09340, México*; [4]*Dept. of Chemistry, University of Florida, P.O. Box 117200, Gainesville, FL 32611*

Proposal Title

Through-Bond Interactions in Nanoscale Self-Assembly (CNMS2004-016) and *Theory-Guided Design of Supramolecular Wires for Optoelectronic Applications* (CNMS2007-029)

Research Achievement

Nanoscale self-assembly of donor-σ-acceptor molecules: Self-assembly lies central to the implementation of a bottom-up approach to design functional organic materials and represents a promising strategy to control bulk electronic and optical properties.[1] Over the past several years, researchers at the University of Florida and Center for Nanophase Materials Sciences (CNMS) at ORNL have shown, through a joint experimental and theoretical study, how the self-assembly of rather "unconventional" donor–acceptor molecules may lead to their broad application in materials science, supramolecular chemistry, and organic electronics.

Molecules containing a donor and acceptor group separated by an insulating spacer (donor-σ-acceptor molecules) have been largely unexplored with respect to their self-assembly and supramolecular electronic properties, despite early enthusiasm.[2] Demonstrated in 2005 was that 1-aza-adamantanetriones (AATs) **1** (Fig. 1a), one class of donor-σ-acceptor molecules, could be designed to rapidly self-assemble in organic solution to form gels and homogeneous fibers (Fig. 1b), and that this macromolecular behavior responded dramatically to chemical modifications of the monomers.[3,4] What has emerged since, through extensive first principles calculations, is a detailed description of the AATs at the monomer, dimer, and multimer levels and a new approach to one-dimensional supramolecular wires based on the systems that have easily tunable electronic and physical properties.[a–c]

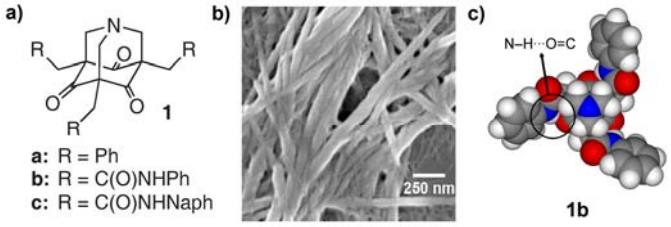

Fig. 1

Both many body perturbation theory (MBPT) and density functional theory (DFT) calculations have identified a propeller-shaped conformation of the AATs **1** as the lowest energy form, additionally stabilized for amide derivatives (e.g., **1b** and **1c**) by weak intramolecular hydrogen bonds (Fig. 1c).[a,b] These gas-phase features are in excellent agreement with experimental data. Theory further shows the proclivity of AATs of this shape to organize into head-to-tail stacked arrays in the gas phase (shown in Fig. 2a for **1a**), a process driven by dipolar and dispersion forces.[a,b] That aromatic stacking interactions are important is shown through the more robust solution-phase self-assembly behavior of naphthyl derivative **1c** versus phenyl derivative **1b**, an observation that agrees well with predicted dimer binding energies (Table 1).[5]

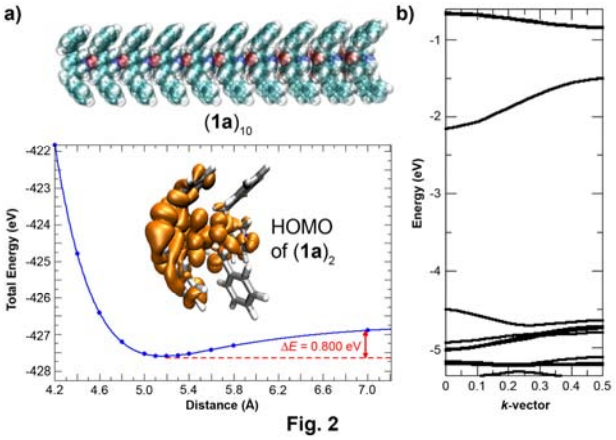

Fig. 2

The simulated X-ray diffraction (XRD) pattern obtained from the optimized supramolecular structure for **1a** also compares favorably to the experimentally-measured XRD spectrum of **1a** as a powder.[a]

Emergent electronic structure and a new class of supramolecular wires: Upon self-assembly of the AATs into 1-D periodic arrays the frontier molecular orbitals are delocalized, spanning the entire system, through the saturated tricyclic cores of the monomers (Fig. 2).[b] The nature of the dispersion is shown by the frontier molecular orbitals of the dimer of **1a** (HOMO shown in Fig. 2a inset) and the electronic band structure for the $(\mathbf{1a})_{10}$ assembly (Fig. 2b); the latter can be tuned from the insulating regime to the semiconducting regime by suitable chemical functionalization of the core (Table 1). For example, the supramolecular bandgap spans from 2.3 eV for **1a** (Fig. 2) to 1.5 eV for the triamides AAT **1b** and **1c**.

Table 1. Calculated properties of dimers (assemblies) of **1a–c**.

parameter	$(\mathbf{1a})_2$	$(\mathbf{1b})_2$	$(\mathbf{1c})_2$
binding *E* (eV)	0.40	0.35	0.83
intercore distance (Å)	5.1	5.5	4.9
LUMO–LUMO transfer integral (eV)	0.25	0.16	0.40
E_{gap}[a] (eV)	2.3	1.5	1.5[b]

[a] From plane-wave pseudopotential calculations. [b] This system also exhibits an indirect bandgap of 0.99 eV.

Future Work

We have shown how tunable through-bond donor–acceptor interactions, shape, and aromatic interactions can direct the self-assembly of donor-σ-acceptor molecules in solution and the gas phase. Rigorous theoretical characterization has revealed a supramolecular electronic structure and a conceptual framework for achieving charge transport characteristics from such systems that differ from traditional π-conjugated materials. In future work we will pursue a) strategies to enhance the AAT core-to-core interactions in solution, b) derivatives that show useful macromolecular phases, and c) the design of new synthetic architectures that can exploit through-bond donor–acceptor interactions in the context of supramolecular assembly and novel electronic structure.

References

1) Schenning, A.; Meijer, E. W. *Chem. Commun.* **2005**, 3245–3258.
2) Aviram, A.; Ratner, M. A. *Chem. Phys. Lett.* **1974**, *29*, 277–283.
3) Li, H.; Homan, E. A.; Lampkins, A. J.; Ghiviriga, I.; Castellano, R. K. *Org. Lett.* **2005**, *7*, 443–446.
4) Lampkins, A. J.; Abdul-Rahim, O.; Li, H.; Castellano, R. K. *Org. Lett.* **2005**, *7*, 4471–4474.
5) Sumpter, B. G.; Meunier, V.; Yuan, L.; Castellano, R. K., manuscript in preparation.

Publications

a) Sumpter, B. G.; Meunier, V.; Vázquez-Mayagoitia, Á.; Castellano, R. K. "Investigation of the Nanoscale Self-Assembly of Donor-σ-Acceptor Molecules" *Int. J. Quantum Chem.* **2007**, 107, 2233–2242.

b) Sumpter, B. G.; Meunier, V.; Valeev, E. F.; Lampkins, A. J.; Li, H.; Castellano, R. K. "A New Class of Supramolecular Wires" *J. Phys. Chem. C.* **2007**, 111, 18912–18916.

c) Yuan, L.; Sumpter, B. G.; Abboud, K. A.; Castellano, R. K. "Links Between Through-Bond Interactions and Assembly Structure in Simple Piperidones", *New J. Chem.* **2008**, 32, 1924–1934 (identified as a "hot article").

Dirac Materials

Hari Dahal, J.-X. Zhu, Alexander Balatsky
Center for Integrated Nanotechnologies, Los Alamos National Laboratory

Tim Wehling, Alexander Lichtenstein,
University of Hamburg

Hari Manoharan, Laila Mattos,
Stanford University

M. Crommie, V. Brar, Y. Zhang
University of California, Berkeley

Scientific Thrust Area: Theory and Modeling of Nanoscale Phenomena

Projects: Controlling the Kondo Effect in Graphene (H. Manoharan); Controlling Electron and Phonon Interactions in Graphene (M. Crommie)

Research Achievement:
Recently a new single layer material -- graphene has been discovered.[1] This is a material where Dirac points in the fermionic spectrum lead to a very unusual transport properties and other electronic signatures like impurity states.[2,3] We will argue that these properties are not unique to graphene and in fact are a direct consequence of Dirac spectrum in fermionic excitation sector. We point strong similarities with d-wave superconductors,[4] superfluid 3He, p-wave superconductors and with other materials exhibiting Dirac electronic spectrum and offer a unifying perspective on the discussion about nanoscale electronics in these materials. We argue that discovery of graphene signifies the emergence of a new class of materials, that we call Dirac Materials, the class where nontrivial properties emerge as a direct consequence of Dirac spectrum of excitations.

In recent work in CINT in collaboration with users from Stanford, we have addressed the local electronic properties of graphene such as impurity states,[2,3] Kondo effect,[5] and inelastic electron tunneling spectroscopy (IETS) in graphene [6] (UC Berkeley user project).

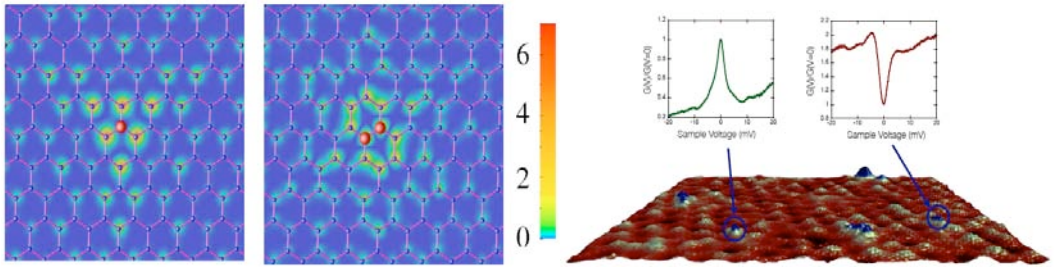

Fig.1. Right panel:Impurity induced modifications of Local Density of States in graphene. [2,3] Left panel: Local Density of states near Co impurity atom on graphene, Kondo peak and dip are observed, depending on position of an atom.[5]

Future Work: We plan to develop microscopic theory of Kondo effect using realistic band structure calculations. We plan to further develop theory of Inelastic Electron Tunneling Spectrosopy (IETS) in graphene.

References:

[1] K. S. Novoselov, A. K. Geim, S. V. Morozov, D. Jiang, Y. Zhang, S. V. Dubonos, I. V. Grigorieva, and A. A. Firsov, Science **306,** 666 (2004).

[2] T. O. Wehling, A. V. Balatsky, M. I. Katsnelson, A. I. Lichtenstein, K Scharnberg, R. Wiesendanger, Phys. Rev. B **75**, 125425 (2007).

[3] Hari P. Dahal, A. V. Balatsky, Jian-Xin Zhu, Phys. Rev. B **77,** 115114 (2008).

[4] A. V. Balatsky, I. Vekhter, J. X. Zhu, Rev. Mod. Phys. **78**, 373 (2006).

[5] Laila Mattos, and Hari Manoharan, (unpublished).

[6] T. Wehling, et. al., Phys. Rev. Lett. **101**, 21608, (2008).

Publications:

1. T. O. Wehling, A. V. Balatsky, M. I. Katsnelson, A. I. Lichtenstein, K Scharnberg, R. Wiesendanger, Phys. Rev. B **75**, 125425 (2007).
2. Hari P. Dahal, A. V. Balatsky, Jian-Xin Zhu, Phys. Rev. B **77,** 115114 (2008).
3. A. V. Balatsky, I. Vekhter, J. X. Zhu, Rev. Mod. Phys. **78**, 373 (2006)
4. Laila Mattos, and Hari Manoharan, (in preparation).
5. T. Wehling, et. al., Phys. Rev. Lett. **101**, 21608, (2008).

Dispersions of Nanoparticles in Polymers: Interfacial and Bulk Behavior

Amalie L. Frischknecht[1], Erin S. McGarrity[2], and Michael E. Mackay[3]

[1]*Sandia National Laboratories, Albuquerque, NM*
[2]*Michigan State University, East Lansing, MI*
[3]*University of Delaware, Newark, DE*

Scientific Thrust Area: Theory and Modeling of Nanoscale Phenomena
Proposal Title: Effects of Nanoparticles on Polymer Film Dewetting

Research Achievement

Polymer nanocomposites display a variety of unique features when the nanoparticle radius is smaller than the radius of gyration of the polymer, including miscibility of the nanoparticles in the polymer and assembly of the nanoparticles at surfaces. Thin films of these blends have many possible applications such as chemical sensors, computer memory, supercapicitors and flexible organic solar cells. The realization of these technologies depends on understanding and controlling the interactions in the system to obtain self-assembled, functional nanostructures. Of particular interest to us is the interplay of entropic effects and van der Waals interactions, which are key in thin film stabilization and placement of the nanoparticles at particular interfaces. We are using various theoretical techniques to elucidate the mechanisms involved in these nanoparticle/polymer composites.

Polymer/Nanoparticle Blends at a Substrate

In thin films of polystyrene (PS) nanoparticles blended with PS homopolymer, we have shown that the nanoparticles form a monolayer on the substrate. Since the polymer and nanoparticles are chemically compatible, the forces driving the nanoparticles to the substrate are thought to be entropic in origin [1]. The presence of about a monolayer of nanoparticles at the substrate has the additional surprising property of preventing the dewetting of the films.

We modeled this system as a mixture of hard spheres and freely jointed hard chains, near a hard wall. Using a fluids density functional theory (DFT), we showed that there is a first order phase transition (see Fig. 1) in these blends in which the nanoparticles expel the polymer from the substrate to form a monolayer at a certain nanoparticle concentration. The nanoparticle transition concentration depends on the length of the polymer and on the nanoparticle diameter. The phase transition is due to both packing entropy effects related to size asymmetry between the components, and to the polymer configurational entropy, justifying the so-called "entropic push" observed in experiments. The magnitude of the free energy gain upon addition of nanoparticles is consistent with experiment.

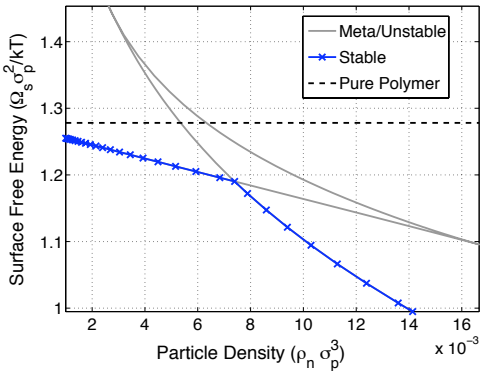

Fig. 1: Free energy curve showing a change in slope at the phase transition.

Bulk Mixtures

Neutron scattering experiments by the Mackay group showed that for PS nanoparticles blended in PS, the polymers undergo a significant amount of chain expansion as the nanoparticle volume fraction increases [2]. This is surprising in that chain expansion costs free energy, which should therefore make the nanoparticles less miscible in the polymer, but the nanoparticles were indeed miscible. There is considerable controversy in the literature over whether the addition of nanoparticles to a polymer melt causes chain expansion. To address this question, we performed self-consistent polymer reference site model (SC/PRISM) theory calculations. PRISM is a liquid state theory that predicts the equilibrium structure of polymeric fluids. In self-consistent PRISM theory, the intramolecular structure of the polymer chains is calculated by performing a single-chain Monte Carlo simulation, in a solvation potential provided by PRISM theory that represents all the intermolecular interactions in the system. This allows a determination of the radius of gyration R_g from the single chain simulation, without the computational cost of performing a many body simulation in a dense fluid.

In the first SC/PRISM calculations on nanoparticle/ polymer blends, we find that the nanoparticles do indeed perturb the polymer chain dimensions. Fig. 2 shows the value of R_g, relative to the value for the pure polymer melt R_{g0}, as a function of nanoparticle volume fraction φ_n. The polymers expand with increasing nanoparticle volume fraction, in semi-quantitative agreement with our experimental results.

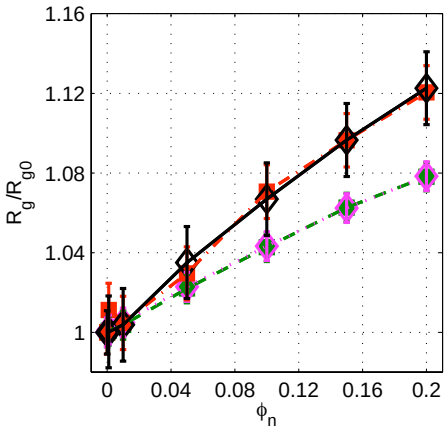

Fig. 2: Chain expansion for nanoparticles of diameters 5 (squares) and 6.2 (diamonds) for chains of length 40 (lower curves) and 80 (upper curves).

Future Work

We plan to explore the effects of attractive interactions on the phase transition described above for nanoparticle/ polymer blends near a substrate. We will also extend the fluids-DFT to include liquid/vapor interfaces in order to model truly thin films. These results will be compared with experimental results on other nanoparticles, such as CdSe quantum dots, mixed in polymers.

References

[1] R. S. Krishnan et al., J. Phys. Condens. Matter 19, 356003 (2007).
[2] A. Tuteja, P.M. Duxbury, and M.E. Mackay, Phys. Rev. Lett. 100, 077801 (2008).

Publications

1. E.S. McGarrity, A.L. Frischknecht, L.J.D. Frink, and M.E. Mackay, “Surface-induced first-order transition in athermal polymer-nanoparticle blends,” Phys. Rev. Lett. 99, 238302 (2007).
2. E. S. McGarrity, A. L. Frischknecht, and M. E. Mackay, “Phase behavior of polymer nanoparticle blends near a substrate”, J. Chem. Phys. 128, 154904 (2008).
3. E. S. McGarrity, P. M. Duxbury, M. E. Mackay, and A. L. Frischknecht, “Calculation of entropic terms governing nanoparticle self-assembly in polymer films,” Macromolecules 41, 5952 (2008).
4. A. L. Frischknecht, E. S. McGarrity, and M. E. Mackay, “Expanded chain dimension in polymer melts with nanoparticle filles,” submitted to Phys. Rev. Lett. (2009).

Role of Cel7A Linker in Enzymatic Hydrolysis of Cellulose Chains: A Simulation Study

Xiongce Zhao[1], Courtney Taylor[2], Clare McCabe[2], William S. Adney[3] and Michael E. Himmel[4]

[1]Center for Nanophase Materials Sciences, Oak Ridge National Laboratory, Oak Ridge, TN [2]Department of Chemical and Biomolecular Engineering, Vanderbilt University, Nashville, TN [3]National Renewable Energy Laboratory, Golden, CO [4]Chemical and Bioscience Center, National Renewable Energy Laboratory, Golden, CO

Proposal Title: Computational Studies of Nanoscale Biocatalytic Mechanisms Relevant to Biomass Conversion

Plant biomass represents an abundant source of fermentable carbohydrates, which when converted to fuels such as ethanol, holds the potential for significant environmental, economic, and strategic gains. Currently, chemical or biological conversion of biomass is too costly to permit ethanol to compete as a viable alternative fuel; hence, there is a need to understand and ultimately engineer the nanoscale mechanisms of the depolymerization of cellulose.

Cellobiohydrolase I (CBH I), from *Trichoderma reesei*, is one of the most active cellulases known. This enzyme hydrolyzes cellulose in a "processive" manner, moving along a cellulose chain liberating cellobiose residues. For this reason, CBH I has been cited as an example of nature's nanomachines[1,2]. CBH I is a multi-domain enzyme, consisting of a large catalytic domain containing an active site tunnel and a small cellulose binding domain (CBD) joined to one another by a 26 amino acid linker peptide (Fig. 1). While much is known about the structure and composition of the CBD and catalytic domain a complete CBH I structure has not been solved. The linker domain plays a significant role in enzyme function (mutation studies show reduced or full negation of enzymatic activity on crystalline cellulose when the linker is removed); however, although the amino acid sequence in the polypeptide chain of the linker is known, the biophysical nature of the linker structure, its role in hydrolysis, and its relation to the catalytic and binding domains is unknown.

The primary aim of this work is to elucidate the nanoscale mechanism of action of CBH I on cellulose. It is believed that the enzyme moves along a single cellulose chain in a processive manner oscillating between an extended and compressed state, in a caterpillar like motion. Due to the flexibility of the linker, the CBD can remain bound to one site of the cellulose while the enzyme hydrolyzes the cellulose chain within a 4 nm range. Once the linker becomes compressed to a very short distance, it has been hypothesized that the energy of the linker will be enough to free the cellodextrin chain from the CBD and allow the enzyme to

progress down the cellulose chain[3]. Using computational methods we are probing the validity of the proposed mechanism by which the linker moves along a cellulose chain. Ultimately, we would like to understand the mechanism of binding and catalysis in this system, with the goal of optimizing the nanoscale action of the enzyme, and eventually designing more effective versions of this enzymatic nanomachine. We believe the knowledge gained will also provide insight into nature's design of nanoscale devices, which will be useful in the development of biomimetic nanodevices.

Research Achievement:

Free energy calculations of the linker peptide in water have shown the linker exhibit two stable states at lengths of 2.5 and 5.5 nm during a extension/compression process, with a free energy difference of 10.5kcal/mol between the two states separated by an energy barrier. The switching between these stable states could support the hypothesis that the linker peptide has the capacity to store energy in a manner similar to a spring. Our simulations also indicate that the free energy of the linker depends on the existence of the cellulose substrate. In particular, a free linker shows distinct free energy profiles compared with that of the linker above a cellulose surface, which implies that the interaction with the cellulose surface plays at least a partial role in determining any energy storage feature in the linker[6].

Future Work:

Simulations will be performed to probe the influence of the stretching/compression pathway and the role of the surface and interaction of the sugar residues on the linker backbone with the cellulose surface. We will also be studying mutated linkers that have been studied experimentally at and shown to have a reduced activity.

References:

[1] See, e.g., G. Cook, H. Brown, D. Sandor, E. Ness, and T. LaRocque, "Unraveling the Structure of Plant Life," National Renewable Energy Laboratory 2003 Research Review, http://www.nrel.gov/research_review/pdfs/36178c.pdf

[2] Clare McCabe, Thomas Schulthess, Peter Hirschfeld, Jackie Chen, Andy McIlroy, Gil Weigand, Yury Gogotsi, Andy Felmy, Jeff Nichols, Thomas Zacharia, Walt M. Polansky, and Michael Strayer, "Scientific Impacts And Opportunities For Computing," 2008, Office of Advanced Scientific Computing Research, Office of Science, Department of Energy, available on the web at http://www.sc.doe.gov/ascr/ProgramDocuments/Docs/ScientificImpacts&Oppor.pdf

[3] L. Zhong, J. F. Matthews, M. F. Crowley, T. Rignall, C. Talon, J. M. Cleary, R. C. Walker, G. Chukkapalli, C. McCabe, M. R. Nimlos, C. L. Brooks, M. E. Himmel, and J. W. Brady, "Interactions of the Complete Cellobiohydrolase I from Trichoderma reesei with Microcrystalline Cellulose Ib," *Cellulose*, **15** (2) 261-273 (2008).

[4] Zhou CG, Schulthess TC, Torbrugge S, Landau DP, “Generalised Wang-Landau algoritm to continuous models and joint density of states,” Phys. Rev. Lett., **96**, 120201 (2006).
[5] X. Zhao, T. R. Rignall, C. McCabe, W. S. Adney, M. E. Himmel, “Energy Storage Mechanism of the Trichoderma reesei Cel7A I Linker Peptide from Molecular Dynamics Simulation,” *Chemical Physics Letters*, **460** 284–288 (2008).
[6] X. Zhao, C. Taylor, C. McCabe, W. S. Adney, M. E. Himmel, “Role of Cel7A Linker in Enzymatic Hydrolysis of Cellulose Chains: A Simulation Study,” *in preparation*, (2009).

Publications:

X. Zhao, T. R. Rignall, C. McCabe, W. S. Adney, M. E. Himmel, “Energy Storage Mechanism of the Trichoderma reesei Cel7A I Linker Peptide from Molecular Dynamics Simulation,” *Chemical Physics Letters*, **460** 284–288 (2008).
X. Zhao, C. Taylor, C. McCabe, W. S. Adney, M. E. Himmel, “Role of Cel7A Linker in Enzymatic Hydrolysis of Cellulose Chains: A Simulation Study,” *in preparation*, (2009).

Understanding the Conductance of Single-Molecule Junctions From First Principles

S. Y. Quek[1], H. J. Choi[2], S. G. Louie[1,3], M. S. Hybertsen[4], L. Venkataraman[5,6] & J. B. Neaton[1]

[1]*Molecular Foundry, Lawrence Berkeley National Lab, Berkeley, CA 94720, USA*

[2]*Dept. of Physics and IPAP, Yonsei Univ., Seoul, Korea*

[3]*Dept. of Physics, Univ. of California, Berkeley, CA 94705, USA*

[4]*Center for Functional Nanomaterials, Brookhaven National Lab, Berkeley, CA 94720, USA*

[5]*Dept. of Applied Physics and Applied Mathematics, Columbia Univ., New York 10027, USA*

[6]*Center for Electron Transport in Nanostructures, Columbia Univ., New York 10027, USA*

Scientific Thrust Area and Relevant Molecular Foundry Proposals. A fundamental challenge in nanoscience is to understand and control charge transport in molecular-scale devices. In close collaboration with experimentalists, we are developing and applying theoretical methods to understand measurements of charge transport properties in single-molecule junctions. Some of the work summarized below has been carried out within the context of the following user projects:

- *Conductance of Pyridine Linked Single Molecule Junctions,* L. Venkataraman (Columbia), Mark S. Hybertsen (BNL)
- *Conductance of Amine Linked Single Molecule Junctions,* L. Venkataraman (Columbia), Mark S. Hybertsen (BNL)
- *Aromatic Molecular States at Metal Surfaces,* M. S. Hybertsen, G. W. Flynn, Columbia University

Research Achievements. Recently, the electrical conductance of single-molecule junctions—small aromatics linked to macroscopic gold electrodes by amine and pyridine endgroups—has been reliably and reproducibly measured using modified break junction techniques [1,2]. These and other contemporary experiments provide an opportunity to benchmark standard first-principles methods while quantitatively exploring foundational concepts in molecular-scale charge transport. In recent User and internal research projects, we have developed and used a scattering-state technique [3] based on density functional theory (DFT) to understand reported transport measurements of single-molecule junctions. Using a physically motivated approximate self-energy correction based on GW calculations of a model metal-molecule interface [4], we

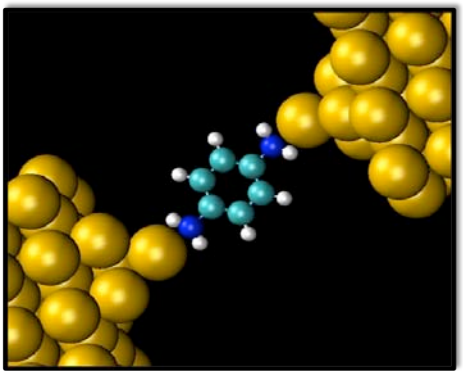

Fig. Atomic structure of benzene diamine, bonded to Au adatoms in a metal-molecule junction, optimized with DFT.

have worked closely with Foundry Users to study quantitatively how binding geometry [5], link chemistry [6], and molecular chain length affect transport properties [7] and, in some cases, lead to novel phenomena, such as mechanically-controlled conductance switching [6]. The importance of electronic level alignment at nanoscale interfaces for understanding conductance—and explaining these experiments—is emphasized in light of our results.

Future Work. We will continue our efforts toward developing an understanding of the physics of charge transport and energy conversion in molecular nanostructures and at organic-inorganic interfaces. Initially, we plan extend our existing theoretical approaches beyond the linear response regime to handle finite bias voltages, compute IV characteristics, and explore nonlinear phenomena associated with single-molecule junctions. We have also begun applying our methods to single-molecule heterojunctions, metal-molecule junctions consisting of "*pn*" donor-acceptor moieties relevant to organic photovoltaics, with the long-term goal of gaining deeper insight into fundamental electronic processes in solar energy conversion and catalysis.

References

[1] L. Venkataraman, J.E. Klare, I.W. Tam, C. Nuckolls, M.S Hybertsen, and M. Steigerwald, "Single-Molecule Circuits with Well-Defined Molecular Conductance", Nano Lett. **6**, 458 (2006)

[2] L. Venkataraman, J.E. Klare, C. Nuckolls, M.S. Hybertsen and M. L. Steigerwald, "Dependence of Single Molecule Junction Conductance on Molecular Conformation", Nature **442**, 904 (2006)

[3] H. J. Choi, M. L. Cohen, and S. G. Louie, "First-principles scattering-state approach for nonlinear electrical transport in nanostructures", Phys. Rev. B **76**, 155420 (2007)

Relevant Molecular Foundry Publications

[4] J. B. Neaton, M. S. Hybertsen, and S. G. Louie, "Renormalization of Molecular Electronic Levels at Metal-Molecule Interfaces," Phys. Rev. Lett. **97**, 216405 (2006)

[5] S. Y. Quek, L. Venkataraman, H. J. Choi, S. G. Louie, M. S. Hybertsen, and J. B. Neaton, "Amine-Au Linked Single-Molecule Junctions: Experiment and Theory", Nano Lett. **7**, 3477 (2007)

[6] S. Y. Quek, M. Kamenetska, M. L. Steigerwald, H. J. Choi, S. G. Louie, M. S. Hybertsen, J. B. Neaton, and L. Venkataraman, "Mechanically-Controlled Binary Conductance Switching of a Single-Molecule Junction", Nature Nanotechnology **4**, 230 (2009)

[7] S. Y. Quek, H. J. Choi, S. G. Louie, and J. B. Neaton, "Many-Electron Effects in Off-Resonant Tunneling in Single-Molecule Junctions", submitted (2009)

Dynamics of pattern-forming and self-assembing soft nanostructured materials

Stephen Whitelam
Molecular Foundry, Lawrence Berkeley National Lab, Berkeley, CA 94720, USA

Scientific Thrust Area and Relevant Molecular Foundry Proposals

The Theory Facility at the Molecular Foundry seeks to understand the principles that underpin the self-assembly and organization of 'soft' materials comprised of nanoscale components bound together by forces comparable to thermal forces. Guided by the simple ideas and unifying principles of statistical mechanics, we we work in collaboration with experimentalists to understand the dynamics through which nanoscale components, both biological and inorganic, associate. Here we present an overview of work from three current collaborations: the *in vitro* crystallization of of bacterial S-layer proteins (with the DeYoreo and Bertozzi groups, Molecular Foundry); the self-assembly of functionalized peanut-shaped colloids (with the Bon Group, Warwick University, User project *Assembly of Anisotropic Particles and their Interaction with Soft Interfaces*); and pattern-forming dynamics of nanostructured actin networks *in vivo* (with T. Bretschneider and N.J. Burroughs, Warwick University).

Research Achievements, resulting publications, and future work

- *S-layer protein crystallization.* Demonstrated that a minimal model of associating monomers with competing nonspecific and specific ('lock-and-key') interactions can mimic experimentally observed crystallization dynamics. We are exploring this model to identify the design principles by which protein-protein interactions select their dynamic assembly pathway [Fig. 1].
- *Peanut-shaped colloid assembly* (User project with S.A.F. Bon): Used molecular simulation to identify morphologies of colloidal assemblies accessible to functionalized peanut-shaped colloids as a function of peanut shape. We are currently comparing theory and experiment, and plan to use the theoretical program to help design novel colloidal assemblies. Manuscript in preparation.
- Actin network pattern-forming dynamics: Demonstrated that dynamics of nanostructured actin cytoskeleton in single-celled *Dictyostelium* can be reproduced by a continuum reaction-diffusion dynamics. S. Whitelam, T. Bretschneider and N.J. Burroughs, *Phys. Rev. Lett.*, in press.

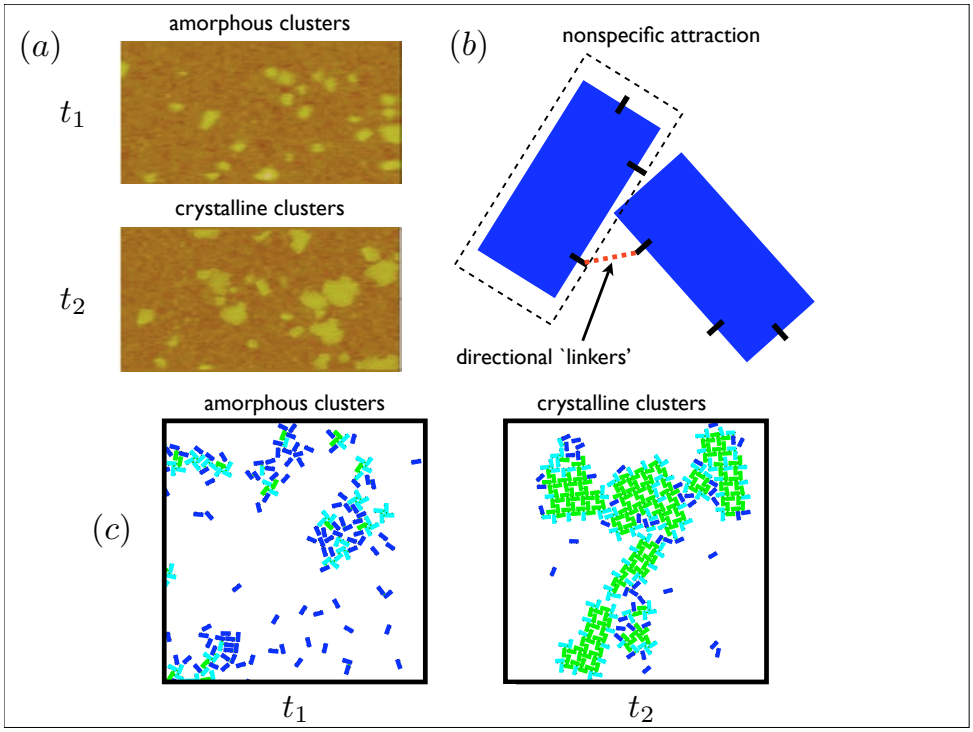

FIG. 1: (a) Bacterial S-layer proteins form, on lipid bilayers, amorphous clusters that spontaneously order and become crystalline on a timescale of minutes [DeYoreo and Bertozzi groups, Molecular Foundry]. (b) A statistical mechanical model of hard rectangles ('monomers') equipped with both nonspecific attractions and directional 'linkers' can (c) recapitulate this complex dynamics. Such models offer insight into the 'design principles' underlying biological assemblies, and allow systematic exploration of the competing roles of phase separation and phase ordering that operate here and in myriad other systems.

X-Ray Probes

Hard X-ray Kinoform Lenses

K. Evans-Lutterodt, A. Stein, A.F. Isakovic
Brookhaven National Laboratory

Research Achievement

Using micro-fabrication facilities at the CFN, BNL, we have fabricated and successfully tested low-loss kinoform lenses for hard X-rays photon energies as low as 7.3keV, and energies as high as 30keV. Focusing hard x-ray photons is technically challenging due to the relatively low values for the real part of the refractive index, and relatively large imaginary or absorptive part of the refractive index. Kinoform lenses are a relatively recent addition to the limited set of focusing options for hard X-rays. There has been steady progress in the quality of hard x-ray focusing optics, and this, in conjunction with brighter synchrotron sources, has enabled spot sizes as small as 100nm and below. These focusing optics enable one to perform spatially resolved versions of widely used characterization techniques such as x-ray diffraction, EXAFS, and other x-ray spectroscopies. Kinoform lenses have lower absorption and larger apertures, than the equivalent refractive-limit lens. We present measurements and simulations of the effectiveness of kinoform lenses. Additionally, using the same micro-fabrication techniques, we have also fabricated low loss Fresnel prisms for hard X-rays. The prism and lens are two of the fundamental building blocks for more complicated optical systems and combinations of these two optical elements should result in interesting and useful high resolution synchrotron based

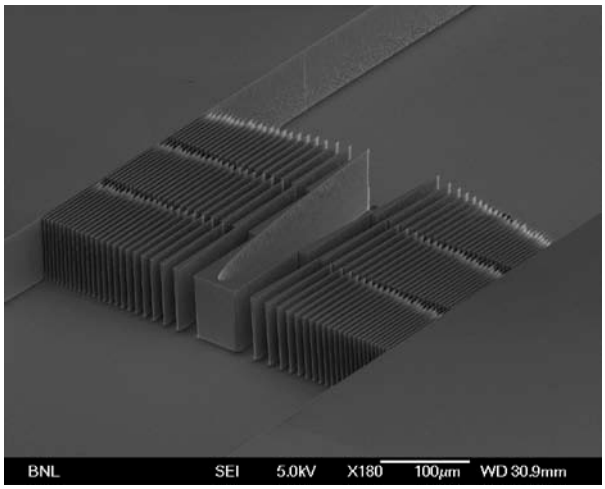

applications, for example phase contrast imaging.

Future Work

Our near term goals are fabricating lenses with diffraction limited resolutions in the 20nm to 50nm range. We are also deploying the lenses in more difficult situations, such as existing bending magnet beamlines with imperfect optics already in place. These bending magnet applications require optics with larger apertures.

References

1. K. Evans-Lutterodt, J. Ablett, A. Stein, C. Kao, D. Tennant, F. Klemens, A. Taylor, C. Jacobsen, P. Gammel, H. Huggins, G. Bogart, S. Ustin, and L. Ocola, "Single-element elliptical hard x-ray micro-optics," Opt. Express 11, 919-926 (2003).
2. K. Evans-Lutterodt, A. Stein, J. M. Ablett, N. Bozovic, A. Taylor, and D. M. Tennant, ”Using Compound Kinoform Hard-X-Ray Lenses to Exceed the Critical Angle Limit”, Phys. Rev. Lett. 99, 134801 (2007)
3. Isakovic, A. F., Stein, A., Warren, J. B., Narayanan, S., Sprung, M., Sandy, A. R. & Evans-Lutterodt, K. “Diamond kinoform hard X-ray refractive lenses: design, nanofabrication and testing”, J. Synchrotron Rad. 16, 8-13., (2009).

Nanofabrication of High-Aspect-Ratio Zone Plates for Hard X-rays

Ming Lu, Derrick C. Mancini, Leo Ocola, Ralu Divan
Center for Nanoscale Materials, Argonne National Laboratory
9700 S. Cass Avenue, Argonne IL 60439

Scientific Thrust Area: Nanofabrication and Devices

Research Achievement:

Zone plates are diffractive lenses composed of concentric rings of phase-shifting material whose period changes along the radius. The focal spot size is proportional to the outermost ring width. In the hard x-ray region, no effective refractive lens is available due to weak interaction between materials and hard x-rays. Zone plates are among those few optics which can focus to the diffraction limit for hard x-rays. The optimal efficiency of a zone plate, however, is determined by the thickness of the phase-shifting layer, which ranges from hundreds of nanometers to several microns, depending on the material and working x-ray wavelength. Therefore, it is challenging to fabricate hard x-ray zone plates with better than 50-nm resolution due to the high aspect ratios required. Our current work focused on taking advantage of the capabilities of our 100-KeV electron beam lithography system for the development of nanofabrication techiques for hard x-ray zone plates.

Current commercial hard x-ray zone plates [1] are fabricated by using electron beam lithography (EBL) to pattern the a thin resist layer, and the use oxygen reactive ion etching to transfer the pattern into a thicker underlying layer that acts as a mold for gold electroforming. We have demonstrated the ability to use hydrogen silsesquioxane (HSQ) as a negative resist for high-aspect-ratio patterning using 100 KeV EBL [2]. We then employed HSQ and EBL to directly pattern the molds for gold electroforming hard x-ray zone plates, which is relative simply compared with commercial process. 1-μm-thick gold zone plates with 80-nm-wide outermost zone were successfully fabricated with this process. While higher resolution zone plates could be patterned, their aspect ratio was limited by electron scattering effects.

A multi-pass technique was initially developed for high-resolution (below 20-nm) soft x-ray zone plate fabrication [3], in which odd- and even-numbered rings are patterned and electroplated separately. The success of this technique relied upon a unique customized EBL system that has sub-pixel overlay alignment capability. Our numerical simulation shows the performance of a zone plate made with multi-pass technology is not very sensitive to alignment accuracy. A zone plate with alignment error no larger than half of the outermost zone width can keep most of the resolution and more than 90% of the efficiency. With our well-calibrated, state-of-the-art commercial EBL system, the overlay alignment can be controlled to 10 nm or less. It is a maximal misalignment budget good for the zone plates with 20 to 30 nm outermost zone width, which can be a breakthrough for hard x-ray zone plates.

By combining the multi-pass technique with an "in-situ" electroplating technique [4] and a resist contrast enhancing technique, we have successfully demonstrated the nanofabrication of gold zone plates with 30-nm-wide outermost zones and 500-nm-thick phase shifting layer. The best alignment error was determined to be about 10 nm. The outermost zone width and thickness have not yet reached the limit of the fabrication technology and with room to improve the aspect ratio of hard-x-ray zone plates.

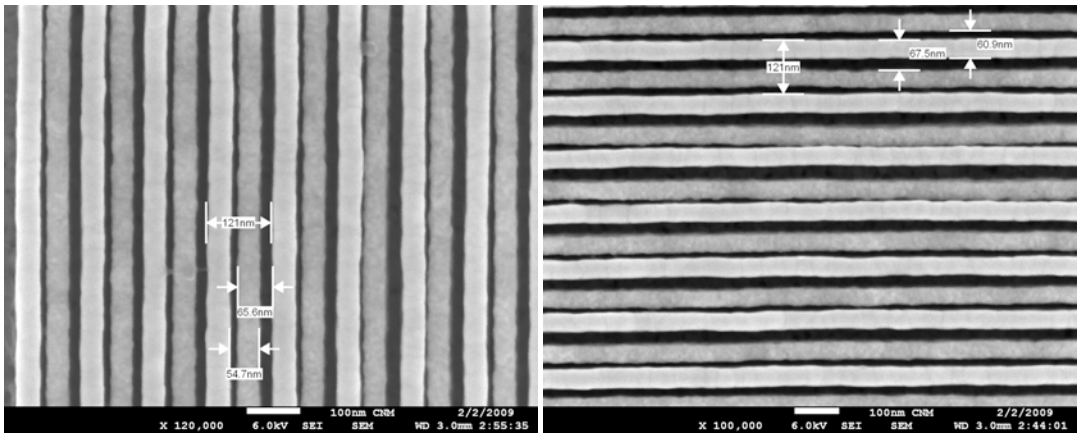

Fig. 1. SEM micrographs of a 500-nm-thick zone plate with 30 nm nominal outermost zone width. The measured misalignment error is about 6.5 nm (5.5 nm at X-direction and 3.3 nm at Y direction).

Future Work:

We will continue to advance the state-of-the-art of hard x-ray zone plate fabrication by employing new methods and materials for high-aspect-ratio nanopatterning of zone plate structures.

References:

1. W. Yun, M. Feser, A.F. Lyon, F. Duewer, Y. Wang, "Pathways to sub-10nm x-ray imaging using zone plate lens," in "Design and Microfabrication of Novel X-Ray Optics II," Proc. SPIE 5539, 133–137 (2004).
2. L.E. Ocola and V.R. Tirumala, "Nanofabrication of super-high aspect ratio structures in HSQ from direct-write e-beam lithography and hot development," presented at EIPBN 2008.
3. W. Chao, B.D. Harteneck, J.A. Liddle, E.H. Anderson and D.T. Attwood, "Soft X-ray Microscopy at a Spatial Resolution better than 15 nm," Nature, 435, 1210-1213 (2005).
4. R. Divan, D. Mancini, N. Moldovan, B. Lai, L. Assoufid, Q. Leonard, and F. Cerrina, "Progress in the fabrication of high-aspect-ratio zone plates by soft x-ray lithography," in "Design and Microfabrication of Novel X-Ray Optics," Proc. SPIE 4783, 82–91 (2002).

Publications:

M. Lu, L. E. Ocola, R. Divan, D. C. Mancini, "Fabrication of high-aspect-ratio hard x-ray zone plates with HSQ plating molds," in "Nanoengineering: Fabrication, Properties, Optics, and Devices V," Proc. SPIE 7039 (2008).

M. Lu, R. Divan, L. E. Ocola, D. C. Mancini, "Fabrication of High Resolution Hard X-ray Zone Plates Using Multi-pass Technology with a Commercial Electron-beam Lithography Tool," to be presented at HARMST 2009 and to be submitted to Microsystems Technologies.

A Path Towards Nanofocusing of X-rays: Multilayer Laue Lenses

Jörg Maser,[1,2] Hanfei Yan,[4] Hyon Chol Kang,[5] Robert P. Winarski,[1] Martin V. Holt,[1] Chian Liu,[2] Ray Conley,[4] Stefan Vogt,[2] Albert T. Macrander,[2] and G. Brian Stephenson[1,3]

[1]Center for Nanoscale Materials, Argonne National Laboratory, Argonne, Illinois 60439, USA.
[2]X-ray Science Division, Argonne National Laboratory, Argonne, Illinois 60439, USA
[3]Materials Science Division and Center for Nanoscale Materials, Argonne National Laboratory, Argonne, Illinois 60439, USA
[4]National Synchrotrn Light Source II, Brookhaven National Laboratory
[5]Advanced Photonics Research Institute, Gwangju Institute of Science and Technology, Gwangju 500-712, Republic of Korea

Research Thrust Area

The possibility of imaging at near-atomic resolution using short-wavelength x-rays has been a dream ever since the nature of x-rays was first understood nearly 100 years ago. Although hard x-rays can in principle be focused to spot sizes on the order of their wavelength (0.1 nm), this limit has never been approached because of the difficulty in fabricating the optics – indeed, it has not even been clear what type of optics will work.

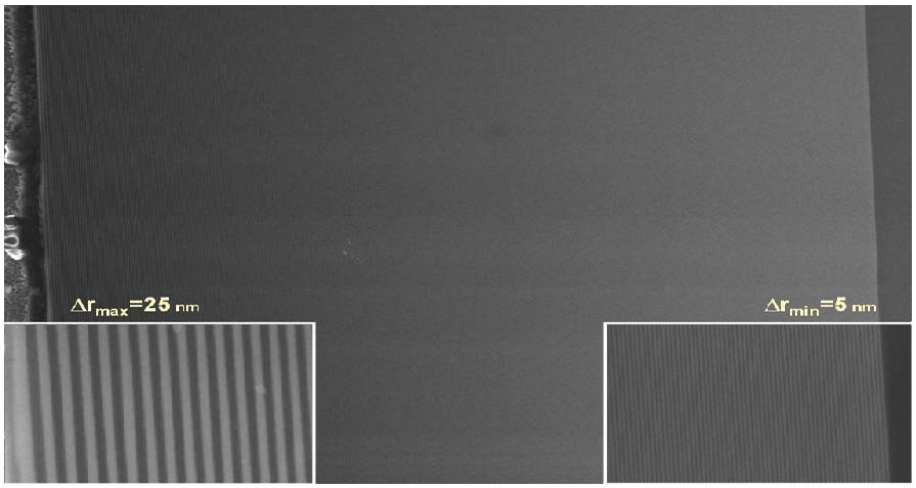

Fig. 1. Multilayer Laue Lens Structure. A total of 1588 layers have been deposited, with inner layer spacing of 25 nm and outer layer spacing of 5 nm. The structure has been thinned to a thickness of 16 μm, optimized for focusing x-rays with a photon energy of 20 keV

Research Achievement

Multilayer Laue Lenses[1] are diffractive x-ray optics with the capability to focus x-rays to focal spots of well below 10 nm. MLL's are fabricated by coating a flat substrate with alternating layers of nanometer thickness, with d-spacing varying to allow focusing of

diffracted x-rays into a single spot. The approach allows deposition of the smallest layers first, thereby reducing the effect buildup of errors has on the focusing properties. Thin cross sections of the multilayer are made following deposition. Such an individual MLL section allows focusing of x-rays in transmission (Laue) diffraction geometry. Crossing two such linear zone plate sections will allow 2-dimensional focusing.

We have shown theoretically that a resolution of 5 nm should be achievable using the non-optimized geometry we are currently fabricating, and that approaching 1 nm with an optimized geometry is feasible. We have experimentally demonstrated a line focus with a width of 16 nm at photon energies of 20 keV and 30 keV[2], with diffraction efficiencies of 30% and above 15%, respectively.

Future Work

We have designed a MLL Microscope that is capable of two-dimensional focusing of x-rays. We will also design optimized MLL structures capable of focusing below 5 nm. We plan to demonstrate a two-dimensional x-ray focus using the existing structures, proceed to 2D focusing with optimized structures, and apply the hard x-ray nanobeams to problems in materials science and nanoscience.

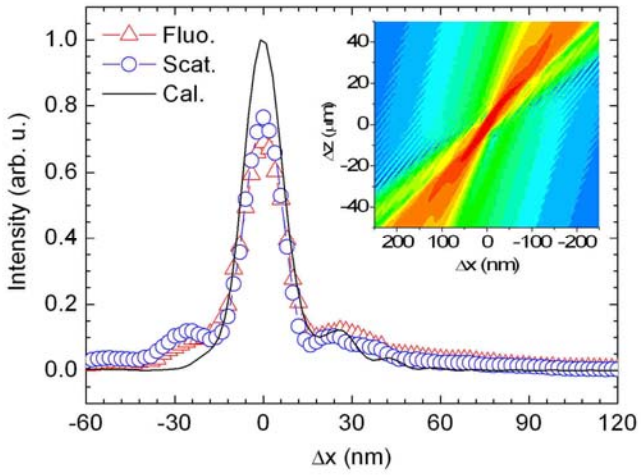

Fig. 2. Focusing of 20 keV X-rays. A line focus of 16 nm has been demonstrated.

Publications

[1] H.C. Kang, J. Maser, G.B. Stephenson, C. Liu, R. Conley, A.T. Macrander, S. Vogt, Phys. Rev. Lett. **96**, March, 127401-1-127401-4 (2006).
[2] Hyon Chol Kang, Hanfei Yan, Robert P. Winarski, Martin V. Holt, Jörg Maser, Chian Liu, Ray Conley, Stefan Vogt, Albert T. Macrander, G.Brian Stephenson, "Focusing of hard x-rays to 16 nanometers with a multilayer Laue lens," Appl. Phys. Lett. **92**, 221114-1-221114-3 (2008).

Other Topics

Heterogeneous Photophysics and Photochemistry of Luminescent Ruthenium Complexes: Implications in Sensor Design

J. N. Demas[1], Kaleem J. Morris[1], James H. Werner[2] and Peter M. Goodwin[2]

[1] *Chemistry Department, University of Virginia, Charlottesville, VA 22904*
[2]*Center for Integrated Nanotechnologies, Los Alamos National Laboratory, Los Alamos NM*

Proposal Title: Heterogeneity effects in luminescence based sensors

Research Achievements

Luminescence-based sensors are tools in bio and environmental analysis including nanosensors that can be incorporated into cells and patterned microsensors used in DNA identification. Many sensors use immobilized luminophores. Polymers are a common support because of easy fabrication and versatile properties. Unfortunately, sensor properties frequently fail to make a clean transition from solution to the solid state. The basic chemistry and photophysics can change (e.g., pKs, binding constants, lifetimes) and well-behaved solution responses can become highly non-ideal with no good models for these changes. These problems complicate the rational design of new sensor systems, and the prevalent view is that much of the non-ideality arises from heterogeneity of the domains in which the sensor molecules partition.[1] As sensors become smaller heterogeneity issues become a more important factor in predicting performance and obtaining reproducible calibrations. For example, using fluorescence microscopy we have established that **micro**heterogeneity is the source of nonlinear Stern-Volmer responses in some quenching based oxygen sensors, and that the non-ideal behavior at the microscope's optical resolution is consistent with nanoheterogeneity (i.e., heterogeneity that is below optical resolution).[2] The ultimate, and probably most common, form of nanoheterogeneity in polymer supports is where every molecule including nearest neighbors can be in spectroscopically distinguishable environments. Fundamental questions concern the existence, the structure, and origins of underlying nanoheterogeneity as well as its role in the design of well-behaved sensors.

Our work is devoted towards the development of biological and environmental sensors based on luminescent transition metal (e.g., Ru(II), Os(II), Re(I) and Ir(III)) complexes. In particular, we pioneered their use in oxygen and pH sensing and are applying them to metal ion sensing.[3] These sensors can be used in a wide variety of analyses where another response can be converted into one directly measurable by our complexes. Applications include diabetic glucose microsensors where glucose oxidase catalyzing glucose oxidation with consumption of oxygen is monitored with an oxygen sensor. Non-ideality is still one of the largest problems in developing new systems and refining existing ones. While we successfully developed microheterogeneity analyses,[2] we had considered direct observation of nanoheterogeneity in these systems out of reach. However, Hochstrasser recently demonstrated that our sensor molecules could be studied at the single molecule level on quartz and the responses of each molecule could be measured independently.[4] A heterogeneous response was obtained for the different molecules. However, quartz surfaces are not polymers and their results do not address the issues in real sensors. Here we examine heterogeneous photochemistry and photophysics of sensor at submonolayer surface levels as well as preliminary results on single molecule studies on glass surfaces and in polymers.

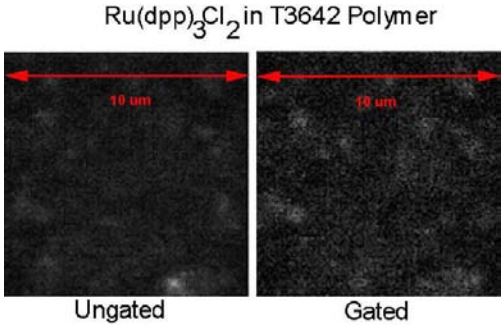

The figure shows single ruthenium $Ru(dpp)_3^{2+}$ molecules (dpp= 2,2'-4,7-diphenyl-phenanthroline) **in a polymer matrix** (T3642 =poly(timethylsilyl-methylmethacrylate)) oxygen sensors. This is a major accomplishment due to the larger polymer backgrounds. The figure compares ungated and time gated confocal images obtained using pulsed excitation and time-gated

photon detection. This approach allows substantial background reduction due to the long lifetimes of the Ru(II) complexes. These preliminary measurements establish unambiguously that we can detect single $Ru(dpp)_3^{2+}$ molecules against the polymer background.

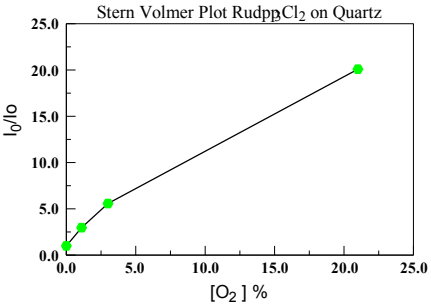

Because SMD with Ru complexes is very difficult due to their long lifetimes (microsecond), we have been developing the confocal lifetime system to examine nanoheterogeneity photophysics and photochemistry using submonolayers rather than SMD. Using the related $Ru(bpy)_3Cl_2$ (bpy=2,2'-bipyridine) and $Ru(dpp)_3^{2+}$ we find that the lifetimes are multi-exponential and the Stern-Volmer quenching plots for oxygen quenching are nonlinear indicating that different molecules have different sensing properties.

Further, the photochemistry is heterogeneous with the extent of photolysis as shown by the non-exponential emission intensity as a function of photolysis time and nonlinear Stern Volmer plots (see figures). The photochemistry is dependent on the complex and the presence of oxygen. Oxygen can either stabilize or destabilize different complexes, presumably due to the relative stability of the complex to attack by reactive singlet oxygen formed on quenching and the degree of quenching of the excited state before it can directly decompose.

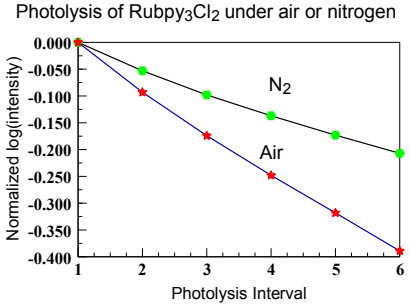

Longer lived, more sensitive molecules can photobleach more readily than shorter lived molecules. Thus, on partial photodecomposition, the oxygen sensing properties of $Ru(bpy)_3Cl_2$ change. It has been widely assumed that lifetime-based sensors are largely immune to photodecomposition; this work establishes that this is not always true. This result has implications for low level sensors in cellular imaging and biomedical analysis where photodecomposition is likely to be a more serious problem.

Finally we found one sample of $Ru(dpp)_3^{2+}$ on quartz that aggregated into domains, possibly nanocrystals. These domains showed oxygen quenching behavior similar to that of single molecules. This is totally unexpected as macro and microcrystals show no oxygen quenching.[2] The figure shows these particles, which are quenched like single molecules but are clearly some sort of $Ru(dpp)_3^{2+}$ aggregate as evidenced by their high emission rates and the absence of single step photobleaching.

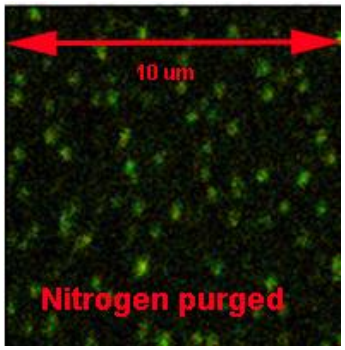

This submonolayer work demonstrates that we can study nano-heterogeneity in polymer-supported sensors without SMD. Implications to sensor design will be discussed.

Future Work

We will improve the S/N in SMD to get quantitative quenching data (e.g., better filters and polymer clean up). We will examine individual single sensor molecule responses and measure the responses of ensembles of individual molecules. This will allow direct proof of sensor nanoheterogeneity and provide the underlying fundamental distribution. These data can help develop reliable behavior modeling and design of improved systems. We will explore the originals of the quenchable nanofeatures.

References

[1] B. A. DeGraff, J. N. Demas, Reviews in Fluorescence 2005, Volume 2, Eds. C. Geddes and J. R. Lakowicz, Springer Science, 125-151.
[2] R. D. Bowman, K. A. Kneas, J. N. Demas, A. Periasamy, Microsc. Microanal., **2003,** 211, 112-120**.**
[3] J. R. Bacon and J. N. Demas, Anal. Chem. **1987**, 59, 2780-85.
[4] Erwen Mei, Sergei Vinogradov, Robin M. Hochstrasser, J. Am. Chem. Soc. **2003**, 125, 13198-13204

Oxygen-deficient 1D-nano-metal oxides and their energy applications

W. Q. Han [1], L. Wu [2], W. Wen [3], H. Li [4], Y. Zhang [5], Y. Zhu[2], J. C. Hanson[3], J. A. Rodriguez [3]*

[1]Center for Functional Nanomaterials, Brookhaven National Laboratory, Upton, NY 11973
[2]Condensed Matter Physics and Materials Science Department, Brookhaven National Laboratory, Upton, NY 11973
[3]Department of Chemistry, Brookhaven National Laboratory, Upton, NY 11973
[4]Institute of Physics, Chinese Academy of Sciences, Beijing 100080, China
[5]Department of Physics and Astronomy, State University of New York, Stony Brook, NY 11794
Corresponding e-mail: whan@bnl.gov

Metal oxides, with their extensive variety of electronic- and chemical-properties are invaluable for fundamental research and for technological applications alike. Oxygen vacancies in metal oxides alter the spatial distribution of atoms in the material, and thus, change their physical- and chemical-properties. We describe herein the formation, microstructure, and physical properties, of oxygen-deficient 1D ceria, titanium, and the non-stoichiometric Magnéli phases in Ti_nO_{2n-1} nanorods. We discuss the potential energy applications of these forms of the materials, for example, in lithium ion batteries, and in the water-gas shift (WGS) reaction.

One important applications of the WGS reaction ($CO + H_2O \rightarrow H_2+CO_2$) is to minimize the CO content in fuel before it enters the main fuel-cell reaction chamber in a hydrogen car. [1-2] Oxygen-deficient ceria (CeO_{2-x}) is a promising candidate because it readily produces oxygen vacancies in an oxygen-deficient environment by reducing some Ce^{4+} ions to Ce^{3+} ions in the stable fluorite structure.

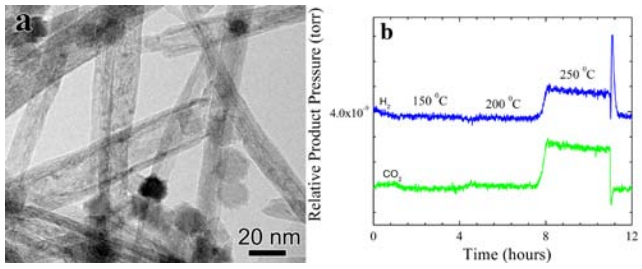

Figure 1(a) TEM image of 1D ceria; (b) WGS activity of pure ceria.

We synthesized polycrystalline 1D-nanostructural ceria by a hydrothermal method. [3] Before using it in the WGS reaction, we activated the 1D-ceria by pre-treating in pure H_2 up to 200 ºC. The *in-situ* time-resolved XRD patterns revealed the retention of the cubic-fluorite structure and average particle size of ceria during the reduction process, although there were major changes in the lattice parameters due to thermal expansion and partial reduction of the cerium oxide. We tested the activity of this pure reduced ceria, without adding any metal catalyst, in the NSLS' beam-line X7B at BNL. The WGS reaction was carried out isothermally in a flow cell at 150-, 200-, and 250- ºC. [4, 5] Figure 1b shows its WGS activity at 200 °C; it is increased further at 250 ºC. Interestingly, a large amount of H_2 was released when we lowered the temperature to room temperature naturally. This finding hints that CeO_2 is suitable for using as a host matrix for storing H_2.

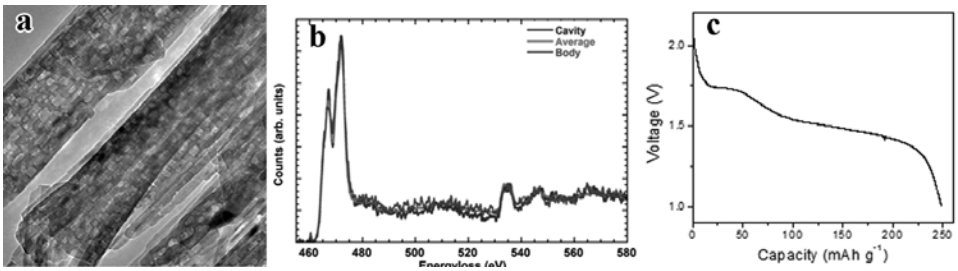

Figure 2(a) TEM image of TiO2 with nanocavities; (b) EELS spectra showing that oxygen deficiency at the inner surface of a nanocavity. (c) Voltage profile of lithium insertion into a TiO_2-nanocavity

We developed a new method to induce the formation of dense, regular nanocavities inside anatase nanorods. [6] Electron-energy-loss spectra show that both the outer-surface of these nanorods and the inner-surface of the nanocavities are oxygen-deficient (Figure 2(b)). We expect that these nanocavities will enhance Li-insertion capacity. Figure 2(c)) shows the voltage profile of lithium insertion into a-TiO_2 NRs with nanocavities. The capacity is close 250 mAh/g, i.e., higher than that for bulk anatase TiO_2 (167 mAh/g), and that for normal anatase nanorods (200 mAh/g). [7]

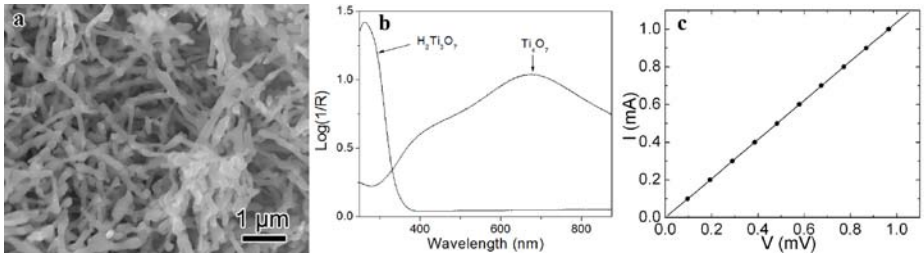

Figure 3(a) TEM image of Magnéli phases in Ti_nO_{2n-1} nanowires; (b) UV-vis diffuse reflectance spectra; (c) Room-temperature I-V curves of Ti_4O_7.

Anatase TiO_2 has poor internal electrical conductivity, so in applying it in Li-ion batteries, conductive carbon black must be added. We developed a novel method to make 1D Magnéli-phases Ti_nO_{2n-1} nanowires, consisting of n–1 TiO_2 octahedral and one TiO octahedral, and thus affected the material's optical- and electrical-conductivity. [8] The light absorption band of Magnéli phases Ti_nO_{2n-1} nanowires covers the full region of visible light, and extends into the near- IR region. The electrical conductivities of Ti_8O_{15} and Ti_4O_7 are, respectively, 0.24 S/cm, and 10.4 S/cm at 300 K. The high electrical-conducting behavior of the Magnéli phases Ti_nO_{2n-1} nanowires points to their potential employment as electrodes, which we soon will pursue.

Acknowledgment: This work is supported by the U. S. DOE under contract DE-AC02-98CH10886 and E-LDRD Fund of Brookhaven National Laboratory.

References

1. M. V. Twigg, Catalyst Handbook, 2nd ed. Wolfe, UK, 1989.
2. Z. Shao, et al., Nature 435, 795 (2005).
3. W. Q. Han, L. J. Wu, and Y. M. Zhu, J. Am. Chem. Soc. 12814, 127 (2005).
4. X. Wang, et al., J. Phys. Chem. B , 109, 19595, (2005).
5. W. Q. Han, et al., J. Phys. Chem. C, 111, 14339, (2007).
6. W. Q. Han, et al., Adv. Mater. 19, 2525-2529 (2007).
7. X. Gao, et al., *J. Phys. Chem. B 108*, 2868 (2004).
8. W. Q. Han, Y. Zhang, Appl. Phys. Lett. 92, 203117 (2008).

Mechanics of Nanoporous Metals

A. Misra, A. Antoniou*, H. Li, J.K. Baldwin, N.A. Mara, D. Bhattacharyya,
E. Akhadov, J.P. Sullivan, M. Nastasi, S.T. Picraux

Los Alamos National Laboratory, Los Alamos, NM
[*]Georgia Institute of Technology

Scientific Thrust Area: Nanoscale Electronics and Mechanics

Proposal Titles: Determining the mechanisms of plastic deformation of metallic nanofoams by atomistic simulations (Michael J. Demkowicz, MIT); Thermal phenomena in micro- and nano systems (Leslie Phinney and Patrick E. Hopkins, SNL).

Research Achievement:

We have synthesized a variety of nanoporous metal films, such as pure Au, pure Pt, and Pt-Ni alloys, by electrochemical dealloying of amorphous metal-silicide films that were either magnetron sputtered or electron beam co-evaporated on a silicon substrate. Electrochemical dealloying selectively etches Si and the remaining metal(s) reorganize to form a three-dimensional porous network where both the ligaments and open cell pores are nanometer-scale. For example, for 20 at.% Pt-80 at.% Si films, the average pore and ligament sizes were 20 nm and 15 nm respectively. The Pt ligaments in these nanoporous films were polycrystalline with a grain size on the order of 5 – 10 nm. Our study has focused on understanding the correlation between synthesis parameters and nanoporous morphologies, mechanical properties, and irradiation stability. The two user projects on nanoporous metals are focused on atomistic modeling of deformation behavior and measurement of thermal properties, respectively.

The key achievements are summarized below:

- Three distinct morphologies (one isotropic and two anisotropic) are reported that depend on the composition and surface topology of the alloy prior to dealloying. There are two levels of anisotropy: micron sized features in the range of 0.1 μm to ~1 μm forming a hyperstructure of either convex or concave features on the free surface. Within each hyperstructure, a 3-D network of polycrystalline Pt ligaments (5-30 nm in length, 5nm grain size) and pores (5-30 nm in size) form. A processing-structure map is developed to correlate np-Pt morphology to the processing conditions, showing that the morphology of the np metal can be controlled by patterning the surface of the as-synthesized alloy prior to dealloying.

- The mechanical properties of nanoporous metal films are investigated through nanoindentation, including compression testing of focused-ion-beam machined micro-pillars, and compared to the properties of fully dense metals as well as macro-scale metallic foams. The dependence of strength is studied as a function of film density as well as ligament size to gain insight on the length scale effects. We observe ultra-high strengths in nanoporous metal films that are not explained by the scaling laws for the strength of bulk metallic foams as a function of foam density (Fig. 1).

- Atomistic modeling is being used by a CINT user to study the unusual nanomechanical behavior of nanoporous metals observed in our experiments. Fig. 2 shows a one million-atom

simulation of a np-Au structure with 3 nm ligament diameter. MD simulation results show that the volume-adjusted yield stress of np-metals is nearly two orders of magnitude higher than that of bulk, single crystal metals. Furthermore, MD simulation show that the onset of plastic yielding in np-metals involves nucleation of plasticity events from free surfaces, as opposed to propagation of pre-existing defects in bulk.

- Ion irradiation (Ne ions, 1 dpa) experiments show insignificant radiation damage in np-metals whereas single crystal full-density films show bubbles and defect agglomerates. Presumably the radiation-induced defects migrate to the surface sinks in np-metals.

Future Work

- Study of ion transport through supported lipid membranes on nanoporous metal films (collaboration with Andrew Dattelbaum, Nano/bio thrust).
- Thermal transport measurements in np-metals using a pump-probe transient thermo-reflectance technique (user project).
- Use of Cantilever Array Discovery Platform^{TM} at CINT to measure the energy dissipation mechanisms in np-metals (collaboration with John Sullivan).
- *In situ* straining in TEM to understand the surface-mediated plasticity in np-metals (collaboration with Jianyu Huang).

Publications

1. J.C. Thorp, K. Sieradzki, L. Tang, P.A. Crozier, A. Misra, M. Nastasi, D. Mitlin, S.T. Picraux, Applied Physics Letters, 88, p.33110-116 (2006).
2. A. Antoniou, D. Bhattacharyya, J.K. Baldwin, P. Goodwin, M. Nastasi, S.T. Picraux, A. Misra, Applied Physics Letters, in review.

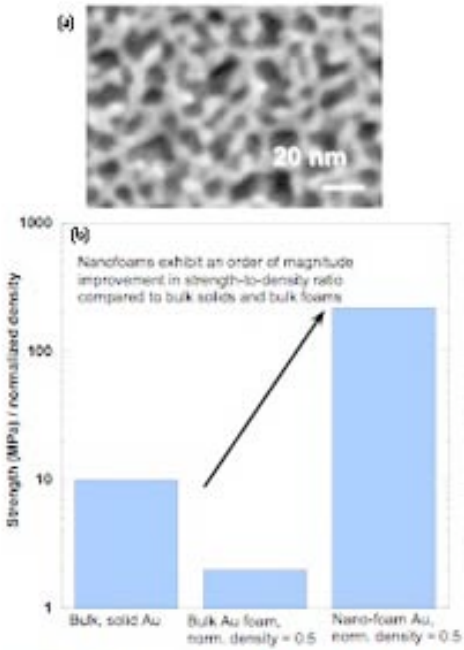

Figure 1 (a) SEM micrograph of a Pt nano-foam; (b) Histogram showing the significant increasing in strength of a nano-foam compared to bulk foam and solid bulk metal.

Fig. 2 Computer generated 3-D structure of np-Au. The simulated structure contains 1 million atoms and has 3 nm diameter ligaments.

Dispensing and Surface-Induced Crystallization of Zeptoliter Liquid Metal Alloy Drops

Eli A. Sutter and Peter W. Sutter
Center for Functional Nanomaterials, Brookhaven National Laboratory
Upton, New York 11973, USA

Scientific Thrust Area

This work is based on in-situ transmission electron microscopy and is carried out primary in the CFN's *Electron Microscopy* facility (E.S.) in collaboration with the *Interface Science and Catalysis* theme (P.S.).

Research Achievement

The controlled delivery of fluids is a key process in nature and in many areas of science and technology, where pipettes or related devices are used for accurately dispensing well-defined fluid volumes. Existing pipettes are capable of delivering fluids with attoliter (10^{-18} L) accuracy at best. Studies on phase transformations of nanoscale objects would benefit from the controlled dispensing and manipulation of much smaller droplets. In contrast to nanoparticle melting whose fundamental pathway was studied extensively, experiments on crystallization, testing classical nucleation theory, are hindered by the strong influence of support interfaces which tend to induce the premature nucleation of the solid phase. Experiments on free-standing fluid drops (e.g., using levitation to avoid melt-support interactions) are extremely challenging.

Here we demonstrate the operation of a pipette specialized for the controlled delivery of individual nanometer sized drops of liquid metals or metal alloys, which is about three orders of magnitude more sensitive than the finest 'universal' pipettes. The pipette, assembled and operated in–situ in a transmission electron microscope (TEM) [1, 2], consists of a semiconductor nanowire (NW), constituting the pipette body, whose tip provides a reservoir of metal semiconductor (Au-Ge) alloy (Figure 1). The entire NW and the Au-Ge reservoir are encapsulated in-situ in a self-assembled multilayer shell of graphene sheets that drives the actuation of the pipette.

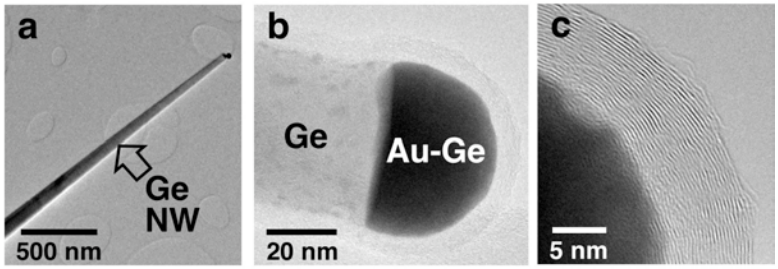

Figure 1: a – Ge nanowire pipette body. b – Fluid reservoir at the pipette tip: Au-Ge alloy melt encapsulated into a multilayer carbon shell (T = 425ºC). c – Pump: carbon shell, made of multiple curved graphene layers, builds pressure on the liquid Au-Ge reservoir.

The device delivers metal alloy melt with zeptoliter (10^{-21} L) resolution (Figure 2). We use this exquisite control to produce nearly free-standing Au-Ge drops suspended by an atomic-scale meniscus at the pipette tip, and to image their phase transformations with near-atomic resolution. Our observations of the liquid-solid transition challenge classical nucleation theory by providing experimental evidence for an intrinsic crystallization pathway of nanometer-sized fluid drops that avoids nucleation in the interior, but instead proceeds via liquid-state surface faceting as a precursor to surface-induced crystallization.

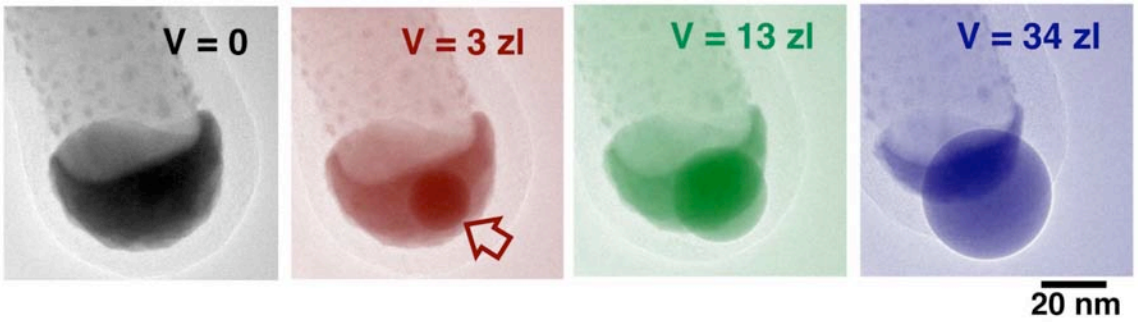

Figure 2: Expulsion of a Au-Ge melt drop during operation of the zeptoliter pipette at 425ºC.

Future Work

Future work will proceed in two main directions – i. graphene shell formation on nanowires from different materials and development of pipettes based on them and ii. establishing the atomic structure of the template for surface-induced crystallization.

Publications

1. P. Sutter and E. Sutter, Nature Mater. **6**, 363 (2007).
2. E. Sutter and P. Sutter, Adv. Mat. **18**, 2583 (2006).
3. BSA 07-37 patent pending.
4. BSA 08-13 patent pending.
5. H. Chiu, S. Kauzlarich, E. Sutter, Langmuir **22**, 5455 (2006).
6. E. Sutter, P. Sutter, R. Calarco, T. Stoica, and R. Meijers, Appl. Phys. Lett. **90**, 093118 (2007).

Quantitative Imaging Analysis Using the Aberration Corrected Scanning Transmission Electron Microscope (Hitachi HD2700C)

Hiromi Inada,[1,4] Dong Su,[1] Lijun Wu,[2] Joe Wall,[3] and Yimei Zhu[1,2]
[1]Center for Functional Nanomaterials, Brookhaven National Laboratory, Upton, NY 11973
[2]Department of Condensed Matter Physics and Materials Science, BNL, Upton, NY 11973
[3]Biology Department, BNL Upton, NY 11973
[4]Hitachi High Technologies Corp., Ibaraki, 312 Japan

The first Hitachi aberration corrected scanning transmission electron microscope (HD2700C STEM) was successfully installed at CFN. The instrument has a cold-field-emission electron source with high brightness and small energy spread.[1] The excellent electro-optical design and aberration correction make the instrument ideal for atomically resolved STEM (Z-contrast) imaging and electron energy loss spectroscopy (EELS). In our presentation we will show the capabilities of the new microscope.

Research Achievement

We have utilized the instrument to study various energy related materials ranging from superconducting and thermoelectric materials to core-shell nano-electrocatalysts. Although aberration correction improves spatial resolution of the instrument, it does not make image interpretation easier due to the large convergent angles used to gain beam current. To understand the image contrast, we developed our own computer codes based on the multislice method with frozen phonon approximation to calculate annular-dark-field (ADF) images. Figs.1 compare experiment with calculation of $SrTiO_3$ in (001) projection, showing very good agreement. Our study demonstrates that the ADF image contrast (or Z-contrast) does not follow the simple $I \sim Z^2$ or $I \sim Z^{1.8}$ power rule as many expect.[2] Although an ADF image indeed shows Z-dependence contrast, only under very high collection angles (i.e. in a true HAADF mode) it yields strong intensity in high Z atom columns and weak intensity in low Z. The image intensity also strongly depends on sample thickness as well as dynamic and static lattice displacement of the atomic species. To correctly interpret the ADF intensity in STEM images, the effect of atomic thermal vibration (Debye-Waller factor) of the atoms must be taken into account. Even at large collection angles the power law Z-dependence is only valid for very thin specimen.[3]

Future Work

Our goal is to conduct STEM experiment and retrieve quantitative crystal, chemical and electronic information of the materials under study at atomic resolution. We have been working on single atom imaging and spectroscopy to further test and push the resolution limit of the instrument. We also plan to combine STEM with SEM using second and back-scattered electrons to retrieve surface structural information. The ability to image surface and bulk structure simultaneously at atomic resolution will revolutionize the field of microscopy and better serve the scientific needs of our user community.[4]

References and Publications

1 Y. Zhu, and J. Wall, chapter in: *Aberration-corrected electron microscopy, a thematic volume of advances in imaging & electron physics*, ed. Hawkes P W, (Elsevier/Academic Press). pp. 481-523 (2008)
2 S.J. Pennycook "Z-contrast transmission electron microscopy – direct atomic imaging of materials". *Annu. Rev. Mater. Sci.* **22**: 171 (1992).
3 H. Inada, L. Wu, J. Wall, D. Su, and Y. Zhu, Journal of Electron Microscopy, June issue, (2009).
4 Work supported by the U.S. DOE, Office of Basic Energy Science, under Contracts No. DE-AC02-98CH10886.

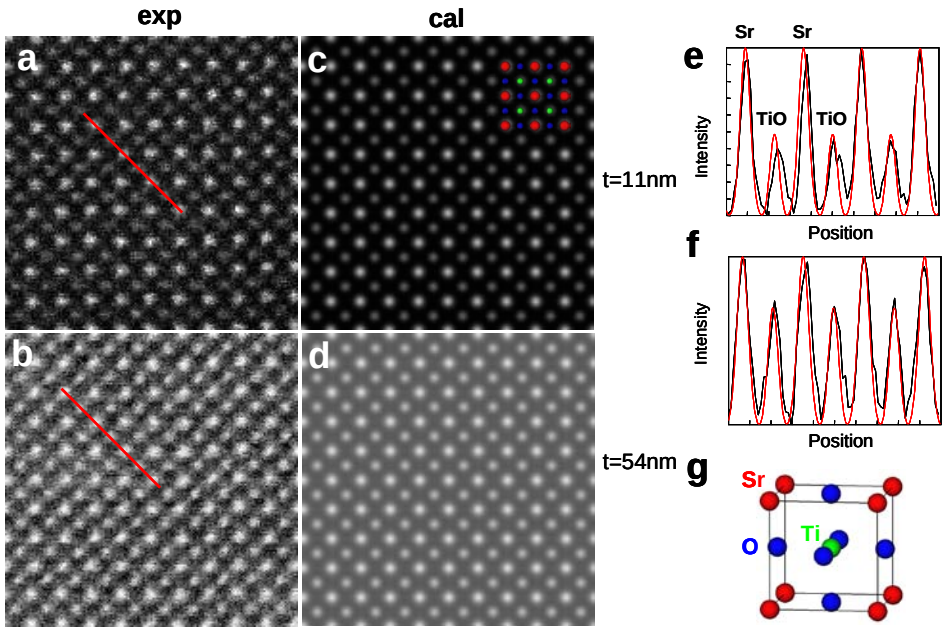

Fig.1 (a-b) Experimental images with convergent angle α=27 mrad and collection angle β=64-341 mrad (a) in thin area, and (b) in thick area. (c-d) Simulated images with (a) thickness=11 nm, and (d) thickness=54 nm, in the image condition of α=27 mrad and β=64-341 mrad. The simulated images are convoluted with a Gaussian point spread function (HMFW=0.09nm). (e-f) Intensity profiles from (a)-(d) with black lines from experiments and red lines from calculations. (g) The crystal model of SrTiO3 where blue dots represent Sr, green dots represent Ti and yellow dots represent O.

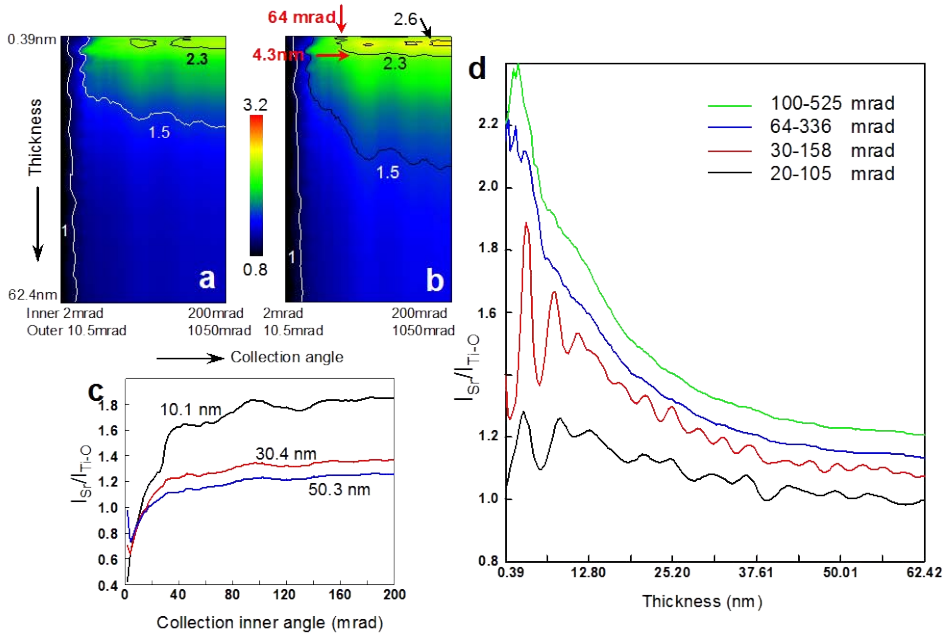

Fig. 2 (a) Intensity ratio I_{Sr}/I_{TiO} with the collection angle increasing from left to right and thickness from top to bottom (Debye-Waller factors B_{Sr}= 0.6214, B_{Ti}= 0.4398 and B_O= 0.7323). (b) Intensity ratio I_{Sr}/I_{TiO} with $B_{Sr}=B_{Ti}=B_O=0.5$. The area with collection angle ≥64 mrad and thickness ≤4.3 nm is considered to comply with a power law Z-dependence (Z^n) with n ranging from 1.77 to 2, as outlined by the intensity contour (>2.6). (c) Intensity ratio profiles of collection angle with thickness being 10.1, 30.4 and 50.3 nm. (d) Intensity ratio profiles of thickness with inner collection angle being 20, 30, 64 and 100 mrad (for details, see ref 3).

Author Index

Participant List

Name	Affiliation	Email
Mark Alper	Lawrence Berkeley National Laboratory	JLEdgar@lbl.gov
George Bachand	Sandia National Laboratories	gdbacha@sandia.gov
Nina Balke	Oak Ridge National Laboratory	balken@ornl.gov
Carl Batt	Cornell University	cab10@cornell.edu
Carolyn Bertozzi	Lawrence Berkeley National Laboratory	crbertozzi@lbl.gov
Anand Bhattacharya	Argonne National Laboratory	anand@anl.gov
Charles Black	Brookhaven National Laboratory	ctblack@bnl.gov
Matthias Bode	Argonne National Laboratory	mbode@anl.gov
Joan Bosworth	Cornell University	jkb27@cornell.edu
Igal Brener	Sandia National Laboratories	ibrener@sandia.gov
Steve Brueck	University of New Mexico	brueck@chtm.unm.edu
Altaf (Tof) Carim	U.S. Department of Energy	carim@science.doe.gov
Kathleen Carrado-Gregar	Argonne National Laboratory	kcarrado@anl.gov
Ronald Castellano	University of Florida	castellano@chem.ufl.edu
Linda Cerrone	U.S. Department of Energy	Linda.Cerrone@science.doe.gov
Bruce Cohen	Lawrence Berkeley National Laboratory	becohen@lbl.gov
Mircea Cotlet	Brookhaven National Laboratory	cotlet@bnl.gov
Peter Cummings	Oak Ridge National Laboratory	peter.cummings@vanderbilt.edu
Hari Dahal	Los Alamos National Laboratory	hpd@lanl.gov
James Demas	University of Virginia	demas@virginia.edu
Jim DeYoreo	Lawrence Berkeley National Laboratory	jjdeyoreo@lbl.gov
Michael Dudley	Stony Brook University	mdudley@notes.cc.sunysb.edu
Bryan Eichhorn	University of Maryland	eichhorn@umd.edu
Kenneth Evans-Lutterodt	Brookhaven National Laboratory	kenne@bnl.gov
Amalie Frischknecht	Sandia National Laboratories	alfrisc@sandia.gov
Oleg Gang	Brookhaven National Laboratory	ogang@bnl.gov
Stephen Gray	Argonne National Laboratory	gray@anl.gov
Jeffrey Greeley	Argonne National Laboratory	jgreeley@anl.gov
Weiqiang Han	Brookhaven National Laboratory	whan@bnl.gov
James Heath	California Institute of Technology	Heath@caltech.edu
Olle Heinonen	Seagate Technology	Olle.G.Heinonen@seagate.com
Jennifer Hollingsworth	Los Alamos National Laboratory	jenn@lanl.gov
James Hone	Columbia University	jh2228@columbia.edu
Robert Hwang	Sandia National Laboratories	rqhwang@sandia.gov
Mark Hybertsen	Brookhaven National Laboratory	mhyberts@bnl.gov
Abdel Isakovic	Brookhaven National Laboratory	Isakovic@bnl.gov

Name	Affiliation	Email
Sergei Kalinin	Oak Ridge National Laboratory	sergei2@ornl.gov
Alamgir Karim	University of Akron	alamgir@uakron.edu
Helen Kerch	U.S. Department of Energy	helen.kerch@science.doe.gov
S. Michael Kilbey II	The University of Tennessee	mkilbey@ion.chem.utk.edu
Harriet Kung	U.S. Department of Energy	harriet.kung@science.doe.gov
Uzi Landman	Georgia Institute of Technology	Uzi.landman@physics.gatech.edu
Xiaogan Liang	Lawrence Berkeley National Laboratory	xliang@lbl.gov
Pao Lin	Northwestern University	pao-lin@northwestern.edu
Yi Liu	Lawrence Berkeley National Laboratory	yliu@lbl.gov
Timothy Long	Virginia Tech	telong@vt.edu
Petro Maksymovych	Oak Ridge National Laboratory	maksymovychp@ornl.gov
Derrick Mancini	Argonne National Laboratory	mancini@anl.gov
Jörg Maser	Argonne National Laboratory	maser@anl.gov
Jimmy Mays	Oak Ridge National Laboratory	jimmymays@utk.edu
Clare McCabe	Vanderbilt University	c.mccabe@vanderbilt.edu
Emilio Mendez	Brookhaven National Laboratory	emendez@bnl.gov
Dean Miller	Argonne National Laboratory	miller@anl.gov
Delia Milliron	Lawrence Berkeley National Laboratory	dmilliron@lbl.gov
Amit Misra	Los Alamos National Laboratory	amisra@lanl.gov
Gabe Montano	Los Alamos National Laboratory	gbmon@lanl.gov
Pedro Montano	U.S. Department of Energy	Pedro.Montano@science.doe.gov
Karren Moore	Oak Ridge National Laboratory	morekl1@ornl.gov
Kaleem Morris	University of Virginia	kjm3c@virginia.edu
Joseph Mougous	University of Washington	mougous@u.washington.edu
Jeffrey Neaton	Lawrence Berkeley National Laboratory	jbneaton@lbl.gov
Frank Ogletree	Lawrence Berkeley National Laboratory	dfogletree@lbl.gov
Deirdre Olynick	Lawrence Berkeley National Laboratory	dlolynick@lbl.gov
Steven Overbury	Oak Ridge National Laboratory	overburysh@ornl.gov
James Perkins	Imperial College London	j.m.perkins@imperial.ac.uk
S. Thomas Picraux	Los Alamos National Laboratory	picraux@lanl.gov
Rpohit Prasankumar	Los Alamos National Laboratory	rpprasan@lanl.gov
Scott Retterer	Oak Ridge National Laboratory	rettererst@ornl.gov
Elena Rozhkova	Argonne National Laboratory	rozhkova@anl.gov
Jim Schuck	Lawrence Berkeley National Laboratory	pjschuck@lbl.gov
Elena Shevchenko	Argonne National Laboratory	eshevchenko@anl.gov
Neal Shinn	Sandia National Laboratories	ndshinn@sandia.gov

Name	Affiliation	Email
Andrew Shreve	Los Alamos National Laboratory	shreve@lanl.gov
Steven J. Sibener	University of Chicago	s-sibener@uchicago.edu
J. Michael Simonson	Oak Ridge National Laboratory	simonsonjm@ornl.gov
David Starr	Brookhaven National Laboratory	dstarr@bnl.gov
Stephen Streiffer	Argonne National Laboratory	streiffer@anl.gov
John P. Sullivan	Sandia National Laboratories	jpsulli@sandia.gov
Ani Sumant	Argonne National Laboratory	sumant@anl.gov
Bobby G. Sumpter	Oak Ridge National Laboratory	sumpterbg@ornl.gov
Yugang Sun	Argonne National Laboratory	ygsun@anl.gov
Eli Sutter	Brookhaven National Laboratory	esutter@bnl.gov
Peter Sutter	Brookhaven National Laboratory	psutter@bnl.gov
Frank Svec	Lawrence Berkeley National Laboratory	fsvec@lbl.gov
Brian Swartzentruber	Sandia National Laboratories	bsswart@sandia.gov
Latha Venkataraman	Columbia University	lv2117@columbia.edu
Akos Vertes	George Washington University	vertes@gwu.edu
Jack Wells	Oak Ridge National Laboratory	wellsjc@ornl.gov
James Werner	Los Alamos National Laboratory	jwerner@lanl.gov
Stephen Whitelam	Lawrence Berkeley National Laboratory	swhitelam@lbl.gov
Gary Wiederrecht	Argonne National Laboratory	wiederrecht@anl.gov
Zhigang Xiao	Alabama A&M University	zhigang.xiao@aamu.edu
Michael Zach	University of Wisconsin, Stevens Point	MZach@uwsp.edu
Nader Zaki	Columbia University	nzaki1@gmail.com
Yuegang Zhang	Lawrence Berkeley National Laboratory	yzhang5@lbl.gov
Yan Zhao	The University of Chicago	yzhao1@bsd.uchicago.edu
Yimei Zhu	Brookhaven National Laboratory	zhu@bnl.gov
Ron Zuckermann	Lawrence Berkeley National Laboratory	rnzuckermann@lbl.gov